

REFERENCE ONLY



2809419834

UNIVERSITY OF LONDON THESIS

Degree phd

Year 2007

Name of Author SATOKO

TANIMOTO

COPYRIGHT

This is a thesis accepted for a Higher Degree of the University of London. It is an unpublished typescript and the copyright is held by the author. All persons consulting the thesis must read and abide by the Copyright Declaration below.

COPYRIGHT DECLARATION

I recognise that the copyright of the above-described thesis rests with the author and that no quotation from it or information derived from it may be published without the prior written consent of the author.

LOAN

Theses may not be lent to individuals, but the University Library may lend a copy to approved libraries within the United Kingdom, for consultation solely on the premises of those libraries. Application should be made to: The Theses Section, University of London Library, Senate House, Malet Street, London WC1E 7HU.

REPRODUCTION

University of London theses may not be reproduced without explicit written permission from the University of London Library. Enquiries should be addressed to the Theses Section of the Library. Regulations concerning reproduction vary according to the date of acceptance of the thesis and are listed below as guidelines.

- A. Before 1962. Permission granted only upon the prior written consent of the author. (The University Library will provide addresses where possible).
- B. 1962 - 1974. In many cases the author has agreed to permit copying upon completion of a Copyright Declaration.
- C. 1975 - 1988. Most theses may be copied upon completion of a Copyright Declaration.
- D. 1989 onwards. Most theses may be copied.

This thesis comes within category D.

☐ This copy has been deposited in the Library of UCL

☐ This copy has been deposited in the University of London Library, Senate House, Malet Street, London WC1E 7HU.

EXPERIMENTAL STUDY OF LATE BRONZE AGE GLASS-MAKING PRACTICE

by

Satoko Tanimoto

Thesis submitted to the University of London
for the degree of Doctor of Philosophy

Institute of Archaeology
University College London

March 2007*

UMI Number: U593461

All rights reserved

INFORMATION TO ALL USERS

The quality of this reproduction is dependent upon the quality of the copy submitted.

In the unlikely event that the author did not send a complete manuscript and there are missing pages, these will be noted. Also, if material had to be removed, a note will indicate the deletion.



UMI U593461

Published by ProQuest LLC 2013. Copyright in the Dissertation held by the Author.
Microform Edition © ProQuest LLC.

All rights reserved. This work is protected against
unauthorized copying under Title 17, United States Code.



ProQuest LLC
789 East Eisenhower Parkway
P.O. Box 1346
Ann Arbor, MI 48106-1346

I, Satoko Tanimoto confirm that the work presented in this thesis is my own.
Where information has been derived from other sources, I confirm that this has
been indicated in the thesis.

Satoko Tanimoto

Abstract:

There is very little known about ancient glass-making practice from the Late Bronze Age (LBA), despite numerous fragments of glass being discovered from LBA archaeological sites, both in Egypt and Mesopotamia. However, for more than 2000 years, two compositional groups of soda-lime-silica glass have dominated the large-scale production of glass in antiquity; namely “LBA glass” of Egypt and Mesopotamia (high magnesium, plant ash based) and the “Hellenistic/Roman glass” (low magnesium, mineral natron based). These two glass groups show unique trends when their compositions are analysed using ternary diagrams, a method developed in petrology. That is, the compositions of most LBA glass can be plotted along different areas/troughs compared to Roman glasses. Their compositions are chemically too homogeneous to be made from the variable raw materials available across chronological periods, vast geographical regions, and colours. Without any solid archaeological evidence available, a scientific approach is necessary to figure out what is causing these trends.

Two glass-making models were tested to identify possible factors that control the composition of finished glass. Once these technical constraints are identified, one can further explore this matter archaeologically (i.e. whether glass-making was centralised, social context of the glass). Moreover, this research paper may contribute fruitfully to the debate on many other unknowns of glass in antiquity, and may eventually give a sensible answer to the fundamental and controversial question; whether glass was made independently from an early period in Egypt, or whether all early Egyptian glass was imported from either Mesopotamia or Asia.

Therefore, my research aims to identify possible factors that control the composition of the finished glass (from variable raw materials) by reconstructing possible LBA glass-making technologies. Then by combining the scientific findings and the archaeological findings, it is hoped to contribute to a better understanding of ancient glass-making in the LBA.

Table of Contents:

Chapter 1: Introduction.....	18
1.1. Aims and objectives of this thesis.....	19
1.2. Overview of thesis structure.....	20
 Chapter 2: Archaeological Evidence.....	 26
2.1. Introduction.....	26
2.2. Glass-making vs. glass-working, organisation of workshops in the vitreous industry, and the social context of glass.....	30
2.2.1. Terminology: glass-making vs. glass-working.....	30
2.2.2. Workshop organisation.....	33
2.2.3. Position of glass in LBA society.....	37
2.3. Known glass workshops in Egypt and Mesopotamia, dating to the Late Bronze Age (about 1500-1000 BC).....	46
2.3.1. Mesopotamia: site evidence in chronological order.....	46
2.3.2. Egypt: site evidence in chronological order.....	65
2.4. Short summary/interpretation of evidence given in section 2.3.....	76
2.5. Work based on Amarna.....	80
2.6. Work based on Qantir.....	86
2.7. Introduction of scientific work on LBA glass.....	89
 Chapter 3: Scientific Approach.....	 95
3.1. Background.....	95
3.2. Methodology.....	109
3.2.1. Methodology of experimental work.....	109
3.2.2. Methodology of analytical work.....	115
3.2.3. Data handling for plotting ternary graphs.....	123

Chapter 4: Melt-Solid Interactions (“partial melting model - PMM”, earth alkalis)..... 124

4.1.	Terminology: Partial melting vs. devitrification.....	125
4.2.	Review of the literature (mostly technical glass industry).....	127
4.3.	CaO vs. temperature.....	132
4.3.1.	PMM: composition (CaO content) vs. firing temperature.....	134
4.3.2.	PMM: quality of glass (“Egyptian” vs. “Roman”).....	145
4.4.	MgO vs. CaO on temperature, viscosity, crystal growth, and the MgO content of LBA glass.....	149
4.4.1.	MgO vs. CaO contents on temperature, and viscosity.....	150
4.5.	CaO and chlorine.....	153
4.6.	Summary and interpretation for earth alkali contents in SLS glass.....	158

Chapter 5: Melt-Melt Interactions (“two melts model- 2MM”, alkalis)..... 166

5.1.	Review of the literature.....	168
5.2.	Na ₂ O/K ₂ O System – 1.....	170
5.2.1.	Base A-4, 5, 6 + NaCl (series 2-1 to 2-4).....	177
5.2.2.	Base A-4, 5, 6 + KCl (series 2-1, 2-5 to 2-7).....	180
5.3.	Na ₂ O/K ₂ O System – 2: Base A-7, 8, 9 + NaCl + KCl (series 3-1 to 3-3).....	184
5.4.	Summary and interpretation for alkali proportions in SLS glasses.....	190

Chapter 6: Archaeological samples from Qantir..... 195

6.1.	Description of the Qantir glass samples.....	196
6.1.1.	Sample-1: #00/0472,01.....	198
6.1.2.	Sample-2: #92/0589b.....	200
6.1.3.	Sample-3 and -4: #88/0517,01and #88/0517,04.....	201

6.1.4. Sample-5: #88/0671c.....	202
6.1.5. Sample-6: #96/0759.....	203
6.1.6. Sample-7: #98/0844.....	205
6.2. Microscopic examination.....	206
6.3. Composition of Qantir glass samples.....	208
6.4. Glass-making practice at Qantir.....	214
6.4.1. CaO content & firing temperature.....	214
6.4.2. Raw materials.....	218
Chapter 7: Archaeological Implications.....	221
7.1. Homogeneity of LBA glass.....	221
7.1.1. Colorants and opacifiers used in LBA Egyptian glass.....	224
7.1.2. Glass composition differences among LBA sites.....	225
7.1.3. Interpretation of the variables in chemical composition of LBA glasses by comparing with the finds from the experimental melts.....	273
7.2. Variability of plant-ash glasses in general, grouping potentials.....	274
Chapter 8: Summary and Outlook.....	280
8.1. Summary of outcomes from the research on the relevant archaeological publications.....	284
8.2. New Contributions from this research.....	286
8.2.1. Replications of two possible glass-making models.....	286
8.2.2. The comparison of the base glass compositions.....	297
8.3. Human agency as the remaining aspect: how influential ?....	303
8.4. Future Outlook.....	304












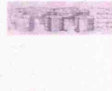
List of Tables:

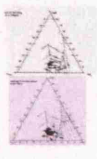






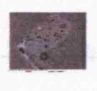
Table #		Page
Table 2.1:	Shortland's (2000b: Table 7-3) list of several historically recorded names and titles of craftsmen at Amarna.	42
Table 2.2:	Shortland's (2000b: Table 7-4) list of several historically recorded names and titles of Egyptian faience makers.	43
Table 2.3:	Summary of LBA Mesopotamian sites with glass finds.	78
Table 2.4:	Summary of LBA Egyptian sites with glass finds (including Uluburun).	79
Table 3.1:	Summarised compositions of plant ash (published) from various geographical locations.	97-99
Table 3.2:	Comparison of the variability among published chemical compositions of plant ash and those of LBA glasses.	100
Table 3.3:	The published salt contents of plant ash from various geographical locations.	105-107
Table 3.4:	The published salt contents of natron from various geographical locations	108
Table 3.5:	Accuracy and precision of acquired data (glass standards).	120
Table 4.1:	Semi-quantitative analysis of various crystalline areas seen in melt #14* (measured by SEM).	140
Table 4.2:	Semi-quantitative analysis of various crystalline areas seen in melt #02* (measured by SEM).	142
Table 4.3:	Compositions of glass melt, all fired at 1000 °C (no MgO, Al ₂ O ₃ , and Cl in the batch).	143
Table 4.4:	Compositions of glass melts, prepared for the quality comparison of the formed melts, Egyptian vs. Roman trough.	147



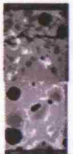
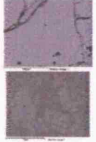
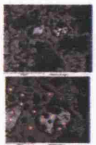

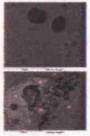
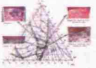
Table 4.5:	Compositions of glass melt with batch compositions chosen along Egyptian trough and all fired at 1150 °C (fixed 2 wt% Cl, no MgO in the batch).	156
Table 4.6:	Compositions of glass melts with batch compositions chosen across 900 °C isotherm and all fired at 980 °C (fixed 2 wt% Cl, no MgO in the batch).	157
Table 5.1:	Compositions of glass melt with various alkali concentrations [wt%].	174
Table 5.2:	Potassium oxide contents of glass melt with various alkali concentrations (extra alkalis, either NaCl or KCl was added) [wt%].	179
Table 5.3:	Compositions of glass melt with various alkali concentrations (extra alkalis, both NaCl and KCl were added together) [wt%].	187
Table 6.1:	Average compositions of Qantir glass samples, both newly obtained and published [wt%].	210
Table 6.2:	Reduced average compositions Qantir glass samples both newly obtained and published [wt%].	211
Table 7.1:	Colorants and opacifiers used in LBA Egyptian glass (Shortland 2002: Table 1).	225
Table 7.2:	Average compositions of various glass samples from Nuzi [wt%] (Brill 1999a, b).	227
Table 7.3:	The seven base oxide compositions of various glass samples from Nuzi [wt%] (Brill 1999a, b).	228
Table 7.4:	Average compositions of various glass samples from Tell Brak [wt%] (Brill 1999a, b, Oates <i>et al.</i> 1997).	230
Table 7.5:	The seven base oxide compositions of various glass samples from Tell Brak [wt%] (Brill 1999a, b, Oates <i>et al.</i> 1997).	231
Table 7.6:	Average compositions of various glass samples from Nimrud [wt%] (Reade <i>et al.</i> 2005: Table 1).	235

Table 7.7:	The seven base oxide compositions of various glass samples from Nimrud [wt%] (Reade <i>et al.</i> 2005).	235
Table 7.8:	Average compositions of various glass samples from Malkata [wt%] (Brill 1999a, b).	239
Table 7.9:	The seven base oxide compositions of various glass samples from Malkata [wt%] (Brill 1999a, b).	240
Table 7.10:	Summarized compositions of glass samples from Amarna [wt%] (modified from Shortland (2000b, Shortland & Tite 2000), by adding data from Brill (1999 a, b) where possible).	242
Table 7.11:	The seven base oxide compositions of various glass samples from Amarna [wt%] (Shortland 2000b, Shortland & Tite 2000, Brill 1999 a, b).	243
Table 7.12:	Average compositions of various glass samples from Lisht [wt%] (Brill 1999a, b).	246
Table 7.13:	The seven base oxide compositions of various glass samples from Lisht [wt%] (Brill 1999 a, b)	247
Table 7.14:	Average compositions of various glass samples from Uluburun shipwreck [wt%] (Brill 1999a, b).	251
Table 7.15:	The seven base oxide compositions of various glass samples from Uluburun shipwreck [wt%] (Brill 1999a, b).	251
Table 7.16:	Comparison of the base glass composition between Mesopotamian and Egyptian LBA glasses* [wt%].	256
Table 7.17:	Reduced compositions of various LBA cobalt-blue glass samples [wt%] (data from Oates <i>et al.</i> 1997, Rehren 1997, Brill 1999a, b, Shortland 2000b, Shortland 2002, Reade <i>et al.</i> 2005, Schoer & Rehren 2007).	260-265

List of Figures:

Plate	Figure #		Page
	Figure 2.1:	A limestone relief from the Amen-Re temple at Karnak depicting glass among semi-precious stones (Sherratt & Sherratt 1991: 386; Fig.2).	40
	Figure 2.2:	Map of Mesopotamia showing glass-related LBA archaeological sites (Moorey 1994: 3).	46
	Figure 2.3:	A small lump of glass from Eridu (Abu Shahrein, BM 115474). Image: courtesy of the British Museum.	49
	Figure 2.4:	Moulded blue glass female mask from Tell al Rimah (Carter 1965: 55, Fig. 8).	55
	Figure 2.5:	Fragments of glass mosaic from Tell al Rimah (Stern & Schlick-Nolte 1994: 46, Fig. 39).	55
	Figure 2.6:	Unique glass vessel fragments from Tell Brak decorated with pattern of rosettes and triangles (Oates <i>et al.</i> 1997: 84, Figure 122).	59
	Figure 2.7:	Mosaic glass fragments from Dur Kurigalzu (Baqir 1946: Plate XX, Fig. 15).	61
	Figure 2.8:	Map of Egypt showing glass-related LBA archaeological sites.	65
	Figure 2.9:	Glass rods, canes and vessel fragments from Malkata (Mass <i>et al.</i> 2002: 68, Figure 1).	66
	Figure 2.10:	Various glass rods and fragments from Amarna (now in the Petrie Museum, UC 22909-20).	68
	Figure 2.11:	Opaque blue glass ingots from Uluburun shipwreck.	70
	Figure 2.12:	Petrie's reconstruction of the glass-making process. Pans are supported on the inverted cylindrical vessels now suggested by Nicholson to be crucibles/ingot moulds (Nicholson & Henderson 2000: 199; Figure 8.1).	82

	Figure 3.1:	Plots of reduced LBA glass compositions from the published works (a) from Rehren 2000, Figure 1 (b) updated figure, including more published data (Qantir samples, Lilyquist & Brill 1993, Rehren 1997, Shortland 2000b).	102
	Figure 3.2:	(a)~(c) Plots of reduced Roman glass compositions (Rehren 2000b).	103
	Figure 3.3:	The SLS ternary system with no MgO (Shahid & Glasser 1972).	112
	Figure 3.4:	The SLS ternary system with 5 wt% MgO (Shahid & Glasser 1972).	113
	Figure 3.5:	Peak intensities for sodium (red), silicon (green), and calcium (blue) respectively in glass (spot-analysis). This figure shows sodium readings of glass standard Corning A dramatically drops while the readings of silicon and calcium remains consistent over time.	116
	Figure 3.6:	Peak intensities for sodium (red), silicon (green), and potassium (blue) respectively in glass (spot-analysis). This figure shows both sodium and potassium readings of glass standard Corning D decrease while the readings of silicon and calcium remains consistent over time.	117
	Figure 3.7:	Peak intensities for sodium (red), silicon (green), and calcium (blue) respectively in glass standard Corning A (area analysis, x 800 magnification). At this magnification, measured intensities stayed stable indicating no soda migration.	118
	Figure 4.1:	SEM (BSE) image showing distribution of crystalline phases within glassy phase. Lime-rich crystalline phases (in white colour) diffusing into pseudo-wollastonite and wollastonite phases (light grey areas), suggesting these crystalline phases were formed by semi-reacted raw materials.	127

	Figure 4.2:	Cross section of one of the experimental melts (incomplete melting) showing the clear transparent glass (lower half) and the opaque, with a high proportion of residual crystalline matter (upper half) (image taken by Shugar).	135
	Figure 4.3:	Separation by simple hand picking after crushing (image taken by Shugar).	136
	Figure 4.4:	SEM (BSE) image of quartz grains (dark) and lime-rich areas (bright) seen in the experimental melts (PMM), (a) Melt #11 and (b) Melt #15 (images taken by Shugar).	137
	Figure 4.5:	SEM (BSE) images of wollastonite crystals seen in (a) melt #57 (no MgO, Egyptian trough, 1100 °C isotherm, underfired at 1080 °C) and (b) melt #06 (no MgO, Roman trough, 1000 °C isotherm, fired at 1000 °C).	138
	Figure 4.6:	SEM (BSE) images showing mixture of various crystalline phases within melt #14 (no MgO, Egyptian trough, 1100 °C isotherm, fired at 1000 °C); (a) overview (b) enlarged image showing lime-rich nucleus (numbers show where semi-quantitative data was taken, see Table 4.1).	139
	Figure 4.7:	SEM (BSE) image showing another type of nucleus formation with its surrounding phase.	140
	Figure 4.8:	SEM (BSE) images showing mixture of various crystalline phases within melt #02 (Egyptian trough, 1000 °C isotherm, batch composition, fired at 1000 °C); (a) overview (b) enlarged image showing lime-rich nucleus (numbers show where semi-quantitative data was taken, see Table 4.2).	141
	Figure 4.9:	Juxtaposition of glass formation and composition for melts #14 (top left), #02 (bottom left), #06 (bottom right), and #10 (top right), all fired at 1000 °C (modified figure from Shugar & Rehren 2002: 4).	143


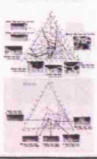



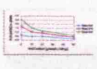
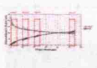
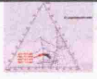
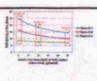
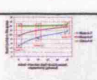




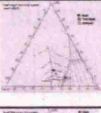

	Figure 4.10:	(a)~(f) Comparison of the quality of glass produced (images taken by Shugar). Individual batch composition was chosen from both the Egyptian and the Roman trough at the specified temperature and fired at the temperature shown above.	146
	Figure 4.11:	Comparison of the quality of glass across 1000 °C isotherm (each batch compositions are shown in wt%). (a) all fired at 980 °C (no MgO). (b) all fired at 1000 °C, with 5 wt% MgO.	148
	Figure 4.12:	Correlation between lime and chloride content in the glass when glass batch compositions were selected along the Egyptian trough (shown as grey circles, respectively).	155
	Figure 4.13:	Correlation between lime and chloride content in the glass when glass batch compositions were selected along the 900 °C isotherm (shown as grey circles, respectively).	155
	Figure 5.1:	Spatial separation of glass and residual salt material (clear glass phase can be seen below the residual salt material). (a) above and (b) cross section.	173
	Figure 5.2:	Potash content in the glass with increasing amount of NaCl. The minimum potash content in the glass is approximately 0.5 wt%.	179
	Figure 5.3:	Alkali oxide contents in the glass with increasing amount of KCl.	182
	Figure 5.4:	Plots of reduced compositions of experimental melts (Series 2-1, 2-5 to -7).	182
	Figure 5.5:	Potash content in the glass with increasing amount of alkali chlorides.	188
	Figure 5.6:	Soda content in the glass with increasing amount of alkali chlorides.	188
	Figure 6.1:	The image of a glass sample series, #00/0472. The arrow highlights the actual sample mounted for analysis, #00/0472,01, above.	199

	Figure 6.2:	Cross-section through Sample 00/0472,01 (image taken by Excavations Qantir). The mounted sample originates from the left section.	199
	Figure 6.3:	Mounted glass sample #00/0472,01 (image taken by Th. Rehren).	200
	Figure 6.4:	White glass plate, #92/0589b (image taken by Excavations Qantir).	201
	Figure 6.5:	White glass plate, #92/0589b in cross-section (image taken by Excavations Qantir).	201
	Figure 6.6:	The image of a glass sample series, #88/0517 (taken by Excavations Qantir). The two samples mounted for analysis (#88/0517,01 and #88/0517,04) are highlighted by the arrows, above (the larger piece is #88/0517,01).	202
	Figure 6.7:	The image of a glass sample series, #88/0671c (taken by Excavations Qantir). The sample is about 12 mm long.	203
	Figure 6.8:	Images of glass sample #96/0759, (a) overall view and (b) cross-section, mounted in resin (both images taken by B. Schoer).	204
	Figure 6.9:	A small glass droplet, #98/0844 (image taken by B. Schoer).	205
	Figure 6.10:	Optical microscope image of quartz grain in the Qantir glass sample #88/0517,01. Width of image c. 2 mm.	206
	Figure 6.11:	SEM (BSE) image of quartz grain in the Qantir glass sample #88/0517,04, with corrosion (dark) starting at the cracks surrounding same quartz grains (centre and left).	207
	Figure 6.12:	Plots of reduced Qantir glass compositions; semi-finished glass (#88/0517,01 and 04; X), #98/0844 (O), and the others (●).	216
	Figure 6.13:	SEM (BSE) image of crushed quartz from the Qantir sample (image taken by P. Connolly).	219
	Figure 7.1:	Plots of reduced chemical compositions of LBA cobalt-blue (top) and copper-blue (bottom) glasses.	266

Acknowledgements:

	Figure 7.2:	Plots of reduced chemical compositions of LBA red (top) and purple (bottom) glasses.	267
	Figure 7.3:	Plots of reduced chemical compositions of LBA green (top) and yellow (bottom) glasses.	268
	Figure 7.4:	Plots of reduced chemical compositions of LBA white (top) and black (bottom) glasses.	269
	Figure 7.5:	Plots of reduced chemical compositions of LBA colourless glasses.	270
	Figure 7.6:	Combined plots of reduced chemical compositions of LBA red, purple, green, yellow, white, black, and colourless glasses.	270

Acknowledgements:

I would like to particularly thank Professor Thilo Rehren for his continuing support and supervision throughout the research, and Dr David G. Jeffreys, Dr Roger Matthews, and Dr Bill Sillar for their advice on the archaeological elements. The staff of the Wolfson Archaeological Science Laboratories, especially Kevin Reeves, have also given great advice and valuable technical support. This research would not have been possible without Dr Aaron Shugar's initial pilot study and Dr Edgar Pusch's excavation, and their generous donations of samples and images that helped me further extend my studies.

I would also like to thank David Park for inspirational cups of coffee and entertaining conversations that have kept me fascinated in the Conservation field and reminded me why I really wanted to pursue my PhD and not go off the rails.

My greatest thanks go to my Father, Mother and to Simon Hill. Without their continual warm support and encouragement throughout my academic years none of this would have been possible.

Experimental Study of Late Bronze Age Glass-making Practice

Chapter 1: Introduction

The glazing of stones such as quartz and steatite, as well as the making of faience, had been known since Predynastic times (5300-3000 BC; all the chronology used in this thesis is based on *The Oxford History of Ancient Egypt* (Shaw 2000) for Egypt, and on *Excavations at Tell Brak* (Matthews 2003: 5) and *The Oxford Encyclopaedia of Archaeology in the Near East* (Meyers 1997) for Mesopotamia). Thus, the routine production of an artificial glass phase was mastered many thousand years ago. In fact, several Egyptian faience workshops are known, ranging from a possible Middle Kingdom (2055-1650 BC) example, through the New Kingdom (1550-1069 BC), to the Ptolemaic/Roman period (332 BC-AD 395) (Nicholson 1993), and the production technologies are well understood (Kaczmarczyk & Hedges 1983; Vandiver 1983).

Objects made entirely of glass, however, are extremely rare before 1500 BC, and not attested in Egypt before the late Middle Kingdom (Shaw & Nicholson 1995: 112). Despite their relatively frequent appearance from then onwards in both Mesopotamia and Egypt, only a few workshops are known to have produced glass artefacts, and little is known about the actual glass-making practice. As will be shown, the archaeological record is either not present, or not clearly identified and understood; this is to a great extent due to the fact

that there is too little known about glass-making and in particular the kind of waste materials associated with it, making it so difficult to identify the relevant evidence.

1.1. Aims and objectives of this thesis

This thesis has two main aims, namely first to contribute to the understanding of the physical and chemical reactions which take place during glass-making within a framework of Late Bronze Age materials and technologies, and then to use this better understanding to identify the possible nature of glass-making remains, and how these immanent factors govern glass composition and constrain glass-making practice. It is hoped that this will help to identify and interpret possible glass-making remains in the archaeological record, and to reveal the cultural (or configurational) parameters at work in LBA glass-making.

In the past, our understanding of LBA glass-making was very limited by the lack of archaeological excavations of glass factories. The key site, Amarna, is mostly for glass-working but reveals little about glass-making activity. Thus, my study of LBA glass-making had to develop its own parameters, starting with the observed homogeneity of LBA glass compositions, and looking for technical explanations for this. The homogeneity is seen as a major feature of LBA glass, and has been used as an argument for centralised and very conservatory glass-making practice. If, however, different glass-making centres are thought to operate during the LBA, then another explanation for this homogeneity has to be found, possibly based on technical processes as first suggested by Rehren (2000a, b).

The research is placed within the ongoing wider research programme based at the excavations directed by Dr Edgar Pusch, Pelizaeus-Museum Hildesheim, at the ancient Ramesside capital of Piramesses in the eastern Nile Delta. Here suspected evidence for glass-making was identified during the period of this research project, and a preliminary study of that material will be used to test some of the results from my work.

Several main objectives were set to achieve these aims. First, the relevant archaeological literature was studied for descriptions of glass-making remains or workshop evidence, both from Mesopotamia and Egypt. Then, two processes that could influence the glass composition during glass-making were explored. The “Partial Melting Model (PMM)” is thought to influence the earth alkali oxide content of the glass, while the “Two Melt Model (2MM)” is thought to influence the alkali oxide content of glass. Both models were tested through series of experimental melts under controlled conditions in the laboratory, focussing on the concentrations of calcium oxide (lime) and potassium oxide (potash), respectively. Parallel to this, the published data of LBA glass objects were studied to test whether the suggested homogeneity of glass composition is true, or whether regional or colour-specific differences can be found which would already indicate de-centralised and possibly changing glass-making. Finally, the experimental data was tested by comparing it to some new archaeological finds of semi-finished glass from Dr Pusch’s excavations, and to published data of LBA glass objects. Based on this data, the aim is to suggest future work to further develop ideas concerning the organisation and practicalities of LBA glass-making.

1.2. **Overview of thesis structure**

Chapter 2 summarises the current understanding of glass workshops, and the archaeological evidence for the production and working of glass proper (i.e. excluding faience and the other glazed materials) during the Late Bronze Age (LBA, see below for more specific time frame) in Egypt and Mesopotamia. Particular emphasis will be put on the two sites of Tell el-Amarna and Qantir-Piramesses in Egypt, and some of the ongoing work based on the material evidence from these two sites.

The geographical framework of this research is consciously limited mainly to Mesopotamia and Egypt unless otherwise noted, leaving aside the Aegean (except for the Uluburun shipwreck), and other parts of Asia etc. This is mostly a reflection of the virtual absence of published evidence for glass workshops in areas outside Mesopotamia and Egypt during the Late Bronze Age. The low-magnesia, high potash glass from Fratessina in Italy, although of LBA date, is fundamentally different from the plant-ash based Middle Eastern high-magnesia soda-lime-silica glass (Angelini *et al.* 2004) and will therefore not be considered here. This chapter will show that glass was intentionally manufactured in Western Asia from at least as early as 1500 BC (Tatton-Brown & Andrews 1991). As will become clear, until recently, no incontrovertible archaeological evidence had been found for the making of glass from primary raw materials in either Egypt or Mesopotamia, which would be the only certain proof for primary glass-making at a specific location and provide sufficient technical detail to reconstruct LBA glass-making practice. The site of Qantir-Piramesses was only identified as a glass-making site in 2005, when the main part of this research was already concluded.

In the absence of archaeological evidence, a series of experiments was designed based on two closely linked aspects, to better understand the reactions and processes that take place during LBA glass-making; these are reported in Chapters 3 to 5. The key purpose of these experiments is firstly to experimentally identify technical constraints within the glass-forming reactions, and then to prepare the ground for developing possible glass-making scenarios for the LBA. This process is very important since it will hopefully enable us to better evaluate to what extent the composition of finished glass is controlled by human behaviour and by chemical reaction, respectively.

My research aims specifically to understand the mechanisms that control the base glass composition during glass-making from complex and variable raw materials. The working hypothesis is that the primary glass-forming processes result – through a series of chemical reactions and exchange processes – in the very uniform base glass composition observed in LBA glasses, despite the inevitable variability of the raw materials (Rehren 2000a, 2000b). To properly interpret this homogeneity requires first to identify to which extent the nature of the primary glass-forming reaction controls the primary glass composition, and to which extent human influence, such as choice of raw materials and operating parameters, affect the glass composition. This observed chemical homogeneity is evidently central to the discussion of regional versus centralised glass-making.

Chapter 3 sets out the Methodology used throughout the experimental and analytical work, as well as the handling of data for graphical presentation.

Chapter 4 focuses on the role which incomplete melting plays for the level of earth alkali oxides. In modern glass-making technology, all the raw materials are placed in one crucible and all the raw materials will react completely, without any residual materials, to form a clear glass. However, recent ethnographic studies of traditional glass-making practice, for example from India (Sode & Kock 2001), indicate that this need not have been the case in pre-modern glass-making. Rather, it appears that the primary glass-making resulted in a glass phase mixed with substantial amounts of residual crystalline material, and required further processing such as selection based on visual appearance and additional melting to produce clear glass.

This chapter explores in some detail the “Partial Melting Model (PMM)” put forward by Rehren (2000a, 2000b) as a possible explanation of the compositional homogeneity of many LBA glasses. It builds on earlier preliminary work by Shugar and Rehren (2002), and focuses on the glass forming reactions involving residual and newly-formed crystalline phases. It is shown that these interactions influence selectively the earth alkali oxides, with CaO being controlled by the melting temperature. The effect of crystal formation on the MgO content is briefly discussed based on a review of technical literature and some preliminary analytical data from archaeological finds from Qantir.

Chapter 5 is an investigation of the interaction between a soda-lime-silicate melt and a co-existing salt melt. This aims at understanding the influence that the non-reactive compounds of the plant ash can have on the final glass melt, particularly with reference to the alkali oxides. The data clearly shows that the

presence of chlorine, in the form of sodium chloride and potassium chloride, has a direct and systematic influence on the alkali oxide concentrations, and provides the basis for a functional model to explain the observed modification of the ceramic in the glass-making vessels recently identified at Qantir.

In combination, these two chapters demonstrate how the investigation of by-products (i.e. residuum, crystals / salts) of ancient glass will help us to better evaluate past technologies, in particular to what extent the composition of finished glass is controlled by configurational factors of human behaviour (i.e. choice of materials etc.) and by inherent factors such as chemical reactions, respectively. The fundamental choice between one or the other melting system (e.g. "Egyptian" cotectic trough or "Roman/Hellenistic" cotectic trough, see Chapter 3) is configurationally determined, as evident from the very strong correlation between the two systems, and their cultural affiliation (LBA vs. Hellenistic/Roman). Thus, configurational and inherent factors overlap in the glass-making process. For archaeology, the configurational or cultural factors are of particular interest, and it is hoped that, by studying the extent and in particular the limitation of the inherent factors, the configurational factors will become more clearly visible from this overlapping picture. In addition, the research will attempt to infer from the data indications of the methods and materials of glass manufacture and to seek criteria that might serve as guides for the identification of procedures and methods in LBA glass-making practice.

Chapter 6 is a brief account of the investigation of some archaeological samples of partly-fused or semi-finished glass from Qantir, Egypt. This

material became available only towards the very end of my research, and offers an opportunity to compare the experimental results to the archaeological reality. However, no comprehensive analysis of the material is possible at present, limiting this to a very preliminary report.

Chapter 7 looks in some detail into the published analyses of major and minor oxides in LBA glasses from Mesopotamia and Egypt, comparing their compositions between different sites and between different colours. Although this approach is limited by the nature of the available data, it does not show that there are systematic differences between sites and between colours, indicating that further analyses of trace elements may reveal more pattern between glass compositions.

Chapter 8 attempts to place the findings of the experimental work within the context of their possible archaeological significance, and offer some suggestions for further work in this field.

If the detailed scientific investigations can be matched successfully with the archaeological evidence, one of the more fundamental questions in ancient glass archaeology, such as “Why is LBA glass in the Middle East chemically so homogeneous, and specifically why is the cobalt-blue glass different?” could be discussed on a better basis.

Chapter 2: Archaeological Evidence

2.1. Introduction

The use of glass in the LBA Middle East centres on two large cultural regions, Mesopotamia and Egypt. It is widely accepted that glass was probably invented in Mesopotamia, and that the earliest glass artefacts were produced there as well. Although the earliest glass has been found in 20th century BC contexts, regular and large-scale glass production does not occur before the 16th century BC (see later section 2.3.1.). The use and working of glass in Egypt occurs only 50 to 100 years later, and was stimulated and influenced by Mesopotamian material. This undisputed primacy of Mesopotamian glass-making, however, does not preclude the possibility that glass was later also fused from primary raw materials in Egypt (Nicholson & Henderson 2000).

In addition to the earlier dates of the archaeological evidence for glass in Mesopotamia, the most common Bronze Age names for glass are taken from Hurrian and Akkadian (ancient languages of Anatolia and Mesopotamia). These are the terms *ephliakku* and *mekku* respectively (Nicholson 1993). The use of these foreign names in texts of the New Kingdom, in Egypt, may reflect the exotic origin of glass, supporting the hypothesis that glass first came to Egypt from Mesopotamia. However, there are also Egyptian names for glass; *iner en weden* or *aat wedhet*, both meaning literally “stone of the kind that flows” (Tatton-Brown & Andrews 1991: 26), indicating a technical familiarity with this material in Egypt as well.

These early names provide interesting insights into the way glass was

perceived during the LBA. Petrie's observations of finds from his excavations and the referring to glass as a kind of stone, led him to suggest that the idea of early Egyptian glass was, in the first place, not to be transparent, but something that would emulate known precious stones, such as turquoise or lapis lazuli, which are opaque. The main purpose of the glass was to reproduce the stone as closely as possible (Petrie 1926). Evidence for coloured glasses to imitate precious stones also comes from two distinct types of cuneiform texts from Mesopotamia. The first type of cuneiform text includes economic records and letters, both private and official, which date from as early as the middle of the second millennium BC and later. In the texts, the existence of coloured glasses is clearly mentioned to imitate rare and precious stones, especially lapis lazuli. Reference is made either directly by describing the stones as artificial, or by stressing that the stones mentioned are genuine. Another designation of artificial lapis lazuli appears in a text from Dur Kurigalzu (see section 2.3.1., below). The second type of the text, probably originating from the second millennium BC but recorded much later, sheds light on the history of glass in Mesopotamia. It consists of word lists in which certain denominations of glass appear (Oppenheim *et al.* 1970). Among 20,000 fragments of clay tablets found from the palace in Nineveh, the library of king Assurbanipal (668–627 BC), there are a few dozen broken pieces containing prescriptions for the making of coloured glasses, named “glass texts” by Oppenheim (Oppenheim *et al.* 1970: 4).

In addition, Oppenheim (Oppenheim *et al.* 1970: 19) called attention to the very rare appearance in texts of the Ur III period of a material known as *anzahhu* (Sumerian AN.ZAH), once as a bowl, once as a raw material, among

the word lists. He believed it to be a “primary glass”; that is, a key intermediate material in the production of a finished glass as well as another material called *busu* (Loding 1981). The *Chicago Assyrian Dictionary* interprets it as “an imperfectly fused, crude, frit-like glass” (Moorey 1994: 191). However, Foster (1979) has taken it to be a kind of rock, perhaps a type of quartzite (finely ground). Whatever the case, and the available evidence is indecisive, it does not provide certain evidence for glass production at this time (Moorey 1994).

The Mitannian region, in modern-day Syria, has been suggested as the location of the earliest glass workshops in Mesopotamia (Freed 1981). In fact, various ingots of glass have been recovered from several sites in Mesopotamia (see section 2.3.1.). These include the “Mitanni Palace” at Tell Brak (Oates *et al.* 1997: 81). At Kar-Tukulti-Ninurta and Nuzi, glass ingots have been found in contexts that are dated to the 13th and 14th centuries BC (Shortland 2000b). However, the findings give little more information than that glass was available in Mesopotamia in this form at this time (Nicholson & Henderson 2000).

It is important to note that there is still much uncertainty about dating of the glass objects/fragments found. Uninscribed objects, if they belong to a medium like pottery, whose stylistic development has been studied systematically, can be dated relatively easily, compared to glass, according to where they seem to fit in the art historical evolution of their type. Birgit Schlick-Nolte (Nolte 1968) was the first to apply art historical methodology – particularly the classification of surface decoration – to the study of glass vessels, devising groupings of vessels into workshops according to the

similarity of their surface decoration. However, this methodology still left many glasses broadly dated “Amenhotep III to Ramesses II” (Kozloff *et al.* 1992: 375) since there is little understanding of either glass-making or -working technologies used in the LBA that could aid in a closer chronological assignment of individual finds.

The most securely dated examples of glass do not appear in Egypt until the 18th Dynasty (1550-1295 BC; New Kingdom). There are examples of glass earlier than this, but the attributions of many of these are still controversial (Lilyquist *et al.* 1993). The most secure pre-18th Dynasty glass includes two scarabs from the 12th Dynasty (1850-1773 BC, Middle Kingdom), one opaque blue and another turquoise blue, both inscribed for officials and firmly dated. Many of the other artefacts previously thought to have been of glass are now placed in other material categories, but it is nonetheless clear that glass was on occasion produced before the New Kingdom in Egypt (Shortland 2000b). It is believed that glass vessels were made in Egypt during the reign of Thutmose/Tuthmosis III (1479-1425 BC), which is earlier than any physical evidence of glass workshops that have been discovered. Thutmose began a series of Asiatic conquests (such as into Palestine and Syria) in 1481 BC, and it has been argued that the military campaigns brought back Asiatic glass-workers to set up a glass vessel industry in Egypt (Frank 1982). It was initially believed that the extensive use of cobalt in Egyptian glass (as a colouring agent) suggested a Mesopotamian connection (Frank 1982). However, later research identified an Egyptian cobalt source (Kaczmarczyk 1986, Shortland *et al.* 2006), and will be discussed further below (see section 2.7.).

A major impression emerging from most studies of archaeological glass is that there is very little firm evidence for the physical origin of the glass that was worked into artefacts, and even less for the practicalities of the glass making in either Egypt or Mesopotamia. Thus, any attempt to study Late Bronze Age glass production has to be based on a novel approach, that overcomes the limitations of currently available archaeological data and materials.

In summary, my research will focus on aspects of the production of LBA glass, particularly between 1500 BC (when glass industries were apparently well developed and glass was routinely produced) and 1000 BC. This cut-off point, 1000 BC, was chosen to coincide with the earliest known production of natron-based glass around 1000 BC, as reported by Schlick-Nolte and Werthmann (2003), whereas typical LBA glass is plant-ash-based. The change from one alkali source (plant ash) to another (natron) has major implications for the production process of glass; hence, this study will focus on plant-ash-based glass only.

2.2. Glass-making vs. glass-working, organisation of workshops in the vitreous industry, and the social context of glass

2.2.1. Terminology: glass-making vs. glass-working

The archaeological literature is relatively non-specific in its use of the term glass-making, glass-working, or glass workshops. However, for a better understanding of the practice and organisation of LBA glass-making and -working, a clear distinction needs to be made between glass-making (the primary production of glass from its raw materials; silica, lime and alkali) and glass-working (the manufacture of artefacts from existing glass, such as ingots

or scrap glass; cullet), as the apparatus and pyrotechnology involved are quite different; glass-making usually requires significantly higher temperatures in order to flux the silica source. The techniques of making glass from its raw materials requires a very different set of skills than glass-working, and is at the centre of my research. It is a matter of discussion whether the colouring process is seen as a part of glass-making or glass-working. Recently, it has been argued that during the LBA the coloration of glass is more closely related to glass-making than glass-working (Rehren *et al.* 2001). Unfortunately, the two sets of activities are in their practical aspects not well understood, archaeologically not well defined, and hence difficult to separate based on the published evidence from many glass-related archaeological sites. Thus, it is first necessary to develop defining criteria that can be applied to the published evidence for glass workshops in order to identify glass-making vs. glass-working, or simple use of glass.

It is widely accepted that glass-making during the LBA was based on a two-component recipe, with silica as the main ingredient and soda-rich plant ash as the flux. Colorants and opacifiers were further components that were added to the glass batch, but as my research focuses on understanding the primary glass-making this is not further considered here. The main silica source was either crushed quartz pebbles as already suggested by Petrie (1926), or desert sand as suggested or implied by several authors (most recently Nicholson and Henderson 2000). However, the most recent interpretation of the silica source for LBA glass production is crushed quartz pebbles, rather than sand (personal communication Freestone). The use of mineral natron has recently been suggested for cobalt-blue glass from Amarna

(Shortland & Tite 2000, and see below). The raw materials were ground, mixed and fused together to form the glass; there is no regular waste material such as slag during metallurgical processes, which would remain. Any incompletely fused material is likely to have been recycled and re-used in the next melting cycle, making it difficult to archaeologically identify glass-making from its waste.

Rehren (1997) has argued that LBA Egyptian glass-making is archaeologically visible as fragments of cylindrical crucibles. The recent identification of so-called Reaction Vessels (Rehren & Pusch 2005) in addition to the cylindrical crucibles from the glass-making workshop in Qantir-Piramesses offers a further diagnostic artefact type for glass-making; however, it is possible that fragments of reaction vessels were overlooked in earlier excavation practice (Rehren personal communication), and therefore are not reported in the earlier literature.

Glass-working in contrast is characterised through the presence of waste glass such as monochrome rods or semi-finished or malformed objects; several archaeological sites are known to have produced such material (see e.g. Amarna, below), and the careful study of these finds has helped archaeologists understand and reconstruct some of the main glass-working techniques. In particular, the production of core-formed vessels has attracted much attention (Stern & Schlick-Nolte 1995), and some lapidary techniques are also known to have been used.

The mere presence of increased numbers of glass objects at an

archaeological site, fragmentary or not, is in itself not evidence for the former presence of a glass workshop. Instead, it more likely indicates a site occupied or used by the glass-using elite of high-ranking officials, priests or members of the royal families.

Several excavation reports use the term 'glass slag', and use it as a justification to suggest that there was a glass workshop nearby. However, glass slag is a rather vague term, which has not been defined properly, and a range of fused materials can appear glassy without necessarily being waste of a glass-making or glass-working process. Thus, for the purpose of the discussion later in this chapter of the archaeological evidence, reports of glass slag in the literature have been taken as a generic indication of glass workshops, but not as diagnostic for a specific type of activity.

2.2.2. Workshop organisation

Based on the separation of glass-making and glass-working, Rehren and co-workers suggested that workshops can be divided into Primary and Secondary Workshops. In this model, primary workshops are specialised in the production of artificial materials from raw materials, using chemical reactions to transform substances (i.e. glass-making). Secondary workshops in contrast re-shaped and worked a given material (such as in the form of glass rods, canes, or ingots) into finished products, often physically combining glass of various colours, albeit without much changing the composition of the materials involved (i.e. glass-working) (Rehren *et al.* 2001).

The conceptual separation into primary and secondary glass workshops has

been useful in identifying the organisation of glass production in the Late Roman period (Freestone *et al.* 2002). While Late Roman glass production is similar in principle, it differs considerably in the details from LBA glass workshop organisations in such important factors as scale of production, affiliation of workshops and craftspeople, and the underlying macroeconomic context. Therefore, it is unlikely that the details of this model can be used to identify the LBA glass production; instead, a different type and level of organisation has to be assumed.

It is highly suggested from Petrie's excavations at Tell el-Amarna (Nicholson 1995a, 1996, Shortland 2000a, Shortland & Tite 2000) and from the recent work at Qantir-Piramesses (Rehren & Pusch 1997, 2000, 2005, Rehren *et al.* 1998, 2001) that glass-making and glass-working workshops were not placed in isolation (also see sections 2.5. and 2.6., Work based on Amarna and Qantir). It is believed to be carried out alongside faience production, and possibly other pyrotechnical crafts, such as Egyptian blue production and metallurgy (Boyce 1989, Hamza 1930, Mass *et al.* 2002, Rehren 1997).

The technical and organisational aspects of faience production were intensively studied (e.g. Shortland 2000a, 2000b, Tite 1987, Tite & Bimson 1986, Tite *et al.* 1983). However, the separation of skills required at primary and secondary workshops, as defined above, is less clear when it comes to faience workshops. This is because in terms of high temperature processes faience is a one-step product. The raw materials are mixed and formed into the intended shape while cold. The shaped body is then allowed to dry and fired, during which process the glaze develops. Following this, there is little

working to be done once a faience object is being made, except for the mechanical assemblage of individual pieces to more elaborate or large architectural items. Thus, while the glass phase and the raw materials used in faience production are similar to those used for glass-making, there are significant differences in the practices and organisation of the two crafts, and the evidence from faience workshops can not be used to interpret glass-making or glass-working.

Another artificial material frequently mentioned in connection with Egyptian glass is Egyptian blue, which was made and worked alongside glass as well. The primary production of Egyptian blue involves specialist raw materials and chemical reactions, similar to glass-making. The secondary workshops are based on cold processes, involving grinding for pigment production and painting. Thus, it may be assumed that Egyptian blue making and glass-making are organised in a similar way, and that one can distinguish between Egyptian blue primary workshops where required skills involve high temperature operations for the production of cakes and slabs, and Egyptian blue secondary workshops, where these intermediate products are processed rather than produced (Rehren *et al.* 2001). However, no primary production workshops for Egyptian blue are known, and the suspected similarity can therefore not inform the discussion of the organisation of the glass workshops. Egyptian blue cakes and slabs are long known from Egyptian sites such as Amarna and Qantir (see next section, 2.3.2.). Thomas (2000, cited in Rehren *et al.* 2001: 230) proposed that recent evidence from Zawiyet Umm el-Rakham, a Ramesside fort near the Libyan coast some 300 km west of Alexandria, indicates that such pigment cakes were traded together with other pigment

cakes for further working and consumption at some considerable distance from the primary production site. Thus, the mere discovering of such cakes does not constitute evidence for the local production of Egyptian blue.

The concept of long-distance trade of cakes or ingots of finished raw material, to be manufactured into objects at a place separate from the place of primary production, is applicable to glass as much as to Egyptian blue. Indeed, the evidence for glass ingots from LBA shipwrecks confirms this. The complex nature of the cargo of these ships, however, does not help in identifying the place of origin of the glass. Indeed, even the direction of sailing of the Uluburun vessel, the most prominent LBA ship and carrying large numbers of glass ingots, is unknown (Pulak 2003, 2005, 2006). Therefore, as regards the organisation of different workshops and archaeological sites related to glass-making and -working, one has to differentiate between primary production, possible long-distance transport, and secondary production. The correct identification of activities from the archaeological evidence is crucial for their interpretation; section 2.3. will try and apply the criteria mentioned above for the identification of primary versus secondary workshops based on the published literature.

The frequent mentions of glass imports into Egypt raise the question about the ability of glassworkers in that country to produce their own glass. If all glass were traded into Egypt in the form of foreign ingots then the Egyptians would have merely worked these into vessels, using their artistic skills. Petrie (1894; 1926), Nicholson (1993), Rehren (1997), Rehren and Pusch (1997, 2000, 2005), Shortland (2000a, 2000b), Shortland & Tite (2001) and Rehren *et al.*

(2001) have suggested that glass-making most likely did happen in Egypt, i.e. that glass was made from the raw materials. Rehren and co-workers (2001) and Rehren and Pusch (2005; 2006) argue that most glass workshops produced glass only in certain colour(s), and that some readymade glass ingots in possibly other colours were imported into Egypt. However, this is difficult to prove from the published archaeological data. Therefore, any contribution of primary production, trade and working has to be considered when assessing the individual sites. Before this, however, it is important to address some non-technical aspects of glass in ancient Egypt.

2.2.3. Position of glass in LBA society

The aim of my research is to determine to what extent the composition of the finished LBA glass is controlled by human factors (i.e. choice of materials, recipes, furnace conditions etc.) and/or chemical factors. For this, it is also important to discuss the socio-economic background of glass in order to understand the social context within which choices are made in each manufacturing process, as artisan's techniques give us not only a general insight into their social organization but also may be a good indicator of how much the people's choice would have an effect on the material itself (Lemonnier 1986).

Therefore, the possible human factors and the social context of the glass are discussed below by defining the nature and the significance of glass-making and the social position of the craftsmen involved in glass-making within the LBA setting.

2.2.3.1. Value of glass

Glass was first produced mainly to imitate precious stones, such as turquoise and lapis lazuli (Nicholson & Henderson 2000, Nolte 1968, Oppenheim *et al.* 1970, Petrie 1926, Shortland 2000b, 2001). Glass was noted in the Bible as being precious as rubies and gold in both Egypt and Mesopotamia (Freed 1981). In fact, there is a cross-over in usage of glass and the other precious materials (i.e. gold, lapis lazuli) that can be seen in numerous LBA artefacts. That is, both glass-inlays and gold-inlays can be seen in faience design and usage of lapis lazuli and blue glass can be seen in similar design in other crafts. This trend is also visible in the most prestigious and high status objects. For example, there are two objects from Tutankhamen's grave dated to the end of the 18th Dynasty (Tiradritti 1999). One is the innermost coffin (JE 60671, shown in Tiradritti, 1999: 232), made entirely from thin gold sheet decorated with finely executed chasing and with multi-coloured glass inlays. Another is the funerary mask of Tutankhamen (JE 60672, shown in Tiradritti, 1999: 235), made of solid gold with decorations in carnelian, lapis lazuli, turquoise and glass. The mask was discovered in the innermost layer of his complex coffin. The mask shows the King wearing the *nemes* headdress and the false beard made of gold framework with blue glass inlays. Multi-coloured glass inlays were also used on the chest part of the mask to form a broad collar. This usage of glass clearly demonstrates how highly it was valued by Egyptians.

In addition, glass had sufficient intrinsic value to be a gift suitable for the highest nobility and was also a valuable commodity for trade (Nicholson 1993). In fact, glass was sent between Egyptian and Mesopotamian kings and was mentioned repeatedly in the Amarna Letters (EA14, 25, 148, 235, 314, 323,

327 and 331); for translations see Moran (1992). For example, in the letter EA14, glass is not only mentioned to be imported into Egypt but also is mentioned among gifts sent by Amenhotep IV / Akhenaten (1352-1336 BC), the Egyptian king, to Burnaburiash, the king of Karaduniash (Babylon) (Moran 1992). However, it is not clear from the letters whether the glass was exchanged in the forms of glass ingots and/or glass objects. More textual evidence comes from the reliefs in the temple of Amen-Re at Karnak (modern Luxor), built by Tuthmosis III. The reliefs show that some Mesopotamian glass was given to the temple as tribute for Tuthmosis' victories in the Levant, see Figure 2.1 (below) for the relief (Sherratt & Sherratt 1991: 386, Fig. 2; Shortland 2001). The Karnak reliefs/texts list glass among the gifts sent by the king of Ashshur (Assyria), the king of Sangar (Babylon), and the Hittites. For example, reliefs in the Jubilee Hall in Karnak list gifts sent by the king of Sangar to Tuthmosis III that are 0.73 kg of "true lapis lazuli" and 2.2 kg of dark-blue glass, usually translated as "man-made lapis lazuli" (Nolte 1968: 8). One of the reliefs at Karnak records ten registers of gifts from the Levant to Amen-Re in thanksgiving for Tuthmosis' victories. In the reliefs of this kind, the objects are generally listed strictly in order of value and occasionally the text(s) come with both pictures of the objects and written labels, as in this case (Shortland, in press). According to priority, objects in the top five registers are marked as follows; gold, two registers of objects of silver, one of "semi-precious stone", and two registers with objects of copper (Shortland 2001: 213). Within the objects of "semi-precious stone", there are illustrations of five baskets containing round or irregular lumps. The first three baskets contain blue lumps and the remaining two baskets contain blue-green lumps (Shortland 2001: 213). The text associated with the illustrations notes as

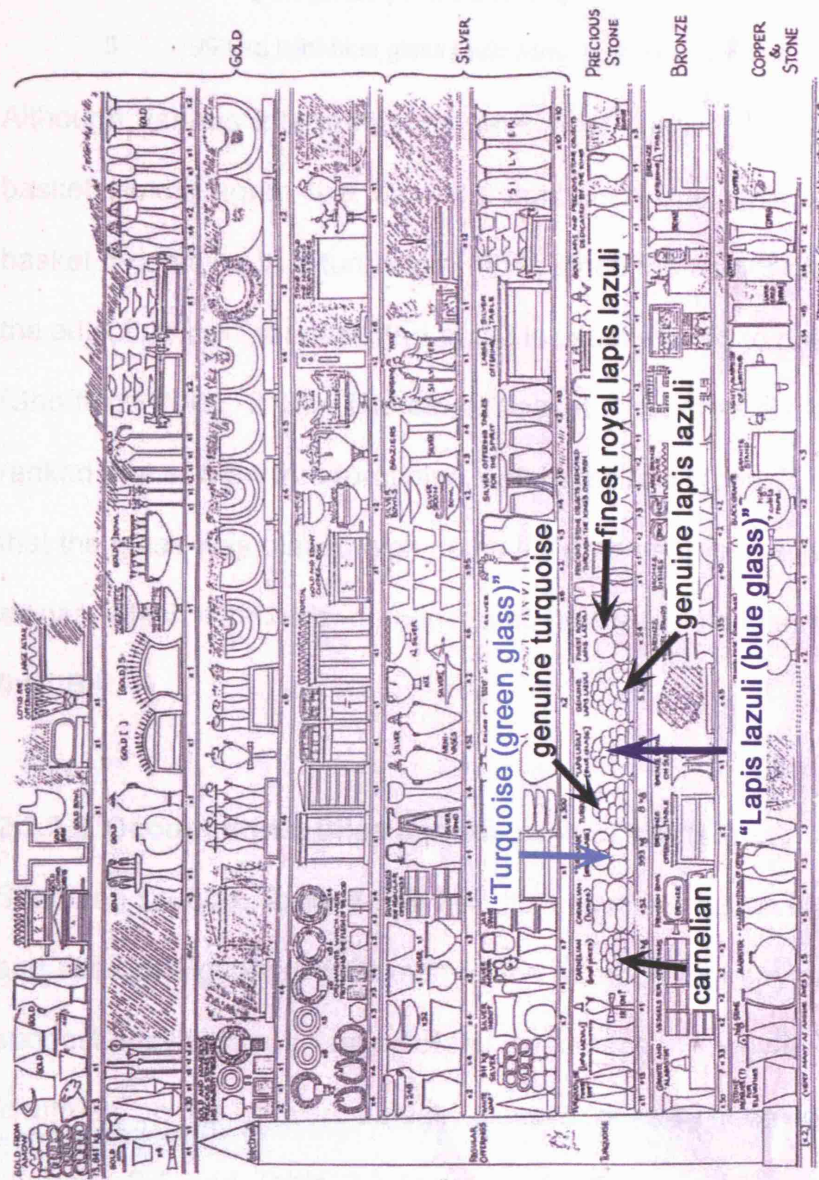


Figure 2.1: A limestone relief from the Amen-Re temple at Karnak depicting glass among semi-precious stones (Sherratt & Sherratt 1991: 386, Fig. 2)

follows:

1. 24 lumps of dark-blue glass (*transliteration of the original text: ḥsbḏ Men-ḥpr-R^c ḥrtt 24*)
2. 51.8 kg lapis lazuli (*ḥsbḏ m³ dbn 569*)
3. >54 kg, <90 kg dark-blue glass (*ḥsbḏ Men-ḥpr-R^c dbn 600...*)
4. 8.5 kg turquoise (*mfkt dbn 93 kt 2*)
5. 993 kg light-blue glass (*mfkt Men-ḥpr-R^c dbn 10913.8*)

Although various interpretations have been applied to this depiction of five baskets, most agree that basket 2 contained true lapis lazuli (*ḥsbḏ m³*) and basket 4 contains true turquoise (*mfkt*), since the use of phrase “*ḥsbḏ*” without the adjective “*m³*” for baskets 1 and 3 is usually taken to mean dark-blue glass (Shortland 2001: 213). Therefore, basket 3 contains dark-blue glass that is ranked higher than true turquoise, semi-precious stone. Once again, the fact that the glass was placed high in the list at the same level with semi-precious stones, which it imitates, demonstrates how valuable this material was during the LBA.

2.2.3.2. Occupational titles and the rank of craftsmen

Shortland (2000b: Table 7-3 & 7-4) lists several historically recorded names and titles of Egyptian craftsmen in the vitreous industry which may lead to suggest possible organisation of the workshops. However, it is not clear if the ‘craftmen’ on the list were actually glass-workers. These lists are shown here as Table 2.1 and Table 2.2 (below). According to Shortland (2000b), “*irw*” could mean maker or worker, and “*ḥsbḏ*” means “blue stone” referring to lapis lazuli and/or to blue glass and by some scholars to faience, depending on the context. However, this latter interpretation is less likely since there is another term, *thnt*, often used to describe faience. In addition, by judging from the fact

that the usage of the phrase “*hsbd*” and the glass industry both started to develop during the New Kingdom whereas lapis lazuli had been worked in Egypt since Predynastic times, it is fair to judge that the phrase “*irw hsbd*” used in the tables refers to either (blue) glass-maker or (blue) glass-worker rather than to lapis lazuli worker. The remaining section of the title, such as “*imy-r*” and “*hry*”, describes the rank of the craftsman and it is often placed before “*irw hsbd*” suggesting there were at least three occupational ranks in the following order: overseer (“*imy-r*”), chief (“*hry*”), and the ordinary “*irw hsbd*”. Besides, the phrase describing where or for whom the craftsman worked is often placed after “*irw hsbd*”. For example, the phrases “*n nb tʿwy*” and “*n Jmn*” refer to the King or court worker and the temple of Amun, respectively, suggesting glass workshops being placed within the nearby palace and temple (see below). Having official titles/names and ranks for the craftsmen involved in Egyptian vitreous industry demonstrates how well the industry was recognised and organised. However, the knowledge of ancient Egyptian language is so vague that a full linguistic interpretation is pending. Therefore, the phrases of titles and ranks of workers mentioned in these tables only apply within the vitreous industry and it is difficult to infer anything about their wider social rank from this interpretation.

Table 2.1: Shortland’s (2000b: Table 7-3) list of several historically recorded names and titles of craftsmen at Amarna.

Table 7-3 : Titles of craftsmen at Amarna.

	title in translation	house/tomb	references
“Overseer”			
Hatay ²	Overseer of works	T34.1	Frankfort and Pendlebury (1933)
“Chief craftsman”			
Thutmose ¹	Chief of works, the sculptor	P47.1-3	Borchardt and Ricke (1980)
Iuty ³	Chief sculptor	Tomb of Huya	Davies (1906)
Maanakhtuef ¹	Chief of builders	M47.3	Borchardt and Ricke (1980)

¹ Borchardt and Ricke (1980), ² Frankfort and Pendlebury (1933), ³ Davies (1906)

Table 2.2: Shortland's (2000b: Table 7-4) list of several historically recorded names and titles of Egyptian faience makers.

Table 7-4 : Titles of faience makers.

	title	period	type of object
"Overseer of faience makers"			
Debehenni ¹	<i>imy-r ḥnsw</i>	13th Dynasty, King Hor	coffin inscription
Oennou ²	<i>imy-r irw ḥsbḏ</i>	19th Dynasty	papyrus
"Chief faience maker"			
Hesay ³	<i>ḥry irw ḥsbḏ n nb tswy</i>	New Kingdom	funerary stela
Plahmose ⁴	<i>ḥry irw ḥsbḏ n nb tswy</i>	New Kingdom	papyrus
"Faience maker"			
Rekhamun ⁵	<i>irw ḥsbḏ n Jmn</i>	19th Dynasty, Ramesses II	faience funerary stela

¹ Bourrain (1996), ² Papyrus Vatican 64, Bellon (1987), ³ Cairo JE25641, Gaballa (1979).

⁴ Papyrus Krakow MNK IX-75211-4, Luft (1977), ⁵ National Museum of Scotland A.1956.153, Friedman (1998)

2.2.3.3. Controlled and centralised operation

Most of the published LBA glass findings tend to come from either palace complex or temple sites (see next section 2.3.). It is possible that some of the glass workshops were under direct court control. Therefore, expeditions to obtain alum, a source of precious and important cobalt colorant to imitate lapis lazuli, would presumably have been controlled by the court (Nicholson & Henderson 2000). In fact, scientific research on LBA Egyptian cobalt-blue glasses highly suggests that an alum-based cobalt colorant with the same chemical composition was used to make those glasses (see section 2.7. for more details). This might suggest that only the royal workshops had access to precious cobalt, although further work is needed (Nicholson 1993).

2.2.3.4. Religion

Henderson (1991) and Oppenheim (Oppenheim *et al.* 1970) argue that glass recipes were kept strictly secret as for the ritual significance in the glass-making process. The group of cuneiform texts ("Glass texts", see

section 2.1.) is so far the only existing evidence that contained prescriptions for making coloured glasses and highly suggest that the ritual formed an important part of the manufacturing process (Henderson 1991). Cuneiform texts were generally kept in private or royal libraries. The glass texts were kept in the library of king Assurbanipal (Ninevah) when found (Oppenheim *et al.* 1970), again suggesting the court involvement in glass industry mentioned above. According to the texts, a favourable month for a propitious day was chosen to set up glass-making kiln(s) and then Kubu-images were placed not to allow any stranger/outsider around the kiln(s). Moreover, on the day when all the raw materials were to be fired, a sheep sacrifice was placed in front of the Kubu-image (Oppenheim *et al.* 1970). However, Oppenheim (Oppenheim *et al.* 1970) claims that these instructions were formulated by scribes who had never produced glasses, and they were later copied by other scribes who were even more removed from the actual chemical processes, which may indicate that the texts do not reflect actual glass-making practice. It can be argued that the emphasis on ritual and magic aspects reflects a world more familiar to the scribes than the actual technical operations, which therefore receive less attention or are copied with less control over correct procedures.

Putting all four reasons mentioned above together, it is clear that glass was once considered equal to precious stones, its production required specialized skills and the processes may have been kept secret and thus it is possible that only selected craftsmen were able to produce glass. Furthermore, glass may have been produced under some restrictions of royal control and glassmakers that knew special tricks could be held in high social esteem (Nicholson 1993). We will probably never know whether the earliest glassmakers in Egypt were

prisoners of war (brought back by Thutmosis III from a series of Asiatic conquests, see above) or whether they followed voluntarily with the Egyptian armies from Mesopotamia to serve new patrons. There is also the question of imported artisans or locally trained craftsmen under foreign supervision (Freed 1981). For example, Moorey (2001: 4) and Shortland (2001: 1-2) quote the passage in the Old Testament (Hebrew Bible, 2 *Chronicles* 2: 14-16), a description of Hiram of Tyre, the Phoenician craftsman sent by the City's ruler, of the same name, to assist King Solomon with the construction and furnishing of the Temple in Jerusalem in the tenth century BC: "he is an experienced worker in gold and silver, copper and iron, stone and wood, as well as in purple, violet and crimson yarn, and fine linen; he is also a trained engraver who will be able to work with your own skilled craftsmen and those my lord David your father, to any design submitted to him". Although the time at which this was written is later than the LBA, Moorey (2001) argues that the biblical passage epitomizes the exchange of skilled craftsmen amongst the royal courts of the Near East and Egypt during the LBA as a matter of diplomacy in times of peace, as well as the versatility of the best of them. Although glass was not specifically mentioned in the passage, it is possible that the imported or imprisoned Mesopotamian craftsmen, who had the know-how of producing glass, used raw materials available locally in Egypt (such as Egyptian cobalt). The only certain thing is that the highly skilled craftsmen must have had some conception of its practical and social function as this determines the choice of raw materials and techniques to be used.

Lastly, while the various social and ritual aspects of LBA glass-making as

summarized above give some interesting insight into its role in New Kingdom Egypt, there is nothing in those aspects that would explain the tight chemical composition of most LBA glasses. Therefore, further research based on practicality of glass-making (i.e. chemical processes and the inherent parameters of glass-forming reactions) needs to be conducted.

2.3. Known glass workshops in Egypt and Mesopotamia, dating to the Late Bronze Age (about 1500-1000 BC)

2.3.1. **Mesopotamia: site evidence in chronological order** (see Figure 2.2 (Moorey 1994: 7), for the locations).

Figure 2.2 (right):
Map of Mesopotamia showing
glass-related LBA archaeological
sites (Moorey 1994: 3).



Early primitive glass

Since Beck's (1934) fundamental review of the earlier evidence, 28 examples dating from 4000 – 1600 BC, there has been remarkably little progress in the study of the earliest glass reported from both Near East (Mesopotamia) and Egypt, however, the database is increasing gradually (Moorey 1994). Beck (1934) highlighted the difficulty of identifying the early evidence since only 17 of the 28 examples turned out to be glass, 13 glass beads and 4 glass objects. Some of the remaining 11 turned out to be different materials (e.g. faience, rock crystal), some modern and

some unconfirmed if they were even glass.

The earliest, safely dated, glass bead yet reported from the Near East is probably that from Tell al-Judaiah in the Amuq Plain of Syria, where it was attributed to phase G (Amuq Phase G), dated to the earlier third millennium BC (Early Bronze Age, 3100-2900 BC) (Braidwood & Braidwood 1960, cited in Moorey 1994: 190). It is a well-preserved short, oblate spherical bead, pale yellow-green in colour.

Other early examples of glass beads have been found from several other Near Eastern archaeological sites, such as Nuzi, Nippur, and so on (Moorey 1994). A cylinder seal, still on its copper pin, was found from Nuzi and assigned by Boehmer (1965, cited in Moorey 1994: 190) to the later Akkadian period (2150–2100 BC). Two glass beads were found at Nippur directly associated with tablets of the Akkadian period (2300-2100 BC) in what was taken to be a secure context (Gibson 1990). There are more glass beads findings, but the attributions of many of these are still controversial. In fact, the supposed early “glass” beads from Tell Farah (Shuruppak) with a date before 3000 BC were later determined to be made from rock crystal that looks like glass (Beck 1934). However, safely stratified examples such as, a bead from a grave at Tel Dan (Israel), and several beads in composite necklaces from another grave at Dinkha Tepe (Iran), indicate the occasional use of glass, much of it probably formed as a by-product from faience and metal-working (Meyers 1997).

Early proper glass

Early glass fragments have been reported from excavations in levels of the

Akkadian period at Tell Brak, including a piece of what appears to be a raw glass, cylindrical in shape (2.4 x 2.2 cm as extant), bluish-white in colour. This was found from a well-stratified Akkadian context in Area FS (locus FS 1826, Level 5) (Oates & Oates 1991a). Of equal significance is a pale blue-green chipped glass rod from the main level of the Northern Palace at Tell Asmar in the fill of Room E16: 16 (Delougaz *et al.* 1967). The rod is about 1.1 cm in diameter, 3.3 cm in length, and 6.3 g in weight (Beck 1934). Frankfort (Frankfort 1934, cited in Moorey 1994: 191) himself dated it to the Gutí period (2334-2112 BC) or “more probably to that of the dynasty of Akkad (2371-2100 BC)”. Beck (1934) published two technical comments on this find and reported that the glass is very pure; it has a few small bubbles but is surprisingly free from striae or inclusions of quartz fragments or dirt.

Perhaps the most famous and the earliest piece of raw glass from Mesopotamia is the small lump (Figure 2.3, BM 115474, 3.8 x 3.4 x 3.3 cm), excavated at Abu Shahrein (Eridu) by Hall in 1919, now in the British Museum (Barag 1985). Hall found a lump of opaque blue vitreous paste, which he recognized as a true glass, in the rubbish but not on the floor of the house, immediately beneath the Bur-Sin [(from the reign of) Amar-Sin] pavement (Hall 1930). It was dated to the dynasty of Akkad or the early Ur III period (2100-1950 BC) (Barag 1970, 1985, Moorey 1994). Beck (1934) concluded that the specimen was intended for carving or to have been re-melted and moulded to the desired shape, or even, it may have been ground up for glazing. In any case, it was probably a manufacturer’s piece of material and the probability is that it was to be processed in the immediate neighbourhood of where it was found. The glass is pure ultramarine in colour and has been

analysed by Garner (1956), who identified the colorant as arsenical cobalt ores, either *cobaltite* or *erythrite* (0.15 % of cobalt with 0.49 % of copper; although the amount of copper is much higher, it has a much weaker colouring property and would hardly affect the colour) and attributed to an Iranian source by its chemical composition. Another famous glass piece is a fragment of a translucent glass rod, in pale blue-green colour, found at Eshnuna. According to the excavation report, the context of this rod fragment can safely be dated to the late Sargonic period (in the 23rd century BC) (Barag 1970).

Figure 2.3: A small lump of glass from Eridu (Abu Shahrein, BM 115474). Image courtesy of the British Museum.

There is nothing in the material record before the Kassite / Mitanni period (1550-1275 BC) in Mesopotamia to indicate anything other than an infrequent and irregular production of glass, which showed little, if any, appreciation of the material's special properties. The isolated finds dated before the middle of the second millennium BC have sometimes been explained as no more than compositions intended as faience, which turned completely vitreous when over-fired, whilst the glass tubes, the lump of glass from Eridu (above), and a pale blue-green chipped glass rod from Tell Asmar (above) have been seen as by-products of glaze manufacture. Thus, they would hardly substantiate the existence of a distinct, controlled production of glass, as might be assumed from some readings of contemporary texts, such as cuneiform texts (668-627 BC) (Moorey 1994).

It is towards the end of the Middle Bronze Age, some time in the 16th century BC, when the first evidence appears in Western Asia to suggest major technological changes in the manufacture of glass, involving the appearance of new production techniques (e.g. fusing, maverling, trailing), the use of special tools, and the inclusion of different metal oxides to provide a range of colours not commonly used, if used at all, in earlier times (Moorey 1994). Examples of moulded blue glass, star-shaped disk pendants, nude-female plaques and spacer-beads found at Nuzi (below) have been identified as oriental imports (Barag 1970). A survey of finds made in excavations on Mesopotamian sites suggests that core-formed glass vessels – the earliest technique for making glass vessels – appear during the 15th century or already in the second half of the 16th century BC. The earliest example of a core-formed vessel was found in level VI (second half of the 16th century BC) at Alalakh, north Syria, during Sir Leonard Woolley's excavation.

The best indication of glass production in Mesopotamia comes from some palace/temple complexes and graves such as the "Mitannian Palace" (built in the early 13th century and made of mud-bricks) at Tell Brak (Oates 1982, Oates & Oates 1991a, Oates *et al.* 1997), Kar-Tukulti-Ninurta, Nuzi (Stratum II), and Assur (Barag 1970), in contexts around the 14th to 13th centuries BC (see below for more details on each sites). Large and small ingots of glass as well as fragments of glass were recovered from these three sites suggesting that each site was an industrial area. However, the findings do little more than indicate the wide currency of glass in ingot form.

Most of the glass findings at Nuzi, equally well known for the associated faience and glazed terracotta, were concentrated in the destruction level of Stratum II (Starr 1939), which Stein (1989) dates 1425 BC, at the earliest, and 1375 BC, at the latest. Starr (1939) also found glass beads in grave 5A (attributed to Stratum IV) and Stratum II. Several pins with large glass beads were found from Stratum IV. One was a plain, straight copper pin of even diameter, 14 cm long, with a large glass bead, 15 mm in diameter, serving as a bead, in much sounder condition than the majority of the Nuzi glass beads found in Stratum II. Since such “bead-heads” (Moorey 1994: 190) on pins had earlier been made of lapis-lazuli, the association of the earliest glass, as the earliest faience, with the reproduction of semi-precious stones is evident. Unfortunately, Starr (1939) did not illustrate this find. Vandiver (1982, 1983) has begun to examine the technology used at the Nuzi industry and her work has already shown the usage of various techniques and their sophistication (the range of chemical compositions was relatively limited, though the number of colorants was large). Vandiver (1983) concluded that a well-developed glass technology was present in the Near East at Nuzi well before the destruction of the site at about 1400 BC. The glass finds at Assur (below), another site with an active faience industry at the same time, are mostly dated to the 13th century and again display considerable technical variety. In addition, an important collection of glass was found at Tell Rimah, once again, where a faience and frit industry was active (Moorey 1994). These sites suggest that the Mesopotamian glass-making was carried out alongside faience production, as was believed for Egyptian glass-making, and this will be discussed later. Moreover, the texts from the royal palace at Dur Kurigalzu (Gurney 1953) indicated that the workmen at Dur Kurigalzu were being issued with a variety of

precious materials for palace decorations, suggesting Mesopotamian royal and temple workshops are likely to have included glass-makers, as at Nuzi, Assur, Tell Rimah, and Brak.

In addition, debris from a possible glass workshop, including traces of kilns, was found by Mallowan (1954, 1966), at Nimrud (possibly Neo-Assyrian period, 1000-612 BC), later to be called “Burnt Palace” (Moorey 1994: 194), see below for more details.

2.3.1.1. Nuzi

Nuzi (modern Yorgan Tepe) is located near Arapkha (modern Kirkuk) in northeast Iraq about 130 miles north of Baghdad. Nuzi was excavated between 1925 and 1931 by a joint expedition of the American School of Oriental Research in Baghdad and Harvard University (Vandiver 1982, 1983).

The mound of Nuzi was occupied intermittently from around 5000 BC to about 400 BC. Only the Stratum II level (mid-14th century BC) was extensively excavated. However, enough was recovered from the earlier and later levels to permit an outline of the site's occupational history.

A collection of glass, along with ceramic and metal artefacts was removed chiefly from Stratum II, a date nearly contemporary with Amarna (Egypt). No cemeteries were excavated at Nuzi II, so all the glass came from the town, where it was concentrated in “Temple A” and in “The Palace”, with further finds in the “House of Shilwi-Teshub” (Room 44, Court 15 & Court 7) and in “Room C22”. Fragments of segmental glass ingots (lumps) and glass vessels were

found at the site along with numerous glass beads (Barag 1970: 136).

Three lumps of dark blue, partly translucent glass (4.7 x 5.5 cm; 5.0 x 2.6 cm; 5.2 x 2.9 cm) and seven small chips, which all seem to have belonged to one ingot, were found at the site named as "C 62" (Barag 1970: 140-1, Moorey 1994: 196). However, unfortunately, this site was not marked in the excavation plans so the exact location of C 62 is unknown. Moreover, no industrial debris or raw glass has been published from this site (Barag 1970, Moorey 1994).

One of the more remarkable discoveries about the glass found at the site is that a significant number of beads (especially unpierced ones, more than 16,000), in various styles, had been part of the architectural decoration, though no wall was preserved to a great enough height to show exactly how. This discovery was substantiated by the discovery of an unbaked brick in which had been set a row of elliptical and circular eye-beads (Starr 1939).

Many fragments of core-formed glass vessels (whose shapes include goblets, piriform bottles, shallow bowls and stands) and moulded glass objects were found from the site (Barag 1970).

Objects of moulded blue glass, various star-shaped disk pendants (their length varies between 5–6 cm; thickness 1 cm), nude-female plaques (extant length 3.4 cm; width 2.1 cm; thickness 1.9 cm) and spacer-beads found from Temple A in archaeological contexts of the 16th or 15th centuries BC, have been identified as oriental imports (Barag 1970).

Barag (1970) has provided the basic typological study of the vessels, but much remains to be done on the other glass objects. Apart from a shallow monochrome glass bowl, the reported Nuzi glass vessels were polychrome, with blue as the primary base colour (the greenish appearance of some fragments was caused by deterioration of the blue); thread decoration was in white, yellow, orange (amber), and pale blue; rim twists were of blue and white or brown and white (Barag 1970, Moorey 1994).

2.3.1.2. Tell al Rimah

Tell al Rimah is located 184 km northwest of Nuzi (Vandiver 1982), 13 km south of Tell Afar, in the Sinjar area (Oates 1965). The site was occupied from the time of Samsi-Adad I of Assyria (1852-1819 BC) to Middle Assyrian with a terminal date of 1250 BC (Oates 1966). Excavation works had started as early as 1964 and continued till 1971, mainly by David and Joan Oates.

Various core-formed vessels were found both in complete form and in fragments from Phase II of the temple found on Area A and also from the ruins of the palace on Area C and from a grave in Area D (Barag 1970). The date of Phase II of the temple is suggested contemporary with Nuzi II (Oates 1965, 1966) and suggested as around 1650-1350 BC (Carter 1965).

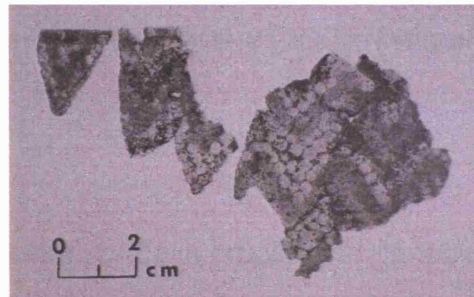
Glass objects from the temple (Area A) include various glass beads, a miniature glass plaque pendant with a nude female figure in high relief (which may be identified with the goddess Ishtar), and a miniature glass mask pendant, probably representing Humbaba. Fragments of glass vessels built up of sections of red, green and white glass rods arranged in a zigzag mosaic

pattern were also found from the temple (Oates 1965). Furthermore, Carter (1965) reported more detailed glass findings from Area A, including a round-faced female mask with fluted hair or cap (Figure 2.4, several naked goddess plaques, all possibly moulded in blue glass, and a tiny hedgehog amulet and the female mask which seems to be entirely original to the site. More fragments of glass mosaic in black, white, green, and yellow, were also found from Area A (Carter 1965, Stern & Schlick-Nolte 1994: 46, Fig. 39, shown here as Figure 2.5).



Figure 2.4 (left): Moulded blue glass female mask from Tell al Rimah (Carter 1965: 55, Fig. 8).

Figure 2.5 (right): Fragments of glass mosaic from Tell al Rimah (Stern & Schlick-Nolte 1994: 46, Fig. 39).



The grave (Area D) findings include a broken glass cylinder seal and a glass bottle in a poor preservation condition, approximately contemporary with Phase II of the temple. The glass bottle was 17.5 cm in height, with a cylindrical neck on an ovoid body and an almost pointed base. It was coloured with an inlaid pattern of yellow, white and orange festoons on a light blue background. Fragments of glass vessels (above) have been found from the temple, from the same Phase II, but this glass bottle was the only completed form among glass vessel findings from the site (Oates 1967).

Unfortunately, Oates did not report on any further details of glass object findings from the palace (Area C). However, Carter (1965) who was in charge

of the excavation of Area C has reported a few glass beads and several fragments of sand-core vessels, in a mid-2nd millennium context, a greenish-white glaze covered in a brown herring-bone design, found from Area C (Level 2).

2.3.1.3. Kar-Tukulti-Ninurta (Tulul al-'Aqar)

The Assuritu Temple was built at Kar-Tukulti-Ninurta, on the east bank of the Tigris, opposite to Assur (below) by Tukulti-Ninurta I (1243-1207 BC) (Oates 1965). Kar-Tukulti-Ninurta was excavated between 1986 and 1989 by the Free University of Berlin. The site is believed to be occupied during the Middle Assyrian (1600-1000 BC) and Neo-Assyrian periods (1000-612BC) (Dittmann 1990).

Fragments of a segmental glass ingot, cast in a concave crucible, in dark blue glass, in context of the 14th to 13th century BC, were found at the site, as well as at Nuzi (above) (Moorey 1994). Unfortunately, there is no further information on this site.

2.3.1.4. Assur: mostly dated to 13th century BC

It is located near the present day city of Qalat Sharqat, on the western bank of the Tigris. Excavation of Asuur began in 1847 by a British archaeologist, Austen Layard, and in 1904 by Dr. W. Andrae, for the Deutsche Orientgesellschaft. Clay tablets were found from these excavations that show the record and the layout of the site. These tablets enabled archaeologists to identify the remains of the site (The Minnesota State University EMuseum website, www.mnsu.edu/emuseum/archaeology/sites/middle_east/assur.html,

visited in 2006, Anonymous). Since then Assur had been excavated by various archaeologists.

Core-formed glass vessels and shards of them were mostly found in graves (notably in tombs 37 and 133), which held glass contemporary with that from Nuzi (Stratum II), and in various parts of the Ishtar Temple built by Tukulti-Ninurta I as well as the Assuritsu Temple, above (Barag 1970).

Two piriform bottles with knob bases were found from Tomb 133. Another piriform bottle found from Tomb 37 has analogies in style among the find from Nuzi II (Barag 1970). Galling reported two glass-pins found in the tomb and dated them to about 1000 BC (Barag 1970). In spite of the poor preservation of colours, it is certain that blue, brown and white were used as base colours. Colours used for decoration are blue, turquoise, yellow, white and red-brown (Barag 1970).

Unfortunately, the finding on the glass has not yet been fully published (Barag 1970, Moorey 1994). Cullet (i.e. raw glass or fragments of broken glass from a cooled melt, or scrap/waste glass intended for recycling) was also found, reinforcing the case for local production (Barag 1970, Moorey 1994). The finding certainly indicates a local glass-working industry of all kinds (mosaic and core-formed vessels, inlays, and probably plaques) as well as complementary production of artefacts in glassy (sintered quartz) materials.

2.3.1.5. Tell Brak

Tell Brak is one of the most important multi-period archaeological sites in

Upper Mesopotamia (Matthews 2003), and lies in north-eastern Syria, close to the modern borders of Iraq and Turkey. The archaeological findings at Brak represent continuous occupation from at least as early as 6000 BC until 1200 BC. During the 23rd century BC the city served as a provincial centre of administration under the Akkadian kings of southern Mesopotamia. Brak maintained its importance in the 2nd millennium, when it was a major city of the Mitanni Empire (Oates & Oates 1991b). The Mitanni Palace was populated by a largely Hurrian-speaking population and was one of the major powers in the Late Bronze Age world (Oates *et al.* 1997).

Brak was initially excavated by Max Mallowan in 1937 and 1938, sponsored by the British School of Archaeology in Iraq, with the findings in the contexts of the fourth millennium BC and the late third millennium BC (Mallowan 1947). However, most of the glass findings from the site come from the later excavation by David and Joan Oates (Oates & Oates 1994), started in 1976.

By far the majority of the glass objects from Brak came from Level 2 of Area HH (latest occupation in the Mitanni Palace and Temple; early in the 13th century BC), which produced over 73 registered items excluding the beads. Significant numbers of glass beads were also found in all levels of Area HH (dates between 1800-1200 BC; Oates & Oates 1994), but the vast majority came from the destruction level of the Palace and Temple (Level 2) (McDonald 1997). However, unfortunately, most of the materials found at Brak were severely damaged in the Middle Assyrian sack, and only small shards - many of the over 100 fragments were only a few mm across; the largest measured 3.0 x 1.5 cm - have survived (Oates *et al.* 1997).

The most remarkable glass vessel found at Brak is certainly unique: a small bowl or cup found smashed into such tiny pieces that the shape could not be reconstructed. The vessel was decorated with pattern of rosettes and triangles, each consisting of groups of tiny yellow and white glass globules less than 1 mm in diameter (Oates *et al.* 1997: 84, Figure 122, shown here as Figure 2.6). It seems that these tiny balls of glass were set into the surface of the vessel, and probably protruded very slightly. The end product closely resembles contemporary granulated patterns on gold jewellery, an example of which was also found at the site in the Mitanni shrine (Oates *et al.* 1997). In addition, six fragments of glass vessels were recovered from levels pre-dating the final Mitanni occupation. It must be emphasized, of course, that the total amount of material from these levels is relatively small, and no statistical

Figure 2.6: Unique glass vessel fragments from Tell Brak decorated with pattern of rosettes and triangles (Oates *et al.* 1997: 84, Figure 122).



comparison can be made with Level 2. Of these earlier pieces, the most interesting piece is another unusual mosaic glass vessel, comprised of four fragments found from a Trench D, Level 5 (early Palace occupation; around 1550 BC) house, perhaps the earliest mosaic glass yet found. The body is composed of alternating rhomboids of dark blue and white opaque glass, set at an angle of the vessel surface (Oates *et al.* 1997).

Among the most interesting objects in our context, for my research, are light and dark blue glass ingots and ingot fragments and many miscellaneous

pieces of cullet, strongly suggesting that glass objects were being manufactured at the site by the 14th century (from analysis of a small glass ingot from HH 427, dating around early 14th century, by Henderson, cited in Oates *et al.* 1997: 95-98). A total of 13 ingot fragments were found from the Mitanni palace at the site. However, whether the raw glass was made at the site is still a question that we cannot answer on existing evidence (Oates *et al.* 1997). The best-preserved ingot (consisting of two fragments; one of 2/3 of the complete ingot and another accounting for the rest) came from the doorway between Room 5 and Room 7, a possible store for the adjacent possible glass workshop, where another similar ingot fragment was found. The ingots' shapes are similar to those of slightly concaved crucibles, having the relatively complete fragments measuring 15 cm in diameter. Most of the ingots and cullet were of light blue opaque glass (copper colorant), though some dark blue opaque examples were also recovered, presumably coloured with cobalt. Further ingot-like pieces, also from Room 5, have been identified by Brill as possible glass "waste", the crucible-shaped lumps consisting of layers of two colours, a "dark amber glass coating a flat piece of white opaque glass" (Oates *et al.* 1997: 86). Fragments found in corridor 6 seem also to have been waste glass, again consisting of layers of dark amber and white opaque colours (Oates *et al.* 1997).

2.3.1.6. Dur Kurigalzu (Aqar Quf): the Kassite capital

Dur Kurigalzu is located north of Sippar, west of Bagdad, part of the site called Tell el-Abyad. The site was excavated from 1942 through 1945 by Taha Baqir and Seton Lloyd in a joint excavation by the Iraqi Directorate-General of Antiquities and the British School of Archaeology in Iraq (Baqir 1946). Glass

fragments along with glass plaques and mosaics were recovered from the royal palaces of the Kassite dynasty, in contexts dated mainly from the mid-13th to the mid-12th centuries BC (Baqir 1946, Moorey 1994). However, a fragment of mosaic glass was dated to the mid-14th century (below).

A plaque (6 mm thick), unfortunately fragmentary, where the pattern is formed by opaque, greenish-black glass squeezed in its soft state to form a background for shaped inlays of some whitish paste, came from the debris of the staircase in chamber no. 48 at the second level from the top (Baqir 1946).

A fragment of mosaic glass – made of small round glass rods, in various colour, stuck together by some black material – was found in a context of the final phase of Level IV (dates around the mid-14th century BC) (Barag 1970). Other mosaic glass fragments, a ring base of a bowl, were found in the ramp-chamber no. 76. It consists of closely packed multicolour glass/paste with both faces smooth (Baqir 1946: Plate XX, Fig. 5, shown here as Figure 2.7, Barag 1970).

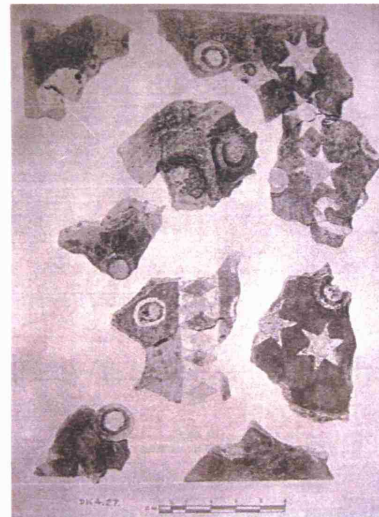


Figure 2.7: Mosaic glass fragments from Dur Kurigalzu (Baqir 1946: Plate XX, Fig. 15).

According to the texts found from the site, there were two palaces which once existed at the site: called “the Palace of the Stag” and “the Palace of the Mountain Sheep” (Gurney 1953: 21). Gold, silver, and precious stones were used to decorate various parts of these palaces (Gurney 1953). In addition, one of the texts from Level II (room 4), dated to the third year of King

Kashtiliash(u) IV (1232–1225 BC), refers to glass given to artisans for decoration in the Palace of the Stag (Gurney 1953). The text also refers to the lapis lazuli coloured glass inlays destined for a statue to be made for the palace (Oppenheim *et al.* 1970). The published information on these glass finds is limited to the more general types (more information is given about the tablets themselves or the architectural plan of the site) and little or no reference is made to shards of vessels.

2.3.1.7. Nimrud, The Burnt Palace: Neo Assyrian period

Nimrud is situated north of Assur, between the rivers Tigris and Greater Zab (eastside of Tigris). Glass-related finds come from the excavation of the site that started in 1949 by Mallowan (1954), on behalf of the British School of Archaeology in Iraq and the British Museum. The occupation of the site runs from the beginning of the 9th until the end of the 7th century BC. Most areas of the palace were assumed to be set up during the reign of Sargon, between 722-705 BC (Mallowan 1954).

Although the Nimrud glass finds do not fit in my research's timeframe (1500–1000 BC), this site will be included here since at least some of the Nimrud glass is determined as plant-ash-based by Brill's (1999a) analysis. This matter will be discussed further in the later chapter (see Chapter 7, section 7.1).

The finds consist of five vessels, about 150 vessel fragments and a multitude of inlays used almost exclusively for ivories. Most of the glass varies in colour from a practically clear to a pale green or pale yellow material. The most

renowned glass object from Nimrud is the alabastron, of thick greenish glass, with the name of Sargon II and two lions engraved on its shoulder (now in the British Museum; BM 90952). Most vessels were initially assumed to be made by the lost-wax process, followed by grinding and polishing (Mallowan 1954, Saldern 1966).

In addition, two disks of opaque blue glass had probably been formed in rough moulds, whilst at least two pieces of blue cullet, or unshaped fused glass, to be used as raw material were also recovered. These findings suggest that glass-working facilities have existed at Nimrud (Saldern 1966).

In fact, Mallowan (1954, 1966, Saldern 1966) found traces of kilns and a glass-worker's kit, including one specimen of sealing wax red glass, probably from a crucible, on the south side of room 47 of the Burnt Palace. Two separate kilns both with long, narrow, rectangular flues/drafts were found at the south end of room 47. These kilns were in such poor condition that unfortunately it was only possible to trace a part of their outline.

The average thickness of the glass fragments from Nimrud fluctuates around 0.2 to 0.3 cm, with some going up to 0.6 cm. However, it is important to note that about one sixth of the fragments are of extremely thin glass, with some shards being "paper-thin", raising the question of the technique of manufacture. The technique of manufacture must have been more refined than is generally assumed. Although once it was believed that Assyrians had used the lost-wax process (Mallowan 1954, Saldern 1966), more modern literature suggest the process is unlikely to have been used (because of the viscous nature of the

glass). The extreme thinness of the fragments lead one to believe that they were familiar with other methods not explicable in the light of our present knowledge (Saldern 1966). This lead even to a revision of the date of the findings, because the date and the sophistication of the technologies do not seem to match.

However, the revised British Museum Carbon-14 dating of the charcoal offers a most probable range of 860-740 BC (59 % probability) and 440-380 BC (16 % probability) (Freestone: personal communication with Moorey, 1988). Therefore, Mallowan's (1954) original dating of this working debris to the Neo-Assyrian period, rather than later, seems to be correct.

Overall, without direct evidence for places of manufacture, the sources of glass found in Mesopotamia remain controversial. That is, although it has been believed that glass was initially invented in Mesopotamia, all the glass related evidence found are glass-working remains, rather than those of glass-making. This lack of evidence for glass-making may be due to the fact that finds of earlier Mesopotamian glasses were almost always ill-preserved and friable because of soil conditions of the region being less favourable than those of Egypt (Harden 1956, Moorey 1994). In addition, very early glasses invented in Mesopotamia may be decomposed completely due to their poor quality. Moreover, it is not surprising that ill-preserved glasses from Mesopotamia took some time to get attention, compared to well-preserved polychrome glass objects from Egypt. Therefore, archaeological finds of second-millennium BC glass in Mesopotamia are still bewilderingly sporadic and random leaving Egypt with more significant archaeological evidence

relating to glass.

2.3.2. Egypt: site evidence in chronological order (see Figure 2.8 for site locations, except for Uluburun).

As noted glass is much more widely identified in LBA Egypt and this section therefore concentrate on the seven archaeological sites in Egypt with postulated glass workshops dating to the New Kingdom; these are Malkata, el-Amarna, Kom Medinet Ghurab, el-Mansha, el-Lisht, Tell el-Yahudiya and Qantir (Kozloff *et al.* 1992, Rehren & Pusch 2000, 2005), as well as the evidence of trade in glass ingots is the Uluburun shipwreck (Bass *et al.* 1989, Pulak 1998, 2006).

Figure 2.8 (right):
Map of Egypt showing glass-related LBA archaeological sites.



2.3.2.1. Malkata (west bank at Thebes)

The large-scale glass artefact production during the reign of Amenhotep III (1390-1352 BC) is first suggested by finds from Malkata, a palace complex at Thebes (the capital of ancient Egypt). Malkata seems to have been the original source of the conglomerate glass bowls known from numerous fragments at the site, and which are the precursors of the true mosaic glass (Nicholson & Henderson 2000). However, most of the excavated material from Malkata has subsequently been lost and only a few glass rods can now be

found (Mass *et al.* 2002: 68, Figure 1, shown here as Figure 2.9). Only preliminary reports were ever published (Tytus 1903, Newberry 1920, Shortland 2000b). In one of the preliminary reports, Newberry (1920) claims that small crucibles containing dark blue glass and a quantity of different coloured glass rods were found when he was digging at the site with R. de P. Tytus (1903) in 1901. H.E. Winlock and A. Lansing also found various glass manufacturing elements such as glass slag, fragments of crucibles, dozens of glass rods and a few test droplets of glass during their excavation in 1917-18, on behalf of the Egyptian Expedition of the Metropolitan Museum (Keller 1983).

Figure 2.9 (right): Glass rods, canes and vessel fragments from Malkata (Mass *et al.* 2002: 68, Figure 1).



2.3.2.2. Ghurab

Ghurab is located in the Faiyum. It is likely to have been a glass artefact production centre similar to Malkata, operating from the reign of Amenhotep III (1390–1352 BC) to that of Ramesses II (1279–1213 BC; Tatton-Brown *et al.* 1991). A perfect bottle of the time of Amenhotep III, another bottle that can be dated to the reign of Tutankhamen (1336-1327 BC), and a bowl and several bottles of the reign of Ramesses II, have been found at Ghurab (Newberry 1920). Petrie (1891) reports that he found three glass vessels that dated to Tutankhamen by assumption from the delicate little blue pendants found with it and claimed that the skill of this glass-making is surprising. A great number of beads, now in the glass department of the British Museum, were also found by Petrie. However, considering the fact that the dating merely depends on

assumption and that evidence was found (by Petrie) suggesting foreigners' residence on the site, further research is necessary to make precise comment on the glass vessels found from the site.

In addition, Nicholson and Henderson (2000) claim Petrie recovered a collection of moulds from the site suggesting the Ghurab factory produced mainly glass amulets, whose manufacture required much less technical sophistication than vessel production since old scraps of glass could be melted down and manipulated very easily into moulds. However, these findings were from domestic contexts, and the moulds may have been possibly used for making faience rather than for making glass artefacts. Although a small square enclosure that may have been a trace of 'glass factories and lime kilns' were mentioned by Brunton and Engelbach (1927:3), the only glass from this site is objects, not workshop debris. Therefore the presence of a glass workshop is rather unproven, leaving uncertain the exact nature of activities carried out here.

2.3.2.3. Tell el-Amarna

The site of Amarna is in Middle Egypt, roughly half way between the ancient capitals of Memphis (Cairo) and Thebes (Luxor). Amarna was the new capital city of the so-called heretic Pharaoh Akhenaten (Amenhotep IV; 1352–1336 BC) after Thebes.

Many glass rods and fragments of glass (Petrie called these "manufacturing wastes", which are now in the Petrie Museum, such as UC22909-20, see Figure 2.10) along with crucible-like jars were found from the site, highly

suggesting the existence of glass-working workshop(s) at the site. The total amount of glass fragments is given as 750 pieces, found from the rubbish mounds, 38 from the palace, and none from elsewhere (Petrie 1894). The colours are very varied, and in sorting over hundreds of the glass rod finds, it seemed as if no two pots of glass had been quite alike; so that a few pieces of each batch might be found, but no exact match beyond those. There are purple, opaque violet, light and dark blue, green, yellow, opaque red, brown, black, and white. Most of these colours occur in both transparent and opaque, especially the blues and greens that were unlimited in variety of tones (Petrie 1894). One of the glass rods (now in the Petrie Museum, UC 22923, 38 mm in length) shows marks from rolling on a textured surface such as wood or stone. Some of the rods end in blobs of glass which show the marks of pincers indicating how they were removed from the batch (Nicholson 1993).

Figure 2.10:
Various glass rods
and fragments from
Amarna (now in the
Petrie Museum, UC
22909-20).

Petrie discovered shallow saucer-shaped pans (10 inches across, 3 inches deep, and 1/4 inches in thickness) that he believed were for fritting raw materials; these, he suggested, stood on inverted cylindrical vessels (100 mm in height), also found from the site, whose external sides and bases show clear runs of glass. Measurements of these cylindrical vessels found from the site are summarized and published by Nicholson and co-workers (Nicholson *et al.* 1997). However, Petrie's interpretation was questioned by Turner (1954a) and

later by Nicholson (1993) (see later section 4 for more details). In addition, a total of 13 coarse-textured lumps of blue frits (11 cobalt-blue and 2 copper-blue) were found not only in association with shallow pans but also adhering to the cylindrical vessels and other ceramic fragments (Nicholson 1995b). Both blue frits and 19 blue glass fragments found from Amarna were analysed by Tite and Shortland (Shortland & Tite 2000, Tite & Shortland 2003) and will be discussed in more detail in section 2.5.

At Site O.45.I of Amarna (Nicholson 1995a), there are four furnace structures in all; one is certainly a pottery kiln, another may be for pottery or faience/pigment-making while the two largest are believed by Nicholson to be suitable for glass-working or possibly glass-making (Jackson *et al.* 1998). However, there is no claim from him that these furnaces were indeed used for glass-working, as mentioned earlier (personal communication with Nicholson in 2003). Therefore, we still do not know whether the Amarna workshops were mainly for glass-making or glass-working (see later section 2.5., below).

2.3.2.4. Uluburun

The Uluburun shipwreck site is located off the south-western Turkish coast, about 8.5 km southeast of Kas. Uluburun (written Ulu Burun in earlier publications) is the southernmost point of the coast. The wreck lay only 60–70 m off Uluburun's east face and about 400 m from the tip of the "Grand Cape" (Pulak 1998). Excavations by the Institute of Nautical Archaeology (INA), at Uluburun (Bass 1986, 1987, Bass *et al.* 1989) have yielded significant amounts of fragments of circular glass ingots of different colours (Pulak 1998). The ship carried products of at least seven cultures – Mycenaean Greek,

Canaanite, Cypriot, Egyptian, Kassite, Assyrian, and Nubian. Timber from the wreck has recently been dated to 1316 BC, by dendrochronology (Kuniholm *et al.* 1996, Pulak 1998). This dating was strongly supported by the recent unpublished radiocarbon dating of short-lived materials (e.g. olive pits, terebinth resin, twigs etc.) that suggest a 95 % probable sinking date of the ship of 1343-1314 BC (Pulak 2006). The latter dating seems to be more likely considering the similarity in the base glass compositions of Amarna glass and Uluburun glass ingots (see Chapter 7, below for details).

Initially, some opaque, cobalt blue glass ingots (diameter; about 6 inches = 15 cm, average thickness; two and a half inches = 6 cm, average weight; about 2.3 kg, see Figure 2.11) were found from a sandy gully, at the depth of about 160 feet (about 45 m) (Bass 1987, Pulak 2006). At present, from subsequent surveys and further excavation of the same area, approximately 170 ingots in total are known and that the predominant colour is cobalt-blue. However, there are ingots of copper-blue (21 ingots, in turquoise blue), orange-yellow, and purple (2 ingots) (Nicholson *et al.* 1997, Pulak 1998, 2006). The thickness and diameters of glass ingots seems to vary with the colour. The cobalt-blue glass ingots are generally larger (in their diameter) and thicker than those of the copper-blue glass ingots. The cobalt-blue glass ingots have an upper surface diameter exceeding 13 cm (up to 15.5 cm) with the thickness above 5.0 cm,

while copper-blue glass ingots usually have an diameter of less than 13 cm with typically 3.5 cm in thickness (Nicholson *et al.* 1997).

Figure 2.11 (left): Opaque blue glass ingots from Uluburun shipwreck.

The analyses of the glass ingots by Brill have shown that they are chemically identical to blue glass in Egyptian bottles and Mycenaean medallions dating from the same period as the shipwreck, leaving the direction of the ship unknown (Bass 1987). However, Uluburun glass ingots clearly show concentric ridges and grooves on their undersides which are matched in negative by similar structures on the interior of the cylindrical vessels from Amarna (Nicholson & Henderson 2000, Nicholson *et al.* 1997, Pulak 2006). Nicholson and his co-workers (1997) made a comparison between the ingot moulds from Amarna and those of Qantir (see below) and highly suggested that the Uluburun ingots might even have come from Amarna. On present evidence, ingot moulds (the cylindrical vessels) from Qantir seem to be several centimetres smaller (in diameter) and taller (in height) than those of most Uluburun ingots (Nicholson *et al.* 1997).

Moreover, a recent work by Shortland (2000b) shows one of the two purple glass ingots analyzed from Uluburun is chemically similar to a purple glass fragment found from Amarna.

2.3.2.5. Qantir

Qantir-Piramesses is located 100 km northeast of Cairo, in the eastern Nile Delta. The site was an industrial and military complex, dating to around the time of Ramesses II (1279-1213 BC) and was excavated first by Hamza (1930) and later by the German mission from the Peabody-Museum, Hildesheim (directed by Dr. Edgar Pusch). The excavations at sites Q I and Q IV at Qantir-Piramesses so far indicate a dominating specialisation on copper-related compounds such as bronze, red glass, Egyptian blue and

faience, while pottery production obviously took place outside the excavated area (Rehren *et al.* 1998, 2001)(see section 2.6., for more details).

The most prominent glass object from the site is the complete ingot of red glass (JdE 64296, 10 cm high, 13 cm in diameter), now in the Egyptian Museum in Luxor, found by M. Hamza in 1928. The circumference is circular for the most part, but with a spout-like protrusion at one side. The sidewalls of the ingot are almost cylindrical, with a slightly decreasing diameter downwards. The base part shows a curved profile. The ingot is now discoloured and the colour of the side and base surfaces is of a pale to dark green, while the top surface is distinctly blackened to a depth of about 1 mm. On close examination, an original dark red colour is visible underneath the green surface. Together with this glass ingot, a much smaller lump of blue glass (JdE 64679) was also found by Hamza. However, unfortunately, no spatial or stratigraphic details of the exact origin of these finds are known (Rehren & Pusch 2000).

So far, 1100 ceramic fragments related to glass-making have been found from the site representing 250 to 300 individual vessels (90 % of these are crucibles and the rest being jars) possibly used in glass-making and -colouring (Rehren & Pusch 2005). With finds of glass-colouring crucible fragments that have significant amounts of glass adhering to their inside, representing only a fraction of the entire material once present, the production of glass ingots proved to be a large scale operation (Rehren 1997, Rehren & Pusch 1997, Rehren *et al.* 2001). Most of the glass adhering inside is cuprite-red in colour, typical for the site, except for five fragments (e.g. FZN 88/0386b) that have

cobalt-blue and one fragment that has purple glass attached (Rehren & Pusch 2000, 2005).

Similar to the cylindrical vessels found in Amarna, crucibles found from Qantir have been noted to match the ingot of (now discoloured) red glass also found from the site, mentioned above (Rehren & Pusch 2000, 2005).

It is significant that this site has so far not yielded any of the coloured glass rods and glass vessel fragments that are typical of the glass-working sites elsewhere in Egypt. This indicates that the evidence excavated at Qantir is not primarily linked to glass-working, but more to the production of glass ingots which were probably brought to workshops elsewhere. Moreover, a most recent find by Rehren and Pusch (2005), a substantially preserved crucible filled with heavily corroded raw glass (object 00/0344, inventory number 3108), highly supports the idea that the glass was made from raw materials at this site (see more details in section 2.6., below).

2.3.2.6. el-Lisht

El-Lisht is located about 50 km south of Cairo. The site was a pyramid complex from as early as the 12th Dynasty, Amenemhat I (1850-1800 BC). The glass-related finds from Lisht are distributed throughout nearly all areas and date probably to the 20th Dynasty (1190-1075 BC; Ramesside times) or broadly to the second half of the New Kingdom (Keller 1983).

The evidence includes factory material, such as fritting pans for possibly

melting the glass, and manufacturing debris, such as rods, glass slags, and cullets in addition to fragments of crucibles, conical clay stands for holding the crucibles during fusing, pieces of slag from the ovens, samples of the pigments added to the glass, little discs with well-worn edges (possible glass ingots?), pieces of unfinished faience ware and nearly 200 shards of glass vessels (Keller 1983, Kozloff *et al.* 1992, Tour Egypt website, www.touregypt.net/historicalessays/lifeinEgypt12.htm, visited in 2003, Anonymous). There are traces on the inside of some vessels of a clay-and-sand core, revealing the possible glass-working or vessel making technology used (cited from Tour Egypt website, same as above). The rods and cullets are physically poorer in appearance yet are chemically identical to Malkata and el-Amarna glass (informal communication between Brill and Kozloff, cited in Kozloff *et al.* 1992: 378). The site also contains glass vessel fragments of two distinct levels of quality – one of the highest quality similar to that found at Malkata and Amarna; the other, poorer both in design and fabric (Kozloff *et al.* 1992). These materials suggest that the factory at el-Lisht was a poor workshop where 18th Dynasty glass was salvaged from the tombs of nearby Saqqara and recycled to make new vessels (Mass *et al.* 2002). Keller (1983) also commented upon the poor quality of the glass found at Lisht, noting that a) the body fabric of the Lisht vessels contains more and larger bubbles and is generally less well fused than that of Malkata, and b) that the colours are not as clear as at Malkata.

In addition, Cooney (1970, cited in Kozloff *et al.* 1992: 379) also mentioned the site may be one of the illegal operation of pilgrim flasks trade of unknown origin (most likely not in Egypt). However, this report by Cooney is likely to be biased

because of his great admiration for Malkata and Amarna glass (Kozloff *et al.* 1992).

2.3.2.7. Mansha(h)

Manshah is located on the east bank of the Nile, near Abydos, a short distance south from Menshiyeh. Newberry (1920) claims that this site used to be another glass factory of about the same date as el-Lisht (the 20th Dynasty).

Its status as a factory has been questioned by Keller (1983), who assumes that Newberry had simply been told of the site as a source of artefacts looted elsewhere. However, Newberry in fact seems to have visited the site with local Arabs (in 1911) and found some glass slag and a few rods of coloured glass even though the site had been plundered. Newberry was told by the locals that several vases from the site had been sold during the previous season to Luxor dealers. Therefore, unfortunately it is not possible to further speculate either on the nature of this site or on its connections – if any – with other crafts.

Tatton-Brown and Andrews (1991) and Newberry suggest that this site may have taken over from Malkata as the main supply centre for Thebes since the rims of standard Mansha-type vessels have a stylistic holdover from the Malkata site (Kozloff *et al.* 1992, Nicholson & Henderson 2000). However, there is no further information on the actual Mansha-type vessels attributed to the site.

2.3.2.8. Tell el-Yahudiya

Tell el-Yahudiya is located 20 km to the north of Cairo, in the eastern delta, Lower Egypt. The site was a temple complex and/or a possible palace of

Ramesses III (1184-1153 BC). In fact, remains of a colossal statue of Ramesses II have been found and a temple of Ramesses III which was decorated by faience tiles.

From evidence now in the British Museum, Cooney (1970, cited in Kozloff *et al.* 1992: 379) postulated that there was a factory from the Ramesside period at Tell el-Yahudiya, but he felt that its sole purpose was making temple decorations (Kozloff *et al.* 1992) rather than glass vessels. An opaque red glass fragment, possibly a corner element of an ingot, was also collected from this site (Cooney 1981).

However, Cooney's investigations of the glass fragments found by Davies and Carter from the tombs of Ramesses II, Merenptah, and Ramesses IV, suggested that the glass findings at Tell el-Yahudiya are solely heirlooms from the 18th Dynasty (Kozloff *et al.* 1992). In fact, Cooney (1970, cited in Kozloff *et al.* 1992: 379) noted the decoration on one of the fragments as "not of the usual dragged variety but suggesting the heavy, large-scale pattern found on certain vessels of Amenhotep II".

Therefore, it seems more likely that the site used to be for producing faience rather than glass and the site had been neither a glass-working nor –making workshop.

2.4. Short summary/interpretation of evidence given in section 2.3.

The glass-related findings from LBA Mesopotamian and Egyptian sites are summarised in Table 2.3 and Table 2.4 (below). Putting together all that has

been discussed above, there are two fundamental issues when trying to understand glass production practice in Egypt during the New Kingdom. Firstly, there are very few excavations focusing on the glass workshops themselves, such as furnace structure remains. Almost all glass evidence listed above is for consumption in temples and graves, in the shape of vessels and vessel fragments. Birgit Schlick-Nolte (Nolte 1968) has demonstrated that these vessels can be attributed on stylistic grounds to different workshops and traditions; this, however, does not answer the question of the location of these workshops. More importantly, these workshops styles are likely to reflect the artistic working of the glass, and say nothing about the source of the glass-making itself (Rehren *et al.* 2001).

The vast majority of the published evidence for glass-working, both in Mesopotamia and Egypt, relates either to the manufacturing of glass objects (glass rods and such like), or to the long-distance trade in coloured glass ingots (primarily from Uluburun, and the various ingot fragments discovered at other sites; such as Nuzi, Kar-Tukulti-Ninurta, Tell Brak, Qantir, and possibly el-Lisht).

Two sites, however, Amarna and Qantir, have yielded more substantial evidence of glass workshops; these two will be looked at in more detail below to identify their potential to inform us about glass-making practice during the New Kingdom.

In summary, the number of possible glass-working sites or artistic workshops far outweighed the number of possible primary glass-making factories,

suggesting that glass production probably was a centralised practice (see Table 2.3 and Table 2.4).

Secondly, the other major difficulty relates to interpreting the material remains of these workshops correctly (Rehren *et al.* 2001). The published information concerning individual sites is often inconclusive and not supported by full documentation or analyses of finds; furthermore, much of the relevant material is no longer available for study. The evidence also highly suggests that the glass industry operated alongside other high-temperature industries, in

Table 2.3: Summary of LBA Mesopotamian sites with glass finds.

Name	Date (approx)	Finds	Interpretation	Reference
Nuzi	mid 14 th century BC	<ul style="list-style-type: none"> - glass ingot fragments (3) - glass vessel fragments (many) - glass beads (many) 	Consumer goods Artistic workshop	Barag 1970 Vandiver 1983
Tell al Rimah	1650–1350 BC	<ul style="list-style-type: none"> - glass beads - glass plaques (few) - glass vessel fragments (many) - glass mask pendant (few) - glass amulets (few) - a glass bottle 	Artistic workshop	Oates 1965, 1966, 1967 Carter 1965
Kar-Tukulti-Ninurta	14 th to 13 th century BC	<ul style="list-style-type: none"> - glass ingot fragment 	Unknown (not enough info)	Oates 1965 Moorey 1994
Assur	13 th century BC	<ul style="list-style-type: none"> - glass vessels (both complete and fragmentary) - glass piriform bottles (2) - glass-pins (2) - glass cullets 	Artistic workshop	Barag 1970
Tell Brak	early 13 th century BC	<ul style="list-style-type: none"> - glass beads (many) - glass vessel fragments (>100) - a glass bowl/cup - glass ingots (13) - glass cullets (many) - glass 'waste' ('slag') 	(Primary workshop?) Artistic workshop	Oates & Oates 1991a, 1991b, 1994 Oates <i>et al.</i> 1997 McDonald 1997
Dur Kurigalzu (Aqar Quf)	mid 13 th to mid 12 th century BC	<ul style="list-style-type: none"> - fragments of glass plaques & mosaics - text (mentions glass being given for decoration) 	Consumer goods Artistic workshop	Baqir 1946 Gurney 1953 Barag 1970
Nimrud (The Burnt Palace)	early 9 th to 7 th century BC	<ul style="list-style-type: none"> - glass vessels (5) - glass vessel fragments (150) - glass inlays - glass disks (few) - glass cullets (few) - glass 'slag' - kilns (2) - 'glass-worker's kit' 	(Primary workshop?) Artistic workshop	Mallowan 1954 Saldern 1966

Table 2.4: Summary of LBA Egyptian sites with glass finds (including Uluburun).

Name	Date (approx)	Finds	Interpretation	Reference
Malkata	14 th century BC	The excavated materials have been lost. Therefore, finds listed below are only referred to published work. - glass rods (dozens) - crucibles (both complete and fragmentary) - glass 'slag'	Primary workshop Artistic workshop	Tytus 1903 Newberry 1920 Keller 1983
Ghurab	14 th to 13 th century BC	- glass bottles (few) and a bowl - glass vessels (few) and pendants - moulds (possibly for faience) - glass factory remains?	Artistic workshop Consumer goods	Petrie 1891 Newberry 1920 Brunton & Engelbach 1927.
Tell el-Amarna	14 th century BC	- glass rods (> 100) - glass fragments (> 750) - crucibles and pans - glass 'waste' - furnace/kiln (?)	Primary workshop Artistic workshop	Petrie 1894 Turner 1954a Nicholson 1993, 1995, Nicholson <i>et al.</i> 1997 Jackson <i>et al.</i> 1998
Uluburun	14 th to 13 th century BC	- glass ingots (100-200) - glass fragments (> 175)	Trade	Bass 1986, 1987, Bass <i>et al.</i> 1989, Kuniholm <i>et al.</i> 1996, Nicholson <i>et al.</i> 1997, Nicholson & Henderson 2000 Pulak 1998, 2006
Qantir	13 th century BC	- glass ingot (1) - red glass plates - crucible fragments (about 1100, representing >250 crucibles) - glass 'slag'	Primary workshop	Hamza 1930 Rehren 1997, Rehren & Pusch 2000, 2005, Rehren <i>et al.</i> 2001
el-Lisht	12 th century BC	- glass vessel fragments (over 200) - glass rods (several) - glass cullets and glass 'slag' - glass pilgrim flasks - glass little disks (few) - pans and crucible fragments	Artistic workshop Consumer goods	Keller 1983 Cooney 1970
Mansha(h)	12 th century BC	- glass "slag" - glass rods (few)	Unknown (not enough info)	Newberry 1920 Keller 1983
Tell el -Yahudiya	12 th century BC	- glass ingot fragments - the other glass finds turned out to be heirlooms, not original	Consumer goods	Cooney 1970, 1981

particular faience making and Egyptian blue production, leading to the concept of a more generalised vitreous materials industry (Rehren *et al.* 1998, Shortland 2000b). Moreover, it may be possible that glass-making was operated alongside other high-temperature industries (e.g. Qantir bronze industry) while glass-working operated alongside other less industrial artefact production.

Here, one will have to deal with scrambled evidence; an intensive mixture of raw, intermediate, and waste materials including a variety of objects and the remains of often non-diagnostic features. Therefore, there is major uncertainty when attributing some materials from excavated workshops to glass-making or glass-working.

Even less evidence is available from Mesopotamia since no site yet excavated suggests glass production workshops securely dated to the period of interest here (Moorey 1994); therefore, it is at present not possible to provide a definitive archaeological answer to the most fundamental question; whether glass was made independently from an early period in Egypt or whether all early Egyptian glass was imported from either Mesopotamia or Asia. However, two sites have a better record of documentation and study, namely Tell el-Amarna and Qantir-Piramesses, and these will be looked at more closely in the following section.

2.5. Work based on Amarna

The best indication so far for both glass-making and -working comes from Sir Flinders Petrie's excavations at Amarna, where he found a great deal of glass

waste. As mentioned earlier, Petrie discovered many fragments of manufacturing waste, including shallow saucer-shaped pans from the site, and he and Turner (1954a) are the first to discuss glass production in Egypt.

Without evidence of actual glass workshop remains, Petrie (1894) claimed that the sites of 3 or 4 possible glass factory areas and 2 large glazing works were discovered and that the waste was full of glass fragments which show the technology employed. These waste dumps, still visible during much later excavation in 1993 (Nicholson 1995a), are on the eastern edge of the city, and they are still providing much technological evidence.

Petrie distinguished three kinds of vessel used in melting the glass, a shallow, saucer-shaped pan (10 inches in diameter, 3 inches deep, and 1/4 inches in thickness), in which he thought the raw materials were fritted; cylindrical pots (7 inches in diameter and 5 inches deep, externally); and crucibles (about 2 to 3 inches in depth and diameter), in which the possible fritted material was melted to produce glass (Turner 1954a). In an account dating from 1909, Petrie's third type of vessel was listed as "about 4 or 5 inches across" (Nicholson 1995a: 12). He suggested that the fritting-pans were supported in the furnace by a group of the inverted cylindrical jars/crucibles since the jars had glaze run down the side from the close end to the open end, as seen in Figure 2.12, above (Nicholson & Henderson 2000: 199, Figure 8.1). In addition, he also suggested that the glass was made in two stages, first as a frit, which was subsequently melted to form glass (Turner 1954a). This interpretation was first corrected by Turner (1954a) and later by Nicholson (Nicholson 1993, Nicholson *et al.* 1997), who argued that the cylindrical

vessels were more likely to be moulds for ingot production, and demonstrated that they matched very well the almost contemporary glass ingots from the Uluburun shipwreck.

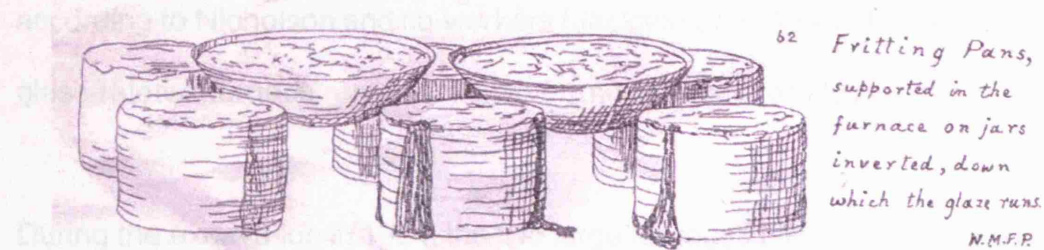


Figure 2.12: Petrie's reconstruction of the glass-making process. Pans are supported on the inverted cylindrical vessels now suggested by Nicholson to be crucibles/ingot moulds (Nicholson & Henderson 2000: 199; Figure 8.1).

Turner (1954a) analysed some of the crucible-like fragments and proposed that because both of the composition of the ceramic and by direct experiment the upper limit of glass-melting temperatures was 1100 °C. The practical limit employed may well have been lower since the presence of alkalis, mixed in the raw materials, acted as a flux. Turner's work in the mid-1950s was clearly groundbreaking and provided the foundation for several decades of subsequent glass research in archaeology. It established for the first time reliable data about glass composition and melting practices through time and space; however, it did not shed much light on the actual glass-making practice at Amarna.

Understanding of the glass-making process in Egypt has been hindered by a lack of identification and study of any actual glass furnaces dating to Pharaonic times. While Petrie's excavations at Amarna yielded much material that had been, or was thought to have been, associated with furnaces, no

actual structures were found, either for glass- or faience-firing. More recently, however, kilns and furnaces were excavated at the northern edge of the site O.45.I of Amarna during excavations in 1993 and 1994. These findings are, according to Nicholson and co-workers (Jackson *et al.* 1998), the only possibly glass-related furnace remains known from New Kingdom Egypt.

During the excavation in 1994, the two large furnaces discovered in 1993 were fully uncovered and proved to be roughly circular. The furnaces are unlike any pottery kiln known from Amarna, and they have complicated brickwork patterns (bricks were approximately 32 cm x 16 cm x 8 cm) that may have been intended to improve insulation, to cope with thermal stresses, and to absorb heat gradually. The subterranean fire pit provides further insulation. The furnaces had an internal diameter of approximately 1.5 m, larger than expected (Jackson *et al.* 1998).

The size of the furnace found at the site has led to suggestions that they could not have been used for glass-making, since it would be impossible to achieve the desired temperatures, particularly without some forced-draft system (Nicholson 1996). In order to test this view, Nicholson and co-workers (Jackson *et al.* 1998) reconstructed a full-size replica of the best-preserved furnace and fired two crucibles; one contained a glass batch (raw materials) and another held green cullet obtained from a broken soda-glass beer bottle. The glass batch comprised plant ash (ash from seaweed, collected from the beach at Penarth in South Wales), and sand collected from Amarna. No lime was added to the mixture (lime will exist in the mixture as the natural calcareous component of the sand and by any calcium oxide in the ash).

Although the results have demonstrated that the furnaces were not too large to achieve the necessary temperatures (temperatures in excess of 1100 °C were readily achieved without draft system) and that they would have been capable of making glass, Nicholson clearly said, at a recent conference (London, December 2003), that there is no claim from him that these furnaces were indeed used for glass-making. Importantly, however, it has been shown by Nicholson and co-workers that the fritting stage may not have been necessary for the glass-making process (Jackson *et al.* 1998).

The distribution of some possible faience workshops at Amarna has recently been published by Boyce (1995) since Petrie (1894: 25) failed to record all the locations where glass and glazing works were found except for one, O.45.I. Boyce (1989, 1995, Nicholson 1995a) argues that, since glass was added to the body material of some faience to make it harder and to extend its colour range during the New Kingdom, glass and faience working could have been considered as the same craft and could have shared the same workshops (and craftsmen). Boyce (1989) then noted that both large and small faience workshops could have co-existed with glass workshops in a manner analogous to that of pottery manufacture at the site. Boyce (1995) also discussed that the making of raw glass may have remained centralised at sites such as O.45.I, which then supplied glass in the form of glass rod or cane to the lesser, smaller workshops. However, Boyce's work on workshops distribution is specifically focused on faience workshops and not particularly on glass workshops. In addition, Shortland's (2000a) later research covering a much wider area of Amarna refined the distribution of faience-making workshops from high concentrations of moulds throughout the site and

suggested that these faience workshops are involved in the manufacture of other vitreous materials, especially glass. He also suggests that these workshops could be the ones originally found by Petrie but which then got lost from the record.

There was a possibility that the furnaces excavated might be related to some process other than glass-making, such as metallurgy. However, examination of the vitrified material (which is known locally as *khorfush*: fused clay) by Shortland and Tite showed that it is the remains of vitrified mud brick and of the “sacrificial render” that lined the furnaces, rather than slag derived from metallurgical processes (unpublished work, cited in Jackson *et al.* 1998: 14). Moreover, since this material, *khorfush*, had been produced at a greater temperature than required for pottery making, and due to numerous finds of glass from the site, glass production seemed to have been the most likely interpretation of these furnaces (Jackson *et al.* 1998).

Shortland and Tite (2000) also analysed eight fragments of blue glass, from the industrial debris surrounding O.45.I furnaces, by scanning electron microscopy (SEM) wavelength dispersive spectrometry (WDS). The results were supplemented by analysis of 11 further fragments of similar glass debris and fragmentary finished objects excavated by earlier expeditions of the site, now held in the British Museum, and the Petrie Museum. Their interpretation is that there are two different types of blue-coloured glass from the site; one made from Egyptian raw materials and another being imported from Mesopotamia (Shortland & Tite 2000). This findings matches Keller’s (Keller 1983, Mass *et al.* 2002) earlier interpretation of the existence of two types of

blue-coloured glasses. According to this, blue-coloured glass found from Amarna and Malkata was using cobalt while the blue-coloured glass found from Lisht was coloured with copper.

It is believed that the cobalt-blue glass was produced in Egypt since cobalt colorants are rare in Mesopotamian glass throughout the second millennium BC (Shortland *et al.* 2006). Therefore, it would be very interesting to know whether the cobalt-blue glasses were an Egyptian speciality and whether the glasses of other colours were produced either in Mesopotamia only and imported into Egypt, or produced in Egypt and Mesopotamia at the same time, since this would suggest a motivation for trade and interaction between different glass workshops during LBA. Tite and Shortland (Shortland 2004, Shortland & Tite 2000, Shortland *et al.* 2006, Tite & Shortland 2003) have directed several analytical studies to identify differing compositions relating to possibly distinct glass-making centres. Analytical studies on these blue-coloured glasses will be discussed in more detail in section 2.7. and in Chapter 7, below.

2.6. Work based on Qantir

The excavations at sites Q I, Q IV, and Q V at Qantir-Piramesses so far indicate a dominating specialisation of copper-related compounds such as bronze, red glass, Egyptian blue and faience, while pottery production obviously took place outside the excavated area. Red glass is particularly difficult to produce, but appears to have been a speciality of the site (Rehren & Pusch 2000). Since the red colorant used was copper oxide with minor amounts of tin oxide, and therefore clearly derived from bronze metal, the

glass workshop was probably associated with the enormous bronze foundry discovered at the site (Rehren *et al.* 1998).

Copper, however, was by no means a scarce or specialised commodity in Egypt. The specialisation therefore which is apparent at Piramesses seems to be governed not mainly by the availability of a specific raw material, but by bringing together of technical skills with which this metal was mastered over a range of chemical compositions, redox conditions (Cu^+) and temperatures. It appears reasonable to assume that the foundation of this industrial complex was a planned act, following the political decision to establish Piramesses as a major settlement in the eastern Delta. No technical or environmental reason for this location of the copper-centred workshops comes to mind, given the ubiquitous availability of metallic copper or bronze artefacts within the New Kingdom, and since none of the raw materials employed (quartz and plant ash) originate from anywhere near the site. One can only assume that skilled labourers were sent to Piramesses early on in the city's history, in a planned act to serve the needs of the rapidly growing capital in highly decorative architectural items (Rehren *et al.* 2001).

In addition, it is important to note that there have been none of the drawn rods or canes of coloured glass nor any significant numbers of fragments of glass vessels found in the excavations at Qantir so far, unlike the large quantity of such materials at Tell el-Amarna and Lisht, the other major New Kingdom glass-working sites in Egypt (Rehren & Pusch 2000). Hence, the glass workshops at Qantir-Piramesses seem to represent primary production rather than secondary working (Rehren 1997, Rehren & Pusch 1997, Rehren *et al.*

2001). This interpretation is central to formulate some of the working hypotheses of my research, see below.

More recent findings seem to prove local glass-making from raw materials (Rehren & Pusch 2005). These include a substantially preserved crucible (object 00/0344, inventory number 3108) filled with heavily corroded raw glass, and numerous other finds which are thought to be semi-finished glass melted during the primary production, but without fully fusing all raw materials. This will enable me to test the partial melting model (Rehren 2000a, b) using real archaeological material, based on the results of my own experimental data. Scientific analyses of these Qantir glass samples are shown in Chapter 6.

Based on the Ramesside workshops in Qantir-Piramesses discussed above, a detailed model for the organisation of LBA glass-making and -working is proposed. The basic difference is between a producer or primary workshop, producing glass from raw materials and forming it into monochrome glass ingots, and that of secondary workshops, working such ingots into objects such as vessels, inlays and beads of different colours. Coloured glass was probably produced at a number of sites, both in Mesopotamia and Egypt, in more common colours, in particular copper blue and turquoise. More rare colours, however, were probably produced only at specialised sites, dependent on specific raw material access and know how. Examples of this specialisation are the production of cobalt blue glass in Amarna and copper-red glass in Qantir. Long distance trade in glass of all colours then allowed artistic centres (= secondary workshops) to work glass of all colours available (Rehren *et al.* 2001). The possible technological steps involved in

the LBA glass industry are also suggested by Rehren and Pusch (2005) that the raw materials were fired initially at temperatures of 900 to 950 °C to produce semi-finished glass (frit). Then coloration and ingot production followed at 1000 to 1100 °C. The partial melting model should provide a method to test this assumption by analysing the semi-finished glass from Qantir, and comparing it to glass compositions from my experimental melts.

2.7. Introduction of scientific work on LBA glass

Using very different methodologies, various scientific approaches have established notable insights into ancient Egyptian glass making and have given sensible answers concerning the raw materials used and to whether the glass was made in ancient Egypt (some scientific studies are already mentioned in detail above).

Many analytical studies, such as those by Sayre (1967, Sayre & Smith 1974), Brill and Lilyquist (Brill 1999a, 1999b, Brill *et al.* 1993, Lilyquist *et al.* 1993, Oppenheim *et al.* 1970), Kaczmarczyk (1986), Shortland (2000b, 2001, 2002), Tite (Paynter & Tite 2001, Shortland & Tite 2000, Tite & Shortland 2003), and the pioneering work of Turner (1954a, 1954b, 1956a, 1956b, 1956c), focussed on identifying first compositional groups among the increasing number of glass analyses, and then to identify the raw materials used in their production and coloration. Fundamental issues were such questions as whether mineral natron or plant ash were used as the flux; and which metal oxides were used as colorants, opacifiers and decolourants. Many of these questions have now been addressed – some, such as choice of colorants have been satisfactorily answered. There appears to be a general silent assumption that already

during the earliest glass-making the final glass composition was equal to the composition of the combined raw materials, as is the case in modern glass-making. However, already Turner (1956c) pointed out that most ancient batch compositions will have contained unreactive salts, and that therefore the resulting glass composition is not necessarily equal to the batch composition. Only very recently has this been further explored by Jackson and Smedley (2004), for European wood ash-based glass. The only changes that are more widely acknowledged are those of glass compositions and colorants used over time, and even then there is hardly ever a discussion why changes may have occurred.

The archaeological and historical evidence (see above) strongly suggests that glass was made in ancient Egypt as well as in Mesopotamia. However, because of the similarity between Egyptian and Mesopotamian glass compositions, especially in the LBA (see below), there is still much uncertainty about where specific samples of glass were actually made. Some authors, e.g. Frank (1982), denied the possibility of independent Egyptian glass-making and maintained that all glass must have come from Mesopotamia. However, this subject was not widely discussed in the literature.

Without any certain archaeological evidence on glass-making, the scientific studies had to approach glass, as a material, from its technological point of view for better understanding. Some experimental studies were based on the available archaeological indications; Turner (1954a) established a possible firing temperature based on the ceramic vessels from Amarna and established the upper limit of glass-melting temperatures as 1100 °C (see section 2.5.,

above). Later, Nicholson and co-workers (Jackson *et al.* 1998) reconstructed a full-size replica of the best-preserved possible glass furnace found at Amarna and used it to melt glass, by mixing sand (collected from Amarna) and plant-ash (obtained by burning seaweed collected from Penarth, South Wales) (see section 2.5.). The experiments demonstrated that the furnaces would have been capable of making glass directly from raw materials, by reaching the firing temperature in excess of 1100 °C, and that the fritting stage might not have been necessary at all.

Other research identified an Egyptian cobalt source (above) by matching the association of the five transition metal oxides (iron, manganese, cobalt, nickel, and zinc) that characterise the Egyptian cobalt-blue glass. The cobalt-rich alums (aluminium magnesium sulphate) were deposited when ancient lakes evaporated, and it is very unlikely that another cobalt deposit could end up with a similar combination of the same five metal oxides, of the same order of magnitude (Kaczmarczyk 1986).

LBA cobalt-blue glass has a very particular chemical composition. That is, cobalt-blue glass is different from copper-blue and other contemporary glasses in that its potash content is typically less than 1 %, and its alumina content is consistently higher than in other glasses, whereas its magnesia content (typically 3-5 %) is similar to those of the other glasses. These characteristics are potentially very important to identify the raw materials used in its production. The difference between plant-ash-based and natron-based glass is the concentrations of both potash and magnesia being roughly 2 to 3 % higher in the former type (Rehren 2001). Therefore, Shortland and Tite's

(2000) early study suggested that the low potash content of cobalt-blue glass indicated the use of natron rather than plant ash as alkali source, and its magnesia content was increased from that expected for natron-based glass by the addition of Egyptian raw material, the cobaltiferous alum colorant from the Kharga and Dakhla Oasis (Kaczmarczyk 1986, Shortland *et al.* 2006). However, this interpretation was questioned by Rehren (2001) for two reasons. Firstly, because it failed to explain why the glass-making process based on mineral natron was kept restricted to the production of one colour only, while at the same time much larger quantities of glass were made using the different alkali source plant ash. Mineral natron (which consists mostly of the sodium carbonate mineral *trona*) is believed to be collected from the natural evaporitic deposit of Wadi Natrun in Egypt. Plant ashes, on the other hand, were produced by burning specific coastal or desert plants that were available both in Egypt and Mesopotamia. The Egyptians, therefore, had access to both types of alkali sources but allegedly limited natron use to only one certain colour within the same workshop site, Amarna. Secondly, Rehren (2001) questioned why, with the concentration of alumina in the alum twice that of magnesia, the relative increase of alumina in cobalt-blue glass is less than half of that of the proposed increase of magnesia, when compared to copper-blue glass. Rehren (2001) instead suggested that the reason for the unusual composition of the cobalt-blue glass was the use of plant ash with a low potash content but with a typical magnesia content. However, he could not demonstrate that such low-potash plant ash was indeed available, as no analyses of Egyptian plant ash were available.

The subsequent publications by Tite and Shortland (2003) extended their

study to include the cobalt blue frits found at Amarna along with the shallow 'fritting pans' and found that in contrast to the cobalt-blue glass, the cobalt contents of the frits correlate with both the alumina and magnesia contents that could explain the unique composition of the cobalt-blue glass compared to the other LBA glasses. They suggest the cobalt-blue glasses are more likely to be produced in two steps, in that the cobalt-rich alum colorant had been pre-treated with natron to form a cobalt-blue frit and then have been mixed together with plant ash and quartz, in contrast to the copper-blue glass that is believed to be produced in one step with plant ash being an alkali source (Tite & Shortland 2003). This interpretation would explain the presence of blue frit found with saucer-shaped pans and crucible fragments since no artefacts made from these frits have been identified from the site (Tite & Shortland 2003). However, Tite and Shortland (2003) note that it is still possible that the cobalt-blue glass was produced directly by mixing quartz, plant ash, and precipitated cobalt hydroxide colorants, as pointed out earlier by Rehren (2001). Overall, there are still considerable gaps in our understanding of the raw materials and production methods of different coloured glasses. My research will contribute to this by looking at two different aspects relevant to the question of cobalt-blue glass production. First, why is the lime content in these glasses the same as in other LBA glasses? If indeed a mineral natron had been used as flux instead of plant ash, and the high magnesia level typical for plant ash glasses is here in fact due to the added colorant, then one needs to explain where the lime content of the glass comes from. In typical LBA glasses, the lime is thought to come with the plant ash. If the lime does not come from the plant ash, does this mean that it comes from calcareous sand instead, as is typically the case for the much later Roman glass production?

However, the latter is unlikely, since the silica source for LBA glass is thought to be crushed quartz pebbles rather than sand. Secondly, is there a mechanism by which the potash content of the glass can be lower than the potash level in the raw materials? That is, can a normal plant ash still produce a glass with particularly low potash concentrations? This will be discussed in Chapter 7, Archaeological Implications.

More recently, Rehren (2000a, 2000b) has pointed out that Egyptian and Roman glass compositions, respectively, are too narrowly defined to be the result of mixing of raw materials that are so variable in composition as plant ash and / or sand. Unfortunately, there are little published compositional data for plant ashes from Egypt, but available data from Brill (1999a) for plant ashes from Western and Central Asia demonstrate their widely varying composition. Consequently, if such is the case, how can it explain the observed chemical homogeneity of LBA glasses? Rehren (2000a, 2000b, 2001, Shugar & Rehren 2002) suggested that this is mostly due to the immanent chemical and physical melting behaviour of the raw materials, resulting in the formation of eutectic melts of a tightly defined composition. This idea forms the basis for the partial melting model (PMM), which requires the presence of a crystalline phase in excess of the amount required for melting at any given temperature. These chemical factors could control the exchange of certain oxides or elements between the glass melt and another phase, namely crystal residue or salt melt, respectively. This will be discussed more in detail in Chapter 3, and tested experimentally (Chapters 4 and 5).

Chapter 3: Scientific Approach

3.1. Background

The previous chapter has given a brief overview of the archaeological, textual and scientific evidence for glass-working and glass-making in LBA Egypt and Mesopotamia. It has been shown that direct archaeological evidence for glass-making at present is restricted to the site of Qantir-Piramesses, with some further evidence for glass-making in Amarna. All other sites concern mostly the production of artefacts from existing glass or the exchange of glass ingots. Textual evidence is limited to the Mesopotamian cuneiform tablets that are well studied and interpreted (Oppenheim *et al.* 1970), but of limited practical value for the research questions at hand. Scientific work has so far concentrated on identifying the most likely raw materials and working temperatures (Turner 1954a, 1956c, Nicholson & Henderson 2000). None of this, however, would explain the observed chemical homogeneity of LBA glass. This can only be explained by an interpretation of the kinetics of the relevant chemical glass-forming reactions, and experimentally reconstructing LBA glass-making technologies, as mentioned earlier.

There is a purely theory-based way to further explore this matter considering different glass-forming models, as first suggested by Rehren (2000a, 2000b). What is here referred to as the “total batch melting model” (Rehren 2000b: 1225) assumes that the composition of archaeological glass formed is equal to the composition of the batch used in its formation, minus the volatile components such as carbon dioxide, water etc. This total batch melting is standard practice in modern glass-making and is based on the availability of

carefully selected and weighed raw materials, as no slag is formed to remove any unwanted or superfluous materials from the batch. There are at least two good reasons to doubt that this model sufficiently explains the very ancient glass-making, and instead to suggest alternative models, namely a “partial (batch) melting model” (PMM) and “two melts model” (2MM, below).

Firstly, LBA glass is chemically too homogeneous across space and time to be made from the very variable raw materials used in the LBA. It is assumed that LBA glass is based on crushed quartz as the main silica source, and plant ash as the main flux providing both soda and lime. Shortland (2005) notes that crushed quartz is almost pure silica, suggesting that all minor oxides such as magnesia, potash and alumina come from the plant ash. There are countless factors that will affect the exact compositions of each raw material. For example, the compositions of the plant and the plant ash yielded from it vary significantly not only between species but also between plants of the same species grown in different geographical locations, harvested at different times, or even different parts of the same plant (Jackson *et al.* 2005, Jackson & Smedley 2004). Misra *et al.* (1993) have shown that the ashing temperature has a significant influence on the ash composition, particularly for potash content (the volatilization of potassium began at ashing temperature of 800-900 °C). Thus, it is surprising to see such a close chemical similarity between glasses from all over Egypt and Mesopotamia (Brill 1999a, 1999b). Plant ash data are very variable for their main components, soda, lime and potash (Brill 1999a, 1999b). The published analytical data of plant ash compositions (Brill 1999b, 1999a, Jackson *et al.* 2005, Tite *et al.* 2006, Turner 1956c) are partially shown in Table 3.1., below. This variability is far greater

Table 3.1: Summarised compositions of plant ash (published) from various geographical locations.

	Location	Description	Sample ¹	[wt%]					Na ₂ O/K ₂ O	CaO/MgO
				Na ₂ O	K ₂ O	CaO	MgO	Na ₂ O/CaO		
Egypt	Wadi Natrun	<i>Salsola</i>	WM1	14.7	3.1	23.1	7.5	0.6	4.7	3.1
	Barnug	<i>Suaeda</i>	WM2	43.4	6.5	5.2	3.9	8.3	6.7	1.3
	Barnug	<i>Suaeda</i>	WM2A	33.3	14.5	7.3	6.6	4.6	2.3	1.1
	Taposiris Magna	<i>Anabasis articulata</i>	WM3	48.9	4.5	2.0	2.0	24.5	10.9	1.0
	Taposiris Magna	<i>Suaeda</i>	WM4	30.9	5.3	13.6	4.8	2.3	5.8	2.8
	Cairo-Alexandria highway	Shrubs (twig only)	653	7.8	18.2	16.1	7.8	0.4	0.4	2.1
	Syria (desert)	Shrub, <i>chinan</i>	1380	31.3	5.2	9.5	6.0	3.3	6.0	1.6
Near East	Syria (desert)	Ash lump, <i>chinan</i> (e)	na ²	28.0	5.5	21.1	0.5	1.3	5.1	42.2
	Syria (desert)	Ash lump, <i>chinan</i>	1381	24.0	15.3	21.2	11.2	1.1	1.6	1.9
	Iraq	Shrub, <i>chinan</i>	1326	42.5	7.0	4.7	12.2	9.0	6.1	0.4
	Iraq (desert)	Shrub	1324	25.5	5.0	13.8	8.0	1.8	5.1	1.7
	Iraq	Shrub, <i>chinan</i>	4401	24.9	6.8	4.0	7.3	6.2	3.7	0.6
	Iran	Ash lump, <i>osnan</i>	1304	41.2	4.5	3.5	10.0	11.8	9.2	0.4
	Iran	Ash lump, <i>osnan</i>	1305	37.3	10.6	6.7	4.0	5.6	3.5	1.7

1: numbers refer to data from Brill (1999b) and capital letters refer to data from Tite *et al.* (2006: Table 1 & 2), otherwise data are from either Turner (1956c: Table VI) or Jackson *et al.* (2005: Table 1).

2: not available. 3: ghar = khar = ishgar = ashgar = *Haloxylon recurvum*.

4: branch and twig samples from a single beech tree (Jackson *et al.* 2005: 791).

5: *Pteridium aquilinum* (Bracken) harvested in different years from the same sampling location (Jackson *et al.* 2005: 791).

Table 3.1: (continued)

		Location	Description	Sample ¹	[wt%]				Na ₂ O/CaO	Na ₂ O/K ₂ O	CaO/MgO
					Na ₂ O	K ₂ O	CaO	MgO			
Near East	Pakistan	Shrub, <i>ghar</i> ³		4405	34.3	14.1	3.0	4.3	11.4	2.4	0.7
	Pakistan	Ash lump, <i>ghar</i> ³		4420	37.3	9.4	1.6	0.4	23.3	4.0	4.0
	Pakistan	Ash lump, <i>ghar</i> ³		4421	34.1	4.2	4.5	4.2	7.6	8.1	1.1
	Pakistan	Ash lump, <i>ghar</i> ³		4422	30.7	5.9	5.0	5.5	6.1	5.2	0.9
	Pakistan	Ash lump, <i>ghar</i> ³		4423	37.7	5.1	4.2	2.9	9.0	7.4	1.4
	Pakistan	Ash lump, <i>ghar</i> ³		4426	32.2	15.4	0.5	0.1	64.4	2.1	5.0
	Pakistan	Ash lump, <i>ghar</i> ³		4432	28.0	4.8	4.6	4.7	6.1	5.9	1.0
	Pakistan	Ash lump, <i>ghar</i> ³		4433	22.3	8.8	7.6	4.0	2.9	2.5	1.9
	Uzbekistan	Ash lump, <i>ghar</i> ³		4447	42.1	7.0	1.0	0.9	42.1	6.0	1.1
	Uzbekistan	Ash lump, <i>ghar</i> ³		4449	8.1	25.8	7.0	15.9	1.2	0.3	0.4
	Uzbekistan	<i>Salsola crassi</i>		4446	40.3	12.3	1.1	2.6	36.6	3.3	0.4
	Levant	Seaweed		654	14.1	18.1	12.4	10.7	1.1	0.8	1.2
	EU	Portugal	<i>Salsola Kali</i>		4403	15.1	1.5	14.5	6.3	1.0	10.1
Greece(Attica-Anavissos)		<i>Salsola Kali</i>		ANAV1	16.9	31.8	15.3	3.9	1.1	0.5	3.9
Greece (Attica-Schinias)		<i>Salsola Kali</i>		SCH1	23.1	19.0	14.4	6.6	1.6	1.2	2.2
Greece (Attica-Schinias)		<i>Salsola Kali</i>		SCH2	19.5	26.3	15.7	5.0	1.2	0.7	3.1
Greece(Crete-Ammoudara)		<i>Salsola Kali</i>		AMM1	24.8	36.2	11.4	2.2	2.2	0.7	5.2
Greece(Crete-Ammoudara)		<i>Salsola Kali</i>		AMM5	19.1	22.2	15.5	6.6	1.2	0.9	2.3
Greece(Crete-Ammoudara)		<i>Salsola Kali</i>		AMM5 _{pH7}	6.7	1.5	56.8	26.0	0.1	4.6	2.2

Table 3.1: (continued)

	Location	Description	Sample ¹	[wt%]				Na ₂ O/CaO	Na ₂ O/K ₂ O	CaO/MgO
				Na ₂ O	K ₂ O	CaO	MgO			
EU	Greece (Crete-Georgiopolis)	<i>Salsola Kali</i>	GEOR1	20.0	39.6	10.3	2.4	1.9	0.5	4.3
	Greece (Crete-Georgiopolis)	<i>Salsola Kali</i>	GEOR4	48.2	26.1	2.1	1.1	23.0	1.8	1.9
	UK (Pembroke-Broad Haven)	<i>Salsola Kali</i>	BH1	15.2	33.4	13.8	6.2	1.1	0.5	2.2
	UK (Pembroke-Broad Haven)	<i>Salsola Kali</i>	BH2	12.3	38.1	10.7	6.9	1.1	0.3	1.6
	UK (Pembroke-FreshwaterE)	<i>Salsola Kali</i>	FE1	18.1	22.6	16.1	7.2	1.1	0.8	2.2
	UK (Pembroke-FreshwaterE)	<i>Salsola Kali</i>	FE2	10.6	28.5	23.2	12.5	0.5	0.4	1.9
	UK (Pembroke-FreshwaterW)	<i>Salsola Kali</i>	FW1	23.7	22.5	11.1	4.1	2.1	1.1	2.7
	UK (Pembroke-FreshwaterW)	<i>Salsola Kali</i>	FW2	19.2	26.3	9.5	8.4	2.0	0.7	1.1
	UK (Pembroke-FreshwaterW)	<i>Salsola Kali</i>	FW3	17.5	18.4	14.6	13.0	1.2	1.0	1.1
	UK (Isle of Mull)	<i>Salsola Kali</i>	IM1	10.9	38.2	19.7	10.2	0.6	0.3	1.9
	UK	Seaweed, kelp	5420	19.4	16.4	11.6	11.2	1.7	1.2	1.0
	UK	Seaweed, kelp	5422	20.8	19.9	9.0	9.0	2.3	1.1	1.0
	UK	Seaweed, kelp	5424	18.7	12.4	9.0	8.0	2.1	1.5	1.1
	UK (Sheffield/Derbyshire)	Beech ^(Fagus sylvatica)	branch ⁴	0.4	18.8	31.1	6.9	0.01	0.02	4.5
	UK (Sheffield/Derbyshire)	Beech ^(Fagus sylvatica)	twig ⁴	0.7	18.2	26.5	6.0	0.03	0.04	4.4
	UK (Sheffield/Derbyshire)	<i>Pteridium aquilinum</i>	"1996" ⁵	0.3	42.5	10.5	5.4	0.03	0.01	1.9
	UK (Sheffield/Derbyshire)	<i>Pteridium aquilinum</i>	"1997" ⁵	2.7	44.2	10.7	5.8	0.25	0.06	1.8
	UK (Sheffield/Derbyshire)	<i>Quercus rober</i>	na ²	0.7	14.5	65.4	4.4	0.01	0.05	14.9

Table 3.2: Comparison of the variability among published chemical compositions of plant ash and those of LBA glasses.

Description	range [wt%]			Na ₂ O/CaO	Na ₂ O/K ₂ O	CaO/MgO
	Na ₂ O	K ₂ O	CaO			
Plant ash	Suaeda	30.0 – 43.4	5.3 – 14.5	2.3 – 8.3	2.3 – 6.7	1.1 – 2.8
	Chinan	24.0 – 42.5	4.0 – 21.2	1.1 – 9.0	1.6 – 6.1	0.4 – 42.2
	Osnan	37.3 – 41.2	4.5 – 10.6	5.6 – 11.8	3.5 – 9.2	0.4 – 1.7
	ghar*	22.3 – 37.7	4.2 – 15.4	2.9 – 64.4	2.1 – 8.1	0.7 – 5.6
	Salsola Kali	6.7 – 48.2	1.5 – 39.6	0.6 – 23.0	0.3 – 10.1	1.1 – 5.2
	Seaweed	14.1 – 20.8	12.4 – 19.9	1.1 – 2.3	0.8 – 1.5	1.0 – 1.2
	Total plant ash	6.7 – 48.2	1.5 – 39.6	0.6 – 64.4	0.3 – 10.1	0.4 – 42.2
LBA glasses	cobalt-blue	16.6 – 22.2	0.3 – 1.9	2.0 – 4.4	9.9 – 57.7	1.9 – 2.8
	copper-blue	11.3 – 23.0	0.6 – 3.7	1.4 – 4.6	4.7 – 18.8	0.9 – 3.1
	Red	16.0 – 19.8	1.6 – 2.1	2.1 – 4.0	9.1 – 10.6	1.4 – 2.5
	Purple	17.7 – 19.1	2.0 – 2.4	1.8 – 2.9	8.0 – 8.9	1.5 – 3.1
	White	16.1 – 17.6	2.1 – 3.8	1.9 – 2.8	4.2 – 8.4	1.4 – 2.5
	Green	14.8 – 18.7	1.0 – 2.4	1.6 – 2.8	6.2 – 17.7	2.2 – 2.3
	Yellow	7.5 – 19.1	1.0 – 3.6	1.3 – 2.7	3.6 – 10.0	1.1 – 2.0
	Black	17.9 – 20.7	2.0 – 2.3	3.2 – 3.4	8.6 – 9.4	1.2 – 1.7
	Total LBA glasses	7.5 – 23.0	0.3 – 3.8	1.3 – 4.6	3.6 – 57.7	0.9 – 3.1

*: ghar = khar = ishqar = ashgar = *Haloxylon recurvum*.

than the observed range in published compositions among LBA glasses (Brill 1999a, 1999b, Rehren 1997, Shortland 2000b), except for the soda to potash ratios (see Table 3.2, above). Moreover, Shortland's (2004) study on the formation process of the evaporitic deposits (mineral natron) between the different lakes of the Wadi Natrun showed that the lakes are seasonal in their deposits with different minerals appearing and disappearing at different times. Thus, even the use of mineral natron does not necessarily produce a more consistent batch composition.

Secondly, not only are LBA glasses chemically homogeneous, but also there is an important trend observed among archaeological glasses. Rehren (Rehren 2000a, 2000b, Shugar & Rehren 2002) observed that the compositions of the majority of LBA glasses, published by Lilyquist and Brill (Lilyquist *et al.* 1993), are closely related to the cotectic trough ("cotectic" is a specialised technical term, describing the troughs in the ternary diagram; see Figure 3.1, below) originating from the eutectic region of the SLS system on the soda-rich side and extending towards more lime-rich compositions. Equally, Roman glasses are almost exclusively found within the more silica-rich cotectic trough (see Figure 3.2, below). Rehren (2000a, 2000b) argues that these glass compositions and the liquidus surface morphology of the relevant phase diagrams are too closely linked to be coincidental, and that the variety in chemical composition is too slight to be derived from initial raw material control. Therefore, there should be some inherent factors within the glass-making system itself rather than some variable or configurational human factors (e.g. choice of materials) that control the composition of glass made with variable raw material compositions. That is, there may be some

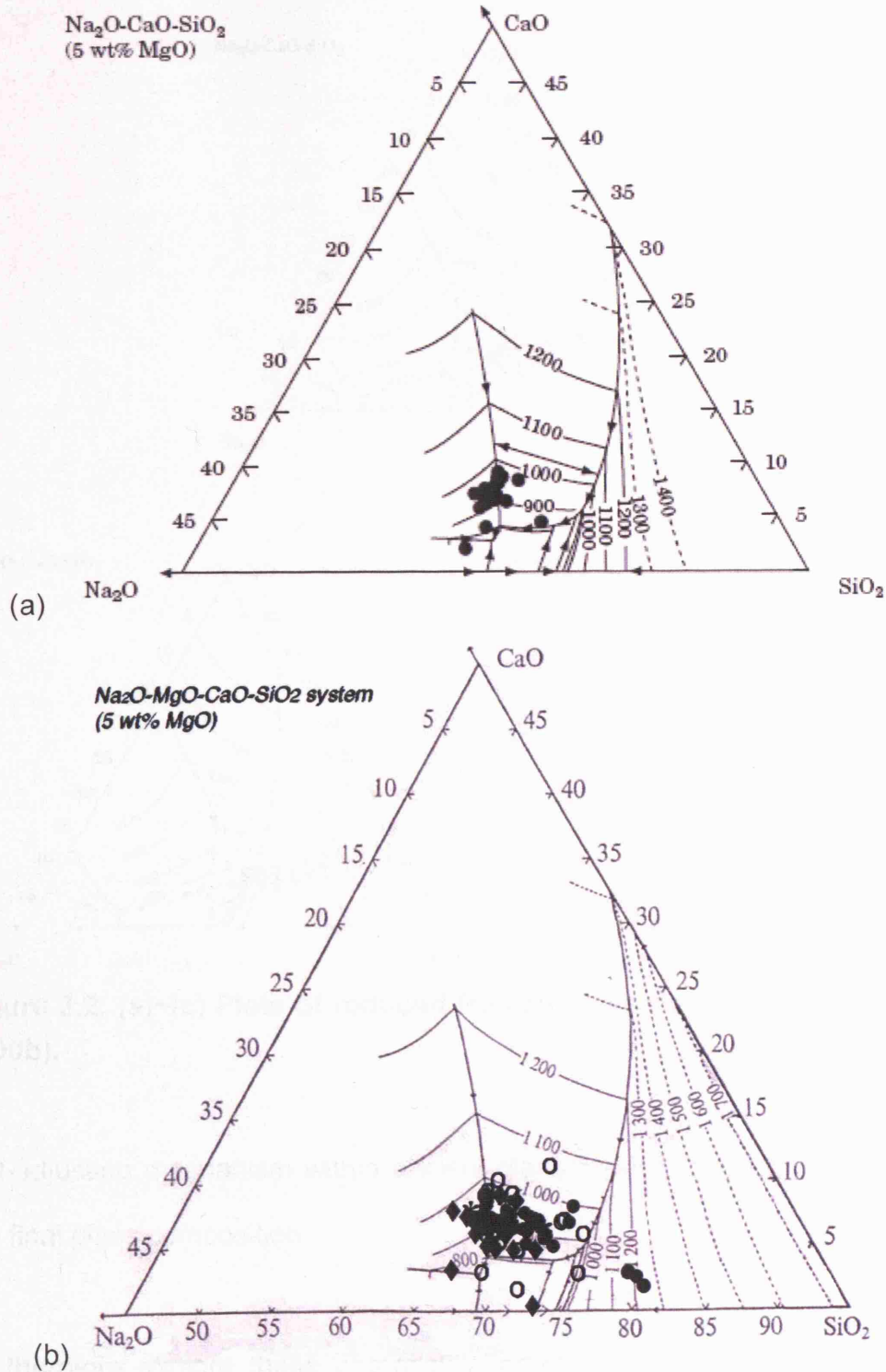


Figure 3.1: Plots of reduced LBA glass compositions from the published works (a) from Rehren 2000, Figure 1 (b) updated figure, including more published data (●: Qantir samples (newly obtained, Schoer & Rehren 2007), ♦: Lilyquist & Brill 1993, Table 2, *: Rehren 1997, Table 3, O: Shortland 2000b, Table 3-2).

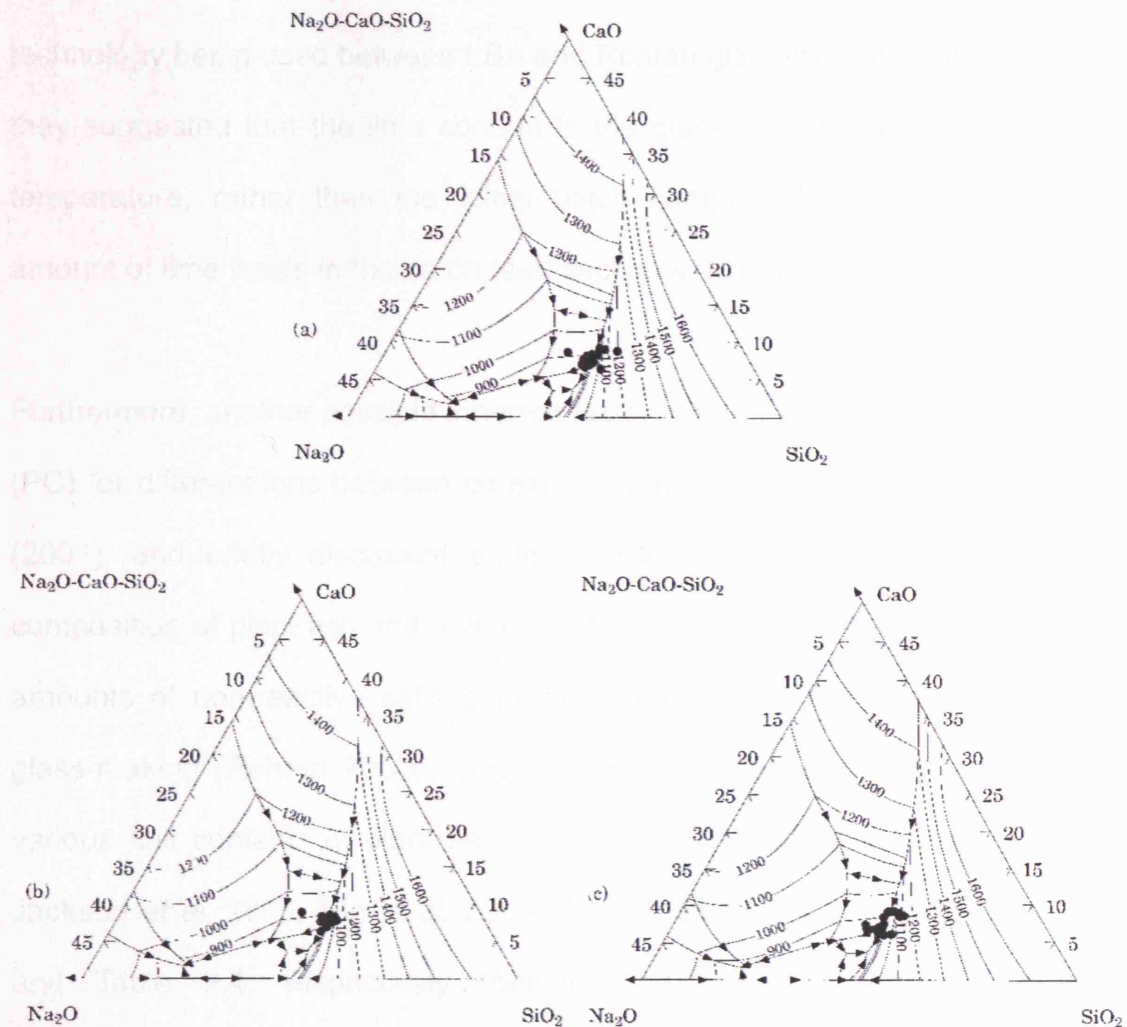


Figure 3.2: (a)~(c) Plots of reduced Roman glass compositions (Rehren 2000b).

self-adjusting mechanism within ancient glass-making being responsible for the final glass composition.

To therefore explore these potential inherent factors, it was suggested to systematically explore these two models, PMM and 2MM. The PMM assumes the formation of a cotectic glass melt in the presence of quantities of crystalline material that act as a buffer or reservoir material from which the melt draws upon as it forms (Shugar & Rehren 2002). With the PMM

approach, Shugar and Rehren (2002) studied the possibility of different technology being used between LBA and Roman glass-making. In particular, they suggested that the lime content in the glass is controlled by the firing temperature, rather than the initial batch composition, when an excess amount of lime exists in the batch (see section 4.3., below, for details).

Furthermore, another possible inherent factor, namely the partition coefficient (PC) for different ions between co-existing melts, was suggested by Rehren (2001), and briefly discussed earlier (section 2.7.). Not only does the composition of plant ash and mineral soda vary, there are always substantial amounts of non-reactive salts present as part of the flux used in ancient glass-making (Rehren 2000b, Turner 1956c). Published analytical data of various salt contents of plant ash and those of natron (Brill 1999b, 1999a, Jackson *et al.* 2005, Tite *et al.* 2006, Turner 1956c) are shown in Table 3.3 and Table 3.4, respectively (below). At melting temperature, the soda-lime-silica (SLS) glass and common chloride- or sulphate-based salts form a system of two immiscible melts, like oil and water. However, exchanges of ions are expected to occur between these two separate melts. The boundary between two melts acts like a permeable membrane and ions can move freely between the two to react, and to concentrate in one or the other (two melts model, 2MM). Silica, for example, partitions completely into the glass melt, while sulphur and chlorine partition preferably, but not completely, into the salt melt. The maximum amount of chlorine that can go into the silicate melt is limited to less than 2 wt% (for details see below). The behaviour of the alkalis under these conditions is as yet unknown, but clearly

Table 3.3: The published salt contents of plant ash from various geographical locations.

	Location	Description	Sample*	[wt%]					
				Na ₂ O	K ₂ O	Cl	SO ₃	CO ₂	%Carbonate**
Egypt	Wadi Natrun	<i>Salsola</i>	WM1	14.7	3.1	13.7	24.8	na***	-86.5
	Barnug	<i>Suaeda</i>	WM2	43.4	6.5	20.0	8.2	na***	50.1
	Barnug	<i>Suaeda</i>	WM2A	33.3	14.5	17.3	7.1	na***	51.7
	Taposiris Magna	<i>Anabasis articulata</i>	WM3	48.9	4.5	34.9	4.2	na***	34.8
	Taposiris Magna	<i>Suaeda</i>	WM4	30.9	5.3	32.8	5.9	na***	3.4
	Cairo-Alexandria Highway	Shrubs (twigs only)	653	7.8	18.2	5.2	12.0	7.8	-15.8
Near East	Syria (desert)	Shrub, <i>chinan</i>	1380	31.3	5.2	15.0	8.1	28.2	44.2
	Syria (desert)	Ash lump, <i>chinan</i> (e)	na***	28.0	5.5	2.1	2.2	34.0	88.8
	Syria (desert)	Ash lump, <i>chinan</i>	1381	24.0	15.3	3.4	2.2	29.0	86.3
	Iraq	Shrub, <i>chinan</i>	1326	42.5	7.0	6.1	2.2	26.4	85.1
	Iraq (desert)	Shrub	1324	25.5	5.0	2.0	1.7	8.6	89.3
	Iraq	Shrub, <i>chinan</i>	4401	24.9	6.8	2.3	1.4	27.0	89.5
	Iran	Ash lump, <i>osnan</i>	1304	41.2	4.5	9.0	0.8	22.0	80.8
	Iran	Ash lump, <i>osnan</i>	1305	37.3	10.6	11.4	1.8	24.8	74.3

*: numbers refer to data from Brill (1999b) and capital letters refer to data from Tite *et al.* (2006: Table 1 & 2), otherwise data are from either Turner (1956c: Table VI) or Jackson *et al.* (2005: Table 1). Branch and twig samples from a single beech tree (Jackson *et al.* 2005: 791). *Pteridium aquilinum* (Bracken) harvested in different years from the same sampling location (Jackson *et al.* 2005: 791).

** : %Carbonate refers to the percentage of total alkali moles present as carbonate. Negative values indicate that there is insufficient soda-plus-potash present to take up all the Cl₂ and SO₃ moles (Tite *et al.* 2006: 1288). ***: not available.

Table 3.3: (continued)

	Location	Description	Sample*	[wt%]					
				Na ₂ O	K ₂ O	Cl	SO ₃	CO ₂	%Carbonate**
Near East	Pakistan	Shrub, <i>ghar</i> ****	4405	34.3	14.1	10.2	4.0	21.8	72.4
	Pakistan	Ash lump, <i>ghar</i> ****	4420	37.3	9.4	8.6	0.1	28.8	82.5
	Pakistan	Ash lump, <i>ghar</i> ****	4421	34.1	4.2	5.0	0.4	23.1	87.4
	Pakistan	Ash lump, <i>ghar</i> ****	4422	30.7	5.9	7.4	0.6	21.7	80.0
	Pakistan	Ash lump, <i>ghar</i> ****	4423	37.7	5.1	28.2	0.7	28.2	38.6
	Pakistan	Ash lump, <i>ghar</i> ****	4424	30.7	5.0	7.9	0.7	21.8	78.2
	Pakistan	Ash lump, <i>ghar</i> ****	4426	32.2	15.4	na***	na***	na***	na***
	Pakistan	Ash lump, <i>ghar</i> ****	4432	28.0	4.8	25.4	0.9	25.4	83.5
	Pakistan	Ash lump, <i>ghar</i> ****	4433	22.3	8.8	15.3	6.3	15.3	80.8
	Uzbekistan	Ash lump	4447	42.1	7.0	15.7	19.4	9.8	38.5
	Uzbekistan	Ash lump	4449	8.1	25.8	1.6	2.6	20.8	87.5
	Uzbekistan	<i>Salsola crassi</i>	4446	40.3	12.3	13.1	23.5	na***	38.7
	Levant	Seaweed	654	14.1	18.1	19.2	16.8	19.8	-14.5
	Portugal	<i>Salsola Kali</i>	4403	15.1	1.5	na***	na***	na***	na***
Europe	Greece (Attica-Anavissos)	<i>Salsola Kali</i>	ANAV1	16.9	31.8	22.6	1.5	na***	44.7
	Greece (Attica-Schinias)	<i>Salsola Kali</i>	SCH1	23.1	19.0	25.1	2.1	na***	33.8
	Greece (Attica-Schinias)	<i>Salsola Kali</i>	SCH2	19.5	26.3	25.5	2.2	na***	34.8
	Greece (Crete-Ammoudara)	<i>Salsola Kali</i>	AMM1	24.8	36.2	18.7	2.1	na***	63.1
	Greece (Crete-Ammoudara)	<i>Salsola Kali</i>	AMM5	19.1	22.2	31.3	1.3	na***	15.7

Table 3.3: (continued)

	Location	Description	Sample*	[wt%]					
				Na ₂ O	K ₂ O	Cl	SO ₃	CO ₂	%Carbonate**
Europe	Greece (Crete-Ammoudara)	Salsola Kali	AMM5 (pH7)	6.7	1.5	0.3	3.1	na***	64.3
	Greece (Crete-Georgioupolis)	Salsola Kali	GEOR1	20.0	39.6	20.9	1.8	na***	57.3
	Greece (Crete-Georgioupolis)	Salsola Kali	GEOR4	48.2	26.1	15.2	0.9	na***	78.5
	UK (Pembroke-Broad Haven)	Salsola Kali	BH1	15.2	33.4	21.4	2.6	na***	44.2
	UK (Pembroke-Broad Haven)	Salsola Kali	BH2	12.3	38.1	25.1	1.7	na***	37.7
	UK (Pembroke-FreshwaterE)	Salsola Kali	FE1	18.1	22.6	13.9	2.0	na***	58.4
	UK (Pembroke-FreshwaterE)	Salsola Kali	FE2	10.6	28.5	18.6	3.2	na***	36.2
	UK (Pembroke-FreshwaterW)	Salsola Kali	FW1	23.7	22.5	30.6	2.1	na***	26.1
	UK (Pembroke-FreshwaterW)	Salsola Kali	FW2	19.2	26.3	27.0	2.2	na***	30.6
	UK (Pembroke-FreshwaterW)	Salsola Kali	FW3	17.5	18.4	16.9	3.3	na***	41.5
	UK (Isle of Mull)	Salsola Kali	IM1	10.9	38.2	7.5	2.7	na***	75.9
	UK	Seaweed, kelp	5420	19.4	16.4	5.1	31.0	1.5	5.8
	UK	Seaweed, kelp	5422	20.8	19.9	19.5	16.0	1.6	13.2
	UK	Seaweed, kelp	5424	18.7	12.4	11.4	23.7	0.9	-5.4
	UK (Sheffield/Derbyshire)	Beech (<i>Fagus sylvatica</i>)	branch	0.4	18.8	na***	1.1	na***	na***
	UK (Sheffield/Derbyshire)	Beech (<i>Fagus sylvatica</i>)	twig	0.7	18.2	na***	1.2	na***	na***
	UK (Sheffield/Derbyshire)	<i>Pteridium aquilinum</i>	"1996"	0.3	42.5	na***	9.6	na***	na***
	UK (Sheffield/Derbyshire)	<i>Pteridium aquilinum</i>	"1997"	2.7	44.2	na***	4.4	na***	na***
	UK (Sheffield/Derbyshire)	Oak (<i>Quercus robur</i>)	na***	0.7	14.5	na***	0.6	na***	na***

Table 3.4: The published salt contents of natron from various geographical locations.

Location	Sample ¹	[wt%]					
		Na ₂ O	K ₂ O	Cl	SO ₃	CO ₂	%Carbonate ²
Wadi Natrun	na ³	13.1	na ³	38.6	18.3	9.3	na ³
Egyptian tomb	655	50.5	0.6	38.9	7.1	8.0	22.0
Egyptian tomb	657	42.7	0.5	14.9	7.4	19.0	57.1
Egyptian tomb	658	41.6	0.6	9.5	6.7	8.5	69.1

1: numbers refer to data from Brill (1999b), otherwise data is from Turner (1956c).

2: %Carbonate refers to the percentage of total alkali moles present as carbonate. Negative values indicate that there is insufficient soda-plus-potash present to take up all the Cl₂ and SO₃ moles (Tite *et al.* 2006: 1288).

3: not available.

very relevant in the context of early glass-making. Both sodium and potassium can go in very high concentrations into the silicate and into the chloride melt. If there is an excess of chlorine in the batch composition, will the salt melt have the same ratio of sodium to potassium as the silicate melt, or will one alkali metal be more likely to partition into the salt melt? This question is particularly relevant for the cobalt-blue glasses from Egypt that have a much lower potash content than all other glasses (Lilyquist *et al.* 1993), and salt partitioning could be one possible way to reduce the level of potash in a silicate glass.

Based on these two speculative glass-forming models (i.e. PMM and 2MM), my research aims to further identify the scientific factors (e.g. temperature,

partitioning behaviour) that determine the concentrations of the minor oxides (such as lime, magnesia and potash) in the glass. For this, a series of experimental melts were done in order to test specific important assumptions of these two models.

3.2. Methodology

3.2.1. Methodology of experimental work

Methodology (common to all series of experiments, unless otherwise stated):

Several series of experimental melts were prepared using controlled chemical-grade raw materials simulating the assumed raw materials of antiquity to explore the hypotheses of system-controlled glass forming behaviour.

Different batch compositions of glasses (below) were prepared from the raw materials, in the ratios described in each relevant section, and melted in crucibles (see each recipe in the relevant sections below for the ratios). While there is almost no archaeological or textual evidence concerning the selection and properties of raw materials and the practicalities of the actual melting schedules, it was decided to use relatively simple modern raw materials, namely silica sand, calcium carbonate, sodium carbonate, magnesium oxide, sodium chloride, and potassium chloride, that are all commercially available.

All the raw materials used were oven dried at 110 °C for 2 hours to remove any moisture and subsequently stored in a desiccator with silica gel. Batches were weighed in to achieve 100 g of final glass, unless otherwise

stated. All measurements were made to one 100th of a gram and the raw materials were thoroughly mixed in a plastic bag. Mullite crucibles from the Department of Engineering Materials in Sheffield (MARCUS) were used to reduce the interaction between the vessel and the formed glass. According to Shugar and Rehren's (2002) experiments, there was only very limited interaction between the crucible fabric and the forming glass, identified by a slightly increased alumina content in the melt, which was only detectable within 50 μm of the crucible wall. They also noted that the potash content, detected by X-ray fluorescence (XRF) analysis as a minor component in the mullite fabric, was consistently below detection limit in the glass.

The filled crucibles were heated in an electrical furnace with heating filaments in the sidewalls at the rate of 3 °C/minute from room temperature to the selected melting temperature in order to prevent the crucibles from fracturing during the heating process. For most experiments, three crucibles were placed in a single row inside the furnace to allow even heating from all sides. For primarily technical reasons, a typical melting time of 16 hours was chosen, enabling me to prepare a series of batches during the day, to start the firing in the afternoon and to remove the crucibles the next morning, unless otherwise noted in the individual section. In Shugar and Rehren's (2002) experiments, extended firing times of up to 40 hours were chosen to check whether these would have a significant effect on the resulting glass; no such effect was observed, reflecting the small batch sizes (100 g/batch). Once the melting schedule was complete, the furnace was allowed to cool letting the temperature inside the furnace to decrease by its nature (approximately at the rate of 3 °C/minute) to room temperature with the crucibles still inside the

furnace for a further 2 hours to reduce mechanical stress in the glass. The cooled crucibles were then cut using a standard petrological saw for macroscopic analyses (see each section for details). Sub-samples were mounted in epoxy resin and ground down on silicon carbide paper before they were polished with diamond paste to 0.25 μm in preparation for further analysis.

3.2.1.1. Melt-Solid Interactions (see Chapter 4, below)

Different batch compositions covering the range of “Egyptian/LBA” (soda-rich cotectic trough) and “Roman” (silica-rich cotectic trough) glasses were melted at temperatures varying between 900 and 1150 °C in the same furnace with the same melting schedule mentioned above. For this section (Melt-Solid Interactions), some experimental glass samples that were produced by Dr. Shugar were re-analysed, and the data integrated in the thesis by the author.

Batch compositions that do not have MgO were selected on the basis of specific points and regions of interest in the SLS ternary system, shown here as Figure 3.3 (Shahid & Glasser 1972: 28; Figure 1). Similarly, the batches with MgO are prepared based on Figure 8 (Shahid & Glasser 1972: 32; Figure 3). Batches were selected at various ideal or set temperatures along certain isotherms across the soda-rich and the silica-rich cotectic troughs, and along these troughs. The batches were then fired at their set temperature, or at lower or higher temperatures from the set batch temperature. That is, a batch situated at the 1000 °C isotherm would, for example, be under-fired to only 980 °C, or fired at the set temperature of 1000 °C, or over-fired at a higher temperature such as 1050 °C, and the resulting glasses are compared.

For example, melt #06 had its batch composition set at 1000 °C on the silica-rich trough and was fired at 1000 °C. Melt #10 had a batch composition set at 1100 °C and was also fired at 1000 °C. Although different quantities of glasses were formed respectively, the compositions of the glass were the same. See Shugar and Rehren (2002) for more details on batch preparation for Melt-Solid Interactions.

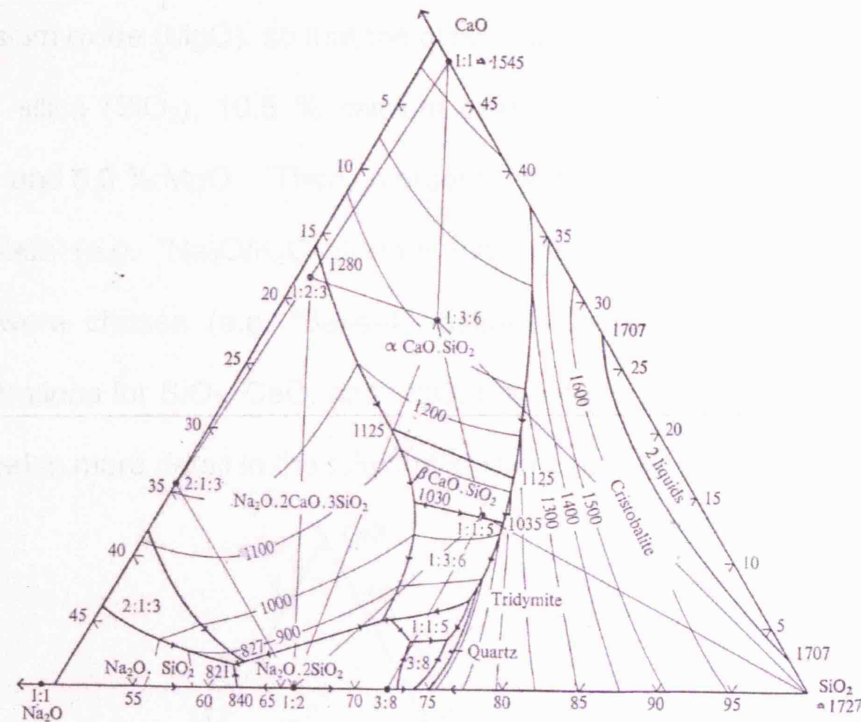


Figure 1. Phase equilibrium diagram for the $\text{Na}_2\text{O}-\text{CaO}-\text{SiO}_2$ system

Figure 3.3: The SLS ternary system with no MgO (Shahid & Glasser 1972).

3.2.1.2. Melt-Melt Interactions (see Chapter 5, below)

A single primary batch composition ("Base A") was selected for all of these experiments from the soda-rich cotectic trough of the SLS ternary diagram, with fixed MgO content of 5 wt%, shown here as Figure 3.4 (Shahid & Glasser 1972: 32; Figure 3), in order to reduce the number of variables in the experiments. This batch composition had an ideal or set melting

temperature as taken from the liquidus surface of the ternary system, of 1000 °C. The batches were then fired at a temperature of 1050 °C, a somewhat higher temperature from the setting to assure all the materials are fully reacted.

Base A (100 g/batch) is composed of 65.0 g of (silica) sand, 18.8 g of calcium carbonate (CaCO_3), 33.3 g of soda ash (mainly Na_2CO_3), and 5.0 g of magnesium oxide (MgO), so that the glass made will have the composition of 65.0 % silica (SiO_2), 10.5 % calcium oxide (CaO), 19.5 % sodium oxide (Na_2O), and 5.0 % MgO. Then, in order to test series of alkalis co-present in the system (e.g. “ $\text{Na}_2\text{O}/\text{K}_2\text{O}$ System (chlorides)””, below), various primary bases were chosen (e.g. “Base-4”, below), derived from Base A (same concentrations for SiO_2 , CaO, and MgO, but different alkali/soda content), as explained in more detail in the relevant sections, below, respectively.

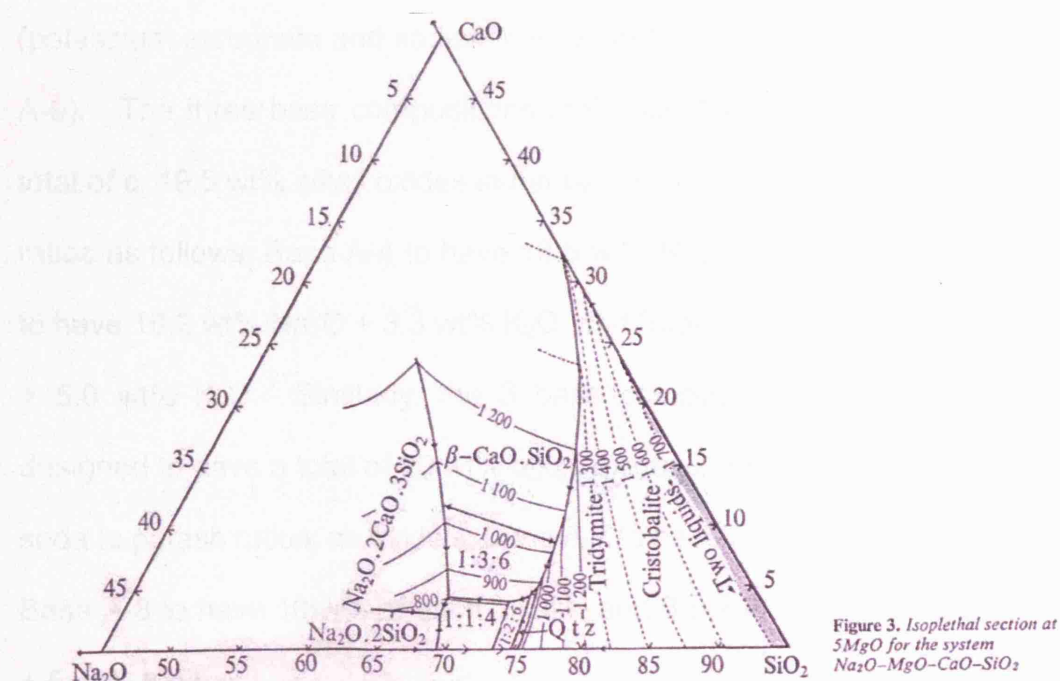


Figure 3. Isolethal section at 5MgO for the system $\text{Na}_2\text{O}-\text{MgO}-\text{CaO}-\text{SiO}_2$

Figure 3.4: The SLS ternary system with 5 wt% MgO (Shahid & Glasser 1972).

In general, appropriate conversion factors were applied respectively to calculate how much of the certain raw material, in weight, is equivalent to that of its oxide form, when glass is formed. That is, 1.71 (molecular weight of Na_2CO_3 /molecular weight of Na_2O) for soda (Na_2O) to sodium carbonate (Na_2CO_3); 1.79 for lime (CaO) to calcium carbonate (CaCO_3); 1 for silica (SiO_2) to silica sand (mainly SiO_2); respectively; 1.39 for magnesia (MgO) to lime; and 1.58 and 1.47 for potash (K_2O) to potassium chloride (KCl) and to potassium carbonate (K_2CO_3), respectively.

Base A was then modified for Base A-4 to A-6 (see Recipe-1) and Base A-7 to A-9 (see Recipe-2, in Chapter 5) to have potash as well as soda. The difference is that the former bases (Base A-4 to A-6) have soda sourced as carbonate form (sodium carbonate) and potash sourced as chloride form (potassium chloride) while alkalis were both sourced as carbonated forms (potassium carbonate and sodium carbonate) in the latter bases (Base A-7 to A-9). The three base compositions in Recipe-1 are all designed to have a total of c. 19.5 wt% alkali oxides in the batch, but with variable soda to potash ratios as follows; Base A-4 to have 18.5 wt% Na_2O + 1.0 wt% K_2O , Base A-5 to have 16.2 wt% Na_2O + 3.3 wt% K_2O , and Base A-6 to have 14.5 wt% Na_2O + 5.0 wt% K_2O . Similarly, the 3 base compositions in Recipe-2 are all designed to have a total of 20 wt% alkali oxides in the batch, but with variable soda to potash ratios, as follows; Base A-7 to have 5 wt% Na_2O + 15 wt% K_2O , Base A-8 to have 10wt% of each alkalis, and Base A-9 to have 15 wt% Na_2O + 5 wt% K_2O .

3.2.2. Methodology of analytical work

3.2.2.1. Electron Probe Microanalysis (EPMA)

The JEOL superprobe JXA 8600 was used for EPMA to determine the composition and homogeneity of the formed glass. The seven elements of the “base glass oxides” (basic components of the glass; Na₂O, K₂O, MgO, Al₂O₃, SiO₂, CaO, and Fe₂O₃) were measured (Lilyquist *et al.* 1993: Table 2). Aluminium and iron were included to check for contamination from the crucible and raw materials. Normally, the formed glass did contain neither aluminium nor iron oxide. The probe is equipped with 3 spectrometers and the machine was set up with an accelerating voltage of 15 keV. A current of 6×10^{-8} A was used to guarantee sufficient count rates and statistical reliability of the data. One major problem with electron microprobe investigations of glass is the migration of sodium during analysis. This migration causes a lower measure of sodium concentration (Figure 3.5, below, shows that Corning Glass Standard A with 14 wt% Na₂O content will be detected as 2-3 wt% only (lowered by 11-12 wt%) after 30 seconds). This measurement was conducted by spot analysis, with a current of 6×10^{-8} A, voltage 15 keV, over a time of 100 seconds without stage movement, i.e. measuring the same area repeatedly to monitor possible soda migration away from the area analysed. In addition, migration of potassium was also observed when Corning Glass Standard D with 11 wt% K₂O and 1.3 wt% Na₂O contents was analysed in the same spot analysis condition (see Figure 3.6, below, showing both measurements were lowered by 1.5 wt% and 0.4 wt% respectively, after 30 seconds). Full compositions of the Corning Glass Standard A and D are published by Brill (1999a: 544).

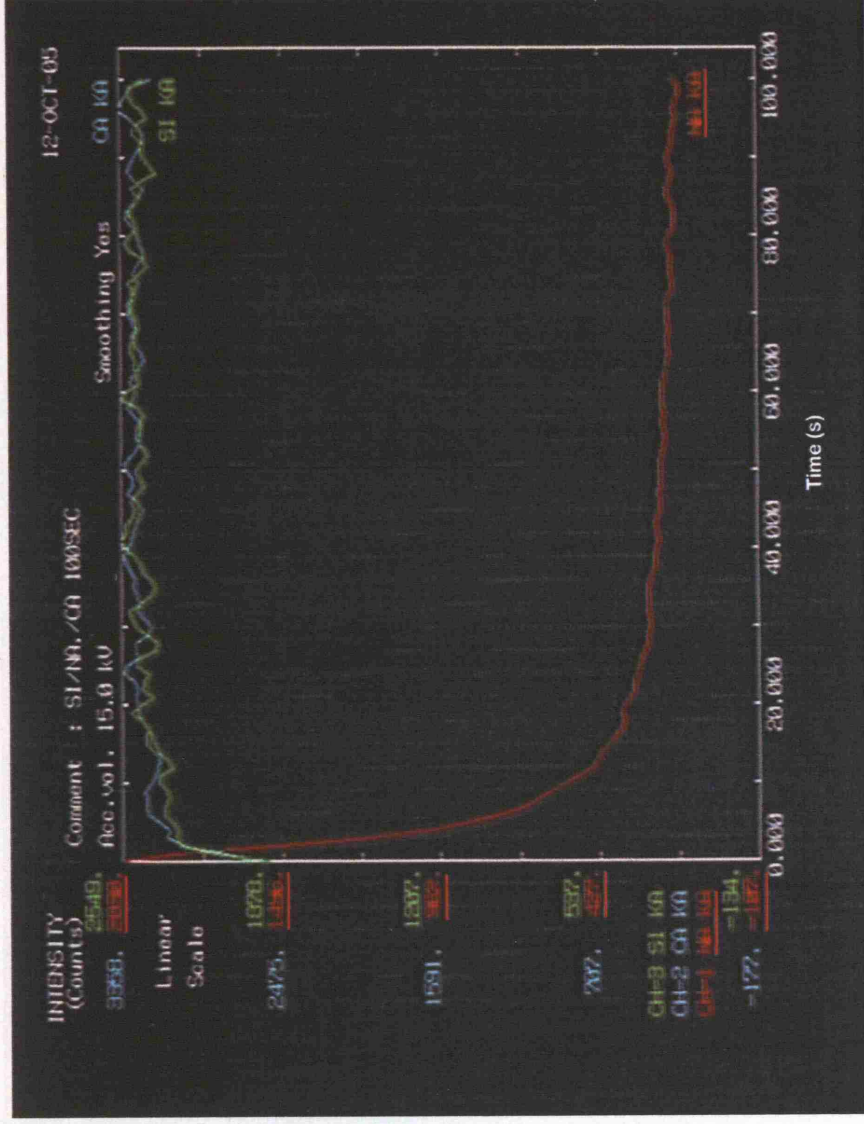


Figure 3.5: Peak intensities for sodium (red), silicon (green), and calcium (blue) respectively in glass (spot-analysis). This figure shows sodium readings of glass standard Corning A dramatically drops while the readings of silicon and calcium remains consistent over time.

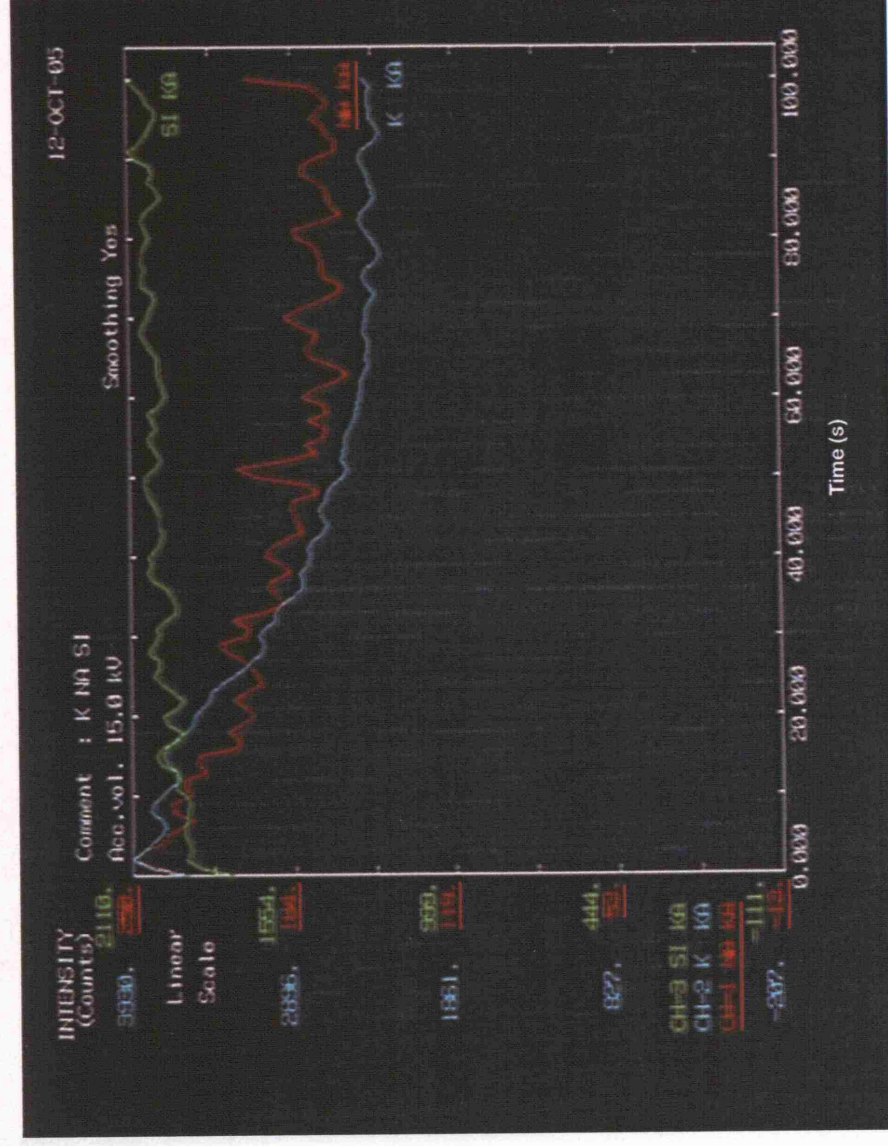


Figure 3.6: Peak intensities for sodium (red), silicon (green), and potassium (blue) respectively in glass (spot-analysis). This figure shows both sodium and potassium readings of glass standard Corning D decrease while the readings of silicon and calcium remains consistent over time.

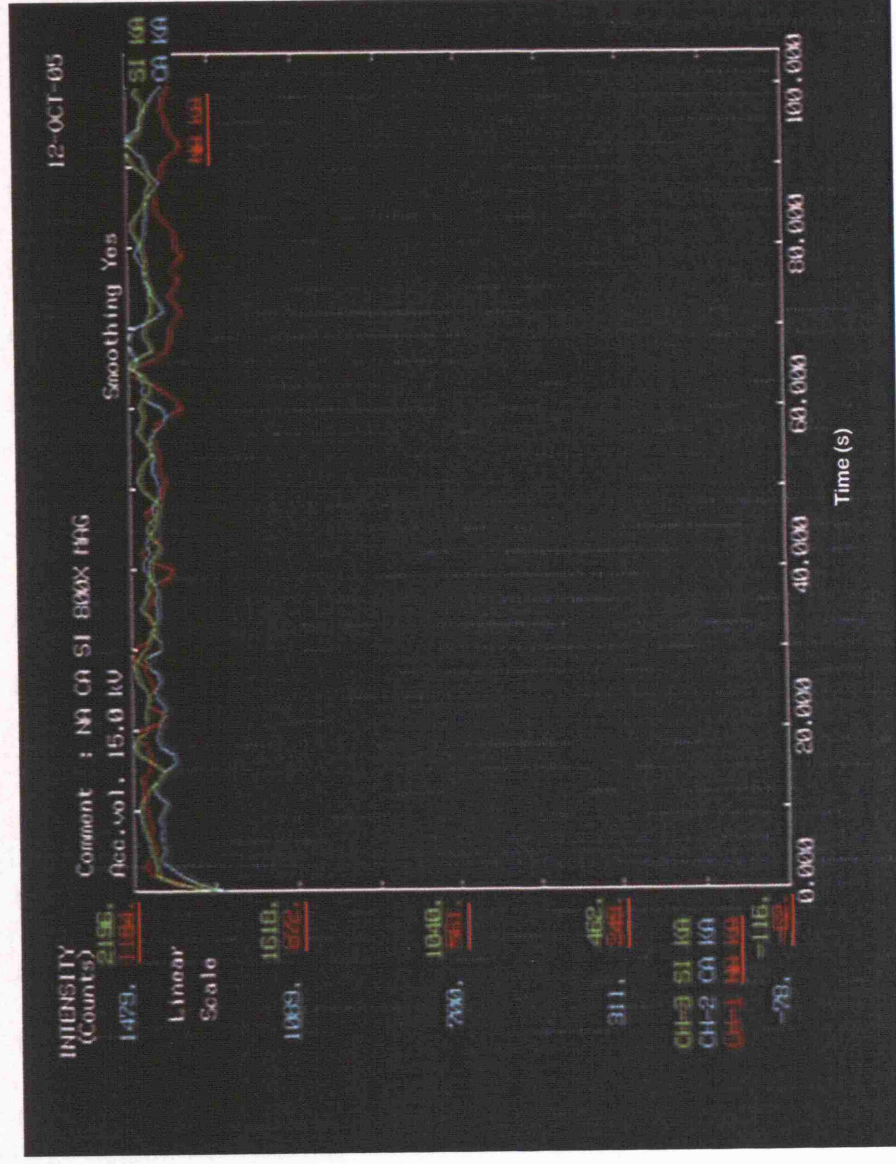


Figure 3.7: Peak intensities for sodium (red), silicon (green), and calcium (blue) respectively in glass standard Corning A (area analysis, x 800 magnification). At this magnification, measured intensities stayed stable indicating no soda migration.

To avoid soda loss, area-scan analyses rather than spot analyses were conducted by EPMA on all the glass samples studied in this research. This method has been tested and established initially by Kevin Reeves and the result is shown below as Figure 3.7 (area analysis with current 6×10^{-8} A, voltage 15 keV, and measured over 100 seconds, using Corning Glass Standard A). Area analysis (at 800x magnification, covering approximately $110 \mu\text{m} \times 80 \mu\text{m}$) was performed over a time of 5 minutes (longer than a typical routine area-scan analysis of about 15 seconds). For experimental glass samples with crystal phases, a clear glassy region is selected to avoid crystal inclusions. At this magnification sodium counts stayed stable over time.

To check the accuracy and precision of the data acquired by EPMA, certified reference glasses (two different glass standards of known composition; DGG-I, and DGG-II, mounted in epoxy resin) were analysed at the beginning of every three samples (since the machine can hold 4 samples; 1 standard + 3 prepared samples at once) or as often as possible and again at the end of the day to check the degree of calibration shift, if any, and also to check the accuracy of the instrument itself. All the chemical compositions presented in this thesis will be given as percents by weight (wt%), and the results normalised to 100 %, unless otherwise mentioned. Pre-normalised totals inevitably were slightly below 100% due to the inherent porosity of most samples and drift in beam intensity. However, the data quality control procedure described above allows us to trust the obtained results since the averages of accuracy of measured seven oxides were reasonable (see Table 3.5 and below for more details).

Table 3.5: Accuracy and precision of acquired data (glass standards).

	Na ₂ O	MgO	Al ₂ O ₃	SiO ₂	CaO	K ₂ O	SO ₃	Cl	Total	Description
1	14.2	4.38	1.26	71.6	6.88	0.38	0.25	0.04	99.2	DGGI (measured on 23/10/2003)
2	14.6	4.52	1.17	71.8	6.89	0.36	0.29	0.03	99.9	same as above
3	14.5	4.47	1.23	71.8	6.86	0.37	0.30	0.04	99.7	same as above
day mean	14.4	4.45	1.22	71.7	6.87	0.37	0.28	0.04	99.6	same as above
4	14.5	4.29	1.18	71.3	6.95	0.37	0.38	0.04	99.0	(26/10/2003)
5	14.3	4.43	1.27	71.4	6.90	0.36	0.34	0.04	99.2	same as above
day mean	14.4	4.36	1.22	71.3	6.93	0.37	0.36	0.04	99.1	same as above
6	14.6	4.62	1.08	70.3	6.85	0.38	0.29	0.04	98.1	(29/10/2003)
7	14.8	4.07	0.93	70.9	6.90	0.36	0.31	0.02	98.3	same as above
day mean	14.7	4.34	1.00	70.6	6.88	0.37	0.30	0.03	98.2	same as above
8	15.0	4.54	1.29	71.1	6.87	0.38	0.30	0.03	99.7	(02/11/2003)
mean	14.6	4.42	1.18	71.3	6.89	0.37	0.31	0.04	99.1	overall mean (DGGI)
theory	15.0	4.18	1.23	71.7	6.73	0.34	0.44	0		"true" value (DGGI)
AAD*	0.4	0.24	0.05	0.4	0.16	0.03	0.13	0.04		
SD*	0.24	0.17	0.11	0.47	0	0	0	0		
	2.7	5.7	4.1	0.6	2.4	8.8	29.5	0		Accuracy [% error]
	1.6	3.8	9.3	0.7	0	0	0	0		Precision
1	13.4	3.53	0.11	72.1	10.3	0.03	0.18	0.03	99.6	DGGII (23/10/2003)
2	13.3	3.63	0.01	72.3	10.4	0.02	0.19	0.03	99.8	same as above
3	13.6	3.61	0.05	72.4	10.3	0.02	0.17	0.14	100.3	same as above
day mean	13.4	3.59	0.05	72.2	10.3	0.02	0.18	0.07	99.9	same as above
4	13.2	3.60	0.04	71.9	10.2	0.02	0.24	0.03	99.3	(26/10/2003)
5	NA*	NA*	NA*	NA*	NA*	NA*	NA*	NA*	NA*	same as above
6	14.2	3.67	0.06	71.2	10.3	0.02	0.20	0.04	99.7	(29/10/2003)
7	14.0	3.66	0.06	71.2	10.3	0.01	0.19	0.04	99.4	same as above
day mean	14.1	3.66	0.06	71.2	10.3	0.02	0.20	0.04	99.5	same as above
8	14.1	3.79	0.11	71.0	10.2	0.02	0.18	0.02	99.4	(02/11/2003)
mean	13.7	3.64	0.06	71.7	10.3	0.02	0.19	0.05	99.7	overall mean (DGGII)
theory	13.8	3.40	0.10	72.3	10.1	0.00	0.27	0		"true" value (DGGII)
AAD*	0.1	0.24	0.04	0.6	0.19	0.02	0.08	0.05		
SD*	0.38	0.07	0.03	0.54	0.06	0	0.02	0.04		
	0.7	7.1	40	0.8	1.9	0	29.6	0		Accuracy [% error]
	2.8	1.9	50	0.8	0.6	0	11	80		Precision

AAD*: average absolute deviation, SD*: standard deviation, NA*: not available.

Accuracy refers to the agreement between the measurement and the “true” (or correct) value and therefore, the true/correct value needs to be known or defined to judge the accuracy. That is, accuracy is measured as % deviation from the true value. That is, accuracy [% error] is calculated by $(\text{true value} - \text{measured value}) \times 100 / (\text{true value})$ or AAD (average absolute deviation) $\times 100 / (\text{true value})$. Precision is expressed as standard deviation (SD) within a number of analyses and depends upon mean. Precision [%] is calculated by $\text{SD} \times 100 / \text{mean}$. That is, precision refers to the repeatability of measurement. The smaller the accuracy value, the better the measurement since the obtained data is closer to the true value(s). However, the repeatability of the data is not necessarily good just because the accuracy value is small. Similarly, the smaller the precision value, the better the repeatability of the measurement. However, the obtained data is not necessarily close to the true value(s). The smaller the precision value, the less the dispersion of data obtained repeatedly.

It is important to note that the values of both accuracy and precision were larger (worse) for minor oxides/constituents and major oxides tend to have smaller (better) values for both. In particular, the values of both accuracy and precision tend to be large (more than $\pm 9\%$) for the oxide contents less than 0.5 wt%, such as alumina, sulphate, chlorides, and potash, while those values becomes much smaller (less than $\pm 2\%$) for the other oxide contents more than 10 wt%, for both reference standards, DGG I and DGG II.

The range of oxide contents in all the experimental glass melts is about 1–65 wt% and major oxides, silica, soda, and lime will be expected to have smaller values for both accuracy and precision, especially silica having the smallest values for both accuracy and precision amongst all the measured elements.

(ii) Scanning Electron Microscope (SEM)

The SEM was used especially for imaging, which would help to identify the characterisation of different crystalline phases within the glass phase. The SEM instrument used for this research is a Philips XL30 Environmental SEM (ESEM) with an INCA Oxford spectrometer package, housed at the Institute of Archaeology. It is equipped with both secondary electron (SE) and backscatter electron (BSE) detectors. The factors affecting SE emission are the morphology of the surface, the beam energy and intensity and, to a lower extent, the density of the sample. Therefore, SE images taken by SEM are good for three-dimensional samples. In contrast, the BSE intensity only depends on the average atomic number of the specimen. Combining both devices, one obtains a great amount of information on the topography and the compositional make-up of the specimens examined. However, all images taken by SEM in this thesis are BSE images since all the samples were polished to form flat surfaces, and therefore had no morphology anymore. Further, the main interest was on compositional differences, best viewed by BSE images.

In addition, the SEM used has attached both wavelength (WDS) and energy dispersive spectrometry (EDS) X-ray microanalysers. The EDS allows measurements in a scanning mode, where an area of up to $\sim 2.5 \text{ cm}^2$ may be analysed, and also spot analyses of particles down to a few μm diameter, and was utilised routinely. The WDS was occasionally used for resolving peak overlaps in some spectra, but predominantly SEM-EDS was used for this research to semi-quantify the compositions of the crystalline phases, for confirmation. Operating conditions for SEM-EDS data collection were as

follows: working distance of 10 mm; accelerating voltage of 20 kV; spot size of 5.0 (INCA conventional units) and process time 4 or 5, corresponding to a detector deadtime of 13-30%; and livetime of approximately 55 seconds. The SEM beam intensity is calibrated with cobalt standard every 2 hours to ensure the consistency of the obtained data. However, this data quality control allows us to trust the obtained results regardless since SEM is mainly used for imaging purposes.

3.2.3. Data handling for plotting ternary graph

In order to check the chemical homogeneity of the LBA glass compositions (e.g. Figure 3.1) and to plot chemical compositions obtained of the formed experimental melts, the following data handling is required. First, the EPMA data had to be reduced to fit into quasi-ternary phase diagrams. That is, the seven measured oxides were reduced to three oxides by mathematically converting alumina and iron oxide contents to “silica” content; similarly potash to “soda”; and magnesia to “lime” (Rehren 2000b: 1226). In this process, factors were applied to the minor oxides to adjust for the differences in molecular weights of the various oxides, namely 1.20 for alumina and 0.75 for iron oxide to “silica”, respectively; 1.39 for magnesia to “lime”; and 0.66 for potash to “soda”. Finally the sums of the three oxides calculated (henceforth labelled silica*/SiO₂*, soda*/Na₂O*, and lime*/CaO*) were normalized to 100 wt% if there is no magnesia in the batch. However, since most of the archaeological glasses and the batches prepared in this paper have a fixed rate of 5 wt% magnesia, the normalization of the final three oxides was done to 95 wt% only to match the appropriate phase diagram as published by Shahid and Glasser (1972), shown earlier (Figure 3.4).

Chapter 4: Melt-Solid Interactions

(“partial melting model - PMM”, earth alkalis)

Glass is a reaction product between raw materials that are initially all present in crystal form. Glass formation is a stepwise process, involving the formation of new, intermediate crystal phases as well as the combination of different phases to form a glass. This means that the formation of glass is not a sudden and complete process, but that there are different stages in which different parts of the batch material have already reacted to form a glass, while others are either partly reacted to form an intermediate crystal phase, or are unreacted, residual due to lack of time or temperature to form a glass. An example for intermediate crystal phases to form is the decomposition of metal carbonates, such as CaCO_3 to form solid CaO and CO_2 gas, or the reaction of CaO with SiO_2 to form wollastonite crystals, CaSiO_3 . These intermediate crystal phases have their own chemical compositions that are typically different from the average batch composition. Another important aspect is the reaction speed; large grains with a relatively small ratio of surface to volume will react more slowly than fine-grained material with a much bigger relative surface. Some components will react more easily than others, such as soda and silica, respectively. Therefore, during glass-formation, the glass will evolve and have different compositions at different stages of the process; therefore, it is bound to have also a different composition than the original batch until all components are fully reacted and molten. Incomplete or partial melting means that there are intermediate lime-rich phases such as wollastonite or residual phases such as silica present when the glass-making process finishes. Areas rich in these phases

will be opaque white in colour, while areas of fully fused glass will be colourless-transparent. If these two areas separate, naturally or through careful manual selection of crushed material, it is possible to obtain a final glass melt which is different from the original batch; in this example lower in lime and silica, and therefore richer in soda.

The main aim of this thesis is to better understand the glass-forming reactions as far as they are relevant for the LBA glass-making; this chapter explores to which extent the earth alkali (lime and magnesia) concentrations of LBA glasses can be controlled by inherent factors and by configurational or cultural factors, respectively. It will also look at the influence which different earth alkali concentrations have on the behaviour of the glass, in preparation for the discussion of the archaeological significance of my research (see Chapter 7).

4.1. Terminology: partial melting vs. devitrification

There are three different types of crystal phases that can be present in glass. The first type is residual phases such as silica grains that have failed to dissolve completely in the melt. The second is intermediate phases that have formed during the glass-forming reactions, but have failed to fully react to form glass. A typical example for the latter is wollastonite, which is often found in glass-making waste (McLoughlin 2003). The third is crystal phases that have formed from existing glass, typically when the glass is held at high temperatures but below the glass transition temperature for a long time, as in glass-working. This last type is known as devitrification.

It is important to distinguish residual or intermediate crystals formed during

partial melting (PMM crystals) from devitrification since PMM crystals are only present in material directly related to primary glass-making, while devitrification is typically observed as a result of glass-working. Thus, the archaeological interpretation of “crystalline-rich glass” will be very different, depending on whether the crystals are PMM crystals or devitrification. Furthermore, PMM crystals can give information about glass-making conditions, whereas devitrification crystals do not give that kind of information. That is, “PMM” describes the situation in glass melting where some parts of unreacted or half-reacted raw materials remain in the glass. This can occur either as a result of wrong batch composition or insufficient melting temperature, or due to local lack of equilibrium conditions or chemical homogenisation, as for instance in areas rich in lime near a former/original limestone particle. “Devitrification” describes the condition of existing glass changing partly or completely to a crystalline structure. This happens typically as an equilibrium process, and the resulting devitrified glass has the same chemical composition as the original glass, just in a different mineralogical arrangement. In addition, it is very important to determine how we should identify each crystalline phase by their spatial distribution (for example, see Figure 4.1 (below) whether the phase is formed directly from incomplete reacting of raw materials or by devitrification). Therefore, it is important to understand how the nature and morphology of the crystal phases differ for these two situations, enabling the identification of one or the other as the main reason for the presence of crystals in the glass, and for correct interpretation.

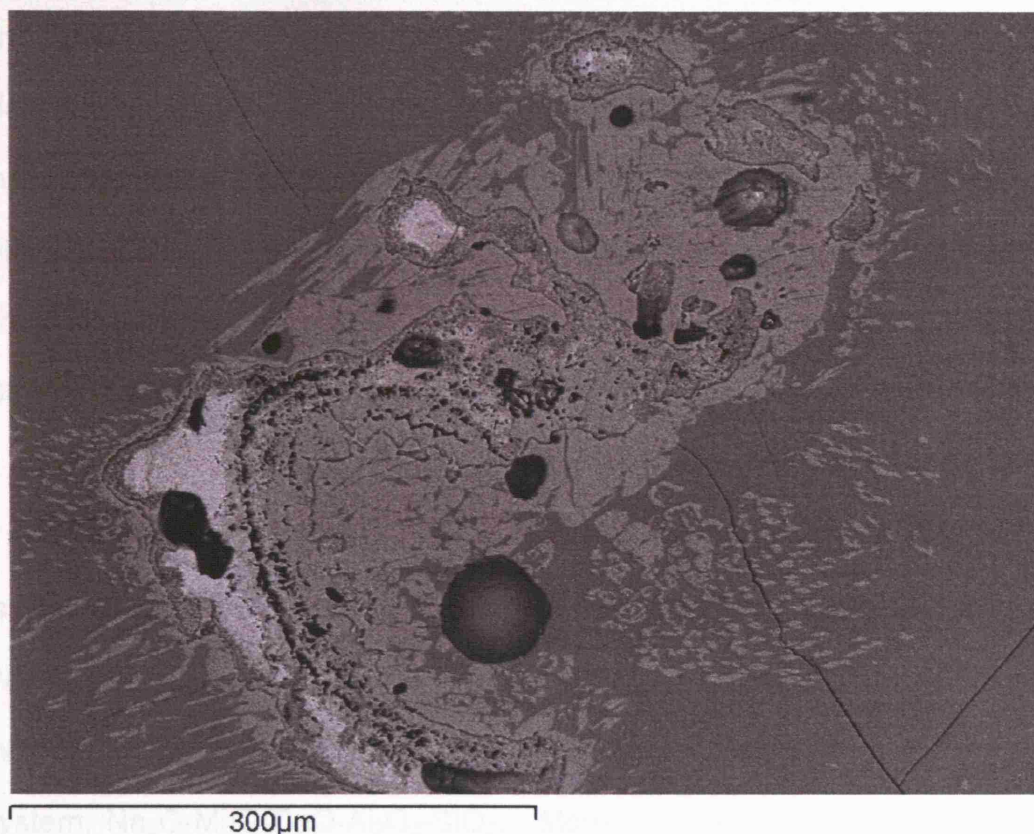


Figure 4.1: SEM (BSE) image showing distribution of crystalline phases within glassy phase. Lime-rich crystalline phases (in white colour) diffusing into soda-lime-silicate phases (light grey areas), suggesting these crystalline phases were formed by semi-reacted raw materials.

4.2. Review of the literature

Soda-lime-silica glass has always been the dominating glass type, from the earliest beginning to the Roman period, and across much of Asia throughout the Middle Ages and early Modern Period. It is the by far most extensively used glass still today. Accordingly, the SLS system is extremely well researched, both in terms of equilibrium or phase diagrams (phase equilibrium), and in terms of engineering behaviour since the early 1900s. However, little was known then about the compounds which are formed by the devitrification of SLS glasses, and the first study to determine the equilibrium relationships between crystalline and liquid phases was published by Morey

and Bowen in 1925 (Morey & Bowen 1925). The nature of glass melting, or glass forming reactions from the batch, melting temperatures, the reactions of the liquid oxide melt with refractories, and the following devitrification products which could originate from the glass are, to some extent, predictable from an understanding of the phase equilibrium in the relevant system (Shahid & Glasser 1972).

It has long been known that the resistance of the glass to chemical attack and to devitrification is improved by adding alumina (Al_2O_3) and magnesium oxide (MgO), respectively (Shahid & Glasser 1972). Therefore, it was a great interest for researchers to understand the phase relations in the quinary system, $\text{Na}_2\text{O-MgO-CaO-Al}_2\text{O}_3\text{-SiO}_2$. Moreover, the crystalline phases that exist within the glass phase that are richer in lime or magnesia than the surrounding glass phase may be the very (possible) buffer materials that affect earth alkali contents in the formed glass. There may be one or several crystalline phases with various earth alkali content within the glass. This is likely to have been devitrite ($\text{Na}_2\text{Ca}_3\text{Si}_6\text{O}_{16}=1\text{Na}_2\text{O}.3\text{CaO}.6\text{SiO}_2$) or pseudo-wollastonite (CaSiO_3) or any other of the relevant phases as a function of the exact composition of the batch (Morey 1930a, b, Morey & Bowen 1925, Rehren 2000b), and will be discussed below.

Firstly, the initial complete phase equilibrium diagrams of $\text{Na}_2\text{O-CaO-SiO}_2$ and $\text{Na}_2\text{O-MgO-SiO}_2$ systems were established by Morey and Bowen (Morey 1930a, 1925) and by Schairer and Yorder (Schairer 1957, Schairer & Yoder 1971: both cited in Shahid & Glasser 1972: 27), respectively. In the $\text{Na}_2\text{O-CaO-SiO}_2$ system, Morey and Bowen's (1925: 243) experiment on SLS

glass showed that devitrite crystals decomposed above about 1000 °C and wollastonite (CaSiO_3) or pseudo-wollastonite being formed instead. This system's phase diagram was revised by Shahid and Glasser (1972) to include the additional primary phase fields of $3\text{Na}_2\text{O} \cdot 8\text{SiO}_2$ (below c. 820 °C) and $1\text{Na}_2\text{O} \cdot 1\text{CaO} \cdot 5\text{SiO}_2$ (between c. 820-830 °C), see Figure 3.3. That is, devitrite phase can be seen only when the glass is fired between 827-1030 °C. The crystalline phases that form below 827 °C are more complicated, including $1\text{Na}_2\text{O} \cdot 1\text{CaO} \cdot 5\text{SiO}_2$, but not relevant for my research here.

Although the full phase equilibrium diagram for the latter system, Na_2O - MgO - SiO_2 , was drawn by Schairer and Yoder in 1971 (Schairer 1957, Schairer & Yoder 1971: both cited in Shahid & Glasser 1972: 27), as mentioned above, many works on the effect of MgO in combination of Na_2O , CaO , and SiO_2 had been studied before then. The effect of MgO was measured by using experimental melts with their lime contents replaced progressively by MgO . Therefore, to be more precise, the quaternary system, Na_2O - MgO - CaO - SiO_2 , was studied by various researchers, such as Morey (1930b) and Owens-Illinois Glass Company General Research Laboratory (1944). In both publications, MgO additions resulted in a large initial drop in liquidus temperature and this matter will be discussed in more detail below (see section 4.4., below).

Secondly, more complicated phase equilibrium systems that contain either alumina and/or potash, in addition to Na_2O - MgO - CaO - SiO_2 , have been studied by various researchers and some of their major findings are summarised below.

In $\text{Na}_2\text{O}-\text{Al}_2\text{O}_3-\text{SiO}_2$ system, albite (sodium plagioclase, $\text{NaAlSi}_3\text{O}_8$) is the primary phase of the glasses with compositions containing alumina as little as 5 wt% (c. 20-23 wt% Na_2O , <5 wt% CaO , and c. 71-74 SiO_2) when fired below c. 800 °C (Moir & Glasser 1976). This albite phase region on the phase diagram expands, as alumina content in the glass increases, not only by moving the phase boundaries between three other primary phases (wollastonite, $\text{Na}_2\text{O}.\text{SiO}_2$, and quartz) surrounding it. However, when alumina content in the glass is more than 15 wt%, one of the surrounding primary phase, $\text{Na}_2\text{O}.\text{SiO}_2$, disappears and nepheline phase appears instead. The effect of certain oxides on crystal growth (Cable & Yang 1993, Swift 1947) varies depending on the compositions of the crystal and the firing temperatures and seems very complicated. Moreover, the effect of alumina on the phase separation was studied by Geotti-Bianchini *et al.* (1998), who showed that not only the addition of alumina increases the stability against devitrification, but also the phase separation is efficiently restrained when more than 1 wt% alumina is present in $\text{Na}_2\text{O}-\text{Al}_2\text{O}_3-\text{SiO}_2$ system when compared to that of $\text{Na}_2\text{O}-\text{CaO}-\text{SiO}_2$ system.

In summary, it is possible to understand some technicalities of past glass-making practice, to some extent, such as the glass forming/melting process (from the batch) and the firing temperatures used from the observed crystalline phases within the glass since the glass-forming process is very different according to the primary phase of that particular batch in a certain condition, such as temperature, viscosity, and crystal growth (e.g. Silverman 1940). Addition of minor oxide(s) to the SLS system expands the phase field where devitrite is the primary crystalline phase towards tridymite (SiO_2) and

makes many of the glasses more difficult to devitrify (Backman *et al.* 1997).

For the purpose of the subsequent presentation of my own research, a brief outline of some relevant aspects of the main SLS system and one of its subsystems – containing 5 wt% MgO – is presented in more detail in this Chapter. This is based primarily on the authoritative compilation by Shahid and Glasser (1972), although some older literature is used as well to highlight specific aspects in each sections discussed below.

What is particularly relevant here is the morphology of the liquidus surface of the system that represents the liquidus temperatures of every given compositions within the relevant glass-forming part of the system. For compositions with 50 wt% and more silica, see Figure 3.4 (above, in Chapter 3). Liquidus temperatures range from a high of 1700 °C for pure silica and temperatures in excess of 1200 °C for compositions with more than about 20 wt% lime to values of less than 800 °C around the eutectic compositions at the bottom of the diagram. The region of interest in this research covers compositions roughly between 65 and 75 wt% silica and less than about 15 wt% lime, and the rest being soda. This region is bordered by a steeply increasing temperature field towards higher silica content (right), and moderately-increasing temperature field towards higher lime content (top & left). The crystal phases that are ideally present in this region of interest (with 5 wt% MgO) are wollastonite (CaSiO_3) and devitrite ($\text{Na}_2\text{Ca}_3\text{Si}_6\text{O}_{16}$), as shown in Figure 3.4. However, the crystalline phases that are present in this region change when there is no MgO in the system (Na_2O - CaO - SiO_2 system, see Figure 3.3) and those phases are wollastonite, devitrite, and



4.3. CaO vs. temperature

The distribution of ancient glass compositions within the ternary phase diagrams shows several interesting characteristics. One is that a clear distinction exists between LBA and Roman glass compositions. Previous research suggested that the LBA glass was typically richer in magnesia and potash than the later glass (Sayre 1967); this is now generally accepted to be due to the use of different raw materials, namely plant ash for LBA glass and mineral natron for Roman glass.

However, once plotted into the SLS diagrams, Rehren (2000a, 2000b) noted an important and quite different separation of the two classes of glass. The LBA glasses almost all plot to the soda-rich side of the eutectic region, and extend up towards higher lime concentrations following the left eutectic trough (see above). The Hellenistic/Roman glasses, in sharp contrast, plot almost exclusively next to the steep silica slope of the eutectic region, and upwards the right-hand eutectic trough that runs towards higher lime contents. This separation occurs regardless of whether one uses the basic SLS diagram or the SLS system with 5 wt% magnesia, and is thus not a function of the presence or absence of this minor oxide. It is this observation, amongst others, that formed the basis to explore experimentally two key aspects of the self-governing properties of the SLS system: the relationship between lime content and temperature, and the preference for one or the other eutectic trough, as a function of process details of the batches and the glass melting furnaces or vessels used in the two respective periods.

The close association of the observed archaeological glass compositions between the two periods and the preference for one or the other of these two troughs strongly indicates that the compositions of these glasses is governed to a considerable extent by the melting characteristics of the system, i.e. inherent and universally valid factors, rather than by culturally determined configurational factors, such as conscious selection and careful mixing of specific raw materials, or choice of firing temperature. However, a configurational factor clearly is at play here too, as seen from the strong cultural link between specific troughs and archaeological periods. As explained earlier (Chapter 1), my research tries to identify cultural behaviour through understanding the extent of inherent factors, and identifying the archaeologically invisible cultural factors once the inherent factors have been removed. One of the interesting factors in ancient glass-making is the firing temperature. It is hoped that by using the universally valid inherent factor in the SLS system that in the PMM determines the composition of the melt as a function of the temperature, we can actually use the glass composition as a thermometer to establish ancient firing temperatures that are an important configurational factor. Before this can be done, it is important to test the validity of the PMM, and in particular the relationship between firing temperature and melt composition.

Preliminary results from Shugar and Rehren (2002) had indicated that under certain circumstances the melting temperature directly controls the content of calcium oxide in the glass melt. Furthermore, the time and temperature required to form a glass are very different for the two major glass compositions, "Egyptian" and "Roman", as discussed in more detail below.

One of the main aims of this research was to test these preliminary results through further experiments, and to expand the experiments to also cover magnesia-rich ("Egyptian") compositions. Therefore, to link the two sets of data together, my research included some of the earlier samples produced by A. Shugar, but more data was added in this research, as mentioned earlier.

4.3.1. PMM: composition (CaO content) vs. firing temperature

Four different sets of A. Shugar's experiments in the magnesia-free SLS system with initial batch compositions across the "Egyptian" and the "Roman" trough were all melted at 1000 °C. These four initial batch compositions were respectively selected where the 1000 °C and 1100 °C isotherms cross either the "Egyptian" (melt #02 and #14, soda-rich) or the "Roman" (melt #06 and #10, silica-rich) cotectic troughs. All four batches were fired at the same temperature, 1000 °C, that is two of them were fired at their set temperature, while two were underfired by 100 °C. The resulting glass compositions were compared to see whether there is any difference in formed glass quality, quantity and composition when the batch is under-fired compared to the one that is fired at the set temperature. This matter will be discussed in more detail below.

Observation of melts:

Macroscopic analyses were conducted to study the nature and the morphology of the formed melts, such as the volume proportion of glass to crystalline phases. This process is very important for crystal identification, as mentioned earlier in this chapter, and it reflects on how LBA glass-makers judged the quality of the glass, in conjunction with temperature, without any

sophisticated analytical instruments.

All melts produced consist of either a crystalline material above the glass phase or a top layer of crystalline material within the glassy product (see Figure 4.2).

Especially melts under-fired from their intended batch firing temperature showed clear evidence of PMM with a clear glassy phase forming under a crystalline section holding the remainder of the partially reacted batch material. This phenomenon varied in proportion with different batch compositions and with the melt temperature but is clearly visible in all samples. Spatial separation of glass and residual crystalline material was typically good enough to allow mechanical separation when about half of the total melt/batch appeared glassy after firing.



Figure 4.2: Cross section of one of the experimental melts (incomplete melting) showing the clear transparent glass (lower half) and the opaque, with a high proportion of residual crystalline matter (upper half) (image taken by Shugar).



Figure 4.3: Separation by simple hand picking after crushing (image taken by Shugar).

Separation by simple hand picking after crushing gave a clean glassy fraction and a residual crystalline-rich fraction (see Figure 4.3). The crystalline residue comprises not only silica but also a range of other binary and ternary oxide compounds (Shugar & Rehren 2002). That is, the crystalline-rich phases within the melt, are comprised of silica, wollastonite, and the mixture of lime-rich soda-lime-silicate phases in various ratios, depending on where the phases were found and the firing temperature and the batch composition of the melt (see below for detail compositions). Residual quartz grains (see Figure 4.4) can be seen throughout the sample but especially near the surface while wollastonite ($\text{CaSiO}_3 = 1\text{CaO} \cdot 1\text{SiO}_2$) crystals were often found near the crucible wall/bottom (see Figure 4.5). For example, SEM (BSE) images of the area comprised of various crystalline phases within melt #14 and melt #02 are shown as Figure 4.6 & 4.7 and Figure 4.8, respectively. The composition of each crystalline phase is summarised in Table 4.1 (melt #14) and Table 4.2 (melt #02). The distribution of the phases, including

residual quartz grains, may reflect how the heat is transferred during the glass-forming process. The presence of a lime-rich nucleus and/or residual quartz grains may tell us whether the glass/melt was produced by primary glass-making process.

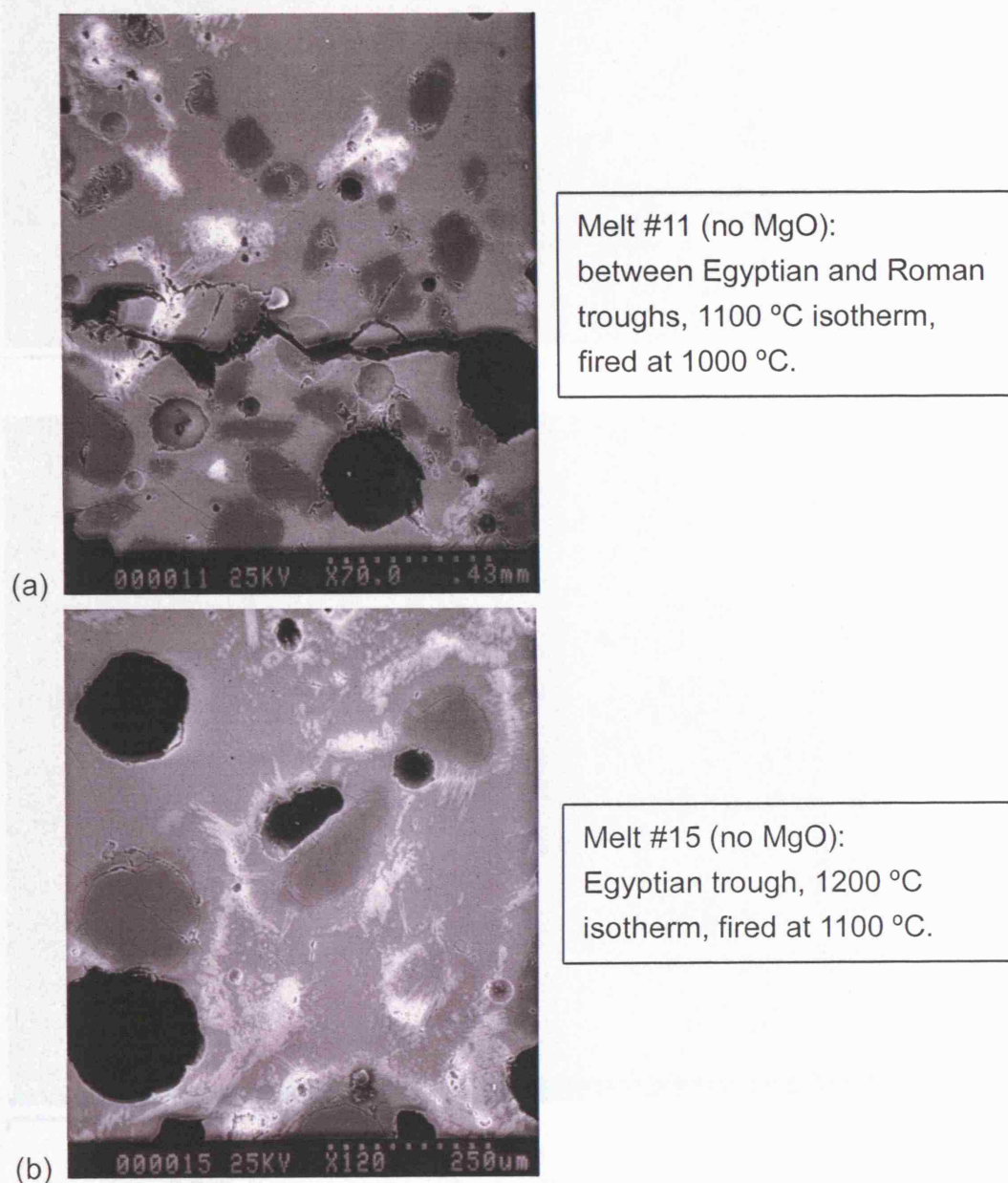


Figure 4.4: SEM (BSE) image of quartz grains (dark) and lime-rich areas (bright) seen in the experimental melts (PMM), (a) Melt #11 and (b) Melt #15 (images taken by Shugar).

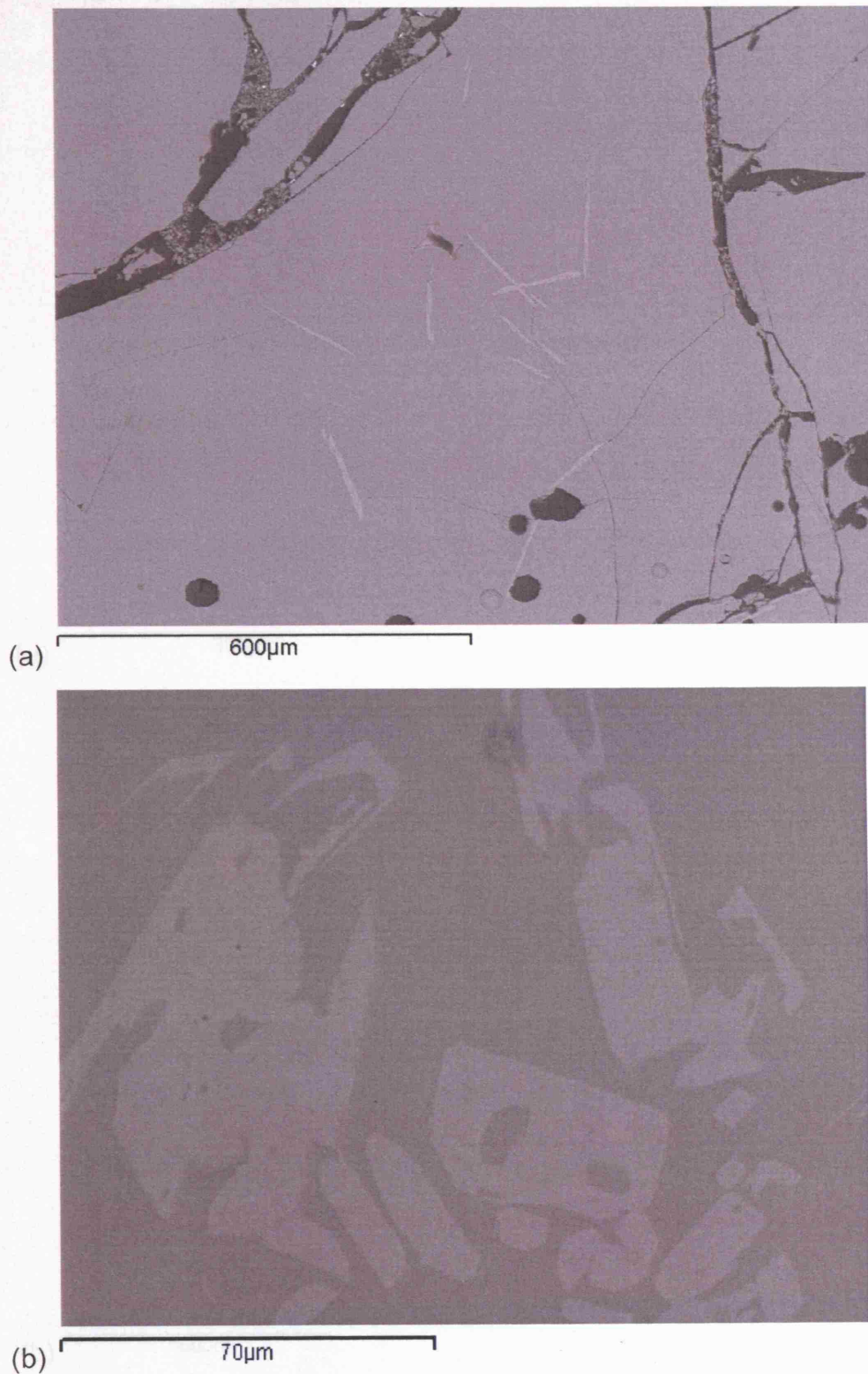


Figure 4.5: SEM (BSE) images of wollastonite crystals seen in (a) melt #57 (no MgO, Egyptian trough, 1100 °C isotherm, underfired at 1080 °C) and (b) melt #06 (no MgO, Roman trough, 1000 °C isotherm, fired at 1000 °C).

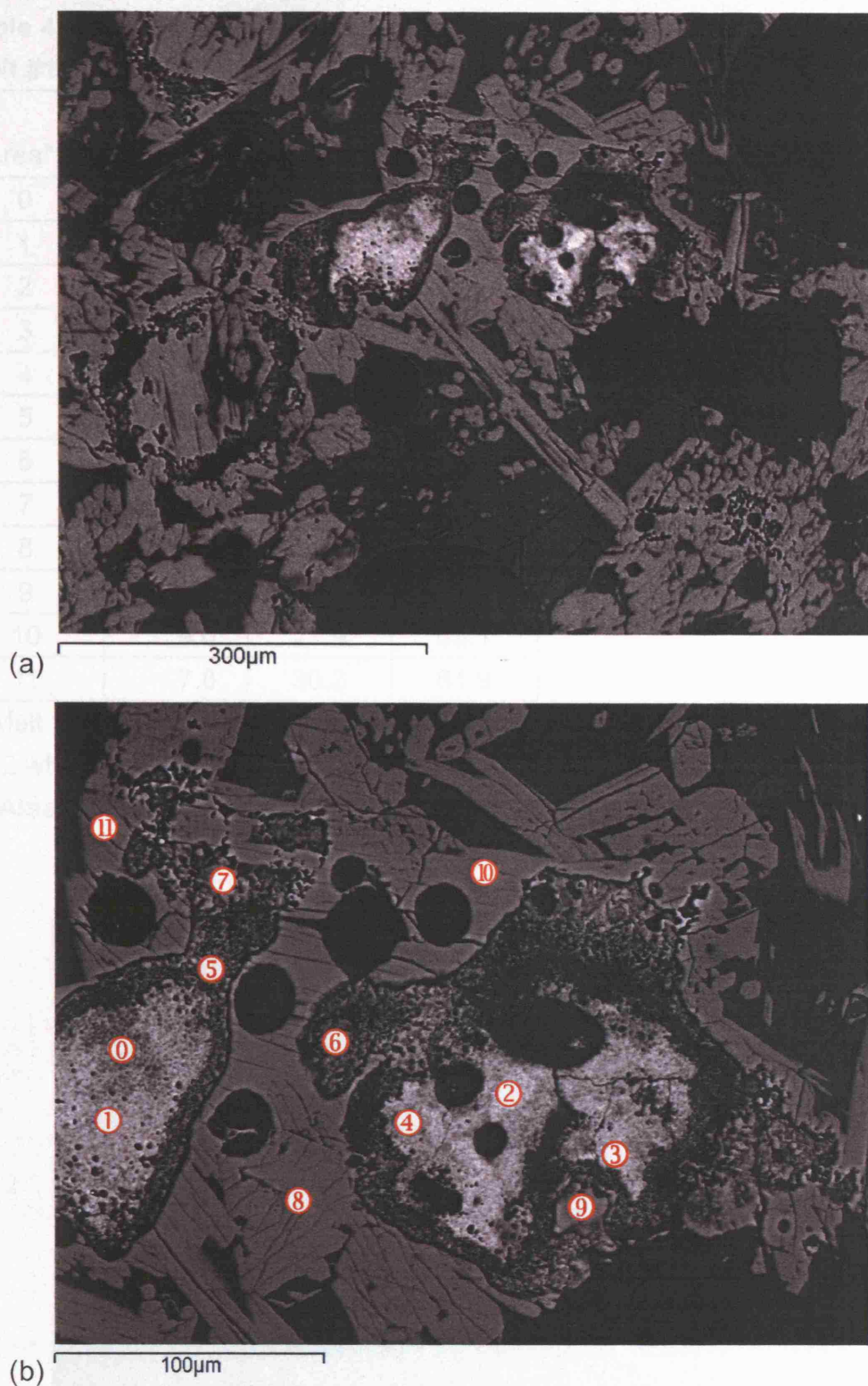


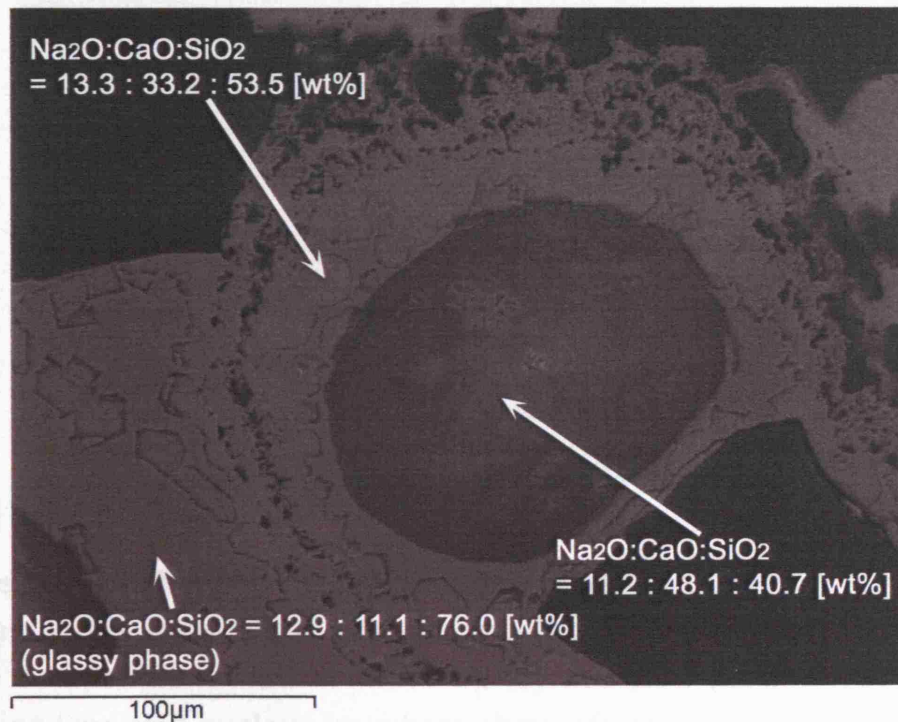
Figure 4.6: SEM (BSE) images showing mixture of various crystalline phases within melt #14 (no MgO, Egyptian trough, 1100 °C isotherm, fired at 1000 °C); (a) overview (b) enlarged image showing lime-rich nucleus (numbers show where semi-quantitative data was taken, see Table 4.1).

Table 4.1: Semi-quantitative analysis of various crystalline areas seen in melt #14* (measured by SEM).

Area**	Weight%			Descriptions of the phase
	Na ₂ O	CaO	SiO ₂	
0	3.2	61.7	35.1	White in BSE image. Heterogeneous. Ca-rich phase (nucleus)
1	3.0	60.2	36.9	
2	2.8	61.6	35.7	
3	3.1	61.4	35.5	
4	2.7	61.4	35.9	
5	13.3	34.0	52.7	Dark grey in BSE image. Heterogeneous.
6	13.6	33.0	53.4	
7	14.2	32.4	53.4	
8	9.6	27.8	62.6	Light grey in BSE image. Homogeneous.
9	9.3	27.8	62.9	
10	9.0	27.9	63.1	
11	7.8	30.3	61.9	

*: Melt #14 has the batch composition of 64.2 wt% SiO₂, 17.6 wt% CaO, and 18.2 wt% Na₂O (Egyptian trough, 1100 °C isotherm, underfired at 1000 °C).

**: Areas analysed are shown in Figure 4.6.

**Figure 4.7: SEM (BSE) image showing another type of nucleus formation with its surrounding phase.**

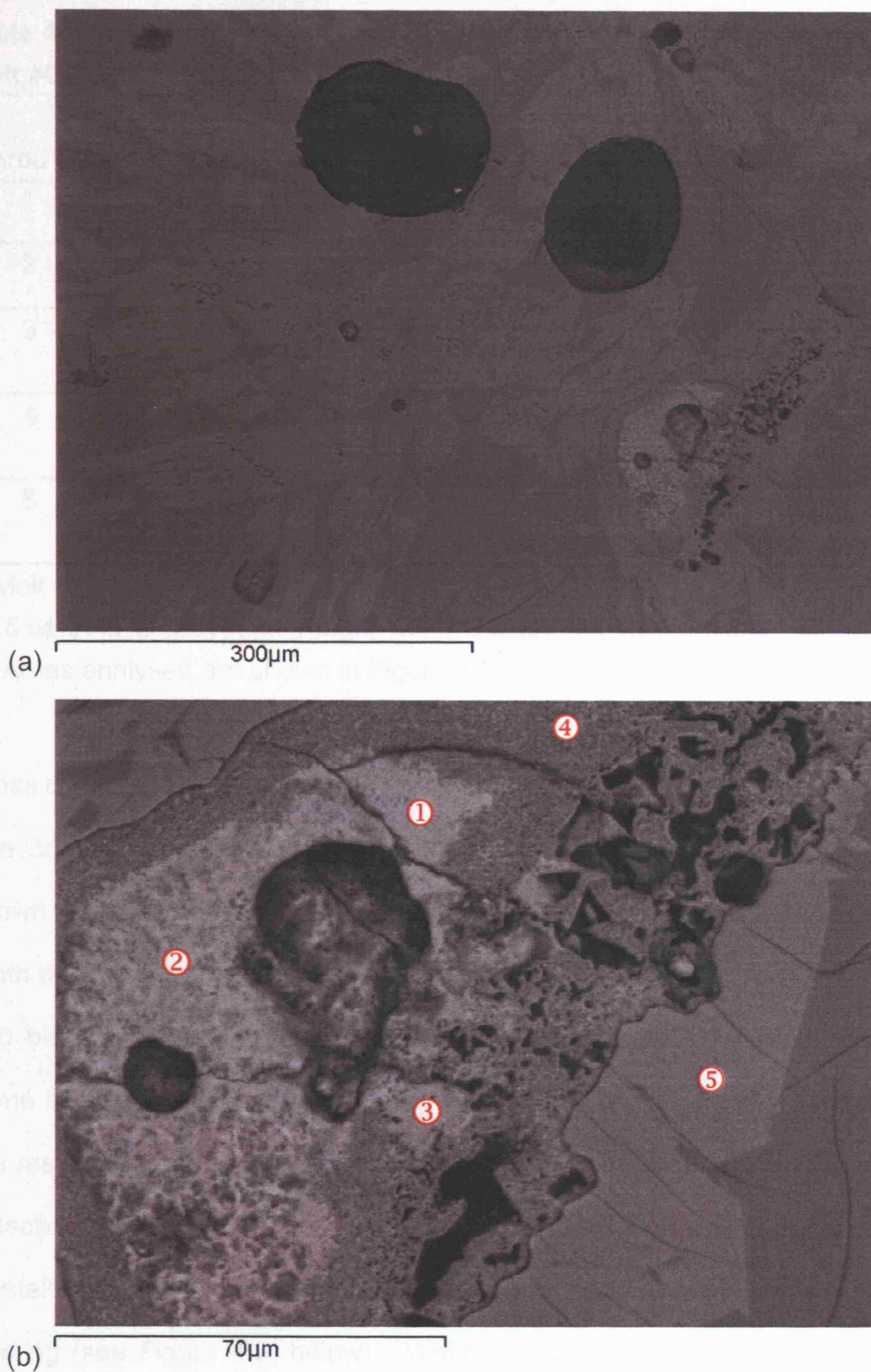


Figure 4.8: SEM (BSE) images showing mixture of various crystalline phases within melt #02 (no MgO, Egyptian trough, 1000 °C isotherm, batch composition, fired at 1000 °C); (a) overview (b) enlarged image showing lime-rich nucleus (numbers show where semi-quantitative data was taken, see Table 4.2).

Table 4.2: Semi-quantitative analysis of various crystalline areas seen in melt #02* (measured by SEM).

Area**	Weight%			Descriptions of the phase
	Na ₂ O	CaO	SiO ₂	
1	3.1	63.4	33.5	White in BSE image.
2	3.0	64.1	32.9	Heterogeneous. Ca-rich phase.
3	7.2	38.5	54.3	White & grey in BSE image. Heterogeneous.
4	12.5	35.0	52.5	Dark grey in BSE image. Heterogeneous.
5	7.2	30.2	62.5	Light grey in BSE image. Homogeneous.

*: Melt #02 has the batch composition of 68.2 wt% SiO₂, 11.3 wt% CaO, and 20.5 wt% Na₂O (Egyptian trough, 1000 °C isotherm, fired at 1000 °C).

**: Areas analysed are shown in Figure 4.8.

Glass composition:

The compositions of batches and their formed glasses, respectively, are shown in Table 4.3 (below). The resulting products of melt #06 and #10 (both belonging to the Roman cotectic trough) were visibly different, with melt #10 being much more crystalline and frothy than melt #06 which showed some clear partial melt of glass forming (see Figure 4.9, below). Similarly, the resulting products of melt # 02 and #14 (both belonging to the Egyptian cotectic trough) were visibly different, with melt #14 being much more crystalline and frothy while melt #02 showed more clear partial melt of glass forming (see Figure 4.9, below). While the amounts of glass differed, the compositions of the glass phase of both melts were almost identical within the analytical accuracy.

Table 4.3: Compositions of glass melt, all fired at 1000 °C (no MgO, Al₂O₃, and Cl in the batch).

melt #	trough	Set batch temperature [°C] and its composition [wt %]				Finished glass composition [wt %]				Note
		temp	SiO ₂	CaO	Na ₂ O	SiO ₂	CaO	Na ₂ O	Total	
06	Roman	1000	73.60	11.60	14.80	73.09	10.25	16.08	99.42	
						73.12	10.19	15.84	99.15	
10	Roman	1100	72.60	15.45	11.95	72.10	10.72	15.66	98.48	underfired
02	Egyptian	1000	68.20	11.30	20.50	68.49	11.28	19.63	99.40	
						67.86	11.42	19.55	98.83	
14	Egyptian	1100	64.20	17.60	18.20	72.00	9.36	19.15	100.51	underfired
						71.79	9.05	19.08	99.92	

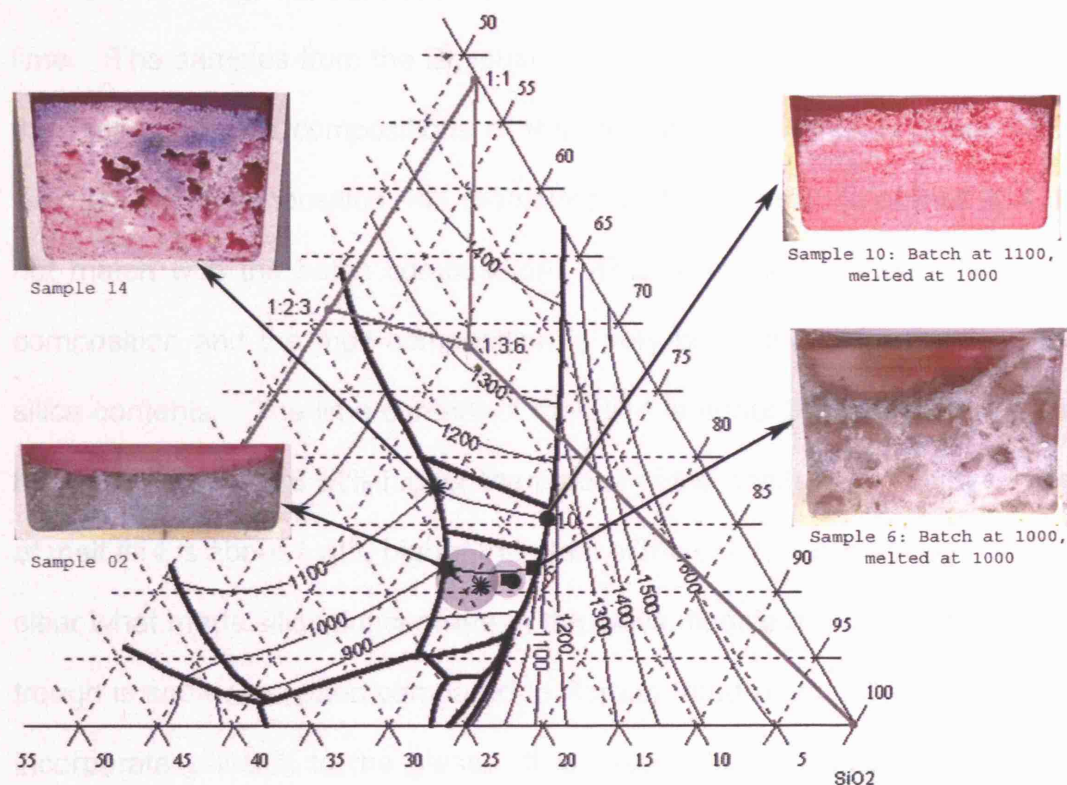


Figure 4.9: Juxtaposition of glass formation and composition for melts #14 (top left), #02 (bottom left), #06 (bottom right), and #10 (top right), all fired at 1000 °C (modified figure from Shugar & Rehren 2002: 4). Their formed glass compositions either from the Egyptian trough or Roman trough were similar and can be plotted in the shaded circle areas, showing that the formed glass composition is determined by firing temperature rather than the initial batch composition.

It is interesting to note that the silica and the lime content in both samples from the Roman trough are about 1 wt% lower than the batch composition of the sample set at 1000 °C; accordingly, the soda content is about 1 to 2 wt% higher than in that overall batch. This difference between the batch composition and the melt composition is much more pronounced for melt #10, set at 1100 °C and underfired at 1000 °C. Here, the silica content of the melt is as set, but the lime content is almost 5 wt% lower, and the soda content is at almost 16 wt%, nearly 4 wt% higher than that of the set composition. Such an increase is only possible with a partial melt which concentrates all the soda in the glass, but not all of the silica, and even less of the available lime. The samples from the Egyptian trough show a peculiar result. While the measured melt compositions of the melt #02 show a fairly good match with the batch composition, the measured melt compositions of melt #14 do not match with the batch composition. This difference between the batch composition and the melt composition is very pronounced for the lime and silica contents. The lime content of melt #14 is about 8 to 9 wt% lower and the silica content is 8 wt% higher than those of the batch. The soda content of melt #14 is about 1 wt% higher than that of the batch. It is not immediately clear what made silica concentrate in the glass, beside the fact that Egyptian trough is soda-rich (when compared to Roman trough) and have more flux to incorporate silica in to the glass. It is reasonable to assume that in this system, silica is much more reactive than lime and therefore enriched in the glass phase.

It is noteworthy that the compositional difference between the batch composition and the melt composition is particularly pronounced for the lime

content regardless of which trough the batch composition was chosen from. In addition, the compositional difference between the batch composition and the melt composition is more prominent amongst the melts from Egyptian trough according to the fired temperature. That is, while melts from Roman trough have similar composition regardless of the batch composition as long as they are fired at the same temperature, melts from Egyptian trough will have very different composition from the batch if not fired at the set temperature. These matters will be discussed in more detail below.

4.3.2. PMM: quality of glass (“Egyptian” vs. “Roman”)

A qualitative comparison of the formed glass fired at the same temperature but belonging to different cotectic troughs, the Egyptian or the Roman trough, was conducted to see whether there is any difference between the two other than their composition.

As seen from initial results shown in Figure 4.9 (above), the quality of glass formed from the Egyptian trough was better (less frothy) than that of the Roman trough even when both were fired at the same ideal temperature. This initial result may suggest that although the Egyptian trough may be more sensitive to the firing temperature, it is easier to form glass in the Egyptian trough than in the Roman trough. Therefore, more work was done to further explore this matter.

The formation of glass occurs much more easily near the soda-rich trough than the silica-rich trough, even for compositions of identical liquidus temperatures. Typically for the Roman silica-rich trough, the total amount of

glass phase visible when fired at the set temperature was far from impressive but enough to form pockets in the residual crystalline matter. In contrast, reasonable glass formation with less and smaller bubbles already occurs in the Egyptian trough at the theoretical/set batch melting temperature, while the Roman trough requires over-firing by at least 50 °C to produce a similar

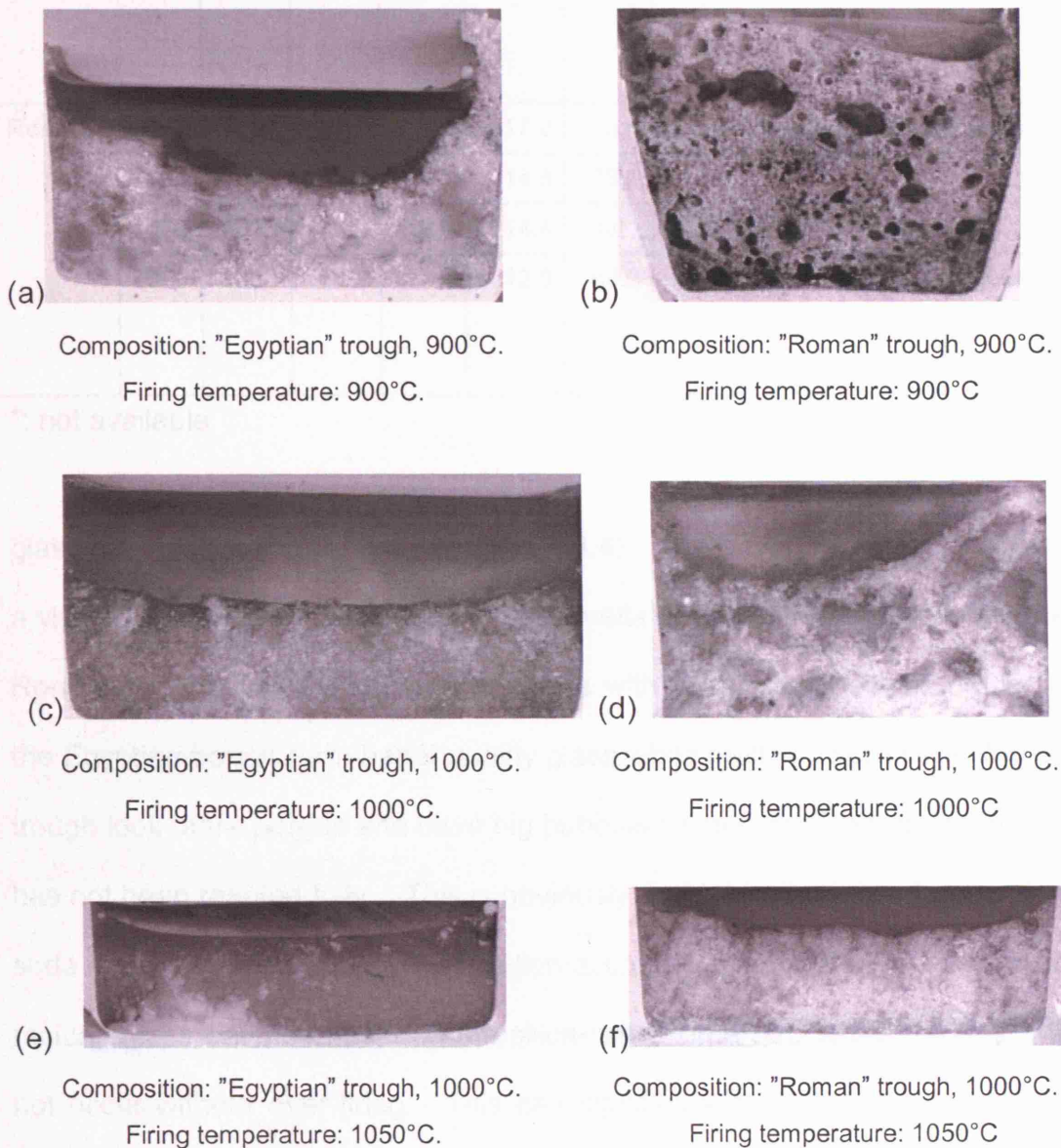


Figure 4.10: (a)~(f) Comparison of the quality of glass produced (images taken by Shugar). Individual batch composition was chosen from both the Egyptian and the Roman trough at the specified temperature and fired at the temperature shown above.

Table 4.4: Compositions of glass melts, prepared for the quality comparison of the formed melts, Egyptian vs. Roman trough.

trough	firing temp [°C]	Set batch temperature [°C] and its composition [wt %]				Average finished glass composition [wt %]				Note
		temp	SiO ₂	CaO	Na ₂ O	SiO ₂	CaO	Na ₂ O	Total	
Egyptian	900	900	69.3	7.8	22.9	68.9	5.7	24.1	98.7	no MgO
	1000	1000	68.2	11.3	20.5	68.2	11.4	19.6	99.2	
	1050	1000	68.2	11.3	20.5	na*	na*	na*	na*	
	1050	1000	64.6	10.7	19.7	70.0	9.0	16.7	96.0 (+ 4.1 MgO)	5wt%MgO
Roman	900	900	74.5	8.3	17.2	73.6	5.4	15.9	94.9	no MgO
	1000	1000	73.6	11.6	14.8	73.1	10.2	16.0	99.3	
	1050	1000	73.6	12.0	14.4	na*	na*	na*	na*	
	1050	1000	74.1	7.9	13.0	68.9	10.4	14.4	93.7 (+ 5.8 MgO)	5wt%MgO

*: not available

glass quality (see Figure 4.10 and Table 4.4). Moreover, Figure 4.11 shows a visible difference of the various formed melts between the Egyptian and the Roman troughs and surroundings. Melts with initial compositions closer to the Egyptian trough form better quality glass while melts closer to the Roman trough look more porous and have big bubbles formed as if the raw materials has not been reacted fully. This is obviously due to the increased amount of soda in the Egyptian trough composition acting as a flux in the glass. When melting glass batches based in the silica-rich, Roman trough, a full melt will not occur without over-firing. This has significant ramifications for furnace design and glass composition and will be discussed in Chapter 7, Archaeological Implications.

In addition, the quality of the formed melts of those having magnesia in the

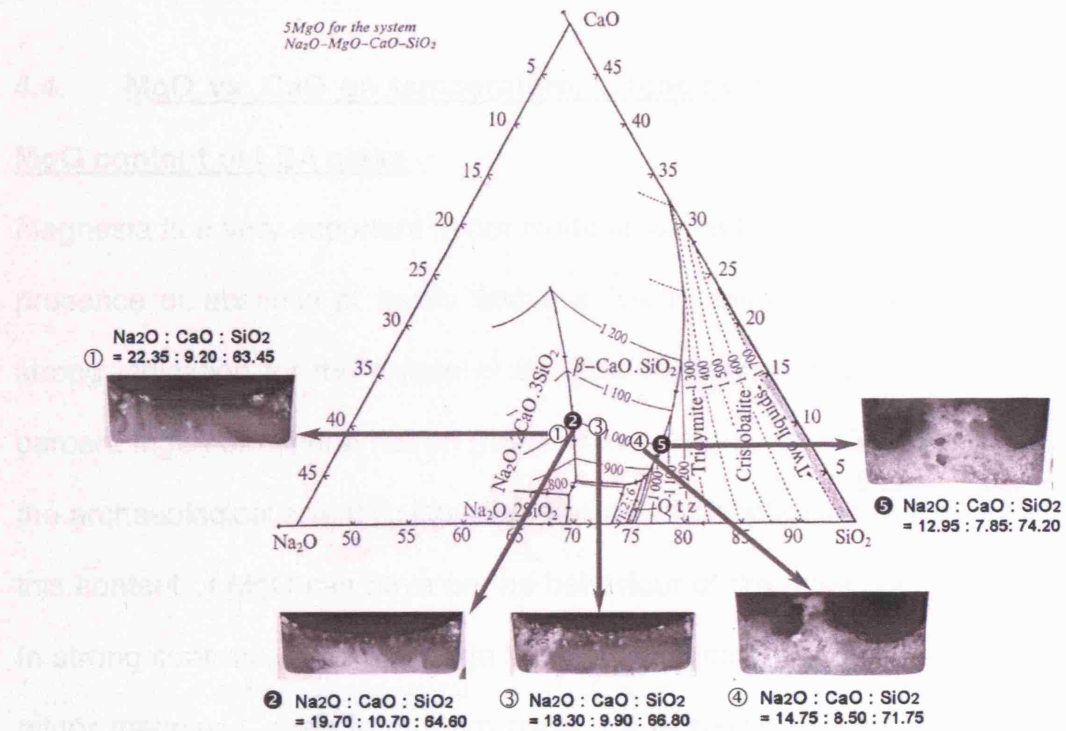
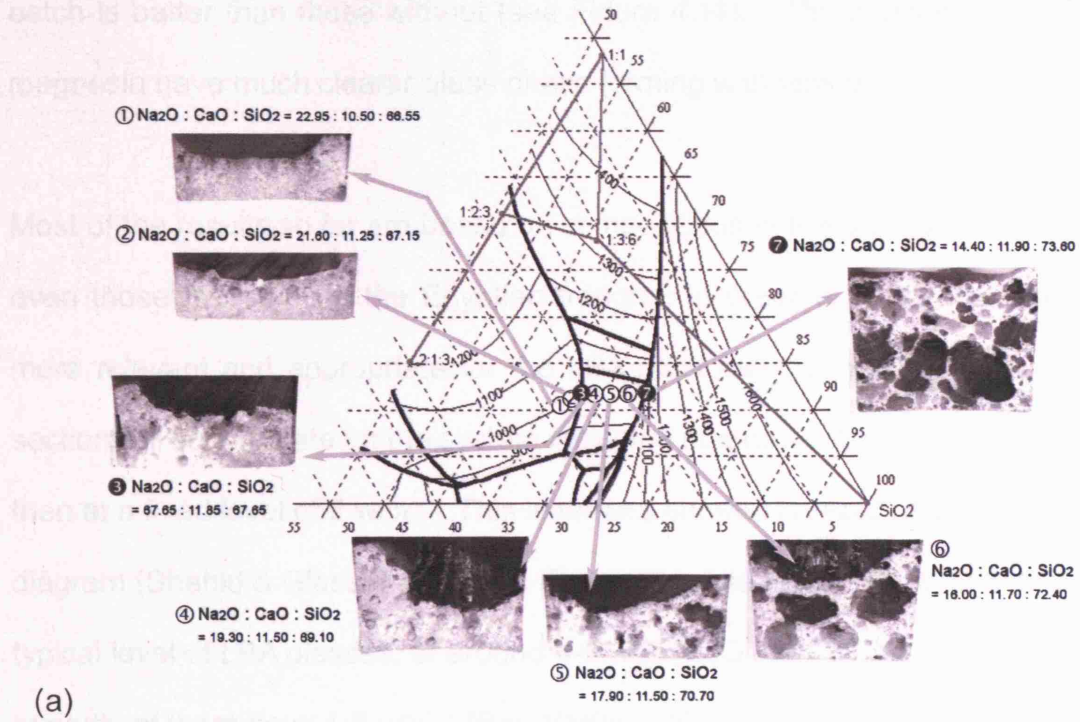


Figure 4.11: Comparison of the quality of glass across 1000 °C isotherm (each batch compositions are shown in wt%). (a) all fired at 980 °C (no MgO). (b) all fired at 1000 °C, with 5 wt% MgO.

batch is better than those without (see Figure 4.11). The melts with 5 wt% magnesia have much clearer glass phase forming with less bubbles.

Most of the results so far are based on compositions in the pure SLS system, even those that refer to the Egyptian trough. In order to make the results more relevant and appropriate for the LBA plant ash glasses, the following section will concentrate on the system including magnesia, first in general and then at a fixed level of 5 wt%. This level was chosen to match the published diagram (Shahid & Glasser 1972: 32; Figure 3), while being very similar to the typical level of LBA glasses, of around 4-5 wt% MgO (overall 3-6 wt%, but the majority of them have 4-5 wt%) (Brill 1999a, 1999b).

4.4. MgO vs. CaO on temperature, viscosity, crystal growth and the MgO content of LBA glass

Magnesia is a very important minor oxide in ancient glass compositions. Its presence or absence at levels above a few percent is usually taken as a strong indication for the nature of the flux, namely plant ash (above a few percent MgO) or mineral natron (below one or two percent MgO). However, the archaeological scientific literature has paid little attention to the effect that this content of MgO can have on the behaviour of the glass, or its formation. In strong contrast, there is a large body of technical literature on the effect of minor magnesia levels in modern glass. It is known that small amounts of magnesia are frequently added to industrial/modern SLS glasses to increase the resistance to devitrification, as mentioned earlier. In the context of my research, it is also important to determine its effect on the liquidus temperature, and on the nature of the crystalline phase appearing as primary

phase in the process of glass melting. The aim of this experiment will be to investigate further the role that the possible crystalline buffer material plays in governing the minor oxide content of the melt.

4.4.1. MgO vs. CaO contents on temperature, and viscosity

Owens-Illinois (1944) studied the effect of substituting magnesia for lime in a 12 wt% CaO base and 10 wt% CaO base SLS glass respectively. The results show that SLS glasses containing CaO and MgO in or up to the dolomitic-lime ratio (i.e. the MgO content of the glass is about 4.4 to 5.0 %, or Ca to Mg ratio about 2:1) have a lower liquidus temperature by up to 80 °C and 50 °C than the respective glasses, containing no MgO. The data for both series had also shown that the total replacement of CaO by MgO results in an increase in liquidus temperature, the increase being greater in the 12 wt% CaO glasses (Owens-Illinois 1944: 222; Figure 1).

The substitution of MgO for CaO results in an increase of viscosity at high temperatures (1150 to 1250 °C) for both series (10 and 12 wt% CaO) of glass throughout the respective composition range. This substitution, however, produces little or no effect on the low-temperature viscosity (at 800 to 900 °C) for compositions up to the dolomitic-lime ratio, but a definite increase in viscosity occurs in composition having a higher MgO content (Owens-Illinois 1944: 223; Figure 2&3).

Therefore, from the results of the effect of MgO on liquidus temperature and viscosity, the optimal melting composition of 12 wt% CaO glass is close to 4 wt% MgO and 8 wt% CaO. Not only is this in accordance with the observed

magnesia to lime ratio in the Egyptian glasses, but also even the primary phase crystallizing on the magnesia-rich side of this eutectic was diopside, as observed in the contact zone, interface between the lime-rich zone of the protective layer and the glass melt, studied by Rehren (1997). The newly formed diopside phase, between formed glass melt and the protective/parting layer, is clearly formed *in situ* by direct contact of glass melt with almost pure lime from the protective material. This diopside phase has equal amounts of magnesia and lime, about 23 wt% each. The formation of this diopside phase seems to have reduced the magnesia content of the adjacent glass by a much larger proportion than its lime content. That is, although the composition of the glass melt formed in this particular crucible sample (FZN 83/0660c) was not available from Rehren's publication (1997: 360), the other Qantir glass samples analysed in his study have an average magnesia content of about 4 wt%, much lower than that of the lime content, about 8 wt%. Rehren's (1997) study demonstrated the interesting example of the potential influence of element partitioning during glass-making, where the saturation of a melt with one component may trigger the precipitation of a multi-element phase and this matter will be discussed in more detail below. Swift (1947: 17; Figure 1) studied the effect of MgO on rate of crystal growth in some SLS glasses. The results show that as MgO was substituted for CaO, the rate of crystal (cristobalite; SiO₂ and devitrite) growth progressively decreased until a minimum rate was reached with about 6 wt% MgO in the glass. However, after this point, the crystals formed changed to diopside and a sodium-magnesium silicate (Na₂O·2MgO·6SiO₂) and the rate of their growth increased with further additions of MgO at the expense of CaO.

Another possibly important buffer material to be considered (in addition to PMM and 2MM) is the fabric of the surface material of the furnace or crucible in which the glass is formed, even though the foremost source for the melt in formation is the batch material. This can be demonstrated for the white, lime-based protective/parting layer of the cylindrical vessels, as mentioned earlier. Rehren (1997) notes that macroscopic evidence indicates only a few areas where the parting layer failed, resulting in glass wetting the siliceous ceramic of the crucible and thus still sticking to the inside of the vessel. This is typically related to (local) over-firing of the ceramic, shown by examination of hundreds of such vessel sherds from Qantir/Egypt, of which an estimated dozen have glass sticking to their interior. EDS analysis of one of the archaeological samples from Qantir showed that the glass within these vessels has twice as much lime than magnesia, i.e. both typical for LBA glass and the ideal ratio as determined by the technical literature. It is important to consider that this glass formed in direct contact with the parting layer that consists of almost pure lime. Rehren's (1997) mineralogical analyses of the reaction zone including the ceramic body, parting layer, and adhering glass revealed the *in situ* formation of a glass phase with similar composition to ceramic body but with 1.0 wt% higher lime content and 1.2 wt% less magnesia content, and diopside crystals ($\text{CaMgSi}_2\text{O}_6$), a phase with an atomic ratio CaO to MgO of 1 to 1 and a weight% ratio of 3 to 2, respectively. This diopside formation reduces the MgO content of the adjacent glass by a much larger proportion than its lime content. This not only in effect caps the magnesia content in glass which is co-existing with a suitable buffer, but more generally illustrates the selective exchange of ions between the melt, its solid surrounding and growing crystals. Thus, the role of the lime-rich layer as a

buffer influences both the total earth alkali content of the melt, and the ratio of lime to magnesia of the melt.

4.5. CaO and chlorine

A further potentially interesting minor component of most archaeological glasses is chlorine. It is typically present at higher concentrations, of around 1 wt%, in LBA glasses than in Roman glasses, where it often only reaches half that value. Chlorine is thought to be a typical component of most fluxes; Brill (1999b, 1999a) reports very variable, and often quite high, chlorine levels for both plant ash and mineral natron (see Table 3.3 and Table 3.4, in Chapter 3). This will be further explored in the next chapter in relation to the alkali content of the glasses. Here, however, it was aimed to explore the possible relationship between chlorine and lime content of the glass. Rehren (2000b) found an approximate inverse correlation between calcium oxide and chlorine content among ancient Egyptian glasses and suggested that the chlorine content may be controlled by the firing temperature. However, when Shugar (Shugar & Rehren 2002) further explored this case, they concluded that the chlorine content in the glass is controlled by its lime content but is neither affected by the soda content nor the melting temperature. Therefore, a series of experiments were conducted to confirm the dependency of chlorine content in the forming glass upon melting temperature and melt composition, re-analysing the experimental melts produced by A. Shugar. In this series of experiments, 2 wt% chlorine (as NaCl) was added to two different series of batch compositions, reducing the amount of soda ash (mainly sodium carbonate) in the batch to account for the contribution of sodium from the salt. For example, 2 wt% Cl (on 100 gram batches) is roughly equivalent to 3.3 g of

NaCl. Therefore, 2.97 g of Na_2CO_3 need to be subtracted from the batch.

A first series of batches (melt #25~28) were chosen along the Egyptian trough with compositions equal to set temperatures from 900 to 1050 °C at 50 °C intervals, and all were fired at 1150 °C to ensure full reaction among the raw materials. The main compositional difference of these batches is the lime content due to the direction of the trough (see Figure 3.3, in Chapter 3). A second series of melts (melt #33~36) was chosen across the 900 °C isotherm. The main compositional differences of these batches are the soda and silica contents, and all were fired at the same temperature of 980 °C to ensure full reaction. The newly obtained compositional data are shown in Figure 4.12, Figure 4.13, Table 4.5 and Table 4.6. Results obtained are almost the same to Shugar and Rehren's (2002) published results.

Results:

A clear inverse correlation was detected between lime and chlorine contents among the melts from the first series (Melt #25~28, see Figure 4.12) while no such trend was found among the melts from the second series (Melt #33~36, see Figure 4.13). The chlorine content is being reduced from an average of 2.0 wt% in melt 25 (an average 7.8 wt% CaO) to an average of 1.3 wt% in melt 27 (an average 14.2 wt% CaO), although all melts were fired at the same temperature of 1150 °C, and sodium contents were maintained around 20 wt% throughout the series (see Table 4.5). In contrast, Figure 4.13 and Table 4.6 show that the soda content in the batch, ranging in this series from 19.8 to 22.1 wt% Na_2O , has little if any influence on the chlorine uptake of the melt. All the melts in this series (Melt #33~36) have similar chlorine and lime

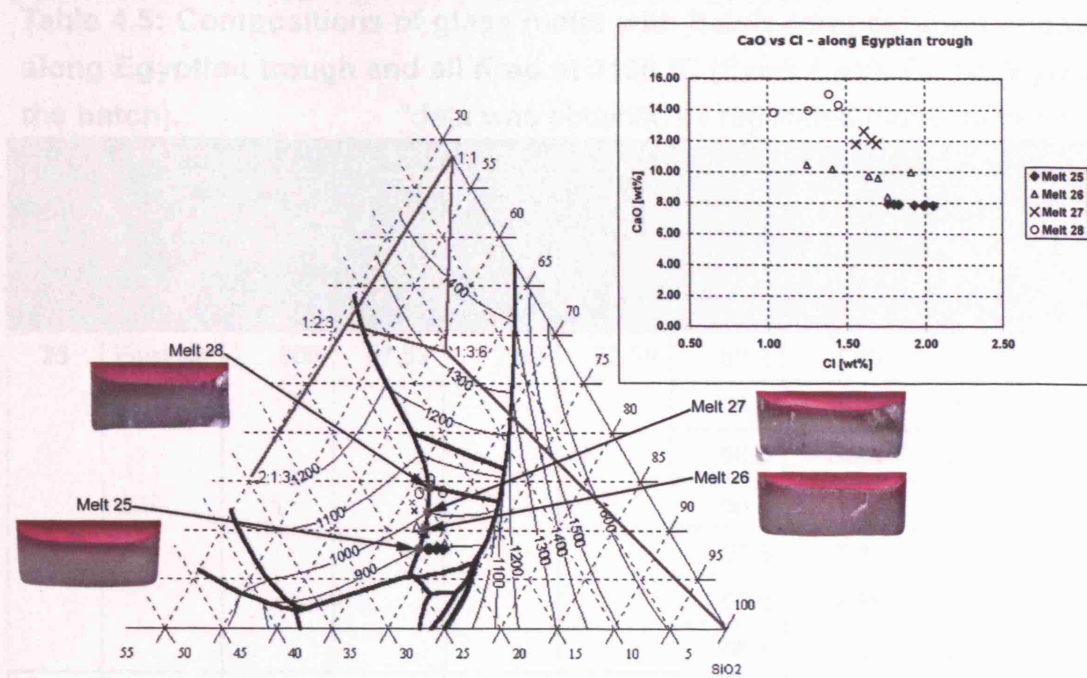


Figure 4.12: Correlation between lime and chloride content in the glass when glass batch compositions were selected along the Egyptian trough (shown as grey circles, respectively).

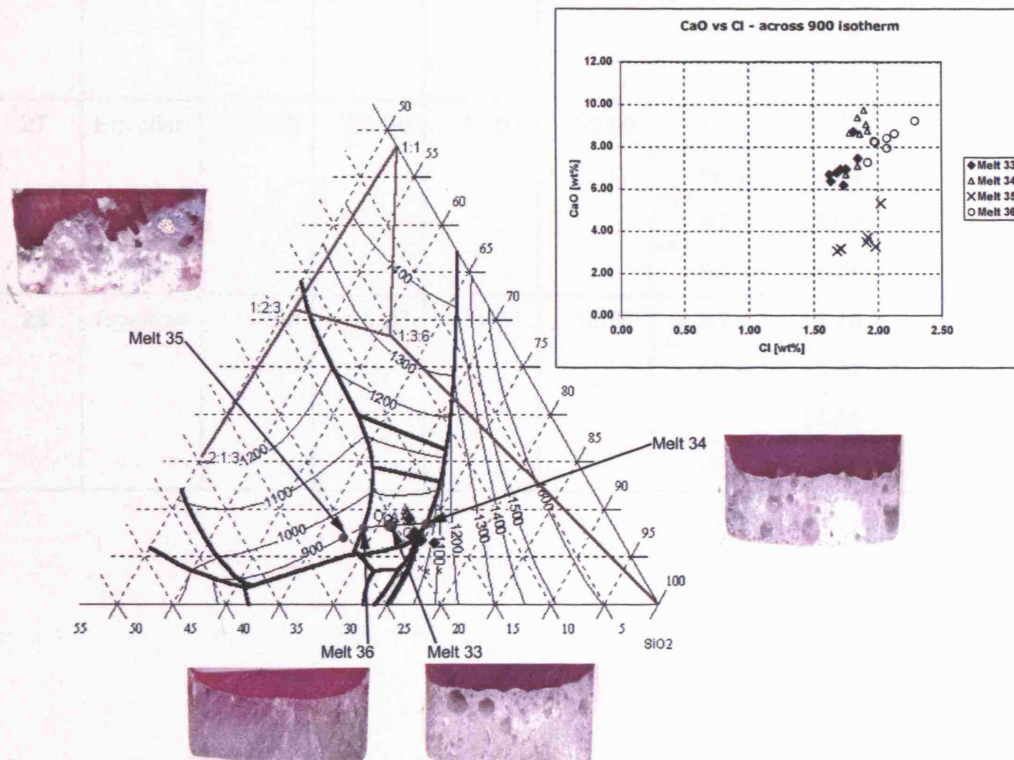


Figure 4.13: Correlation between lime and chloride content in the glass when glass batch compositions were selected along the 900 °C isotherm (shown as grey circles, respectively).

Table 4.5: Compositions of glass melts with batch compositions chosen along Egyptian trough and all fired at 1150 °C (fixed 2 wt% Cl, no MgO in the batch). *data was obtained by replicated measurements.

Melt #	trough	Set batch temperature [°C] and its composition [wt %], all with 2 wt% Cl.				Finished glass composition [wt %]			
		temp	SiO ₂	CaO	Na ₂ O	SiO ₂	CaO	Na ₂ O	Cl
25	Egyptian	900	67.52	7.89	22.59	69.2	7.80	20.1	1.76
						68.9	7.87	21.6	1.80
						68.5	7.86	20.7	1.83
						68.7	7.83	21.9	1.93
						68.8	7.80	21.7	1.99
						69.0	7.86	20.7	2.00
						68.5	7.80	21.4	2.05
26	Egyptian	950	67.03	9.70	21.27	67.2	10.42	21.1	1.25
						69.6	10.14	19.7	1.41
						67.5	9.69	21.2	1.64
						67.4	9.57	21.3	1.70
						67.1	8.35	20.5	1.76
						66.8	9.95	21.6	1.91
27	Egyptian	1000	66.30	11.61	20.09	65.5	11.75	20.9	1.56
						66.2	12.58	19.9	1.61
						65.3	12.03	20.8	1.66
						64.7	11.79	20.7	1.69
28	Egyptian	1050	64.97	14.41	18.62	65.5	13.78	18.1	1.04
						65.8	13.93	18.3	1.26
						67.0	14.99	17.4	1.39
						66.2	14.29	20.0	1.45

Table 4.6: Compositions of glass melts with batch compositions chosen across 900 °C isotherm and all fired at 980 °C (fixed 2 wt% Cl, no MgO in the batch). *data was obtained by replicated measurements.

Melt #	trough	Set batch temperature [°C] and its composition [wt %], all with 2 wt% Cl.				Finished glass composition [wt %]			
		temp	SiO ₂	CaO	Na ₂ O	SiO ₂	CaO	Na ₂ O	Cl
33	halfway between Egyptian and Roman	900	70.70	7.55	20.00	72.3	6.66	18.1	1.62
						72.9	6.35	17.8	1.63
						72.4	6.77	18.3	1.68
						71.9	6.93	17.7	1.71
						73.8	6.18	16.7	1.73
						71.6	6.93	18.2	1.75
						70.7	8.69	17.8	1.81
						71.6	7.42	17.9	1.84
34	Roman	900	72.81	8.23	16.96	71.8	6.67	17.4	1.75
						69.8	8.65	17.5	1.78
						72.3	7.06	17.3	1.84
						70.5	9.36	17.6	1.84
						66.6	8.58	18.0	1.86
						69.2	9.70	17.3	1.89
						70.0	9.04	17.8	1.91
						71.4	8.73	17.5	1.92
35	left side of Egyptian	900	66.64	7.20	24.16	72.8	3.06	21.3	1.68
						73.1	3.17	21.0	1.71
						74.8	3.47	17.3	1.91
						74.1	3.70	19.0	1.92
						74.7	3.27	18.6	1.98
						67.5	5.31	20.7	2.02
36	Egyptian	900	67.86	8.00	22.14	72.2	7.25	18.8	1.92
						70.4	8.25	20.2	1.97
						70.8	8.22	20.0	1.98
						70.8	8.40	19.8	2.07
						69.4	7.92	19.6	2.07
						69.0	8.61	19.7	2.13
						68.7	9.22	20.6	2.29

contents (1.5-2.0 wt% Cl and 6-8 wt% CaO), except for Melt #35, located on the left side of the Egyptian trough (soda-rich region). The surprisingly low lime content of Melt #35 may be due to weighing error or to bad glass formation, as seen from Figure 4.13 that the quality of Melt #35 seems particularly poor (raw materials did not react very well). Therefore, this series of experimental melts were repeated and the same low lime contents were observed again from the melt, which has the same batch composition as Melt #35. However, since glass melting in this region (i.e. left side of the Egyptian trough, soda-rich region) at the higher firing temperature did not show any problem with the quality (see Figure 4.11, above), it was decided not to investigate further on this incidence.

These findings suggest that the chlorine content in LBA SLS glasses is primarily controlled by their calcium oxide content but is affected neither by the soda content nor by the firing temperature. Therefore, chlorine cannot be used as a thermometer, contrary to the earlier suggestion by Rehren (2000b). The observed correlation between lime and chlorine content does exist, but is chemically controlled and not by firing temperature. For the latter, the lime content is a much better indicator, provided one can assume PMM conditions.

4.6. Summary and interpretation for earth alkali contents in SLS glass

Shugar and Rehren's (2002) study had indicated that the concept of partial melts is feasible and probably has a major effect on the melt composition. That is, the production of glass from incomplete melts of batches is feasible

within the technical constraints of ancient glass making practice. The evidence for this can be seen as either a crystalline “cap” above the glass phase, or as pockets of semi-reacted materials within the melt, acting as a buffer for forming glass to draw upon during the melt. The glass phase can then more or less easily be separated from the residual crystalline phase depending on the proportion of glass formed. Following this, re-firing the separated glass fraction at the same or higher temperature at which the initial batch was fired produces a good quality glass ready for coloration or working.

In addition, it has also been shown that during the process of glass formation only a part of the batch fuses to form glass, and that this partial melting produces a glass which is compositionally different from the batch. The difference between batch composition and glass composition is larger for lower melt proportions, and becomes smaller as the amount of melt phase increases until the glass composition reaches the batch composition (minus volatiles) upon complete melting. Incomplete melting is due to two separate, but related effects; reaction kinetics, that is the slowness of reactions taking place, and insufficient temperature to achieve complete melt. In the Late Bronze Age SLS system, characterised by lime as the main buffer material, the calcium oxide content is primarily being controlled by the melting temperature. The experiments showed that the composition of the glass phase regularly matched the composition expected for the melting temperature rather than the initial or set batch composition, with only slight shifts depending on the amount and types of crystals present. The forming melt uses the batch materials, or rather the crystalline material newly formed from reactions within the initial batch material, as a buffer or reservoir to draw

on as the temperature allows. Residual and intermediate phases present in the partially molten material included silica, wollastonite, and the mixtures of phases of lime-rich soda-lime-silicate phases in various ratios, depending on where the phases were found and the firing temperature. A typical distribution of the various soda-lime-silicate phases is shown in Figure 4.6. It represents local heterogeneities of the melt phase near former limestone lumps. The lime rich phase forms a nucleus surrounded by various soda-lime-silicate phases. The compositions of the surrounding soda-lime-silicate phase becomes more rich in silica and soda, having a better reaction among the three, and both Figure 4.6 (underfired) and Figure 4.8 (set temperature) show the nucleus calcium-rich phase diffusing away from the nucleus, as the lime contents of the surrounding phases decreases. It is noteworthy that no soda-rich phase or nucleus formation was observed throughout the samples while residual quartz grains and lime-rich phase were found. This may suggest that within the range of temperature used in this experiment soda melts and reacts quickly and will be distributed into the glassy phase. Moreover, the distribution of the phases, including residual quartz grains, may reflect how the heat is transferred during the glass-forming process. The presence of lime-rich nucleus and/or residual quartz grains may tell us whether the glass/melt was produced by primary glass-making process.

In particular, the results demonstrated that within the pure soda-lime-silica system a batch situated in the soda-rich cotectic trough melts faster and more completely than a batch of the same theoretical melting temperature and similar lime content within the silica-rich cotectic trough. That is, to obtain a

glass (melt) of similar quality in the silica-rich trough ("Roman"), the batch must be over-fired by at least 50 to 100 °C, as compared to the batch in the soda-rich trough ("Egyptian"), situated at the same isotherm. Thus, it is not surprising that early glassmakers used this general ("Egyptian") composition for their glass-making processes. As a result, a typical LBA Egyptian glass tends to plot around the soda-rich cotectic trough, as opposed to Roman glass which forms around the silica-rich cotectic trough. At present, there does not seem to be an inherent factor which would influence the composition of the melt to go either to the Egyptian or the Roman trough; the main difference appears to be the soda content, and as such, it is probably a configurational effect, depending on the overall amount of flux relative to quartz being added to the batch that controls in which cotectic trough the glass finally evolves. This observed phenomenon is clear evidence for the preferred choice of earlier glass-makers for batch compositions closer to the soda-rich cotectic trough for production. This finding probably relates to the lack of suitable refractory materials in the LBA – the clay used for the earliest known melting vessels, LBA glass melting crucibles from Egypt, starts to melt around 1100 °C (Turner 1954a) – which would not allow the over-firing necessary for Roman/Hellenistic glass, stressing the importance of furnace and melting pot design in glass-making practice. The use of a soda-rich batch enabled a suitable melt to occur using less time and/or less overheat to achieve a good quality glass than was necessary for a "Roman" glass composition, with limited fuel requirements and a furnace design within the existing technological reach as defined by ceramic firing and metal melting. Only the progress in furnace design and the development of thermally and chemically more refractory materials from the Iron Age onwards allow the

change to the more silica-rich “Roman” glass formulation (Shugar & Rehren 2002). However, the development of refractory materials is beyond my research object, so it will not be discussed any further.

Owens-Illinois (1944) showed that the substitution of MgO for CaO results in an increase of viscosity at high temperatures (1150 to 1250 °C). This substitution, however, has little or no effect on the low-temperature viscosity (at 800 to 900 °C) for compositions up to the dolomitic-lime ratio. Therefore, the effect of the additional magnesia on the viscosity of the LBA glass melt is insignificant. However, the effect of additional magnesia on the overall temperatures required to melt the LBA glasses is very important. That is, according to published study of Owens-Illinois (1944), the liquidus temperature can drop about 50 °C maximum when there is <5 wt% MgO in the batch, which is the typical magnesia content in the LBA glass.

In addition, Swift (1947) showed that the rate of crystal growth progressively decreased as MgO was substituted for CaO. Thus, the presence of MgO helps to prevent devitrification of glass by increasing viscosity of the melt so the molecules are less mobile to react and form crystals. In fact, the improvement in the quality of formed melts by the presence of MgO can be seen in Figure 4.11.

The results also suggest that the chlorine content in LBA SLS glasses is primarily controlled by their calcium oxide content but is affected neither by the soda content nor by the firing temperature. Therefore, chlorine cannot be used as a thermometer. It is beyond the aim of this project to study the

exact mechanisms controlling chlorine content in glass melts but published work (Gerth *et al.* 1998) shows that the chlorine loss by vaporization as NaCl, or at least Cl from NaCl, below 1200 °C is far too low to be of major effect. An independent recent study by Köpsel (2001) has found that the solubility of halides in glasses does not depend on temperature but rather on the type of halide and the composition of the glass; again, lime rather than soda was found to be the critical oxide. In essence, the investigation of the relationship between the raw materials, the lime content of the glass, and the manufacturing process demonstrate that under Partial Melting Model conditions, and with a lime-rich buffer phase available during the glass-forming reactions, the lime content of the glass is primarily controlled by the melting temperature during glass-making.

Two possible buffer materials that affect earth alkali contents are suggested and discussed here. One is the crystalline phase formed within the glass phase as a result of local heterogeneity, such as semi-reacted raw materials. To identify whether crystals in the glass are indeed residual or semi-reacted raw materials, it is important to establish a way to determine whether the crystalline phase is formed from raw materials or by devitrification. Once this is established, by identifying what crystalline phase(s) is present, one may be able to determine whether a certain archaeological glass was originally made at the site or recycled. The other possible buffer is the fabric of the surface material of the furnace or crucible, in which the glass is formed. This was studied by Rehren (1997) and the interaction between the lime partition layer and the glass was observed, affecting the lime content of the formed glass.

Melting temperatures of around 900 °C, as postulated by Rehren and Pusch (2005) for the initial melting of the raw materials in the reaction vessels, would result in a glass with about 6 wt% CaO, at a nominal level of 5 wt% MgO (see Figure 3.4, in Chapter 3). An increase in temperature to around 1000 °C increases the CaO content to about 10 wt%, provided that a source for the additional CaO is available. In the case of LBA glass-making, this source is the parting layer in the crucibles. In fact, mass balance calculation based on the assumption that the lime present in the parting layer is completely absorbed/transferred into the glass melt, shows the degree of the parting layer effect on the formed glass composition and gives a plausible support to this idea. The parting layer accounts for about 5 % of the volume of a glass ingot by comparing the volume of a typical LBA glass ingot (e.g. about 769 cm³: a typical Uluburun glass ingot, 14 cm diameter x 5 cm thickness) and the volume of the parting layer (0.1 cm thickness) surrounding this glass ingot (about 38 cm³: along its sides and bottom). In addition, by assuming the parting layer is made of pure lime or 50 % lime (the rest being porosity and silica), either additional 5.0 % or 2.5 % (by volume) lime, respectively, will be supplied to the glass on top of the raw materials placed in the reaction vessel. Since density of lime (in general, 3.345, at 20 °C) changes according to the temperature, precise mass balance (in wt%) of lime is not feasible. However, this mass balance calculation highly suggests that at least a few extra wt% CaO can be sourced from the parting layer, if the layer is completely absorbed into the glass phase.

The following section explores the role of the other main minor oxide in LBA glass, potash. It is expected that the addition of potash, in the concentration

range typically found in LBA glasses, may also promote the ease of glass formation. The published data of LBA glass compositions indicate that two different levels of potash exist: most glasses have between 1.7 and 4.3 wt% (average 2.3 wt%) K_2O , while cobalt-blue glass typically has only between 0.5 and 1.9 wt% (average 1.0 wt%) K_2O (Lilyquist *et al.* 1993: 36-39, Shortland 2000b: 17, Tite & Shortland 2003: 286). It is unlikely that the potash content is controlled via a crystalline buffer material, as no likely crystalline phase for this is known. On the other hand, the results of the study of the solubility of chlorine in glass and the published analyses of plant ash indicate that much salt will be present during glass-making. Therefore, the partitioning of potassium between co-existing silicate and chloride phases may play a role in controlling the potash content of the glass. This is explored in detail in the next chapter.

Chapter 5: Melt-Melt Interactions

(“two melts model - 2MM”, alkalis)

The previous chapter explored the interaction of earth alkali concentrations, batch compositions and firing temperatures, and has demonstrated that there is a clear and direct correlation between composition and temperature, provided that a suitable buffer or excess material is present. However, it is long known that another major factor of chemical variability within LBA glasses concerns their alkali concentrations, both in absolute terms and in the ratio soda to potash. Several key issues are to be considered here. It is long known (Sayre 1967, Sayre & Smith 1974) that the LBA plant ash glasses are characterised by somewhat higher potash content than the later Hellenistic and Roman glasses that are based on mineral natron as the flux. This difference is explained by the similar differing soda to potash ratios of plant ash and mineral natron, respectively. However, LBA cobalt-blue glasses are an exception from this rule, having a much lower potash content than other LBA glasses, and more in line with mineral natron based glasses. Their overall alkali content, though, is as high as that of other LBA glasses, indicating that the soda to potash ratio is very different for cobalt-blue and normal LBA glasses. This compositional phenomenon is long known (Sayre & Smith 1974), but a causal explanation for it has been missing so far. Shortland and Tite (2000) suggested that it may in fact be due to the use of mineral natron for this glass colour only. Rehren (2001) challenged this interpretation, mostly on technical grounds, leading to a re-consideration of the evidence and tentative acceptance of a plant-ash based nature of these glasses, possibly diluted with some soda-rich component from the preparation

of the cobalt-containing colorant (Tite & Shortland 2003). At about the same time, Rehren (2000a, 2000b) pointed out that LBA and Roman glasses occupy fundamentally different regions in the soda-lime-silica diagram, characterised by different silica to total alkali contents of the two glass groups. He identified a close relationship of the glass compositions to the eutectic troughs of the ternary systems and suggested that these eutectic troughs govern the overall glass composition; however, no factor was identified which would influence either the ratio of silica to total alkali concentration or the ratio soda to potash in such a way as to explain the observed pattern in the glass compositions.

The presence of non-reactive components, mostly chlorides and sulphates, in the ancient glass batch has been known for centuries, and much industrial research and development work has focussed on making these salts either useable in the glassmaking process, or to reduce their presence in the batch material. Turner (1956c) was probably the first to point out their presence in ancient glass-making. Subsequent experimental work has repeatedly shown their occurrence in major quantities in most plant ashes (Jackson *et al.* 2005, Jackson & Smedley 2004). Also the available analyses of plant ashes and mineral natron (Brill 1999b, 1999a, Tite *et al.* 2006) indicate that both are likely to contain high but variable levels of non-reactive salts, indicating that this aspect is of potentially real significance in ancient glass-making. However, no systematic study of their influence on the composition in the co-existing glass melt has been published. It is the aim of this chapter to begin to investigate the relationship between co-existing silicate glass melt and chloride salt melt under conditions relevant to ancient glass-making

practice. Particular emphasis is placed on the influence that the presence of a salt melt has on the ratio of soda to potash in the silicate melt, and on the relative availability of sodium and potassium for glass-forming when they are provided as either carbonate or chloride. These substantial amounts of non-reactive salts as part of the flux are forming a system of two immiscible melts, the salt buffering the composition of the forming glass, as mentioned above (see Chapter 3). The effect which this has on the potash content of the glass will be investigated in this section.

5.1. Review of the literature

There are only limited relevant published studies on the solubility and the distribution of alkalis between the two melts, glass (silicate) melt and salt melt. Turner (1939) tested the maximum solubility of sodium chloride, the most common chloride to exist in raw materials, in SLS glass by preparing experimental SLS glass samples with various amounts of excess sodium chloride added to the batch, fired at 1400 °C. He determined that there is a maximum chloride content in the glass regardless of the amount of excess NaCl added, suggesting that chlorine content is controlled by the nature of the melt rather than the batch composition, and that there is a limit how much chlorine goes into the glass phase. However, Turner (1939) did not mention anything about the mechanism by which excess NaCl was removed from the glass melt. This could have formed a separate melt, known as galle in traditional glass-making, or evaporated (Gerth *et al.* 1998).

Solubility of chlorine has been much more studied in naturally occurring two-melts system, namely magma. Carroll and Holloway (1994) studied the

partitioning behaviour between melts and aqueous fluids co-existing in magma, in different compositions and conditions, and their data showed low chlorine solubility in silicate melts with a preference for chlorine to concentrate in the co-existing aqueous phase. However, chlorine solubility in silicate melts increased as the amounts of calcium and sodium increased in the magma. The effects of magma composition, pressure, and temperature on the partitioning remained unknown, but are likely to have been significant.

Gammon and co-workers (1969) studied the distribution of potassium and sodium between silicate melts and aqueous chloride solutions using experimentally prepared SLS glass samples, fired between 770 and 880 °C. They noted that the distribution coefficient of potassium and sodium between the aqueous and silicate phase was independent from not only the chloride concentration of the aqueous phase but also from the duration of the firing time in excess of 24 hours. The measured ratio of alkalis in the aqueous phase ($m_{K,aq}/m_{Na,aq}$, where m represents mole per kilogram) was 0.74 ± 0.06 times that of the coexisting silicate melt ($m_{K,silicate}/m_{Na,silicate}$) over the whole range of the temperature used. That is, the value of distribution coefficient of alkalis between the aqueous and the silicate phase ($K_{K,Na} = (m_{K,aq}/m_{Na,aq}) / (m_{K,silicate}/m_{Na,silicate})$) remained consistent around 0.74 regardless of chloride concentrations. For example, the ratio of alkalis in an aqueous phase ($m_{K,aq}/m_{Na,aq}$) is 0.57, between 770° and 880 °C, regardless of the chlorine content. Therefore, the ratio of alkalis in the co-existing silicate melt ($m_{K,silicate}/m_{Na,silicate}$) between 770° and 800 °C is 0.77. Unfortunately, whether one alkali has more tendency to be distributed into the same melt over another alkali is unknown since the exact amount of the alkalis initially

added to the batch is unclear from the publication (since they mixed various alkali-containing minerals to produce the experimental melts). These findings suggest that there is a fixed value of distribution coefficient of alkalis between the two phases (silicate melt and aqueous solution), controlling the alkali ratio in the glass (silicate melt) regardless of the salinity of the aqueous solution that co-exist with the glass phase. In these conditions, sodium has a higher preference for aqueous solution than potassium, which in turn is more enriched in the silicate melt.

However, these geological experiments are not directly comparable to the situation in ancient glassmaking, due to the presence of water and high pressure in the system. Therefore, this thesis presents some basic exploration of the distribution of potassium and sodium between salt melt and silicate melt.

5.2. Na₂O/K₂O System – 1

A total of seven series of batches with different alkali contents were prepared in this section to investigate the partitioning and distribution of alkalis between glass and salt melt, that is whether there is any preference among alkalis for one of the two melts in the extreme scenario. The base glass composition chosen for these series was defined by the crossing of the soda-rich eutectic trough and the 1000 °C isotherm in the SLS system with 5 wt% MgO (Shahid & Glasser 1972). This composition was defined as 65 wt% SiO₂, 19.5 wt% Na₂O, 10.5 wt% CaO, and 5 wt% MgO. Each series consisted of three melts, fired at the same time in the furnace at 1050 °C with increasing amounts of potash substituting for soda. Base A-4 was designed to contain 0.5 wt%

potash, Base A-5 to contain 1.7 wt% potash, and Base A-6 to contain 2.5 wt% potash, each with the potassium provided in the batch as potassium chloride rather than potash (potassium carbonate). Series 2-1 was run to see whether there is any effect of chlorine when there is no excess amount of chloride co-existing (chlorine is only added to the batch as a source for potassium, by adding increasing amounts of KCl while decreasing the amount of soda ash) as a baseline for the following experiments. More specifically, Series 2-2 to 2-7 (see below) were designed to test whether the presence of an excess amount of alkali chloride affects the ratio of sodium to potassium in the glass melt, if both alkalis co-exist in the initial batch, as initially suggested by Rehren (2001). For this, two different forms of chloride were used; first NaCl (Series 2-2 to 2-4) and then KCl (Series 2-5 to 2-7) to test whether the initial form of chloride salt in the batch affects the alkali partitioning.

(Recipe-1) Na₂O/K₂O System – 1 (base batches)

Base A-4 (100 g/batch) = 65.0 wt% SiO₂ (65.0 g of sand), 10.5 wt% CaO (18.8 g of CaCO₃), 5.0 wt% MgO (5.0 g of MgO), 18.5 wt% Na₂O (32 g of soda ash), and 1.0 wt% K₂O* (0.79 g potassium chloride, KCl = 0.5 wt% K₂O).

Base A-5 (100 g/batch) = 65.0 wt% SiO₂ (65.0 g of sand), 10.5 wt% CaO (18.8 g of CaCO₃), 5.0 wt% MgO (5.0 g of MgO), 16.2 wt% Na₂O (28 g of soda ash), and 3.3 wt% K₂O* (2.6 g potassium chloride, KCl = 1.7 wt% K₂O).

Base A-6 (100 g/batch) = 65.0 wt% SiO₂ (65.0 g of sand), 10.5 wt% CaO (18.8 g of CaCO₃), 5.0 wt% MgO (5.0 g of MgO), 14.5 wt% Na₂O (25.0 g of soda ash), and 5.0 wt% K₂O* (3.95 g potassium chloride, KCl = 2.5 wt% K₂O).

* Note: It was planned to use such quantities of raw materials as necessary

to produce 100 g of glass, so that grams of each oxide in the batch equal the weight percent of that oxide in the glass. However, in these batches the oxides in the batches do not add up to 100 wt% due to miscalculation by the author when converting the target K_2O value into KCl to be added to the batch. The weights shown in the brackets here are the actual amounts that were added to the batch, resulting in increasingly lower batch weights as the potash content increases. This has to be considered when comparing the analysed glass compositions to the oxide contents of the prepared batches.

Results:

The formation of glass occurs in all series of melts (Series 2-1 to 2-7), but the degree of separation between glass melt and salt melt differs from sample to sample. Most of the melts produced a residual salt phase that solidified as a salt layer over the glass phase. The spatial separation of glass and residual salt material was generally good enough to allow mechanical separation, especially when more than about 1/6 of the total material appeared as salt phase (over the glass phase) after firing (by simple hand picking or by cracking the salt layer) (see Figure 5.1). Only the melts of A-4 and A-5 did not produce a separate salt layer but formed a clear glass phase without any visible residual salt phase on top. These melts contained an initial amount of less than 1 g Cl, added as KCl. Only for sample A-6, containing 1.4 g Cl as KCl in the batch, there was a little amount of visible opaque residual salt phase over the transparent glass phase, which was almost impossible to separate mechanically from the glass phase. In addition, Base A that contains no chloride formed a clear glass without any residual phase when it was prepared initially before this series of experiments.

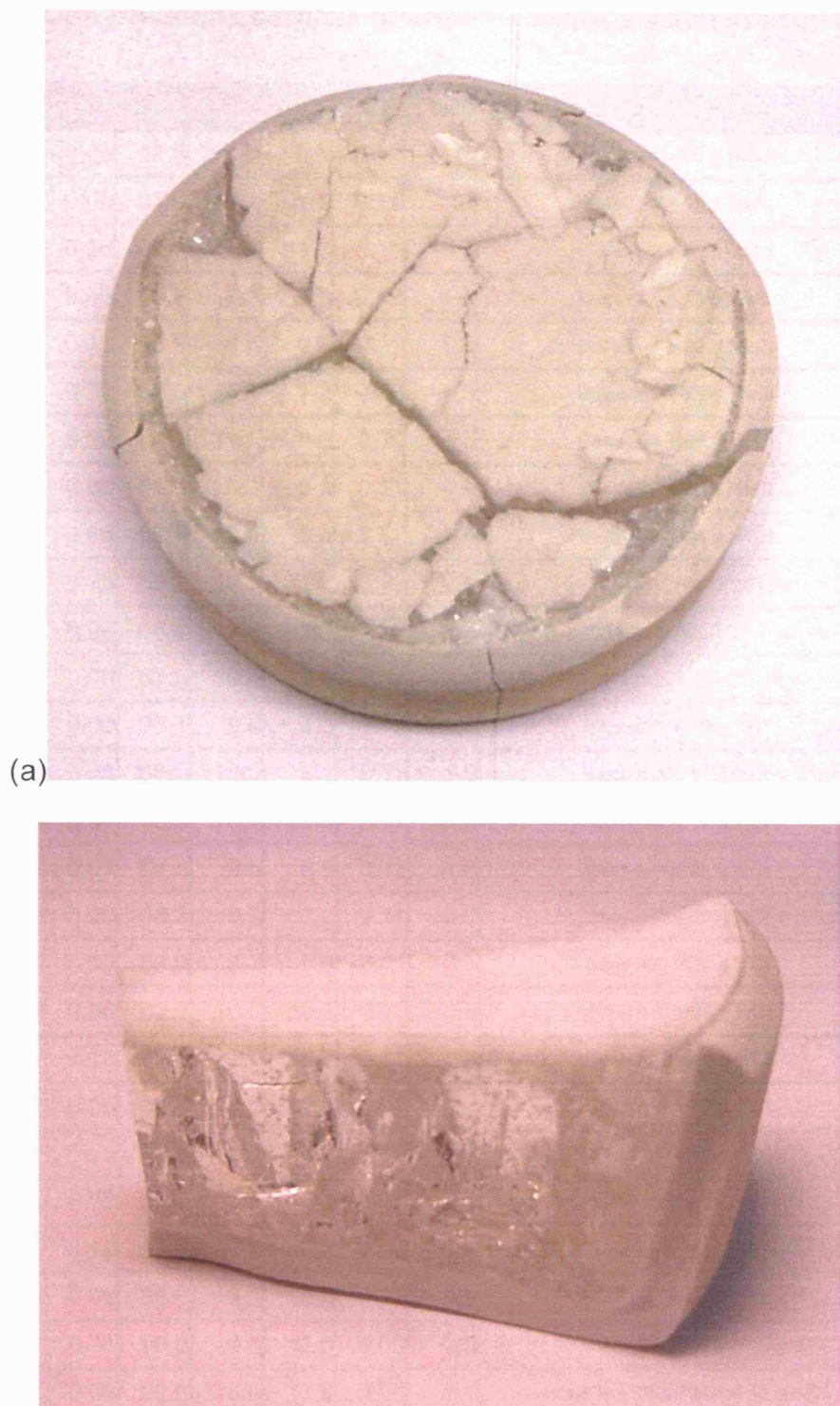


Figure 5.1: Spatial separation of glass and residual salt material (clear glass phase can be seen below the residual salt material). (a) above and (b) cross section.

Table 5.1: Compositions of glass melts with various alkali concentrations [wt%].

Na ₂ O	MgO	Al ₂ O ₃	SiO ₂	CaO	K ₂ O	SO ₃	Cl	Sample Description	
16.3	5.2	0.08	67.3	10.6	0.5	0.12	1.5	Base A-4 + 10 g NaCl	Series 2-2
18.5	59.1	0.06	63.9	11.1	1.1	0.11	1.5	Base A-5 + 10 g NaCl	
14.7	4.4	0.08	67.7	9.4	1.5	0.11	1.3	Base A-6 + 10 g NaCl	
18.3	4.0	0.09	65.8	8.2	0.5	0.12	1.7	Base A-4 + 20 g NaCl	Series 2-3
14.3	4.4	0.12	68.9	8.8	0.9	0.11	1.3	Base A-5 + 20 g NaCl	
15.2	4.5	0.09	67.0	9.5	1.2	0.12	1.3	Base A-6 + 20 g NaCl	
18.8	4.4	0.09	64.1	11.4	0.2	0.11	1.8	Base A-4 + 50 g NaCl	Series 2-4
17.0	5.0	0.09	66.3	10.3	0.4	0.11	1.5	Base A-5 + 50 g NaCl	
16.7	4.3	0.05	67.5	10.4	0.6	0.11	1.5	Base A-6 + 50 g NaCl	
18.5	4.7	0.13	65.2	11.1	0.6	0.12	0.4	Base A-4: 18.5 wt% Na ₂ O*, 0.5 wt% K ₂ O*	Series 2-1
16.3	4.5	0.08	66.1	11.0	1.7	0.13	1.2	Base A-5: 16.2 wt% Na ₂ O*, 1.7 wt% K ₂ O*	
14.4	4.4	0.06	67.5	10.6	2.6	0.13	1.2	Base A-6: 14.5 wt% Na ₂ O*, 2.5 wt% K ₂ O*	
14.6	4.7	0.09	66.1	9.4	4.3	0.12	1.0	Base A-4 + 10 g KCl	Series 2-5
12.7	4.8	0.08	66.2	10.0	5.1	0.11	1.0	Base A-5 + 10 g KCl	
13.2	4.9	0.07	65.5	10.1	5.5	0.11	1.0	Base A-6 + 10 g KCl	
11.6	3.9	0.07	67.5	9.5	6.8	0.11	1.0	Base A-4 + 20 g KCl	Series 2-6
11.9	4.3	0.09	66.3	9.9	7.2	0.11	0.9	Base A-5 + 20 g KCl	
10.4	3.5	0.09	68.9	8.7	7.8	0.11	0.8	Base A-6 + 20 g KCl	
11.3	4.4	0.08	62.0	10.3	10.1	0.11	0.8	Base A-4 + 50 g KCl	Series 2-7
9.0	4.2	0.10	65.8	9.4	10.7	0.11	0.8	Base A-5 + 50 g KCl	
7.6	4.1	0.05	67.4	8.4	11.2	0.11	0.7	Base A-6 + 50 g KCl	
5.0	4.0	0.14	56.9	9.1	24.7	0.01	0.0	Base A-7: 5 wt% Na ₂ O**, 25.5 wt% K ₂ O**	Series 3-1
9.5	4.3	0.11	59.2	9.7	16.3	0.02	0.0	Base A-8: 10 wt% Na ₂ O**, 17 wt% K ₂ O**	
14.1	4.8	0.12	62.2	9.3	8.5	0.01	0.0	Base A-9: 15 wt% Na ₂ O**, 8.5 wt% K ₂ O**	
8.2	4.0	0.09	58.8	9.5	18.3	0.01	0.8	Base A-7 + 10 g NaCl + 10 g KCl	Series 3-2
12.3	4.2	0.11	58.8	9.8	12.5	0.00	0.9	Base A-8 + 10 g NaCl + 10 g KCl	
14.0	4.2	0.08	62.0	10.0	7.6	0.00	1.1	Base A-9 + 10 g NaCl + 10 g KCl	
11.8	4.0	0.10	59.6	9.5	14.3	0.00	0.9	Base A-7 + 25 g NaCl + 25 g KCl	Series 3-3
13.5	3.9	0.09	61.5	9.5	10.0	0.00	1.0	Base A-8 + 25 g NaCl + 25 g KCl	
15.3	3.8	0.09	61.6	9.8	7.2	0.00	10.9	Base A-9 + 25 g NaCl + 25 g KCl	

Na₂O*, K₂O*: added as Na₂CO₃ and KCl respectively to the batch (100 g).

Na₂O**, K₂O**: added as Na₂CO₃ and K₂CO₃ respectively to the batch (100 g). In addition, for potassium content, these values were obtained by applying a factor of 1.7 to the intended amount (e.g. 15, 10, 5 wt% K₂O) in order to balance the number of potassium atoms with that of sodium in the batch.

The analytical results (Table 5.1) of series 2-1, that is the three base glasses A-4 to A-6 with no further added salt, are in close agreement with the weighed-in batch compositions. (Note that the measured silica content in Base A-4 to Base A-6 increases from 65.2 to 67.5 wt%, although in each case 65.0 g SiO₂ were added to the batch. This increase reflects the decreasing total batch weight as mentioned above, resulting in an increase of the silica percentage in the resulting glass. This increase affects pro rata all oxides in the glass, but is most noticeable for the main oxide, silica.) Significantly, the potash content mirrors closely the amount of potassium added as potassium chloride. The chlorine content of the glass is slightly higher than expected; Base A-4 had 0.3 g Cl added as KCl, and the resulting glass has 0.4 wt% Cl. Base A-5 had 0.9 g Cl added, and the glass had 1.2 wt% Cl, indicating that there is another source of chlorine in the batch than the added KCl, possibly impurities in the raw materials. Unfortunately, since chemical composition of the Base A (no Cl added to the batch) melt is unavailable, especially for chlorine reading, it is not possible to confirm whether there is any chlorine in the raw materials as a contamination. However, this possibility is indicated by the presence of 0.1 wt% SO₃ in all analyses (see Table 5.1).

Notably, Base A-6, which contained an estimated 1.4 g of Cl in the batch added as KCl produced a glass with the same 1.2 wt% Cl as the previous glass, despite more chlorine being available in the batch. This indicates that the total chlorine content is capped somewhere near this value. Experiments described in the previous chapter have shown that the total chlorine content of a glass is controlled by the amount of lime in the glass, with chlorine solubility decreasing with increasing lime content. Melt 28 has the comparable lime

content to Base A-6 (14.4 wt% CaO in Melt 28, 10.5 wt% CaO and 5 wt% MgO in Base A-6). The average chlorine content in Melt 28 is 1.3 wt%, very similar to the 1.2 wt% Cl measured in Base A-6. This interpretation of a saturation of the glass in chlorine is further supported by the appearance of a small amount of visible residual salt melt on top of the glass melt, as mentioned earlier.

This experiment has shown that potassium chloride is not completely non-reactive in glass-making. However, its contribution to glass-forming is limited by the amount of chlorine which can be absorbed into the glass, typically of slightly more than 1 wt% Cl, equivalent to about 1.7 to 2 wt% potash. Any additional chlorine will not be incorporated into the glass. Experiments by Gerth *et al.* (1998) have demonstrated that the volatility of chlorine from glasses is very low at temperatures below 1400 °C, and therefore it is unlikely that much chlorine will leave the system as gas. Accordingly, it is likely to form a salt melt, as visually observed. For the salt melt to form, it requires a stoichiometrically defined matching amount of metal ions, and therefore no additional metal ions are added to the melt. Supplementary X-ray fluorescence (XRF) analyses of the excess salt phase from initial screening experiments have shown that these metal ions are invariably alkali metal ions and not earth alkali metal ions (data shown in Appendices). Thus, the chlorine in the excess salt melt requires a molar equivalent of potassium or sodium. This is naturally present as the metal component of the added salt.

The following experiments were done to explore whether potassium has the

same likelihood to enter into the salt melt as sodium, or whether one alkali metal has a stronger affinity to the salt melt than the other, and is accordingly depleted in the silicate melt. In the first series (2-2 to 2-4), it explores how the amount of excess common salt, sodium chloride, has an effect on the potash uptake in the glass, and whether there is a threshold value which can not be removed ('washed out') unless unrealistically high salt quantities are assumed.

5.2.1. Base A-4, 5, 6 + NaCl (series 2-1 to 2-4)

The layout of experiments for this section is as follows;

- Series 2-1: 3 batches; Base A-4, A-5, A-6.
- Series 2-2: 3 batches; Base A-4, A-5, A-6, with additional 10 g sodium chloride, NaCl, respectively.
- Series 2-3: 3 batches; Base A-4, A-5, A-6, with additional 20 g sodium chloride, NaCl, respectively.
- Series 2-4: 3 batches; Base A-4, A-5, A-6, with additional 50 g sodium chloride, NaCl, respectively.

Results:

Series 2-1 had shown that, if there is no additional NaCl in the initial batch, almost all of the potassium present in the batch as potassium chloride goes into the glass phase as long as the solubility of chlorine in the silicate melt is not exceeded, resulting in 0.6, 1.7, and 2.6 wt% K₂O, respectively, in the three melts.

However, the situation changes with the addition of sodium chloride (see

Table 5.2). In the series with 10 g NaCl added to the batches with 0.8 g, 2.6 g, and 4.0 g KCl respectively, the resulting glass has a potash contents of 0.5, 1.0, and 1.5 wt% respectively. The next series, with 20 g NaCl added, resulted in glass with 0.5, 0.9, and 1.2 wt% K₂O, respectively. The third series finally, with 50 g NaCl added, produced glass with only 0.2, 0.4, and 0.6 wt% K₂O, respectively. Very clearly, if there is additional NaCl in the batch, the amount of potassium that goes into the glass phase decreases as the additional amount of NaCl increases (see Figure 5.2). Two fundamental observations stand out: the higher the initial potash levels are the more are they affected than those with lower initial potash levels, and the more common salt is present, the less potash enters the glass. This, however, does not in itself indicate any interaction of the salt melt with the glass melt other than the limited addition of alkali chloride from the salt phase, as already identified in the first series of experiments.

A remarkable feature is the amount of potassium that enters into the glass as a proportion of the total alkali metals present in the batch as chlorides. Base A-4 with 10 g NaCl added has only 0.8 g KCl in it; less than one tenth of the NaCl amount. Despite this, almost all potassium enters into the glass melt, while only a small proportion of the sodium goes additionally into the glass. Similarly, in Base A-6 with 4 g KCl (equal to c. 2.1 g K) and 10 g NaCl, almost one third of the potassium goes into the glass (c. 1.2 g K, expressed as 1.5 wt% K₂O in 118 g/batch; $118 \times 0.015 \times 2K(\text{atomic weight})/K_2O(\text{molecular weight}) = 2 \times 39 / (2 \times 39 + 35.5)$), while hardly any of the additional sodium enters into the glass. At higher amounts of added sodium chloride the absolute figures change in favour of sodium uptake, that is less potassium enters the

Table 5.2: Potassium oxide contents of glass melts with various alkali concentrations (extra alkalis, either NaCl or KCl was added) [wt%].

Base Batch*	Amount of additional NaCl [wt%] added to the batch (100g/batch). Series 2-1 to 2-4.				Amount of additional KCl [wt%] added to the batch (100g/batch). Series 2-1, 2-5 to 2-7.				Note
	0	10	20	50	0	10	20	50	
A-4	0.6	0.5	0.5	0.2	0.6	4.3	6.8	10.1	includes 18.5 wt% Na ₂ O**, 0.5 wt% K ₂ O**
A-5	1.7	1.0	0.9	0.4	1.7	5.1	7.2	10.7	includes 16.2 wt% Na ₂ O**, 1.7 wt% K ₂ O**
A-6	2.6	1.5	1.2	0.6	2.6	5.5	7.8	11.2	includes 14.5 wt% Na ₂ O**, 2.5 wt% K ₂ O**

Base Batch*: All the Base Batch has 65.0 wt% SiO₂, 10.5 wt% CaO, 5.0 wt% MgO.

Na₂O**, K₂O**: added as Na₂CO₃ and KCl respectively to the batch (100 g/batch).

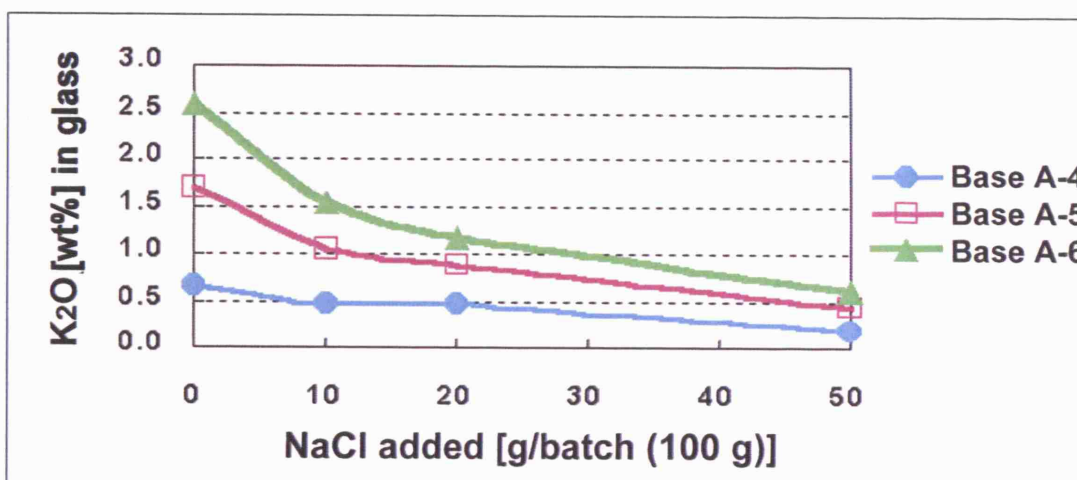


Figure 5.2: Potash content in the glass with increasing amount of NaCl. The minimum potash content in the glass is approximately 0.5 wt%.

glass melt. From batch Base A-6 with 4 g KCl and 50 g added NaCl, only 0.6 wt% K₂O enter the glass, compared to 2.6 wt% in Base A-6 with no added NaCl (above, Series 2-1). The proportional uptake of potassium, however, is much higher than that of sodium, as is evident when the ratio of KCl to NaCl

(4 (gram) to 50 (gram), or 8 %) added as salt is compared to the amount of K_2O (0.6 wt%) in the glass, which is almost 25 % of the maximum possible (2.6 wt%). It appears that under these conditions and at low concentrations, potassium has a stronger preference for the glass than for the salt phase.

The chlorine contents of the glasses are relatively similar to each other, at 1.3 to 1.8 wt%, with an average value of 1.5 wt%. This is about 25 % relative higher than in the Base A-5 and A-6 melts, which had 1.2 wt% Cl. All other oxides in the glasses of these melts remained unaffected, and vary only within the analytical and experimental uncertainty (the low lime content in Series 2-3, of only around 9 wt% rather than 10.5 wt%, is probably due to a weighing error). Thus, the presence of excess salt affects only the alkali metals, but none of the other glass-forming components.

The next set of experiments tested the uptake of alkali metals from the salt phase when potassium chloride is added rather than common salt, NaCl.

5.2.2. Base A-4, 5, 6 + KCl (series 2-1, 2-5 to 2-7)

The layout of experiments for this section is as follows;

- Series 2-1: 3 batches; Base A-4, A-5, A-6.
- Series 2-5: 3 batches; Base A-4, A-5, A-6, with additional 10 g potassium chloride, KCl, respectively.
- Series 2-6: 3 batches; Base A-4, A-5, A-6, with additional 20 g potassium chloride, KCl, respectively.
- Series 2-7: 3 batches; Base A-4, A-5, A-6, with additional 50 g potassium chloride, KCl, respectively.

Results:

Here, the situation is very different from the previous set. The first series produced glass with 4.3, 5.1, and 5.5 wt% potash, respectively. In the second series, the values were 6.8, 7.2, and 7.8 wt% potash, and in the final series, 10.1, 10.7, and 11.2 wt% potash, respectively (see Table 5.2, above). Here, the potash concentration in the glass actually surpassed the soda concentrations, which were down to 11.3, 9.0, and 7.6 wt%, respectively.

Thus, if there is additional KCl in the batch (with no presence of NaCl, sodium is only provided as Na_2CO_3 in the batch), the amount of potassium that goes into the glass phase increases as the additional amount of KCl increases. Notably, as in the previous series, the amount of chlorine in the glass remains near constant, at around 1.0 to 0.7 wt% Cl. Since the excess amount of chlorine can not escape as chlorine gas into the air during the firing, it has to bond with another metal to form the excess salt phase. The magnesia and lime concentrations in these glasses remain almost unchanged, while the soda content decreases massively until there is even less soda than potash, as mentioned earlier. Thus, there is a very clear interaction between the glass-forming system on the one hand and the salt system on the other, with a strong ion exchange that is restricted to the alkali metals.

The uptake of potash in the glass melt is not linear with increasing potassium chloride. There is only a short steep direct correlation where all potassium chloride enters the glass, up to about 2 to 3 wt% potash (see Figure 5.3), equivalent to the concentration range where all chlorine present is absorbed into the glass melt. Once the glass is saturated in chlorine, the uptake of

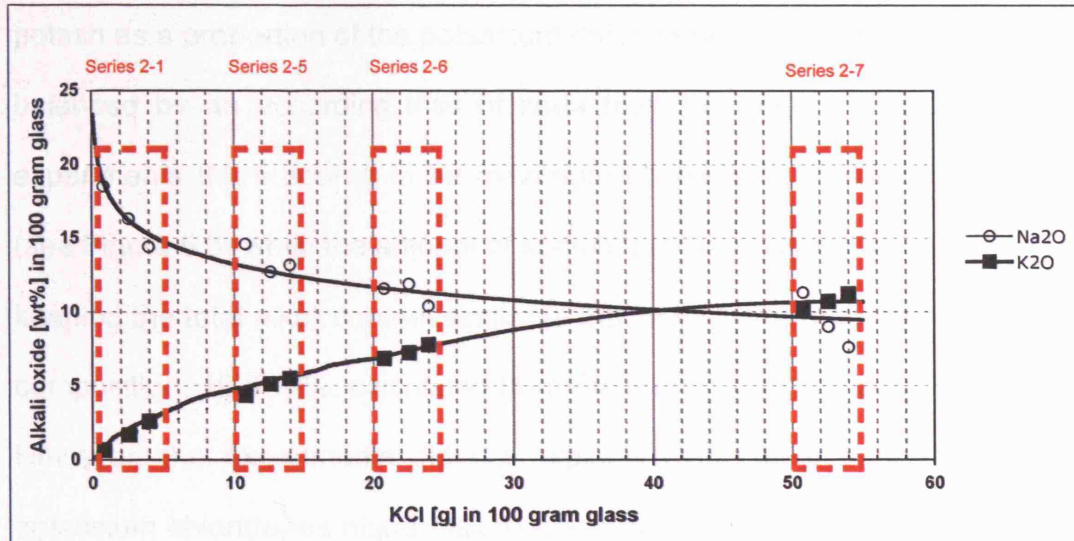


Figure 5.3: Alkali oxide contents in the glass with increasing amount of KCl.

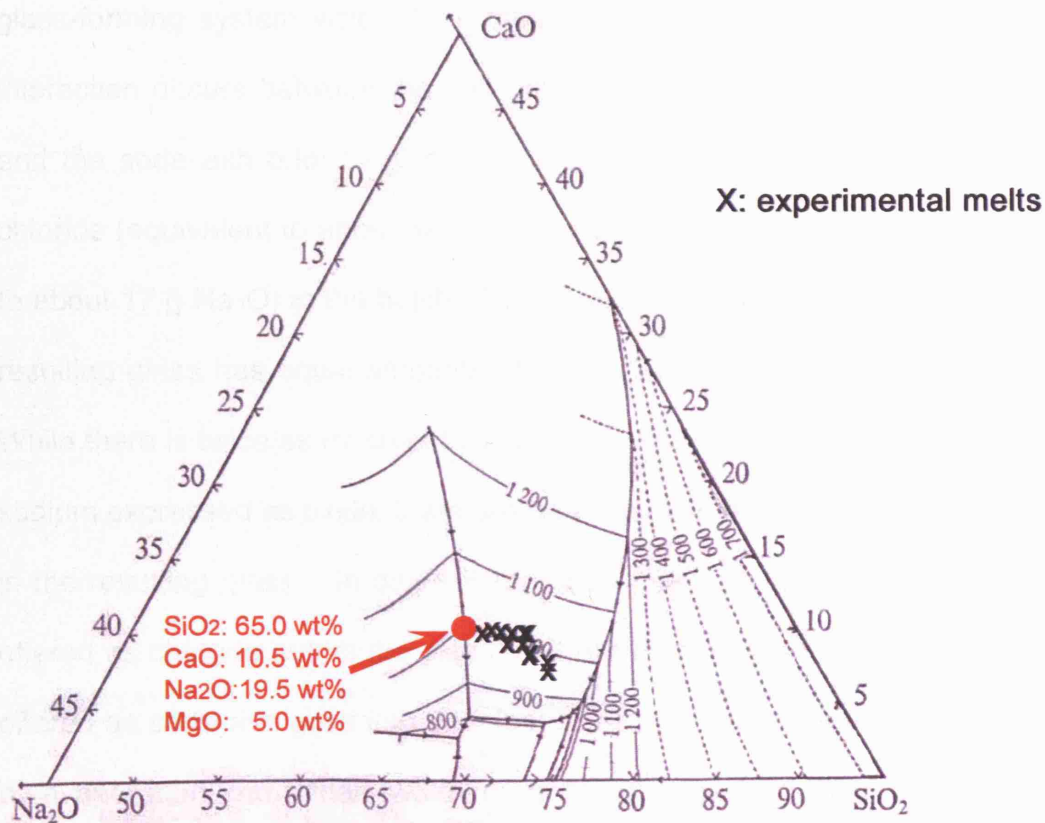


Figure 5.4: Plots of reduced compositions of experimental melts (Series 2-1, 2-5 to 2-7).

potash as a proportion of the potassium chloride offered becomes less, and is balanced by an according loss of soda from the glass system. In these experiments there seems to be maximum potassium content of 10-11 wt% (see Figure 5.3) while the amount of sodium (as Na_2O) in the glass decreases keeping the total alkali content similar to that of the set temperature (1000 °C) composition, 19.5 wt%, calculated from the ternary diagram (see Figure 5.4). However, the experiments did not explore even higher concentrations of potassium chloride, as higher salt to glass ratios were considered unrealistic in ancient glassmaking practice.

While there is a clear and strong interaction between the salt melt and the glass-forming system visible from these results, it is not clear whether this interaction occurs between the salt and the glass melt, or between the salt and the soda ash prior to glass-forming. At about 50 g added potassium chloride (equivalent to about 32 g K_2O) and about 30 g soda ash (equivalent to about 17 g Na_2O) in the batch (Base A-4 and A-5 with 50 g KCl each), the resulting glass has equal amounts of about 10 wt% each potash and soda. While there is twice as much potassium expressed as oxide in the batch than sodium expressed as oxide, there are only equal amounts of potash and soda in the resulting glass. In other words, less than one third of the potassium offered as chloride enters the glass melt, while more than half of the sodium offered as soda ash goes into the glass. Accordingly, and ignoring any loss by evaporation, more than two thirds of the potassium stays in the salt melt, and less than half of the sodium goes into the salt phase. Under these conditions, it appears that potassium has a preference for the salt phase, contrary to the result from the previous series 2-2 to 2-4, above.

In summary, these two series clearly demonstrated that alkali metal ion exchanges take place between the soda-rich glass melt and the chlorine based salt melt. However, the relative preference of the two alkali metals for the two systems, silicate and chloride, are still unclear.

5.3. Na₂O/K₂O System – 2: Base A-7, 8, 9 + NaCl + KCl (series 3-1 to 3-3)

To investigate further the effect of excess alkali salts on the distribution and partitioning of the alkalis between the finished glass and the salt melt, the form of alkalis in the initial batch are unified into carbonated form (K₂CO₃ is used rather than KCl, see Recipe-2, below) and three more series of batches were prepared in this section. This was because there was a difference in their intake behaviour as seen earlier in section 5.2. when soda was initially added in the base batch in the carbonated form while potash was added in the chloride form. Therefore, both alkalis prepared for the base batch were prepared in their carbonated forms to be consistent this time to see whether there is any preference between chloride and carbonated forms, and to see whether the trend observed earlier will change. In addition, this time, both alkali salts, NaCl and KCl, were added together (rather than separately, above) to see whether there is a preference between excess amount of sodium salt or potassium salt. Series 3-1 (below) was designed to test whether there is any difference in alkali distribution when both alkalis exist as the same crystal formation (i.e. carbonated form).

(Recipe-2) Na₂O/K₂O System – 2 (alkalis in the base are both in carbonated forms)

Note: calculations of metal oxides in wt% are based on 100 g/batch. However, most of the raw materials are not in their oxide forms. Therefore, actual glass weight is shown below.

Base A-7 (111 g/batch) = 65.0 wt% SiO₂ (65.0 g of sand), 10.5 wt% CaO (18.8 g of CaCO₃), 5.0 wt% MgO (5.0 g of MgO), 5.0 wt% Na₂O (8.6 g of soda ash), and 15.0* wt% K₂O (37.5 g potassium carbonate, K₂CO₃ = 25.4 wt% K₂O).

Base A-8 (108 g/batch) = 65.0 wt% SiO₂ (65.0 g of sand), 10.5 wt% CaO (18.8 g of CaCO₃), 5.0 wt% MgO (5.0 g of MgO), 10.0 wt% Na₂O (17.1 g of soda ash), and 10.0* wt% K₂O (25.0 g potassium carbonate, K₂CO₃ = 17.0 wt% K₂O).

Base A-9 (104 g/batch) = 65.0 wt% SiO₂ (65.0 g of sand), 10.5 wt% CaO (18.8 g of CaCO₃), 5.0 wt% MgO (5.0 g of MgO), 15.0 wt% Na₂O (25.7 g of soda ash), and 5.0* wt% K₂O (12.5 g potassium carbonate, K₂CO₃ = 8.5 wt% K₂O).

* Note: It was planned to use such quantities of raw materials to produce 100 g of glass, so that grams of each oxide in the batch equal the weight percent of that oxide in the glass. However, in these batches the oxides in the batches do not add up to 100 wt% due to miscalculation by the author when converting the target K₂O value into K₂CO₃ to be added to the batch. The weights shown here are the actual amounts that were added to the batch, resulting in increasingly higher batch weights as the potash content increases. This has to be considered when comparing the analysed glass compositions to the oxide contents of the prepared batches.

The layout of experiments for this section is as follows;

Series 3-1: 3 batches; Base A-7, A-8, A-9.

Series 3-2: 3 batches; Base A-7, A-8, A-9, with additional 10 g sodium chloride, NaCl + 10 g potassium chloride, KCl, respectively.

Series 3-3: 3 batches; Base A-7, A-8, A-9, with additional 25 g sodium chloride, NaCl + 25 g potassium chloride, KCl, respectively.

Observation of melts:

The formation of glass occurs in all batches, but the degree of separation between glass melt and salt melt differs from sample to sample.

Most of the melts produced a residual salt phase over the glass phase, except for the melts of Base A-7, A-8, and A-9 that had no salt component in their batches. However, when the batches Base A-7 and A-8 were fired at their set temperature, some of the content of the crucible seeped through the crucible wall, and the crucibles were stuck onto the furnace floor tile. This is the first time that the content of the crucible (glass melt) flooded. It is to be assumed that this overflow was due to the much higher amount of potassium in the batch compared to the amounts of sodium and silica, to the low viscosity of the alkali-rich melt, and to the failure of the crucible walls.

Results:

Series 3-1, without added salt phase, produced glass with a composition very similar to the batch composition. The apparent differences, such as in the

silica content which is only 57 wt% in the Base A-7, are due to the inadvertently added extra potash from the miscalculation of the batches, resulting in a total weight of 111 g glass rather than 100 g, and accordingly a dilution of all other oxides by more than 10 percent relative. Therefore, the intended 65 wt% silica came out as 57 wt%, and the intended 10.5 wt% lime as only 9.1 wt%. Further distortions are to be expected due to the loss of material when the crucible wall was eroded and some of the melt flooded the furnace floor tile. However, the alkali oxide concentrations are very close to the added amounts (see Table 5.3).

Table 5.3: Compositions of glass melts with various alkali concentrations (extra alkalis, both NaCl and KCl were added together).

Na ₂ O	MgO	Al ₂ O ₃	SiO ₂	CaO	K ₂ O	SO ₃	Cl	Sample Description
5.0	4.0	0.14	56.9	9.1	24.7	0.01	0.0	Base A-7: 5 wt% Na ₂ O**, 25.5 wt% K ₂ O**
8.2	4.0	0.09	58.8	9.5	18.3	0.01	0.8	Base A-7 + 10 g NaCl + 10 g KCl
11.8	4.0	0.10	59.6	9.5	14.3	0.00	0.9	Base A-7 + 25 g NaCl + 25 g KCl
9.5	4.3	0.11	59.2	9.7	16.3	0.02	0.0	Base A-8: 10 wt% Na ₂ O**, 17 wt% K ₂ O**
12.3	4.2	0.11	58.8	9.8	12.5	0.00	0.9	Base A-8 + 10 g NaCl + 10 g KCl
13.5	3.9	0.09	61.5	9.5	10.0	0.00	1.0	Base A-8 + 25 g NaCl + 25 g KCl
14.1	4.8	0.12	62.2	9.3	8.5	0.01	0.0	Base A-9: 15 wt% Na ₂ O**, 8.5 wt% K ₂ O**
14.0	4.2	0.08	62.0	10.0	7.6	0.00	1.1	Base A-9 + 10 g NaCl + 10 g KCl
15.3	3.8	0.09	61.6	9.8	7.2	0.00	10.9	Base A-9 + 25 g NaCl + 25 g KCl

Na₂O**, K₂O**: added as Na₂CO₃ and K₂CO₃ respectively to the batch.

The situation changes again considerably once the salt phase is added to the batches. In Series 3-2, 10 grams each of potassium chloride and sodium chloride are added, and in Series 3-3, 25 grams each. In all cases, there is a clear and strong shift of potassium out of the glass phase and into the salt phase, with a matching increase in soda in the glass (see Figure 5.5 and Figure 5.6). This observation is true regardless of whether the initial alkali

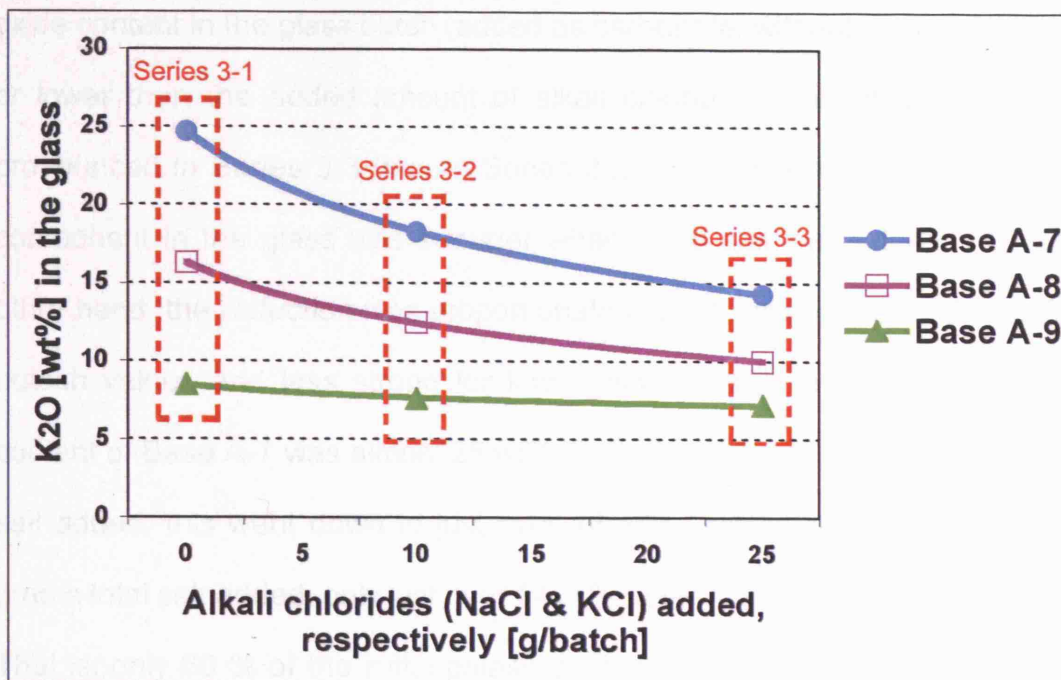


Figure 5.5: Potash content in the glass with increasing amount of alkali chlorides.

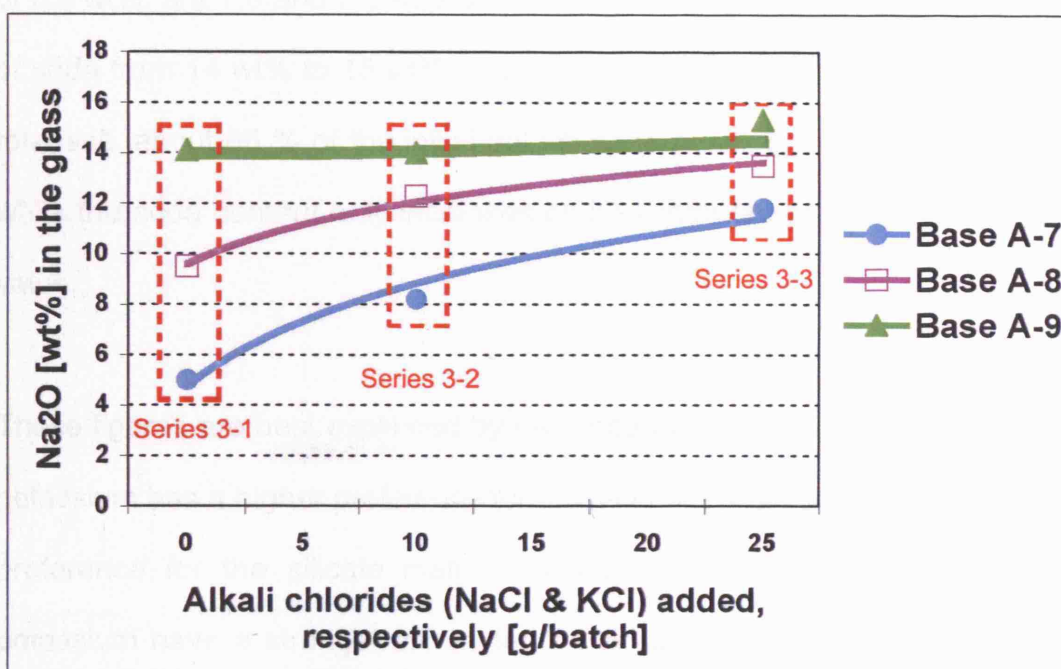


Figure 5.6: Soda content in the glass with increasing amount of alkali chlorides.

oxide content in the glass batch (added as carbonate, without salt) was higher or lower than the added amount of alkali chloride. The effect was more pronounced in Series 3-3 than in Series 3-2, that is the reduction in potash component in the glass was stronger when more salt was added. On the other hand, the reduction was proportionately much stronger for higher initial potash values and less strong for lower initial potash levels. The potash content of Base A-7 was almost 25 wt%; in Series 3-2 with twenty grams total salt added, this went down to just over 18 wt%, and in Series 3-3 with fifty grams total salt added, only just over 14 wt% potash remained in the Base A-7. That is, only 60 % of the initial potash content entered the glass melt in this experiment, while the soda content more than doubles from 5 wt% to almost 12 wt%. The same figures for Base A-9, which has an initial potash content of 8.5 wt%, are 7.6 and 7.2 wt% potash, respectively, and a minimal increase of soda from 14 wt% to 15 wt% only; that is, even after adding fifty grams of total salt, about 85 % of the initial potash content still enter the glass phase, while the soda content only increases by less than ten percent of its original value.

These figures are best explained by two separate trends. On the one hand, potassium has a higher preference for the salt melt while sodium has a higher preference for the silicate melt. On the other hand, lower amounts of potassium have a stronger affinity for the silicate melt than higher amounts. These experiments were designed in such a way that enough alkali oxide was present in the batch as alkali carbonate to bond with all the available silica, and the salt was added as excess alkali chlorides. However, as in the previous series, there is a clear interaction and ion exchange between the

glass-forming system (carbonate and silica) and the salt system, demonstrating that the salts are only nominally non-reactive in the sense that they do not on their own enable the formation of a silicate glass, but that they are still fully reacting with the batch during the glass-forming process. They are not inert, but constrained in their chemical behaviour by the amount of chloride present which requires equivalent molar amounts of alkali metal ions to form the salt phase, once the chlorine saturation level of the glass is exceeded.

In practical terms, the results suggest that when NaCl co-exists with the batch, either alone or in combination with other chlorides, NaCl will be washing some of the potassium out of the glass melt into the salt phase. The earlier results had shown that both sodium and potassium can migrate from the salt phase into the glass phase, increasing the alkali content in the glass at the expense of the other alkali. In this series, with equal amounts of NaCl and KCl added, only the soda level in the glass increased while the potash level decreased.

5.4. Summary and interpretation for alkali proportions in SLS glasses

The results above indicate that the compositions of the glass phase, whose volume and recipe was kept consistent throughout the series, were almost identical (see Table 5.1), except for the sodium and potassium content. Despite the presence of large excess amount of alkali chloride(s) in the batch, chlorine levels throughout the series remained below about 1.5 wt% in soda-rich glasses, and even below 1 wt% in glasses with more than about 5 wt% potash. Previous research (see above, Chapter 4) has shown that the maximum chlorine content in soda-lime-silica glass is negatively correlated

with the lime content, but not affected by variation in soda content. These experiments now show that potash has a similar, if not stronger, effect on maximum chlorine concentrations in these glasses. This confirms the earlier observation that there is a chemically controlled solubility limit of chlorine in the glass, and any excess amount of chlorine will form a separate salt phase that floats on top of the glass melt, and can be easily separated from the glass melt. The metal ions necessary to form this salt phase are taken from the batch. It is important to note that during the glass-forming process significant interaction between the glass-forming components and the salt phase occurs. These interactions and ion exchanges, however, are limited to the alkali metals. There is no noticeable change in the earth alkali concentrations in any of the experiments here, nor was any calcium or magnesium found in the XRF analyses (see Appendices for salt data) of the salt phase after the reactions had occurred.

This demonstrates that the presence of a salt phase in the batch has a potentially strong influence on the alkali composition of the forming glass. The salt phase within the initial batch acts as a buffer or reservoir that can provide alkali metal ions as well as receive them from the glass melt. Thus, the Two Melt Model is highly relevant, but only for alkali oxide content in glass.

The data clearly shows that the alkali metals have different preferential distribution between the two melts (glass and salt melts), as initially proposed. There is a strong tendency for low concentrations of potassium to enter the glass phase even when it is provided as potassium chloride, KCl (salt form) to the batch. Up to a couple of percent this is possible by simple absorption of

potassium chloride, up to the saturation level of chlorine in the glass (Series 2-1). The following series (Series 2-2 to 2-4) had overall low potassium in the batch, provided as chloride, and in the presence of increasing amounts of sodium chloride. The results showed a clear preference for potassium to enter into the glass melt when compared to the much higher available amount of sodium chloride. However, when looking at the absolute quantities involved and estimating the potassium content in the salt phase it becomes apparent that the potassium concentration in the salt phase is higher than in the glass phase.

Adding increasing quantities of potassium chloride to the glass batch instead of sodium chloride confirms the picture of free interaction between the two melt systems, with large quantities of potassium going into the glass melt as potash, and matching amounts of sodium going into the salt phase even if there is no NaCl originally present in the batch. In other words, sodium and potassium can coexist in various ratios and exchange relatively freely between the two melts, but the total content of alkalis ($\text{Na}_2\text{O} + \text{K}_2\text{O}$) in the glass is kept similar to the total alkali carbonate content in the batch. This may appear surprising since the non-stoichiometric glass structure can absorb a very wide range of alkali oxide to silica ratios, and therefore should be able to increase alkali oxide contents in the glass when more alkali metal ions are available in the batch. However, the molar ratio between alkali metals and chlorine in the salt phase has to be kept constant at 1 (KCl or NaCl, or any mixture in between), and there is no significant evaporation loss of chlorine at temperatures below c. 1400 °C (Gerth *et al.* 1998). Therefore, the soda content in the glass is reduced when an excess amount of KCl is

present, even if all the sodium is introduced as Na_2CO_3 and when this is the only alkali carbonate form present in the batch. The total alkali amount in the glass is determined by the amount of reactive carbonate plus a small amount of absorbed alkali chloride, that is, by the batch recipe and not by any temperature or other technical constraint. The ratio of soda to potash within the glass, however, is not equal to the ratio of alkali oxides present as carbonates, but is modified by the interaction with the co-existing salt melt. Both alkali ratio in the salt melt and volume ratios glass melt to salt melt are relevant factors here. This is clearly demonstrated by Series 2-7 with a total batch of 100 g glass-forming material containing 15 to 18 g soda and 51 to 54 g potassium chloride (equivalent to 32 to 34 g potash). The resulting 100 g glass contain 8 to 11 g soda, that is just under two thirds of the total soda initially present in the batch. The other third of the initial total soda content is most likely in the salt phase; with a ratio by weight of 2 to 1 glass to salt, this means that soda is equally distributed between the two melts. The glass also contains 10 to 11 g potash, about one third of the total potassium available in the batch. This means that two thirds of the potassium is present as salt, although the salt melt is only about half the weight of the glass melt. Thus, there is a clear preference of potassium for the salt phase over the glass phase.

The last series was undertaken to test whether the distribution factors for sodium and potassium are strongly influenced by the original type of alkali compound present in the batch or whether the interaction between the two melt systems is complete so that the distribution of the alkali metals between glass and salt melt is independent of the recipe of the batch (Series 3-1 to

3-3). Series 3-3 had again 50 g salt and nominally 100 g glass in the batch, although now equal amounts of sodium chloride and potassium chloride were added and varying quantities of sodium and potassium carbonate were present in the batch. In effect, Series 3-3 contained potassium equivalent to between 24 and 42 g potash in the total batch; the resulting 100 g glass contained between 7.2 and 14.3 g potash, that is again about one third of the total potassium initially present. This indicates that the choice of the alkali compounds plays a less important role in determining the resulting glass composition than overall alkali ratio and glass to salt ratio.

Chapter 6: Archaeological samples from Qantir

The previous chapters have used series of experimental melts to explore the relationship between the firing temperature and the earth alkali content of the glass melt in the presence of a lime-rich buffer material. Other experimental melts have studied the preferential partitioning of alkali elements in the silicate melt in the presence of an excess salt melt, rich in chloride. This has found that the earth alkali content is controlled, or at least influenced, by the firing temperature, and that sodium has a stronger preference for silicate melt while potassium has a preference for chloride melt. The following two chapters will investigate to which extent the results from these technical experiments can be applied to interpret some of the archaeological glass compositions. This chapter focuses on the difference in lime content between semi-finished and finished glass from Qantir in order to test whether there is a difference in theoretical melting temperatures. Chapter 7 will then take a broader view at published LBA glass compositions to look for possible chemical differences between different production regions and colours. Here, particular attention will be paid to the potash content and the overall alkali concentrations.

A series of excavations at Qantir, Egypt, has yielded a significant number of glass and crucible fragments that highly suggest glass-making at this site (Rehren & Pusch 2005; see section 2.3 and 2.6 in Chapter 2 for more details of the site and the excavation works conducted). Scientific study of recent glass findings from Qantir will be discussed in this section. Of particular relevance here are the comparison of finished glass samples (Schoer & Rehren 2007) and analyses of semi-finished glass, as presented for the first

time below. The comparison of the data obtained from the archaeological glasses and those from the experimental melts (above) are hoped to further illuminate the possible glass-making practice at Qantir during the LBA.

6.1. Description of the glass samples

All samples are small fragments of indeterminate shape, weighing between one and four grams. They were excavated in areas rich in glass-related waste material; six originate from site Q IV, squares i/27, f/27, g/27, g/29.30, and h/28, and one from Q V-b/8. These squares are marked through a particular density of glass crucible fragments, ranging from 5 to 52 fragments, as compared to typically just a few finds per square in Q IV. The richest concentrations of glass crucible finds occur in squares h/28 and h/29.30, with 52 and 53 finds, respectively (Pusch & Rehren 2007, 36, Table 06). The relevant layer in Q IV from which these finds originate is dated by the excavator to the reign of Ramesses II, and underlays the royal horse stables dated to Sethos II, possibly late Ramesses II (Pusch & Rehren 2007, 32, Table 05). The layer is mostly re-deposited material rich in baked silt, charcoal, various types of slag, technical ceramic, Egyptian blue, and oxidised mud brick fragments, interpreted to be material accumulated from waste on a workshop floor. The archaeological feature in Q IV are heavily disturbed by the later-addition walls and column foundation pits of the horse stables, and it appears that the layer in question was brought in from elsewhere to level the floor in preparation for building the stables. This same very characteristic mix of materials was found as an *in situ* layer in the immediately neighbouring site Q V, strongly suggesting that the material encountered in Q IV originates from the workshop area in Q V: lowering the ground there, while filling up the

area in Q IV. The final sample analysed here, 00/0472,01, was found in this layer in Q V (Pusch & Rehren 2007, 32-44). The next square, Q V-b/9, yielded a particularly rich workshop assemblage, including the almost complete crucible with a semi-reacted charge still inside, a re-used beer jar sunk into the lime-washed floor and filled to the rim with broken limestone and alabaster fragments, several clusters of white quartz pebbles, and crushing and grinding tools all within two joining rooms. The excavator interprets this as a 'cold' workshop where glass-related raw- and semi-finished materials were prepared, stored and processed, such as breaking open crucibles after firing, crushing quartz pebbles for glass making and limestone to prepare material for the parting layer, etc. (Pusch & Rehren 2007, 45-46). These rooms are separated by a mud brick wall from another pair which has furnace or hearth remains and the characteristic black-and-white slag in it, but is too much disturbed to allow reconstruction.

The finds were too small and too weathered to allow identification in the field, and were selected for analysis as possible semi-finished glass finds due to their generally glassy nature, absence of colorants, and presence of partly visible quartz grain inclusions. Semi-finished glass has been defined by Rehren & Pusch (2005) as glass, which contains still unreacted amounts of silica grains in a glassy matrix, and which is typically not coloured. It is suspected to have been produced in so-called Reaction Vessels at temperatures of around 900 °C, considerably less than the temperatures employed in the glass melting and coloration crucibles, near 1000 or 1050 °C. Most archaeological samples of semi-finished glass are thin films of white material adhering to the ceramic of the reaction vessels, or small fragments

found during the excavation. They are typically very heavily weathered, as is most glass from Qantir due to the environmental conditions.

Additional to most recently published Qantir data (Schoer & Rehren 2007), seven samples of semi-finished glass, find numbers 00/0472,01, 92/0589b, 88/0517,01, 88/0517,04, 88/0671c, and 96/0759, and 98/0844 from Qantir were made available (courtesy of E. Pusch) for analysis and their chemical compositions along with the published compositions (1997: Table 3) of eight finished glass samples are shown as Table 6.1 (full composition) and Table 6.2 (reduced composition) in the later section 6.3 in this chapter. The following is the general descriptions of these newly obtained seven samples.

6.1.1. Sample 1: 00/0472,01

Sample 1 comes from a set of four glass fragments with the find number 00/0472. The sample is from the largest piece, which is heavily weathered glass of white appearance attached to a ceramic layer. During cutting, a small piece dislodged from the inside and this was mounted in resin and polished for further analysis (see Chapter 3 for detailed sample preparations and see Figure 6.1, Figure 6.2, and Figure 6.3 for sample images). The other glass fragments in this set are also heavily corroded and vary in sizes. The glasses seem to be frothy and white in colour (see Figure 6.1 and Figure 6.2). Microprobe analysis showed that no colouring oxide was present in the unweathered glass.



Figure 6.1: The image of a glass sample series, #00/0472 (image taken by Excavations Qantir). The arrow highlights the actual sample mounted for analysis, #00/0472,01, above.



Figure 6.2: Cross section through Sample #00/0472,01 (image taken by Excavations Qantir). The mounted sample originates from the left section. Note the dark ceramic attached to the weathered glass (bottom, centre).



Figure 6.3: Mounted glass sample #00/0472,01 (image taken by Th. Rehren).

Only a small amount of unweathered glass is still preserved in the centre of the mounted sample. The presence of quartz grains in the sample, and its association to the ceramic, indicate that this is semi-finished glass.

6.1.2. Sample-2: 92/0589b

This sample is from a thin plate of glass. Several plates of glass are known from Qantir, mostly of red glass (see Schoer & Rehren 2007); this sample is of a light milky colour indicating that it may be semi-finished glass or coloured in opaque white. Before analysis, no opaque white glass was known from Qantir, therefore this glass was assumed to be semi-finished glass opacified by residual batch material. A small fragment is taken from the unweathered core of sample #92/0589b and mounted in resin for further analysis (see Chapter 3 for detailed sample preparations and see Figure 6.4 and Figure 6.5 for sample images).



Figure 6.4: White glass plate, #92/0589b (image taken by Excavations Qantir).



Figure 6.5: White glass plate, #92/0589b in cross-section (image taken by Excavations Qantir).

6.1.3. Sample-3 and Sample-4: 88/0517,01 and 88/0517,04

The two fragment samples, #88/0517,01 and #88/0517,04, come from a set of

four small glass fragments (see Figure 6.6 for sample image). All glass fragments in this set are heavily corroded and vary in sizes. The glasses seem to be light aqua blue in colour (see Figure 6.6).

These samples have both many quartz grains in the glass matrix, indicating that they are probably semi-finished glass. They appear relatively unweathered, but this may be only the non-corroded core surviving as there are clear signs of a corroded surface on the four fragments.



Figure 6.6: Glass sample series, 88/0517 (image taken by Excavations Qantir). The two samples mounted for analysis (#88/0517,01 and #88/0517,04) are highlighted by the arrows, above (the larger piece is #88/0517,01).

6.1.4. Sample-5: 88/0671c

A small fragment is taken from sample #88/0671c and mounted in resin and

polished for further analysis (see Chapter 3 for detailed sample preparations and see Figure 6.7, below, for sample image). This glass fragment is heavily corroded, but seems to be coloured very dark, black or blue. It has no identifiable artefact shape, and was supposed to be semi-finished glass because of its unusual dark colour, and irregular shape.



Figure 6.7: Image of glass sample #88/0671c (taken by Excavations Qantir). The sample is about 12 mm long.

6.1.5. Sample-6: 96/0759

Sample #96/0759 is a small fragment of corroded glass with no association to technical ceramic. It is superficially corroded to a dirty white colour, but upon cutting revealed a mixed greenish-red body with numerous inclusions of quartz and bubbles (see Figure 6.8). The analysis covered areas of both colours, but no chemical differences were noted, suggesting that the difference is in the

oxidation state rather than the quantity of colorant present (see below for chemical composition).

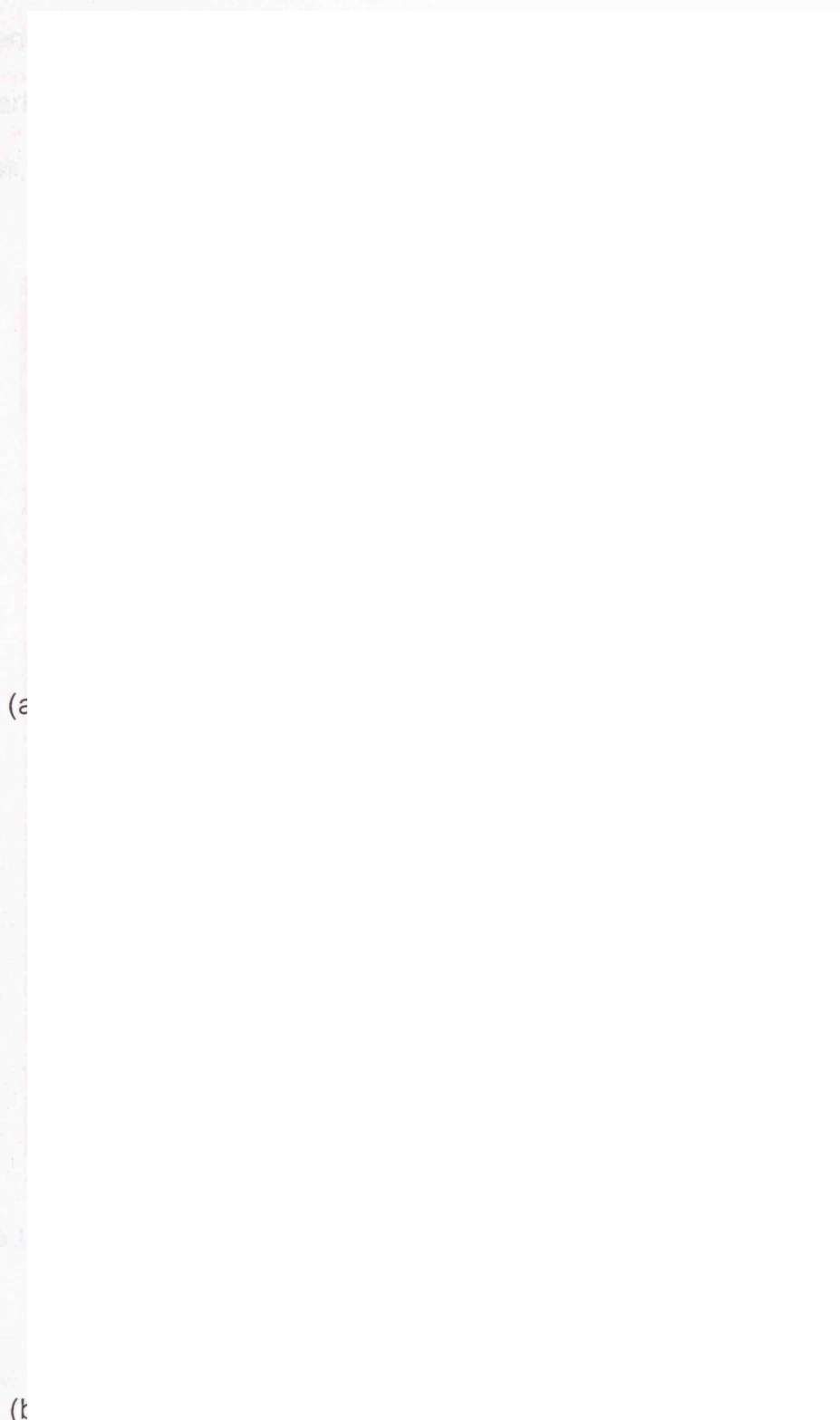


Figure 6.8: The images of glass sample #96/0759, (a) overall view and (b) cross-section, mounted in resin (both images taken by B. Schoer).

6.1.6. Sample-7: #98/0844

Sample #98/0844 is a small droplet of heavily corroded glass; the core though is well enough preserved to allow microprobe analysis. However, the glass is too dark to identify the colour. There are only a few silica grains present in the glass, and no association to technical ceramic.



Figure 6.9: A small glass droplet, #98/0844 (image taken by B. Schoer).

6.2. Microscopic examination

Residual quartz grains are visible in both the polished glass samples #88/0517,01 and #88/0517,04 (see Figure 6.10 and Figure 6.11, below).

The quartz grains are round and have many cracks, probably from the thermal stress during the heating and the reaction with the glass melt. At temperatures above c. 570 °C, quartz expands by about 6 % in volume. At even higher temperature, the quartz grains react with the liquid glass and form a solid bond when the glass cools and solidifies, at about 900 °C. When the glass-with-quartz cools below 570 °C the quartz shrinks again by about 6 vol%. This leads to cracks within the quartz and in the surrounding glass if the entire grain is not able to shrink because of its surface being bonded to the glass matrix.

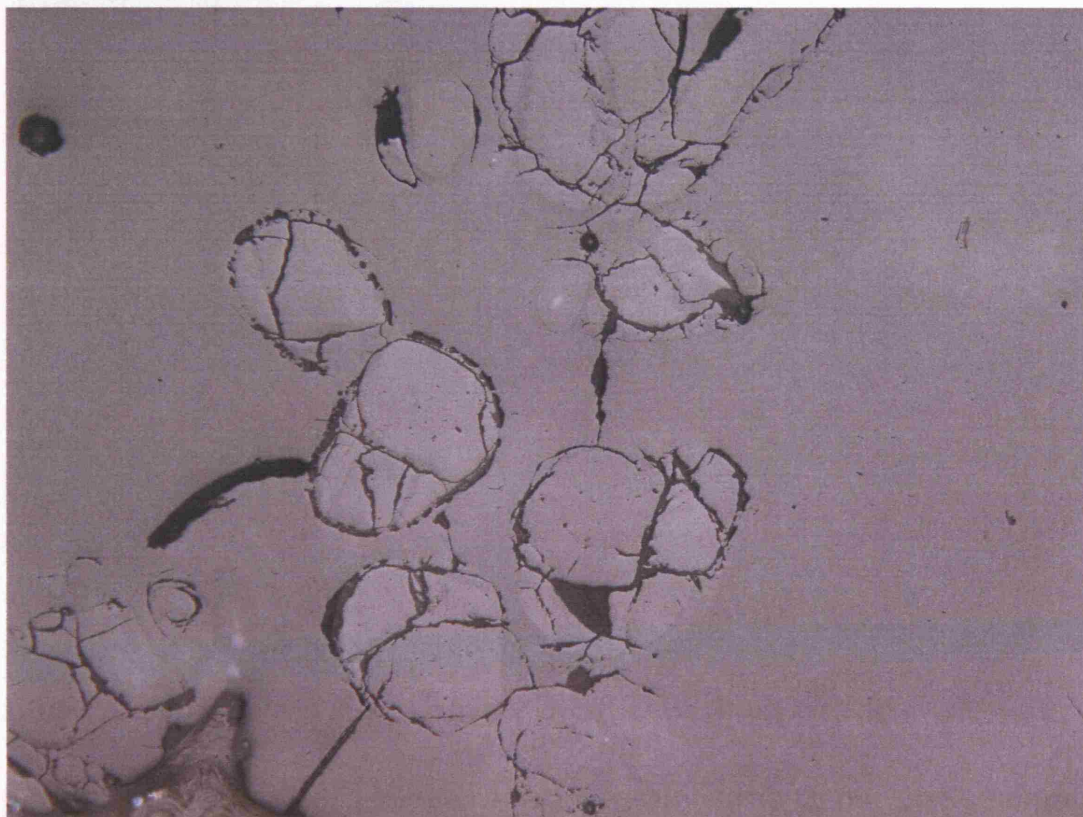


Figure 6.10: Optical microscope image of quartz grain in the Qantir glass sample #88/0517, 01. Width of image c. 2 mm.

SEM analysis was used to see whether there is any diagnostic microstructure that can be used to assess their method of production. Most of the Qantir glasses are heavily corroded, but the clean glass phases appear homogeneous and show almost no microstructure, except for some quartz grains (see Figure 6.11, below, Sample #88/0517,04).

In some areas, the corrosion starts in the cracks surrounding the quartz grains (see below, Figure 6.11, centre top), and the absorption of silica into the glass melt is visible from the erosion bays (e.g., lower left hand corner in Figure 6.11).

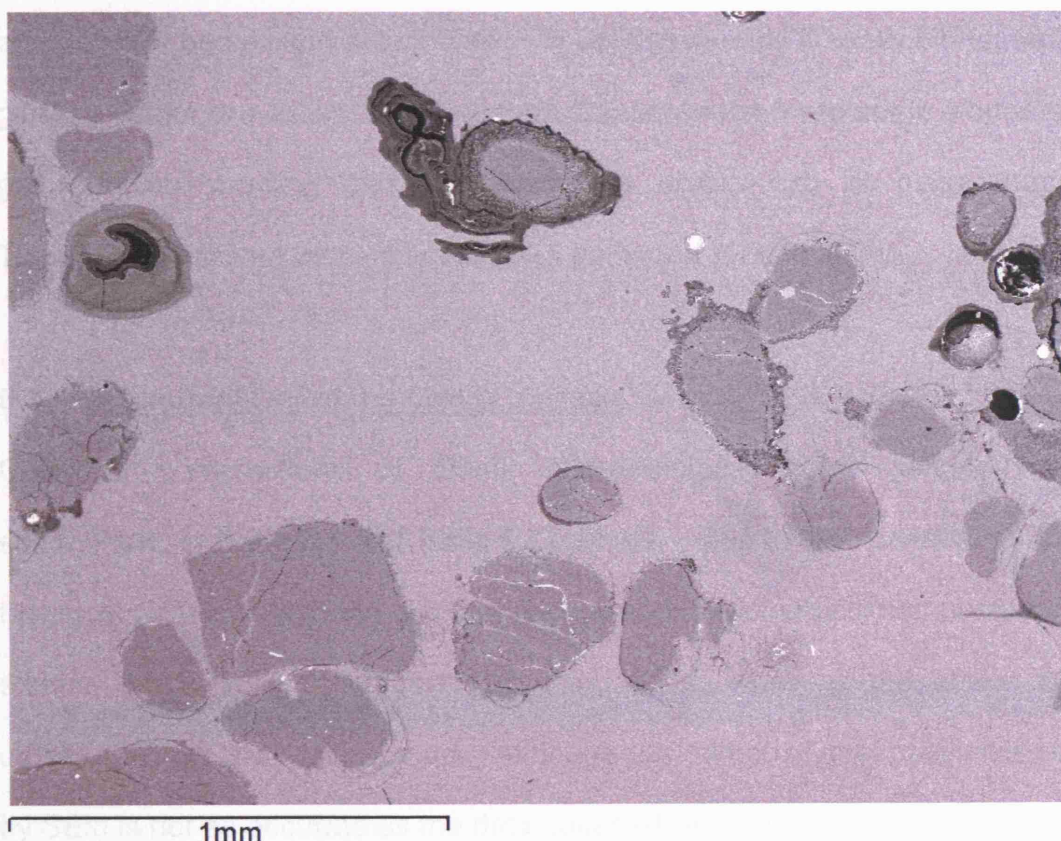


Figure 6.11: SEM (BSE) image of quartz grain in the Qantir glass sample (sample #88/0517,04), with corrosion (dark) starting at the cracks surrounding same quartz grains (centre and left).

However, no lime-rich areas or clusters of wollastonite were found, in contrast to the experimental results (see above, Chapter 4).

In addition, semi-quantitative analysis was conducted on all the clean glass phase areas (i.e. no crystalline material inclusions within the area) of some of the obtained samples, prior to more detailed chemical composition analysis of all the obtained samples by electron microprobe, discussed below.

Glass samples #92/0589b (the white platelet) and #88/0671c (the dark glass fragment) showed no inclusions of quartz crystals. Only sample #92/0589b showed a scatter of tiny small crystals that were further analysed by SEM, and found to be calcium antimonate. Thus, this sample is real white opaque glass, a colour previously unknown from Qantir, and showed some elongated gas bubbles showing that the glass was drawn into its plate shape. Therefore, it was not semi-finished glass as hoped for this study.

6.3. Composition of the Qantir glasses

Chemical compositions of Qantir archaeological glass samples are summarised in Table 6.1 and Table 6.2 (below). Due to time constraints and technical problems with the electron microprobe, the chemical composition of sample 88/0671c was obtained by using SEM, while all the others are obtained by electron microprobe. Although the compositional data obtained by SEM is not as accurate as the data obtained by microprobe, the difference between the compositions of the same glass sample obtained by both SEM and microprobe was close enough for the comparison. The analysis of two samples by both SEM-EDS and EPMA gave an average difference between

the two data sets for the individual oxide contents obtained by SEM to be within about ± 0.5 wt% of the value of the microprobe, except for the silica and soda contents with larger difference of +2.0 wt% and -0.5 to -1 wt%, respectively (see Table 6.1).

Of the glass samples analysed here, only two are so far clearly identified as semi-finished glass, based on their high content of quartz grains (#88/0517,01 and #88/0517,04). However, sample #98/0844 seems to be a semi-finished glass despite having only a few inclusions of quartz grains. Moreover, #96/0759 also has numerous inclusions of quartz grains, but the sample does not seem to be a semi-finished glass due to its colour. Sample #00/0472,01 has just a few quartz grains in the polished surface, and none were identified in the two other samples, the white and black glass, respectively.

The chemical data (Table 6.1) did not reveal the presence of a colorant for sample #00/0472,01, which may have been colourless glass.

Sample #92/0589b has an antimony oxide content of 1.56 wt % and has the highest lime content of 8.0 wt% of all Qantir glass samples analysed here. These contents confirm the glass is opaque and white in colour due to the presence of calcium antimonate.

Sample #88/0671c seems to have a dark-blue colour. However, there was no copper detected in the sample #88/0671c, and no cobalt above the detection limit of the SEM used. Unfortunately, no microprobe data is at present available for this sample, but the composition of the other oxides present, such as alumina, potash and manganese, is very similar to normal

Table 6.1: Average compositions of Qantir glass samples, both newly obtained and published [wt%].

Sample Description	SiO ₂	Na ₂ O	CaO	K ₂ O	MgO	Al ₂ O ₃	Fe ₂ O ₃	TiO ₂	Sb ₂ O ₅	MnO	CuO	CoO	SnO ₂	ZnO	SO ₃	Cl	P ₂ O ₅
#96/0759	overall	11.5	8.66	4.68	3.11	1.59	1.13	0.19	nd	nd	0.34	nd	nd	nd	0.19	0.4	0.48
	red area	10.8	9.26	4.82	3.08	1.60	1.10	0.19	nd	nd	0.34	nd	nd	nd	0.16	0.4	0.60
	green area	12.0	8.23	4.57	3.13	1.59	1.14	0.19	nd	nd	0.35	nd	nd	nd	0.22	0.4	0.39
#88/0517,01	72.4	12.6	5.09	1.81	2.72	1.90	1.90	0.21	nd	0.02	0.15	nd	nd	nd	0.16	0.3	0.25
#88/0517,04	73.4	11.7	4.93	1.85	2.59	2.14	2.09	0.22	nd	nd	0.12	nd	nd	nd	0.14	0.3	0.28
#88/0517,04(SEM)	75.5	10.6	4.4	1.8	2.3	1.7	1.5	0.2	0.4	<0.1	0.3	0.1	0.4	0.2	0.2	nd	0.2
#98/0844	71.6	12.4	5.32	1.83	2.81	1.94	0.94	0.24	nd	nd	nd	nd	nd	nd	nd	0.1	.26
#88/0671c (SEM)	67.7	17.7	6.8	1.1	4.5	0.7	0.4	nd	nd	nd	nd	<0.1	nd	nd	0.4	0.0	0.5
#00/0472,01	62.6	18.6	7.59	1.98	4.75	0.67	0.40	0.06	nd	nd	nd	nd	nd	nd	0.35	1.0	0.22
#92/0589b	63.7	16.0	7.97	2.25	3.80	1.31	0.70	0.11	1.56	nd	nd	nd	nd	nd	0.30	0.9	0.27
#92/0589b (SEM)	65.7	15.5	7.7	2.3	3.7	1.2	0.5	<0.1	1.5	nd	nd	0.0	0.3	nd	0.5	nd	0.2
#80/0044 red 1	62.7	16.3	7.93	1.93	3.46	0.38	0.25	0.04	nd	nd	3.01	nd	0.20	nd	0.23	1.1	0.15
#92/0546 red 2	64.6	15.7	6.58	2.13	4.03	0.47	0.31	0.07	nd	nd	3.58	nd	0.28	nd	0.20	1.1	0.21
#87/1686a red c1	55.3	16.8	6.38	1.73	3.21	0.43	0.29	0.03	1.50	nd	11.22	nd	1.31	nd	0.39	1.1	0.19
#84/1231 red c2	56.3	15.7	6.20	1.81	3.92	0.41	0.30	0.03	1.94	nd	10.13	nd	1.33	nd	0.48	0.7	0.23
#83/0110 light blue	62.8	19.1	7.04	1.99	4.34	0.39	0.27	0.04	nd	nd	2.10	nd	0.19	nd	0.30	1.0	0.20
#83/0744b, 0003 dark blue	66.0	13.9	8.33	1.46	3.75	3.13	0.94	0.12	0.35	0.12	0.06	0.07	nd	0.11	0.17	0.3	0.17
#83/0386b dark blue	61.9	16.5	5.88	0.41	3.85	3.36	2.10	0.13	1.73	0.64	0.03	0.35	nd	0.15	0.22	0.8	0.07
#98/0785, 0005 purple	65.3	17.7	6.47	1.54	3.78	0.50	0.33	0.07	0.02	0.64	0.02	nd	nd	0.02	0.15	1.3	0.16

nd: Not detected (below detection limit). SEM: qualitative data was obtained by SEM (while the others were obtained using electron microprobe). Note: Data shown in *italics* were published by Schoer & Rehren (2007, Table 4a).

Table 6.2: Reduced average compositions Qantir glass samples both newly obtained and published [wt%].

Note: Data shown in *italics* were from Schoer & Rehren (2007, Table 5 & Table 6).

SiO ₂	Na ₂ O	CaO	K ₂ O	MgO	Al ₂ O ₃	Fe ₂ O ₃	TOTAL	fixed to 5%	Reduced & Normalized to 95%			Sample Description
								MgO**	SiO ₂ **	Na ₂ O**	CaO**	
68.2	11.9	8.97	4.85	3.22	1.65	1.17	100	5.00	72.9	15.5	6.7	#96/0759
73.6	12.8	5.18	1.84	2.77	1.93	1.93	100	5.00	78.7	14.2	2.0	#88/0517,01
74.4	11.9	4.99	1.87	2.62	2.17	2.12	100	5.00	79.9	13.3	1.7	#88/0517,04
73.9	12.8	5.49	1.89	2.90	2.00	0.97	100	5.00	78.1	14.2	2.6	#98/0844
68.4	17.9	6.9	1.1	4.5	0.7	0.4	100	5.00	70.0	18.8	6.3	#88/0671c(SEM data)*
65.2	19.4	7.91	2.06	4.32	0.72	0.42	100	5.00	67.0	20.9	7.0	#00/0472,01
66.4	16.8	8.35	2.36	3.98	1.37	0.73	100	5.00	69.4	18.5	7.0	#92/0589b
67.5	17.5	8.5	2.0	3.7	0.41	0.25	100	5.00	69.0	19.2	6.9	#80/0044 opaque red plate 1
68.9	16.7	7.0	2.3	4.3	0.50	0.33	100	5.00	70.4	18.5	6.1	#92/0546 opaque red plate 2
65.7	20.0	7.6	2.1	3.8	0.51	0.34	100	5.00	67.3	21.7	6.0	#87/1686e red 1 (crucible)
66.5	18.6	7.3	2.1	4.6	0.48	0.35	100	5.00	67.9	20.2	6.9	#84/1231 red 2 (crucible)
65.5	19.9	7.3	2.1	4.5	0.42	0.28	100	5.00	66.7	21.5	6.8	#83/0110 light blue
67.2	14.2	9.2	1.5	3.8	3.19	0.96	100	5.00	71.7	15.6	7.7	#87/0744b,0003 dark blue
65.9	17.6	6.3	0.4	4.1	3.57	2.23	100	5.00	71.5	18.3	5.2	#88/0386b dark blue (crucible)
68.3	18.5	6.8	1.6	4.0	0.52	0.35	100	5.00	69.8	19.8	5.4	#98/0785,0005purple (crucible)

*: Only the chemical composition of sample #88/0671c is obtained by using SEM, but all the others are obtained by using microprobe.

**: Data is reduced and handled as mentioned in Chapter 3.

glass from Egypt, and unlike cobalt-coloured glasses. Thus, it is unlikely that the dark colour originates from cobalt in this case, but no other colorant was detected either, such as manganese or iron oxide.

All three glasses mentioned so far have a soda content above 15 wt%, a lime content of 7 to 8 wt%, and a magnesia content of around 4 to 5 wt%, in line with or only slightly higher than other glasses from Qantir, and Egypt in general. Similarly, the other major and minor oxides are present in concentrations as expected, and there is no reason to assume that these glasses are semi-finished, except for the absence of colorants in two of the three samples.

The two glass samples, #88/0517,01 and #88/0517,04, with numerous quartz grain inclusions have a very different composition. As far as their colour concerns, they have both low copper oxide contents of between 0.1 wt% and 0.2 wt%, although this is unlikely to be enough to colour the glass in blue. More importantly, both samples have a high iron oxide content, of around 2 wt%, which is more likely the reason for the aqua colour of the small fragments analysed. In addition, both samples have around 2 wt% alumina, and only around 5 wt% lime and 2.5 wt% magnesia. The iron and alumina levels are much higher than in typical Egyptian glasses and may indicate contamination from Nile clay or ceramic, while the low lime and magnesia concentrations possibly indicate a low firing temperature. The potash content is just below 2 wt% and in line with other glasses, while the soda content of only 12 to 13 wt% is much lower than in most Egyptian glasses.

Sample #96/0759 is characterised by a very high average potash content, of about 4.9 wt%, and relatively low average soda content (11.9 wt%) when compared to the other Qantir samples. Magnesia content is relatively low at around 3 wt%, while the lime content is near usual at about 9 wt%. There is consistently about 0.3-0.4 wt% copper oxide in both the green and the red areas of the glass. This copper oxide content is much lower than the amount found in a typical copper-coloured LBA glasses, and may be due to contamination rather than intentional.

This sample is particularly interesting for its high potash content. This could either indicate variability in the composition of the plant ash used for the making of this glass, or reflect some contamination from fuel ash. The nature of the fuel used in the glass furnaces is not known, but it is very likely that some wood or brushwood was used. The ash of most wood/brushwood is richer in potash than soda, and a certain contribution of fuel ash would explain the high potash content in this sample. Yet another possibility is that the crushed quartz used here is rich in potassium feldspar, either from an unusual quartz pebble or from grinding on a granitic grinding stone. This is based on the composition of a quartz-grain-rich area in the glass indicating positive correlation of potash and alumina; 77.0 wt% SiO₂, 6.6 wt% Na₂O, 3.9 wt% CaO, 4.9 wt% K₂O, 1.3 wt% MgO, 4.0 wt% Al₂O₃, 1.4 wt% Fe₂O₃, 0.42 wt% TiO₂, 0.19 wt% CuO, 0.03 wt% SO₃, and 0.16 wt% Cl. The also elevated contents of iron oxide and titania would then represent the magnetite or ilmenite, frequently present in granite.

The analysis of sample #98/0844 reveals a reasonable composition despite

poor condition of the sample. The magnesia content is less than 3 wt%, the soda content is only about 13 wt%, and the lime content is less than 6 wt% average. The contents of potash, alumina, and iron oxides are within those of the typical LBA glasses, respectively. Noteworthy is the absence of colorant(s).

6.4. Glass-making practice at Qantir

6.4.1. CaO content & firing temperature

Published works (Rehren & Pusch 2005, Turner 1954a) suggest that the firing temperatures used at Qantir workshop(s) are 900-950 °C for initial melting of the raw materials and 1000-1100 °C for the second firing for coloration and ingot production. These firing temperature ranges for Qantir glasses were judged from the degree of colour change and vitrification of the crucibles or ceramics of the reaction vessels. That is, if the crucible fragments are still in the original reddish colour of the Nile Clay fabric, it suggests that the crucible was fired at the lower temperature, in contrast to the grey to blackish colour when fired at the higher temperature up to 1100 °C (the maximum temperature that Nile Clay can withstand). Therefore, if the lime content in the glass is proportional to the firing temperature, as discussed earlier, the lime content in the semi-finished glass should be lower than in the finished glass, supposedly fired at higher temperature.

Compositions of Qantir archaeological samples are shown earlier (see Table 6.1 (full) and Table 6.2 (reduced), above) for comparison. Qantir glasses range from about 4 to 9 wt % CaO, with the three semi-finished glasses (#88/0517,01, #88/0517,04 and #98/0844) having a much lower earth alkali

content than the finished glasses. Figure 6.12 (below) shows the plots of Qantir glass compositions obtained (see Table 6.1 for full compositions). Three aspects are particularly noteworthy of this ternary diagram. First, it is interesting to note that the plots of finished Qantir glasses disperse largely in horizontal direction only. That is, the lime contents of Qantir glasses are somewhat consistent whereas their silica and soda contents vary by each sample, suggesting that there was either some good control over the firing temperature or firing temperature was kept relatively consistent due to technical constraints (i.e. furnace designs) during LBA.

Secondly, three archaeological samples of semi-finished glass were plotted near the 1200 °C isotherm towards the silica-rich corner of the system, which is in a very uncommon part of the diagram. This is in stark contrast to what was expected at the beginning of this analysis and seems to contradict the assumption of a low-temperature firing for semi-finished glass. Indeed, the calculated temperature is in excess of what is assumed the upper limit of Late Bronze Age glassmaking temperatures. However, this seemingly very high temperature is to a large extent due to the particular way in which the analytical data is reduced from the original seven base glass oxides to only three oxides for the ternary diagram. In this process (Rehren 2000b), both alumina and iron oxide are recalculated into silica^{**}. Both samples have about 4 wt% of combined alumina and iron oxide, resulting in a much higher silica^{**} value. Furthermore, due to their low magnesia content of less than 3 wt% and a typical potash content of around 2 wt%, the total difference between the seven base oxides and the reduced three oxides for the ternary diagram is well above the 5 wt% limit below which this reduction can be

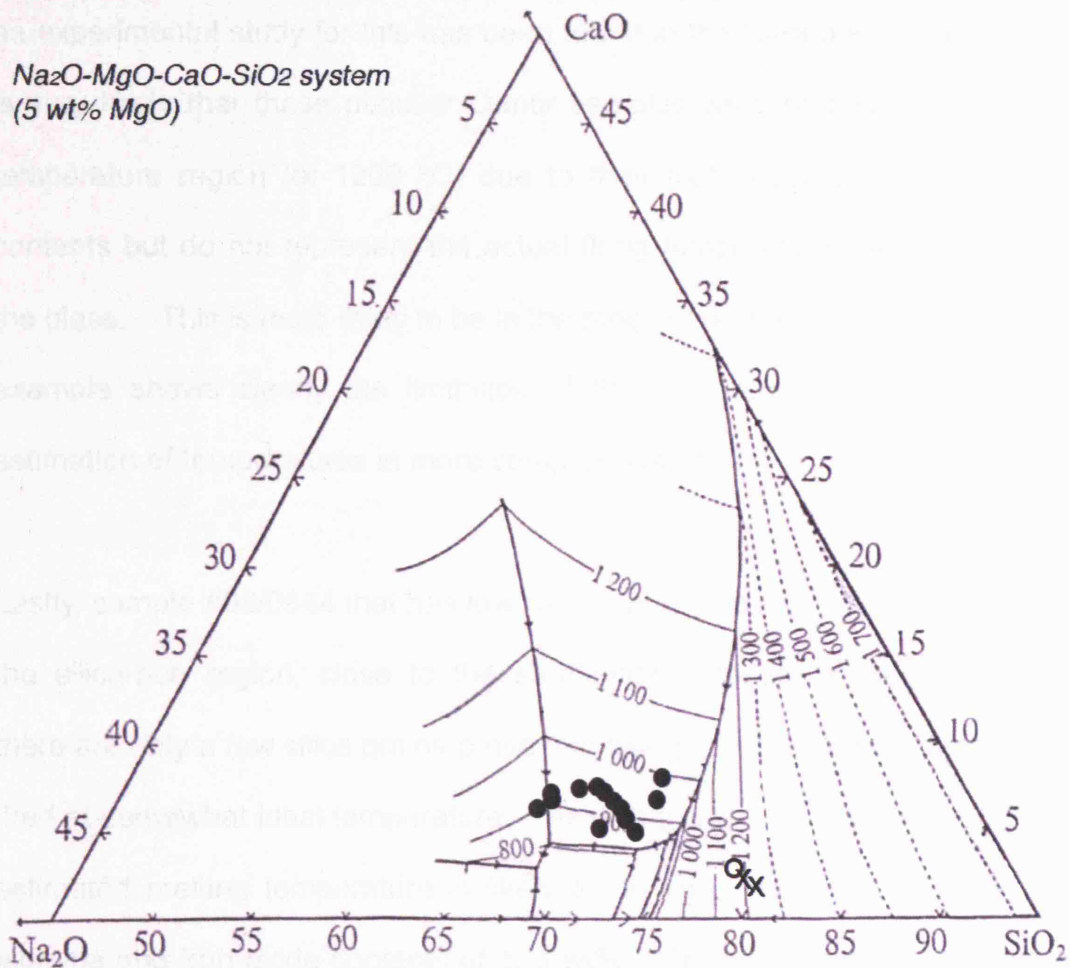


Figure 6.12: Plots of reduced Qantir glass compositions; semi-finished glass (#88/0517,01 and #88/0517,04; X), #98/0844 (O), and the others (●).

considered reasonable (Rehren 2000b). In this case, the iron oxide and alumina levels bring the calculated silica level up from around 75 wt% to near 80 wt%, equivalent to an increase in calculated temperature from around 900 °C to around 1200 °C (see Figure. 6.12). However, Morey (1930c: Fig. 1) has shown in an experimental study on the effect of alumina on liquidus temperatures of SLS glasses that the liquidus temperature will actually be lowered (by about 40-80 °C) by an addition of alumina up to about 2 wt%. In contrast, the liquidus temperatures will go up only when alumina content is more than 2 wt%. A similar effect is to be assumed for iron oxide, although

no experimental study for this has been found in the literature. Therefore, it is very likely that these peculiar Qantir samples were plotted in the higher temperature region (of 1200 °C) due to their high alumina and iron oxide contents but do not represent the actual firing temperature used to produce the glass. This is more likely to be in the range of 900 °C or even less. This example shows clearly the limitation of the 'tool' ternary diagram for the estimation of temperatures in more complex systems.

Lastly, sample #98/0844 that has low lime content (about 5 wt%) plots also in the silica-rich region, close to the semi-finish glasses, above. However, there are only a few silica grains present in this glass, meaning the glass was fired at somewhat ideal temperature. As with the previous two samples, the estimated melting temperature is likely to be very inflated due to the high alumina and iron oxide contents of c. 3 wt%. Therefore, the composition of this droplet may add interesting new information regarding the silica content of the semi-finished glass.

However, the current data is insufficient for the intended purpose of these analyses, namely to test the validity of the partial melting model using real archaeological material, and to determine the probable melting temperature for the primary glass making in the reaction vessels. The only three samples of likely semi-finished glass are contaminated by a certain amount of clay or ceramic material, making it impossible to estimate the original melting temperatures, or at least a temperature difference between the semi-finished and the finished glass. However, it is remarkable that the measured lime and magnesia content in these two samples is well below the typical levels

found in the finished glasses. This indicates that the principle of a relationship between lime content and firing temperature may still be true, even if there is insufficient data to prove it.

6.4.2. Raw materials

Comparison of microscopic examinations result of Qantir samples (above) and that of experimental melts (shown in Figures 6.1-6.9) enable us to speculate about the possible raw materials used in Qantir glass-making.

Quartz pebbles, sand (calcareous sand), plant ash, and natron are the typical raw materials for ancient soda-lime-silica glass-making. Both quartz pebbles and sand are possible source for silica, and they can be distinguished on the basis of the alumina contents in the finished glass (Tite & Shortland 2003). In addition, both plant ash and natron can be the source for soda (flux) and they can be distinguished according to potash and magnesia contents. However, it is very confusing when it comes to the lime content, since both quartz sand and plant ash can provide the typical lime levels (Freestone *et al.* 2000). However, if natron (which is mainly sodium carbonate, Na_2CO_3 , and has few other impurities) can be assumed to be the source of the flux (rather than plant ash which has many impurities), then the lime content of the glass can be used to distinguish between crushed quartz pebbles and quartz sand. Otherwise, it is generally assumed that the bulk of the lime content of LBA glass comes from plant ash (Sayre & Smith 1974, Tite & Shortland 2003).

Bearing this in mind, comparison of the preliminary findings from the microscopic examinations of experimental melts and that of Qantir glass

samples shows interesting difference between the two. Experimental melts were prepared using quartz sand, sodium carbonate, and calcium carbonate. After firing and incomplete fusion, both lime-rich areas/particles, wollastonite, and quartz grains can be seen microscopically. The wollastonite-rich areas are often surrounding porous cores of very lime-rich material, probably remains of the limestone particles from the batch material. Since only quartz grains are visible in the semi-finished Qantir glass samples and the fact that the glass has a rather low lime content, the possible raw materials used in LBA glass-making in Egypt could be crushed quartz pebble and plant ash. In fact, sharp-angular shaped silica crystals can be seen from a peculiar Qantir sample (see Figure 6.13). No full characterisation of mineral phases and grain sizes in plant ash has been found in the literature, but it may be assumed that plant ash contains a very finely intergrown matrix of sodium and



Figure 6.13: SEM (BSE) image of crushed quartz from the Qantir sample (image taken by P. Connolly).

calcium carbonate, with few if any areas rich in calcium carbonate. Therefore, during glass melting no such lime-rich areas and therefore no wollastonite clusters are likely to form. However, more experimental work using real plant ash is necessary, to further explore this matter, but this is outside the scope of this thesis.

On the other hand, published and ongoing analysis of the parting layer in reaction vessels and crucibles from Qantir has shown that wollastonite and diopside form in the contact between the glass and the parting layer, composed of almost pure lime (Rehren 1997; unpublished data). As discussed earlier (Chapter 4, Section 4.4 & 4.6), this has a direct effect on the lime and magnesia content of the glass at least in the vicinity of the parting layer. Ongoing experimental work (Merkel & Rehren 2007) shows that this parting layer is indeed being absorbed into the glass melt, acting as a buffer for the glass melt to take up more lime as the temperature increases. As discussed earlier (Section 4.4 & 4.6), one millimeter of parting layer thickness can increase the lime content of an average glass ingot by 2.5 to 5.0 wt%. Future work will focus on the diffusion profiles for lime from the parting layer into the glass melt as a function of time and temperature, and the homogeneity of individual glass ingots. Only then can we fully understand the archaeological glass compositions and their origins.

However, these findings need to be investigated further. Detailed research on plant ash composition, chemical and mineralogical, and especially for Egyptian sources, is necessary so that these findings will be more conclusive.

Chapter 7: Archaeological Implications

The previous chapters have demonstrated how the configurational parameters of glass-making, such as firing temperature and salt content(s) of the charge, can influence the alkali and the earth alkali oxide concentrations in the finished glass. In addition, it is safe to assume that the raw materials, such as plant ash and quartz are regionally different, and may add a degree of variability to the resulting glass composition. Differences in raw material compositions are likely to be reflected in the minor oxide concentrations, primarily potash, magnesia, alumina and iron oxide, while the firing temperature is likely to be reflected in the lime content normalised to 5 wt% magnesia. The presence of a salt phase is likely to influence the soda to potash ratio, but it is difficult to separate the influence from salt phase from the compositional differences of different plant ashes. This chapter takes a comparative look at the published compositions of LBA glasses from Mesopotamia and Egypt, with particular emphasis on the base glass compositions as defined by Brill in Lyliquist *et al.* (1993), and on the reduced compositions plotted into the ternary phase diagram for soda-lime-silica with 5 wt% magnesia. The glass analyses will be studied by their different colours, following the suggestion of Rehren and co-workers (2001) of a colour specialisation in Egyptian glass-making. Therefore, the nature of the colorant will also be discussed here, although this is only marginally related to the topic of this thesis.

7.1. Homogeneity of LBA glass

This research was started based on the theory that LBA glass compositions

are very homogeneous despite various raw materials available across time and regions (Rehren 2000b). However, as seen from Figure 3.1, this is not as neat and clear-cut as tentatively proposed by Rehren (2000b), and the situation is more complicated with the plots of individual glass analyses more scattered. One important observation is that the data dispersion is bigger horizontally than vertically in the ternary figure. This supports the view that the lime content is controlled by the firing temperature, resulting in less scatter in compositions vertically (only the lime content changes vertically) since the firing temperature used or possible to achieve with ancient glass-making technology was limited at the upper range by the available refractory materials, and at the lower end by the minimum temperatures necessary to make glass. In fact, most of the LBA glass compositions plot between 800 and 1000 °C, which is about the range of the temperature that is believed to be used in LBA glass-making (initial firing and secondary firing) in the published works. However, it is difficult to explain why LBA glass compositions scatter horizontally. Thus, it is important to further investigate what is causing the LBA glass compositions to differ and to scatter horizontally in the ternary diagram. The main compositional differences of horizontally dispersed plots are mainly due to alkali and silica contents in the glass.

Overall, it should be stressed that some of the Egyptian glasses plot a considerable distance to the right from the Egyptian trough, some even reaching the Roman trough. This is in contradiction to the data presented by Rehren (2000a, b), but in good agreement with the experimental results presented in this thesis (see below). The data analyzed here do not plot randomly across the range of potential glass-forming compositions. Rather,

there is a clear pattern in the data, as explained below in more detail. This indicates that there are controlling factors at work, which can be either a direct reflection of raw material choice and batch recipes, or an indirect reflection of furnace temperatures, as argued for the lime content (see above and below). In any case, they represent configurational, that is human, factors and influences, although these are to some extent modulated by the inherent behavior of the glass-forming reactions. There are two main factors controlling the spread of the reduced glass compositions in the diagram, namely the technical limitation in ancient glass-making, such as furnace designs that determines the temperature that can be reached, and variability in the raw materials, especially in plant ash.

In this section published (Brill 1999a, Oates *et al.* 1997, Reade 2005, Schoer & Rehren 2007, Shortland 2000b, Shortland 2002) compositions of LBA glass are compared to figure out which parameters (oxides) actually vary how much. Since a ternary figure uses reduced oxides, it only shows us the spread in silica** to soda** ratios horizontally, it does not reflect the whole glass composition and variability in minor oxides which are included in the reduced data. That is, for example, since the potash content is converted and integrated into soda** content, the reduced data does not reflect the alkali difference in the raw materials used to produce a glass. Therefore, all analyzed oxides in the publications were taken into consideration for the comparison. In addition, since there is a possibility of specialisation in colours produced at each LBA glass workshop as initially suggested by Rehren (1997, 2000a), the published data of LBA glasses were compared by sites (where the glass samples were found) and by their colours to see if there is any trend

present. If there is any trend, an attempt will be made to interpret this using the findings from the experimental melts discussed earlier.

7.1.1. Colorants and opacifiers used in LBA Egyptian glass

Glass consists of various oxides, mainly the seven base glass oxides (silica, alumina, iron oxide, soda, potash, lime and magnesia), any minor oxides and trace elements, notably phosphate, sulphate, titania, chlorine, strontium, barium, zirconium, rubidium and so on, and finally the added colorants and opacifiers and their related elements. These three groups are not independent; the first two are an arbitrary division across geochemical correlations between lime and strontium or potash and rubidium, and the contents of some base and minor oxides will be affected by the addition of colorants and/or opacifiers (see below for more details). The colorants are used either singly or combined to produce various colours of glass. A total of eleven different colours were observed among LBA Egyptian glasses, as published in Shortland (2002: Table 1) and shown here in Table 7.1 (below). As seen from Table 7.1, although four types of metal colorants (Cu^{2+} , Cu^+ , Co, and Mn) and two types of opacifiers (calcium antimonate, $\text{Ca}_2\text{Sb}_2\text{O}_7$, and lead antimonate, $\text{Pb}_2\text{Sb}_2\text{O}_7$) were available during the LBA, not all the possible combinations of colours were used. That is, for example, mixing cobalt and lead antimonate may produce a opaque dark green glass, but there is no such glass that has been found from LBA sites. Shortland (2002) notes that this may be due to the technicality of cobalt, being such a strong colorant that it does not produce a good green glass by simply mixing the two. Moreover, all the colorants occur on their own and mixed with opacifier, except for manganese, which only occurs on its own; there seems to be no technical

reason for this. This may again suggest the existence of specialisation among LBA glass workshops, as mentioned in Chapter 2 (workshop organization section), with some colorants and opacifiers available only at a limited number of workshops.

Table 7.1: Colorants and opacifiers used in LBA Egyptian glass (Shortland 2002: Table 1).

Colorant	Opacifier	Colour produced
None	None	Colourless, amber, or brown
None	Calcium antimonate	Opaque white
None	Lead antimonate	Opaque yellow
Cu ²⁺	None	Translucent blue
Cu ²⁺	Calcium antimonate	Opaque turquoise
Cu ²⁺	Lead antimonate	Opaque green
Cu ⁺	None	Opaque red
Co	None	Translucent dark blue
Co	Calcium antimonate	Opaque deep blue
Mn	None	Translucent purple
Mn---accompanied with Fe?	None	Black

7.1.2. Glass composition differences among LBA sites

Firstly, base glass compositions within the individual LBA sites (both Mesopotamian and Egyptian, including Uluburun, see Chapter 2 for more details on the sites) were compared by colour to see if there is any difference within the glass supposedly produced or worked within the same site, and to see if there is any specialisation in certain site(s), as mentioned above. Secondly, the glass compositions are compared by their colours between Mesopotamian and Egyptian LBA to see if there is any difference in colorant and base glass used in Mesopotamian and Egyptian (see Table 7.1, above)

and to further investigate if there is any colour specialisation between the two. Lastly, all LBA glass compositions were plotted on the ternary diagram by their colours to see if there is any difference in the base glass compositions. Most of the LBA glass composition data used for comparisons were obtained from Brill's publications (1999b, 1999a), with additional data for Tell Brak from Oates *et al.* (1997), Amarna from Shortland (2002), and the newly analysed Qantir samples (Schoer & Rehren 2007).

7.1.2.1. Individual LBA sites

(1) Nuzi

The compositions of Nuzi glasses were summarised and shown in Table 7.2 (full compositions) and Table 7.3 (the seven base oxide compositions), below. There are both coloured and colourless glass samples from Nuzi and the minor oxide contents seem to reflect the usage of the colorant and/or the opacifier to produce certain colours, such as the copper oxide and the antimony oxide contents.

There are four different colours, namely transparent dark blue, transparent light blue, opaque light blue, and amber/yellow. Most of the analysed glasses had a blue colour, either opaque or transparent. There is no cobalt blue glass. A transparent dark blue glass from Nuzi was coloured using copper rather than cobalt. The copper oxide content in the dark blue glass was the highest (2 wt%) while the other blue glasses had about 1 wt% CuO. Antimony oxide was detected only in opaque (light blue) glasses that strongly suggest antimony was added to the batch as an opacifier.

Table 7.2: Average compositions of various glass samples from Nuzi [wt%] (Brill 1999a, b).

Description (n = numbers of samples analysed)	SiO ₂	Na ₂ O	CaO	K ₂ O	MgO	Al ₂ O ₃	Fe ₂ O ₃	TiO ₂	Sb ₂ O ₅	MnO	CuO	CoO	SnO ₂	PbO	NiO	P ₂ O ₅		
Colourless (n = 1)	65.2	17.1	8.8	2.4	5.0	0.8	0.31	0.0	na	0.05	0.0	na	na	0.0	na	0.1		
Trn Dk blue (n = 1)	66.9	14.7	8.4	3.1	3.9	0.4	0.21	0.0	na	0.03	2.15	na	na	0.0	na	na		
Trn Lt blue (n = 4)	68.2	15.7	6.5	2.4	4.5	0.8	0.49	0.0	na	0.03	1.32	na	na	0.0	na	na		
Opq Lt blue (n = 3)	65.1	15.0	8.6	2.8	3.8	0.5	0.63	0.0	2.1	0.03	1.12	na	na	0.0	na	0.2		
Amber or yellow (n = 1)	70.0	13.0	6.0	3.6	5.4	1.0	0.31	0.0	0.1	0.05	0.03	na	na	0.0	na	0.2		
na: not available																		
										Trn: Transparent			Dk: Dark		Lt: Light		Opq: Opaque	

Table 7.3: The seven base oxide compositions of various glass samples from Nuzi [wt%] (Brill 1999a, b).

Description (n = numbers of samples analysed)	Normalised to 100 wt%						
	SiO ₂	Na ₂ O	CaO	K ₂ O	MgO	Al ₂ O ₃	Fe ₂ O ₃
Colourless (n = 1)	65.4	17.2	8.9	2.4	5.0	0.8	0.3
Transparent dark blue (n = 1)	68.5	15.1	8.6	3.2	4.0	0.4	0.2
Transparent light blue (n = 4)	71.9	14.5	6.0	2.2	4.2	0.7	0.5
Opaque light blue (n = 3)	67.5	15.6	8.9	2.9	3.9	0.5	0.7
Amber (or yellow) (n = 1)	70.5	13.1	6.1	3.6	5.4	1.0	0.3

As seen from Table 7.3, all the glasses have similar minor base glass oxide contents; 2-4 wt% of potash, 4-5 wt% of magnesia, below 1 wt% of both alumina and iron oxide. However, the three main base glass oxides (silica, soda, and lime) vary by the colour of the glass. Especially for the silica content that varies a lot from 65-72 wt%. The soda and lime contents of all the glasses were 13-17 wt% and 6-9 wt%, respectively. However, the three types of copper-coloured (blue) glasses (both opaque and transparent, eight in total) are much more similar to each other than the two single colourless and amber glasses, respectively. The latter have both much higher magnesia, but differ widely in their soda and lime content, being the extreme high and low compositions in both.

As discussed in Chapter 2, Nuzi seems to be a glass-working site rather than

glass-making since there is no industrial debris or raw materials published or found from the site. However, the base glass compositions suggest that the copper-coloured blue glasses are from one source. That is, these Nuzi copper-blue glasses may be once produced at the site while the other colours found at the site may be imported from other workshop(s).

(2) Tell al Rimah

There are four different colours, namely, transparent blue, opaque light blue, opaque yellow, and opaque red. However, almost all of Tell al Rimah samples were particularly badly weathered so that published data cannot be used for further comparison.

(3) Tell Brak

The compositions of Tell Brak glasses were summarised and shown in Table 7.4 (full compositions) and Table 7.5 (the seven base oxide compositions), below. There are both coloured and colourless glass samples from Tell Brak. There are about seven different colours in total, namely black, dark blue (some of them defined as opaque but some of them are not clear if it is opaque or transparent), light blue (both opaque turquoise and transparent), opaque yellow, opaque dark amber/brown/yellow, purple, and opaque white. Although most of the oxides analysed vary considerably among Tell Brak glass samples, two dark blue glasses have the typical characteristic of LBA cobalt-blue glass that has high alumina content, while one has the normal low level. However, none of these dark blue glasses have the typical low potash.

In addition, these dark blue glasses, particularly opaque ones, have no MnO

Table 7.4: Average compositions of various glass samples from Tell Brak [wt%] (Brill 1999a, b, Oates *et al.* 1997).

Description	SiO ₂	Na ₂ O	CaO	K ₂ O	MgO	Al ₂ O ₃	Fe ₂ O ₃	TiO ₂	Sb ₂ O ₅ <u>Sb₂O₃</u>	MnO	CuO	CoO	SnO ₂	PbO	NiO	P ₂ O ₅
Colourless (n = 1)	72.2	14.5	9.1	0.1	2.1	1.7	0.16	0.0	na	0.0	0.01	na	0.0	0.1	0.0	na
<u>Black</u> (n = <u>1</u>)	<u>64.1</u>	<u>19.0</u>	<u>4.6</u>	<u>3.4</u>	<u>6.2</u>	<u>0.7</u>	<u>0.3</u>	<u>na</u>	<u>nd</u>	<u>nd</u>	<u>nd</u>	<u>nd</u>	<u>na</u>	<u>nd</u>	<u>na</u>	<u>0.3</u>
<i>Dk blue</i> (n=1 + <u>1</u>)	68.8	12.0	4.1	2.9	4.1	2.2	0.5	<i>nd</i>	0.3	0.2	0.3	0.1	<i>nd</i>	0.1	<i>nd</i>	0.2
	<u>69.9</u>	<u>15.9</u>	<u>5.1</u>	<u>2.2</u>	<u>3.9</u>	<u>0.3</u>	<u>0.2</u>	<u>na</u>	<u>0.1</u>	<u>nd</u>	<u>1.6</u>	<u>0.08</u>	<u>na</u>	<u>nd</u>	<u>na</u>	<u>0.1</u>
Opq Dk blue (n = 1)	70.1	9.7	6.4	2.6	6.5	2.0	1.42	0.1	0.1	0.0	0.75	0.05	na	0.1	0.0	na
Opq Lt blue (n = 3 + 3 + <u>1</u>)	67.6	15.3	8.7	1.8	3.3	0.5	0.19	0.0	1.2	0.0	1.16	na	0.0	0.1	0.0	na
	64.6	15.1	7.6	3.0	5.3	1.2	0.43	<i>nd</i>	3.1	0.1	0.90	<i>nd</i>	<i>nd</i>	0.1	<i>nd</i>	0.2
	<u>63.7</u>	<u>15.0</u>	<u>10.7</u>	<u>2.1</u>	<u>4.2</u>	<u>0.6</u>	<u>0.3</u>	<u>nd</u>	<u>1.1</u>	<u>nd</u>	<u>nd</u>	<u>0.61</u>	<u>nd</u>	<u>na</u>	<u>na</u>	<u>0.1</u>
<i>Trn Lt blue</i> (n = 4)	66.5	16.8	5.3	2.6	5.4	0.5	0.30	<i>nd</i>	<i>nd</i>	<i>nd</i>	1.38	<i>nd</i>	<i>nd</i>	<i>nd</i>	<i>nd</i>	0.1
Opq yellow (n = 1)	73.1	7.5	5.9	1.4	4.9	1.2	0.82	0.0	na	0.0	0.01	na	na	4.6	0.0	na
Opq Dk amber/yellow/ <u>brown</u> (n = 1 + 2 + <u>1</u>)	67.1	16.3	7.3	3.1	5.5	0.4	0.08	0.0	na	0.0	0.01	na	na	0.0	na	na
	69.2	14.6	4.3	2.7	6.0	0.5	0.20	<i>nd</i>	<i>nd</i>	0.1	<i>nd</i>	<i>nd</i>	<i>nd</i>	<i>nd</i>	<i>nd</i>	0.2
	<u>67.7</u>	<u>17.6</u>	<u>4.0</u>	<u>2.6</u>	<u>6.5</u>	<u>0.2</u>	<u>nd</u>	<u>na</u>	<u>nd</u>	<u>nd</u>	<u>nd</u>	<u>nd</u>	<u>na</u>	<u>na</u>	<u>na</u>	<u>0.1</u>
<u>Purple</u> (n = <u>1</u>)	<u>66.0</u>	<u>19.6</u>	<u>4.1</u>	<u>2.0</u>	<u>3.7</u>	<u>2.1</u>	<u>0.4</u>	<u>na</u>	<u>0.1</u>	<u>0.3</u>	<u>0.34</u>	<u>0.04</u>	<u>na</u>	<u>0.1</u>	<u>na</u>	<u>0.1</u>
Opq white (n = 2)	66.5	14.9	8.0	3.1	5.3	0.6	0.31	0.0	1.0	0.0	0.02	na	na	0.1	0.0	na

n: number(s) of sample(s) analysed. na: not available nd: not detected Opq: Opaque Trn: Transparent Dk: Dark Lt: Light

Note: data shown in italics was obtained by J. Henderson and the underlined data was obtained by B. Velde, respectively, both published in Oates *et al.* 1997: Table 6b & Table 7. Their data was obtained mainly from glass beads.

Table 7.5: The seven base oxide compositions of various glass samples from Tell Brak [wt%] (Brill 1999a, b, Oates *et al.* 1997).

Description (n = numbers of samples analysed)	Normalised to 100 wt%						
	SiO ₂	Na ₂ O	CaO	K ₂ O	MgO	Al ₂ O ₃	Fe ₂ O ₃
Colourless (n = 1)	72.3	14.5	9.1	0.1	2.1	1.7	0.2
<u>Black</u> (n = <u>1</u>)	<u>65.2</u>	<u>19.3</u>	<u>4.7</u>	<u>3.5</u>	<u>6.3</u>	<u>0.7</u>	<u>0.3</u>
Dk blue (n=1 + <u>1</u>)	72.7 <u>71.7</u>	12.7 <u>16.3</u>	4.3 <u>5.2</u>	3.1 <u>2.3</u>	4.3 <u>4.0</u>	2.3 <u>0.3</u>	0.5 <u>0.2</u>
Opq Dk blue (n = 1)	71.0	9.8	6.5	2.6	6.6	2.0	1.4
Opq Lt blue (n = 3 + 3 + <u>1</u>)	69.4 66.9 <u>65.9</u>	15.7 16.0 <u>15.5</u>	8.9 7.2 <u>11.1</u>	1.8 3.0 <u>2.2</u>	3.4 5.5 <u>4.3</u>	0.5 1.0 <u>0.62</u>	0.2 0.4 <u>0.3</u>
<i>Trn Lt blue</i> (n = 4)	68.4	17.3	5.4	2.6	5.5	0.5	0.3
Opq yellow (n = 1)	77.1	7.9	6.2	1.5	5.2	1.3	0.9
Opq Dk amber/yellow/ <u>brown</u> (n = 1 + 2 + <u>1</u>)	67.6 71.0 <u>68.7</u>	16.4 15.0 <u>17.8</u>	7.4 4.4 <u>4.1</u>	3.1 2.7 <u>2.6</u>	5.0 6.2 <u>6.6</u>	0.4 0.5 <u>0.2</u>	0.1 0.2 <u>0.0</u>
<u>Purple</u> (n = <u>1</u>)	<u>67.4</u>	<u>20.0</u>	<u>4.2</u>	<u>2.0</u>	<u>3.8</u>	<u>2.2</u>	<u>0.4</u>
Opq white (n = 2)	67.4	15.1	8.1	3.1	5.4	0.6	0.3

Note: data shown in italics was obtained by J. Henderson and the underlined data was obtained by B. Velde, respectively, both published in Oates *et al.* 1997: Table 6b & Table 7.

and very high MgO, showing a very unique composition. A single purple glass also shows high alumina content suggesting alumina-rich cobalt colorant was added with manganese oxide to produce this colour.

The contents of both major and minor base oxides vary considerably by their colours, except for some of the opaque dark amber/yellow glass and opaque white glasses that are both from the 'waste lump' and analysed by Brill (see Chapter 2 for more details), while the others are found as either glass ingots or as vessel fragments, or as beads. However, the opaque yellow glass has a rather low soda content, which is either indicative of heavy corrosion, or of the effect of lead oxide as a flux (but this is unlikely due to the relatively low level of PbO here).

There are 5 different base glass compositions among Tell Brak glasses; 1) low-potash, low magnesia, and high alumina base composition, that suggest the glass is natron-based rather than plant ash based (i.e. colourless glass), 2) low silica, low soda base composition (i.e. black), 3) high alumina (above 2 wt%) base composition (i.e. opaque and transparent dark cobalt-blue glasses), 4) 2-3 wt% potash and 4-6 wt% magnesia, having a typical LBA plant-ash glass base composition and majority of Tell Brak glasses have this base composition (i.e. light copper-blue, dark amber/yellow/brown, and white), and 5) low silica, low soda, similar to black glass base composition, but with high alumina content (i.e. purple).

This inconsistency in glass compositions may be due to the fact (see Chapter 2 for more details) that it is a multi-period archaeological site, although most of the glasses were found from the level which dates to the 13th century BC. However, the colourless glass has a typical Roman composition (low potash and low magnesia) and may be later than LBA. The base compositions of glasses, shown in Table 7.5, are variable, indicating various sources.

However, having 5 different types of base compositions (above) and the fact that the glass samples may come from different periods, it is not clear which type of base glass composition(s) were produced locally, if any.

Therefore, it is still not clear whether glass was locally produced at Tell Brak. The glass samples found only suggest that the site could be a large, long lasting glass workshop.

(4) Nimrud

Although Nimrud dates later than the timeframe of my research, 1500-1000 BC, Nimrud's glasses will be discussed here because Nimrud glass is determined as plant-ash based by Brill's (1999a) analysis, as mentioned earlier (in Chapter 2) and because of the fact that there are very few glass findings available from LBA Mesopotamian sites. However, the most recent chemical analysis of Nimrud glasses (Reade *et al.* 2005) with a further 45 glass samples (while Brill's data published in 1999 had only 24 glasses from Nimrud), mainly blue and colourless glasses, showed that both plant ash glasses and natron glasses were found from the site. Therefore, for this site, not only the comparisons of the chemical compositions of glasses within Nimrud, but also the comparisons of the chemical compositions of Nimrud glasses and the other LBA sites will be conducted here.

There are both coloured and colourless glass samples from Nimrud. There are nine different colours, namely opaque dark cobalt-blue, opaque light blue, transparent blue, transparent dark cobalt-blue, transparent light blue, opaque yellow, opaque red, purple, and green. Copper contents of all the glasses

were reported as copper oxide (CuO), a bivalent form (Cu²⁺), except for opaque red glasses of those were obtained as cuprite (Cu₂O), a monovalent form (Cu⁺).

The most recently published compositions of Nimrud glasses (regardless of their colours), obtained by Reade and her co-workers (2005: Table 1), will be discussed here and the data are summarised and shown in Table 7.6 (full composition) and Table 7.7 (reduced seven base glass oxides). Group 1 glasses have very similar compositions, all having potash contents of about 1.5 wt% and magnesia contents of about 3 wt% (Reade *et al.* 2005). This magnesia content follows more or less a similar make up to plant ash glass. However, the potash content can be seen at the bottom end of the scale of this type of glass (Reade *et al.* 2005). Group 2 glasses have a typical plant ash glass composition of high potash and high magnesia contents. Group 3 glasses seem to have the compositions of natron glasses, having low contents of both potash (1.0 wt%) and magnesia (1.8 wt%). In addition, Group 3 glasses have low phosphate contents of 0.1 wt% whereas plant ash glasses tend to have higher phosphate contents (Reade *et al.* 2005). Group 4, consisting of cobalt-coloured glasses, have the typical characteristic of LBA cobalt-blue glasses with low potash (0.5 wt%) and high alumina (5.7 wt% while the other Nimrud glasses have less than about 1 wt% Al₂O₃) contents. Therefore, the analyses by Reade and her co-workers (Reade *et al.* 2005) strongly suggest that not all the Nimrud glasses are typical LBA Mesopotamian plant ash based glasses as initially suggested by Brill (1999a).

Table 7.6: Average compositions of various glass samples from Nimrud [wt%] (Reade et al. 2005: Table 1).

	SiO ₂	Na ₂ O	CaO	K ₂ O	MgO	Al ₂ O ₃	FeO	TiO ₂	Sb ₂ O ₃	MnO	CuO	CoO	SnO ₂	ZnO	NiO	P ₂ O ₅	SO ₃
Group 1	69.69	13.90	8.66	1.46	3.07	1.00	0.48	0.14	<0.4	0.43	<0.1	<0.1	<0.4	<0.1	<0.1	0.15	0.53
Group 2	60.84	15.98	6.32	3.40	5.18	1.01	0.57	<0.1	2.69	<0.1	2.97	<0.1	<0.4	<0.1	<0.1	0.18	0.52
Group 3	69.85	16.94	6.15	0.95	1.70	0.55	0.28	<0.1	0.92	0.10	1.74	<0.1	<0.4	<0.1	<0.1	0.10	0.54
Group 4	66.28	18.12	2.88	0.45	2.72	5.50	0.85	<0.1	1.71	0.38	<0.1	0.16	<0.4	0.13	0.13	<0.1	0.56

Group 1 glasses consist of colourless, weakly coloured to pink/purple hemispherical bowls.

Group 2 glasses consist of a small group of glasses with a typical plant ash glass composition, high potash and high magnesia.

Group 3 glasses consist of vessels, mainly copper blue with some colourless.

Group 4 glasses consist of 13 cobalt-blue glasses.

Table 7.7: The seven base oxide compositions of various glass samples from Nimrud [wt%] (Reade et al. 2005).

Description (n = numbers of samples analysed)	Normalised to 100 wt%						
	SiO ₂	Na ₂ O	CaO	K ₂ O	MgO	Al ₂ O ₃	Fe ₂ O ₃
Group 1 (n = 8)	70.8	14.1	8.8	1.5	3.2	1.0	0.5
Group 2 (n = 3)	65.2	17.1	6.8	3.6	5.6	1.1	0.6
Group 3 (n = 21)	72.4	17.5	6.4	1.0	1.8	0.6	0.3
Group 4 (n = 13)	68.5	18.7	3.0	0.5	2.8	5.7	0.8

In summary, Nimrud is the latest (9th-7th century BC, see Chapter 2 for more details) site among all the other archaeological sites mentioned in this section and beyond the timeframe of my research. While there are some plant ash glasses present, the majority seem to be already natron-based. Natron based SLS glasses start to appear around 1000 BC (Schlick-Nolte & Werthmann 2003) in Egypt as well. Therefore, it is not surprising that both plant ash and natron based glasses were found from Nimrud. In addition, it may be possible that natron glasses may have been produced from an earlier time but the nature of the natron base glass having lower content of stabiliser, lime, compared to that of plant ash based, made them difficult to survive. However, further work is necessary to better understand the changing glass-making technology around 1000 BC.

For the purpose of this thesis, I will concentrate for further comparisons on the clearly plant ash based glasses of groups 1 and 2.

Although both groups 1 and 2 are plant ash based glasses, the base glass compositions of the two varies for both major and minor base oxides. Therefore, glass samples from Nimrud may not have been produced locally.

As a whole summary, the base glass compositions of Mesopotamian glasses have wide ranges of major base glass oxide contents with much more narrow ranges of minor base glass oxide contents, except for cobalt-blue glasses. LBA Mesopotamian glasses have approximately 65-72 wt% silica, 13-20 wt% soda, 4-11 wt% lime, 2-4 wt% potash, 3-6 wt% magnesia, <1 wt% alumina,

and <0.5 wt% iron oxide. The similarity in potash and magnesia contents, in particular, generally reflects the source of alkalis used to produce the glass (e.g plant ash or natron).

LBA Mesopotamian cobalt-blue glasses were so far found from Tell Brak and Nimrud only. All the Nimrud cobalt-blue glasses have a natron-based glass composition, having a typical LBA cobalt-blue signature of low potash and high alumina content. However, it is noteworthy to mention that the cobalt-blue glasses from Tell Brak show very unique glass compositions, particularly opaque ones, having high alumina with no MnO and with very high MgO. It is interesting that only this particular cobalt-coloured glass has a unique glass composition compared to the other coloured glasses available in Mesopotamia during the LBA.

Glass-making in Mesopotamia during LBA may be centralised to some degree having similar minor base oxide contents, especially magnesia and potash contents. However, from the current published works, it is not clear which site was the major centralised glass-making site, the findings only suggest that glass workshops existed at the site. It is interesting that only one particular colour, cobalt-blue, has a unique base composition and it is not clear whether this particular colour was produced in Mesopotamia or somewhere else.

Since more fundamental evidence for glass-making (i.e. furnace remains, semi-finished glass remains with crucibles etc.) and larger numbers of cobalt-blue glasses were found from LBA Egyptian sites (see Chapter 2 &

Chapter 6), the published glass compositions of glass samples found from LBA Egyptian glass workshop sites will be discussed below to further investigate this matter.

(5) Malkata

The compositions of Malkata glass samples were summarised and shown in Table 7.8 (full compositions) and Table 7.9 (seven base glass oxide compositions), below. Most of the glasses from Malkata were coloured blue and there are five different types of blue, namely transparent dark cobalt-blue, opaque dark cobalt-blue, opaque dark blue, transparent light blue, and opaque light blue. All the light blue glasses are coloured by copper while most of the dark blue glasses were produced using cobalt (with a cobalt oxide content of about 0.1 wt%) and have the typical LBA cobalt-blue characteristic of high alumina content. However, there are some dark blue glass samples from the site with no cobalt detected. There are purple and opaque yellow glasses beside blue from Malkata.

There are four different types of base glass compositions among Malkata glasses; 1) high soda to potash ratio (high soda content) with high alumina content (about 2 wt%) base glass composition (i.e. both transparent and opaque cobalt-blue glasses), 2) a typical Malkata base glass composition, having a typical LBA plant ash based glass composition of 61-64 wt% silica, 18-19 wt% soda, 10-12 wt% lime, 2 wt% potash, and 4-5 wt% magnesia, (i.e. opaque dark blue, opaque light blue glasses, and purple glasses), 3) a distinct low potash and low magnesia (1 wt% and 3 wt%, respectively) base composition similar to the typical natron based glass composition (i.e.

Table 7.8: Average compositions of various glass samples from Malkata [wt%] (Brill 1999a, b).

Description (n= numbers of samples analysed)	SiO ₂	Na ₂ O	CaO	K ₂ O	MgO	Al ₂ O ₃	Fe ₂ O ₃	TiO ₂	Sb ₂ O ₅	MnO	CuO	CoO	SnO ₂	PbO	NiO	P ₂ O ₅
Trn Dk Co-blue (n = 2)	62.9	20.6	7.2	1.5	3.6	1.6	0.84	0.1	1.12	0.1	0.09	0.07	0.0	0.0	0.04	na
Opq Dk Co-blue (n = 2)	61.0	20.0	7.8	1.6	4.1	2.0	0.98	0.1	1.30	0.2	0.51	0.10	na	0.0	0.07	na
Opq Dk blue (n = 1)	55.6	17.1	10.9	2.2	3.7	0.9	1.03	0.1	8.29	0.0	0.03	na	na	0.0	na	na
Trn Lt blue (n = 1)	70.6	14.5	7.6	1.0	2.7	0.7	0.55	0.1	0.92	0.0	0.10	na	0.1	0.1	na	na
Opq Lt blue (n = 2)	59.6	17.1	11.1	2.3	4.1	0.9	0.68	0.1	2.57	0.0	1.35	na	0.2	0.0	na	na
Purple (n = 1)	63.8	17.7	9.7	2.0	4.5	0.8	0.70	0.1	na	0.5	0.01	na	na	0.0	na	na
Opq yellow (n = 1)	64.4	9.7	7.5	1.0	5.7	0.9	1.17	0.1	1.32	0.0	0.05	na	na	7.9	na	na
na: not available	Trn: Transparent			Dk: Dark			Opq: Opaque			Lt: Light						

Table 7.9: The seven base oxide compositions of various glass samples from Malkata [wt%] (Brill 1999a, b).

Description (n = numbers of samples analysed)	Normalised to 100 wt%						
	SiO ₂	Na ₂ O	CaO	K ₂ O	MgO	Al ₂ O ₃	Fe ₂ O ₃
Trn Dk Co-blue (n = 2)	64.0	21.0	7.3	1.5	3.7	1.6	0.9
Opq Dk Co-blue (n = 2)	62.6	20.5	8.0	1.6	4.2	2.1	1.0
Opq Dk blue (n = 1)	60.8	18.7	11.9	2.4	4.0	1.0	1.1
Trn Lt blue (n = 1)	72.3	14.8	7.8	1.0	2.8	0.7	0.6
Opq Lt blue (n = 2)	62.2	17.9	11.6	2.4	4.3	0.9	0.7
Purple (n = 1)	64.3	17.8	9.8	2.0	4.5	0.8	0.7
Opq yellow (n = 1)	71.3	10.7	8.3	1.1	6.3	1.0	1.3

transparent light blue glass), and 4) high silica (71 wt%), low potash (1 wt%), high magnesia (6 wt%) base glass composition (i.e. a opaque yellow glass).

It is interesting to note that the base glass composition of this opaque yellow glass is very different from those of the other glasses, highly suggesting that either this glass has different origin or a different technique was used to produce this colour.

In summary, although Malkata seems to be a large-scale glass-working site rather than glass-making as discussed earlier (see Chapter 2), base glass compositions suggest that glass-making may have taken place at the site, along with glass-working. The fact that some small crucibles containing

dark-blue glass were found and the fact that the majority of the glasses from the site were coloured in blue may suggest that some blue glasses were produced at the site. In fact, the majority of non-cobalt-blue glasses found from the site, except for the transparent light-blue, have similar base glass compositions. Moreover, the purple glass also has a base glass composition similar to the majority of non-cobalt-blue glasses, highly suggesting that glasses having this type of base glass composition were produced at the site. However, although cobalt-blue glasses have the typical LBA cobalt-blue signature of low potash (low potash to soda ratio) and high alumina contents, it is not clear whether these cobalt-blue glasses were produced at the site as well as other blues.

It is interesting to note that a possible natron based transparent blue glass (with no cobalt content) was found from the site and this is the only non-cobalt blue natron based glass found among LBA sites. It may be possible that blue glasses using natron was experimentally produced at the site. However, this is unlikely since natron-based glasses do not appear until much later, around 1000 BC.

(6) Tell el-Amarna

The composition of Amarna glass samples were published by Shortland (2000b: Table 3-2, Shortland & Tite 2000: Table 1) and the compositional data of coloured glass rods published by Brill (1999a, 1999b) is supplemented where only one sample of that colour was analysed by Shortland. The summarized data is shown in Table 7.10 (full compositions) and Table 7.11 (seven base glass oxide compositions), below. All the glass samples were

Table 7.10: Summarized compositions of glass samples from Amarna [wt%] (modified from Shortland (2000b, Shortland & Tite 2000), by adding data from Brill (1999 a, b) where possible). Note: Data obtained from Brill (1999a, b) are shown in *italics*.

	SiO ₂	Na ₂ O	CaO	K ₂ O	MgO	Al ₂ O ₃	Fe ₂ O ₃	TiO ₂	Sb ₂ O ₃	MnO	CuO	CoO	SnO ₂	PbO	NiO	P ₂ O ₅
Cobalt-blue (n = 10)	64.1	19.2	7.8	1.1	3.7	2.4	0.5	0.1	0.3	0.21	0.2	0.2	0.0	0.0	na*	0.1
Copper-blue (n = 9, 6)	65.9	15.2	8.5	2.7	3.8	1.1	0.7	0.1	0.2	0.04	1.5	0.0	0.1	0.0	na*	0.2
	62.4	19.2	8.9	2.1	4.0	0.8	0.5	0.1	0.4	0.08	0.4	na*	na*	na*	na*	na*
Opaque green (n = 1+1)	65.7	14.8	9.1	2.4	4.1	1.1	0.6	0.1	na*	0.00	0.8	0.0	0.1	1.1	na*	0.1
	64.6	17.7	6.3	1.0	2.7	1.0	1.4	0.15	Sb ₂ O ₅ 0.50	0.07	1.8	na*	0.2	2.1	na*	0.3
Opaque white (n = 1+1)	63.8	17.6	9.2	2.1	3.7	0.6	0.3	0.1	2.14	0.06	0.0	0.0	0.01	0.1	na*	0.2
	64.7	17.6	6.4	2.1	3.9	0.9	1.0	0.15	Sb ₂ O ₅ 2.73	0.05	0.0	na*	na*	0.09	na*	0.27
Opaque yellow (n = 1+1)	62.4	17.0	7.4	1.7	3.7	0.4	0.4	0.1	0.5	0.10	0.1	0.0	0.0	5.3	na*	0.3
	61.3	0.6	7.3	2.7	3.9	2.7	1.0	0.1	Sb ₂ O ₅ 0.84	0.05	0.1	na*	na*	4.9	na*	na*
Purple (n = 1)	64.7	19.0	8.7	2.2	2.8	2.2	0.2	0.0	0.07	1.22	0.2	0.0	0.0	0.0	na*	0.2
Opaque red(n=1)	67.4	16.9	7.1	1.6	3.2	1.6	1.3	0.1	Sb ₂ O ₅ 0.35	0.06	na*	na*	0.2	0.0	na*	na*

na*: not available. n = numbers of samples analysed.

Table 7.11: The seven base oxide compositions of various glass samples from Amarna [wt%] (Shortland 2000b, Shortland & Tite 2000, Brill 1999a, b).

Description (n = numbers of samples analysed)	Normalised to 100 wt%						
	SiO ₂	Na ₂ O	CaO	K ₂ O	MgO	Al ₂ O ₃	Fe ₂ O ₃
Cobalt-blue (n = 10)	64.9	19.4	7.9	1.1	3.7	2.4	0.5
Copper-blue (n = 9) (n = 6)	65.9 <i>63.8</i>	15.2 <i>19.6</i>	8.5 <i>9.1</i>	2.7 <i>2.1</i>	3.8 <i>4.0</i>	1.1 <i>0.8</i>	0.7 <i>0.6</i>
Opaque green (n = 1+1)	67.2 <i>68.2</i>	15.1 <i>18.7</i>	9.3 <i>6.7</i>	2.5 <i>1.1</i>	4.2 <i>2.9</i>	1.1 <i>1.1</i>	0.6 <i>1.5</i>
Opaque white (n = 1+1)	65.6 <i>67.0</i>	18.1 <i>18.2</i>	9.5 <i>6.6</i>	2.2 <i>2.2</i>	3.8 <i>4.0</i>	0.6 <i>0.9</i>	0.3 <i>1.0</i>
Opaque yellow (n = 1+1)	67.1 <i>65.5</i>	18.3 <i>17.9</i>	8.0 <i>7.8</i>	1.8 <i>2.9</i>	4.0 <i>4.2</i>	0.4 <i>0.7</i>	0.4 <i>1.1</i>
Purple (n = 1)	66.0	19.4	8.9	2.2	2.9	0.4	0.2

Note: Data obtained from Brill (1999a, b) are shown in *italics*.

coloured glass and there are seven different colours, namely cobalt-blue, copper-blue, opaque green, opaque white, opaque yellow, opaque red and purple. However, since there was only one opaque red colour glass rod analysed by Brill (1999a, 1999b) and its supposed red colorant, copper, was not detected, this red glass sample will be excluded from the discussion here.

The following minor oxide contents clearly show that the formed glass composition reflects the colorant composition and/or opacifier added. There is less than 0.1 wt % manganese oxide in all colours, except for purple glasses with an average of 1.2 wt%. Copper oxide is less than 0.2 wt% in all the colours except for copper blue and opaque green which both having higher contents of 1.5 and 0.8-1.8 wt%, respectively. Overall lead oxide

content is less than 0.05 wt%, except for opaque green and opaque yellow, both having higher contents of 1.0-2.0 and 5.3 wt%, respectively. Similarly, overall average of antimony oxide is less than 0.1 wt%, except for all the opaque coloured glasses (such as, white, opaque yellow, and opaque green). Opaque white has the highest antimony content of 2.0-3.0 wt % while the rest of opaque glasses have that of 0.5 wt%. It is important to note that antimony was not detected from the opaque green sample analysed by Shortland (2000b). This may simply be due to an analytical error. Shortland's (2002) study of glasses that contains lead antimonate (opaque green and yellow) showed lower antimony content compared to the lead content in the glass. His microscopic study of opaque yellow glasses from Amarna showed that the lead antimonate within the glass phase is unevenly distributed and the glass phase has a high lead to antimony ratio. Moreover, his analysis of opaque green glass showed that their lead and antimony levels are only about a third of those of the opaque yellow glasses. Therefore, the opaque green glasses have only a low amount or trace of antimony in the glass phase, considering the lead to antimony ratio is high in opaque yellow glasses.

It is noteworthy to mention that base glass compositions of all the Amarna glasses are very similar, except for cobalt-blue glasses (see Table 7.11, above). That is, particularly the alumina and potash contents in most of the Amarna glass are about 1 wt% (or less) and 2-3 wt%, respectively, except for cobalt-blue with higher alumina content of 2.3 wt% and with lower average potash content of 1 wt% showing a typical LBA cobalt-blue signature. However, the base glass compositions of Amarna glasses across different

colours are more homogenous than any other LBA sites, only cobalt-blue having difference in potash and alumina content. All the remaining five base oxide contents are much more consistent throughout all samples than from any other LBA sites. This homogeneous base glass composition highly suggests that the glasses were locally produced at the site, rather than importing different colours.

In addition, some glass-making debris and rods of different colours were also found from the site and there are many recent publications (Jackson *et al.* 1998, Nicholson 1995a, 1995b, 1996, Shortland 2000a, 2000b, Shortland & Tite 2000) suggesting glass-making from the site, including cobalt-blue glasses.

Therefore, in summary, although the furnace found by Nicholson (Jackson *et al.* 1998, Nicholson 1995b, 1995a, 1996) is not proven to be related to glass-making or -working, glass-making most likely took place at the site. Amarna seems to be a large-scale glass-making and/or glass-working site and most likely one of the major centralised glass workshops during the LBA.

(7) el-Lisht

The compositions of Lisht glass samples were summarised and shown in Table 7.12 (full compositions) and Table 7.13 (seven base glass oxide compositions), below. There are seven different coloured glasses, namely transparent dark blue, transparent light blue, black, purple, opaque green, opaque yellow, and opaque brownish red, that were analysed from Lisht. It

Table 7.12: Average compositions of various glass samples from Lisht [wt%] (Brill 1999a, b).

	SiO ₂	Na ₂ O	CaO	K ₂ O	MgO	Al ₂ O ₃	Fe ₂ O ₃	TiO ₂	Sb ₂ O ₅	MnO	CuO	CoO	SnO ₂	PbO	NiO	P ₂ O ₅
Trn Dk blue (n = 2)	64.3	19.5	7.9	1.8	3.2	0.8	1.17	0.1	na*	0.2	0.81	na*	na*	0.0	na*	na*
Trn Lt blue (n = 2)	65.2	21.1	5.1	2.3	3.4	0.6	0.95	0.1	na*	0.0	1.09	na*	0.1	0.0	na*	na*
Black (n = 3)	65.9	19.4	5.8	2.2	4.0	0.9	1.17	0.2	0.01	0.0	0.22	na*	0.0	0.0	na*	na*
Purple (n = 1)	65.0	19.1	6.7	2.4	4.5	0.8	0.73	0.1	na*	0.5	0.04	na*	na*	0.0	na*	na*
Opq green? (n = 1)	67.8	18.7	7.0	1.1	3.2	0.9	0.99	0.1	na*	0.0	0.02	na*	na*	0.0	na*	na*
Opq yellow (n = 1)	64.4	19.1	7.1	2.0	4.1	0.6	0.83	0.1	0.97	0.0	0.03	na*	na*	0.6	na*	na*
Opq Brownish-red (n = 1)	62.8	19.8	5.0	2.1	3.7	0.7	0.78	0.1	na*	0.0	4.61	na*	0.3	0.1	na*	na*

n = numbers of samples analysed.

na*: not available

Trn: Transparent

Dk: Dark

Lt: Light

Opq: Opaque

Table 7.13: The seven base oxide compositions of various glass samples Lisht [wt%] (Brill 1999a, b).

Description (n = numbers of samples analysed)	Normalised to 100 wt%						
	SiO ₂	Na ₂ O	CaO	K ₂ O	MgO	Al ₂ O ₃	Fe ₂ O ₃
Trn Dk blue (n = 2)	65.3	19.8	8.0	1.8	3.3	0.8	1.0
Trn Lt blue (n = 2)	66.1	21.3	5.2	2.3	3.4	0.7	1.0
Black (n = 3)	66.3	19.6	5.8	2.2	4.1	0.9	1.2
Purple (n = 1)	65.5	19.3	6.8	2.4	4.5	0.8	0.7
Opq green? (n = 1)	68.0	18.8	7.0	1.1	3.2	0.9	1.0
Opq yellow (n = 1)	65.6	19.5	7.2	2.0	4.2	0.6	0.9
Opq Brownish-red (n = 1)	66.2	20.9	5.3	2.2	3.9	0.7	0.8

is important to note that all the blue glasses analysed from Lisht are coloured by copper and there is no cobalt-blue glass found from the site. In addition, LBA Egyptian black glasses were analysed only from this site by Brill (1999a).

There are three different types of base glass compositions among glasses from Lisht; 1) a typical Lisht base glass composition (i.e., both dark and light copper-blue glasses, purple, opaque yellow, red-brown glasses) having 65-68 wt% silica, 19-21 wt% soda, 5-8 wt% lime, 2 wt% potash, 3-4 wt% magnesia, below 1 wt% alumina and iron contents (a typical LBA plan ash base glass composition), 2) high iron (1.2 wt%) base composition (i.e. black glasses), and 3) low potash (1.1 wt%) base composition (i.e. opaque green).

However, considering the fact that the manganese is accompanied by an excess of iron also in black glazing of Egyptian faience (Kaczmarczyk & Hedges 1983), it is not surprising that Lisht black glass is coloured by iron and therefore shows a higher iron content than those of the other Lisht glasses, while there is no manganese oxide detected. Otherwise, all the other six base oxide levels in black glasses are very similar to those of a typical Lisht base glass composition. Therefore, Lisht glasses seem to have a homogeneous base glass composition, except for opaque green glasses. The unique base compositions of opaque green glasses may be due to different sources and/or different techniques used to produce their colours. This homogeneity in base glass composition suggests that some glasses were produced locally at the site.

Although Lisht was initially thought to be merely recycling glasses from Amarna and Malkata, as mentioned earlier in Chapter 2, it is most unlikely that the glasses were recycled at the site due to the homogeneity of base glass compositions among Lisht glass samples regardless of the colour. In addition, this typical Lisht base glass composition has relatively high soda and iron contents and relatively low lime and alumina contents, compared to those of typical base compositions of Malkata and Amarna glasses. Moreover, considering the technicality of recycling LBA glasses, having more polychrome glass vessels/objects than monochrome ones, separating individual colours seems unlikely. This site is also unique being the only LBA Egyptian site without any of the popular cobalt-blue glass.

Therefore, this homogeneity of base glass composition of Lisht glass samples

highly suggest that some glasses were produced locally at the site while some colours were also imported from other sites/sources, rather than recycling.

(8) Qantir

The compositions of Qantir glass samples were summarised and shown earlier in Chapter 6 (Table 6.1 (full compositions) and Table 6.2 (seven base glass oxide compositions)).

There are so far six different colour glasses found from the site; colourless (?), opaque white, cobalt-blue, copper-blue, red, and purple. In particular, red seems to be a specialised colour at the site (see Chapter 2).

There are four different types of base glass compositions; 1) a typical Qantir base glass composition having 65-68 wt% silica, 17-20 wt% soda, 7-8 wt% lime, 2 wt% potash, 4-5 wt% magnesia and below 1 wt% alumina and iron oxide contents (i.e. colourless, red, copper-blue, and purple glasses), 2) a high silica (74 wt%), low soda (12-13 wt%), low lime (5 wt%), low magnesia (3 wt%), high alumina (2 wt%), and high iron (2 wt%) base composition, highly suggesting these glasses are semi-fused or half-reacted raw glasses, 3) a low potash (below 1.5 wt%), high alumina (3-4 wt%) and iron (1-2 wt%) base composition (i.e. cobalt-blue glasses), and 4) a high alumina, high iron (both about ≥ 1 wt%) base composition (i.e. opaque white).

Considering the archaeological findings (see Chapter 2) and the similarity in the base glass composition, including specialised red colour and semi-fused glasses, it is highly supporting the fact that glass-making indeed took place at

Qantir. In addition, the cobalt-blue glasses from Qantir have not only a typical LBA cobalt-blue glass signature of low potash and high alumina contents, but also have a high iron content up to 2 wt%. Qantir cobalt-blue glasses are unique to have such a high iron content compared to the other cobalt-blue glasses found from the other LBA sites, strongly supporting the hypothesis that Qantir was a large-scale glass-making site with specialisation in red colour along with other colours.

(9) Uluburun

The compositions of Uluburun glass ingots were summarised and shown in Table 7.14 (full compositions) and Table 7.15 (seven base oxide compositions), below. All glasses are transparent (no antimony was detected in all the samples) and most of the glasses (75 % of the analysed glasses) are coloured in dark (cobalt-) blue. The remaining are light blue glasses and a single purple glass. Although the most recent published work (Pulak 2006) reports orange-yellow glass being also found from the shipwreck its chemical composition is not available for comparison. This colour range clearly reflects the value of coloured glasses that resembles precious stones, as mentioned above, such as cobalt-blue as lapis lazuli, light blue as turquoise, purple as amethyst, and orange-yellow as possibly gold.

The base glass compositions among Uluburun glasses are similar in major base glass oxides but vary in minor base glass oxides by colours.

It is noteworthy that the cobalt-blue glasses not only have the typical LBA cobalt-blue glass composition signature, but also have a very similar base

Table 7.14: Average compositions of various glass samples from Uluburun shipwreck [wt%] (Brill 1999a, b).

	SiO ₂	Na ₂ O	CaO	K ₂ O	MgO	Al ₂ O ₃	Fe ₂ O ₃	TiO ₂	Sb ₂ O ₅	MnO	CuO	CoO	SnO ₂	PbO	NiO	P ₂ O ₅
Trn Dk blue (n = 9)	67.1	18.5	7.0	1.1	3.0	1.9	0.63	0.1	na*	0.1	0.10	0.05	0.003	0.0	0.03	0.09
Trn Lt blue (n = 2)	68.5	18.8	6.4	1.6	2.7	0.7	0.5	0.1	na*	0.0	0.48	na*	na*	0.0	na*	0.12
Trn Purple (n = 1)	63.9	17.8	9.1	2.2	4.9	0.6	0.71	0.1	na*	0.5	0.02	na*	0.003	0.0	na*	0.19

n = numbers of samples analysed.

na*: not available

Trn: Transparent

Dk: Dark

Lt: Light

Table 7.15: The seven base oxide compositions of various glass samples from Uluburun shipwreck [wt%] (Brill 1999a, b).

Description (n = numbers of samples analysed)	Normalised to 100 wt%						
	SiO ₂	Na ₂ O	CaO	K ₂ O	MgO	Al ₂ O ₃	Fe ₂ O ₃
Trn Dk blue (n = 9)	67.6	18.7	7.1	1.1	3.0	1.9	0.6
Trn Lt blue (n = 2)	69.1	19.0	6.4	1.6	2.7	0.7	0.5
Trn Purple (n = 1)	64.4	17.9	9.2	2.2	4.9	0.6	0.7

glass composition to that of the cobalt-blue glass from Amarna. In addition, the fact that minor base glass oxide contents vary by the colour and the fact that Uluburun cobalt-blue glass ingot matched in negative by similar structures on the interior of the cylindrical vessels from Amarna and also matched with base glass composition, highly suggest that Uluburun cobalt-blue glass was sourced from Amarna.

Uluburun purple glass has a very similar base composition to that of Malkata purple glass. In addition, the transparent light blue glass base composition is similar to those of transparent light blue glasses from Malkata and Amarna, especially for minor base glass oxides (Malkata has better match than Amarna for minor base glass oxides only). The base glass composition of the Uluburun purple ingot is very similar to that of purple glass from Malkata. However, considering the time frame when the ship sank, it is too late for Malkata workshop(s) (unless the dating of Malkata workshop is incorrect) and the time frame matches better to that of Amarna workshop(s).

These similarities in base glass compositions between Uluburun glasses and LBA Egyptian glasses may suggest that all the Uluburun glasses were sourced in Egypt. In addition, the fact that the base composition varies by the colours suggests that there are colour specialisations among LBA Egyptian sites at least.

As an overall summary, the base glass compositions of Egyptian glasses are similar regardless of their colours, except for cobalt-blue glasses. LBA

Egyptian glasses have approximately 65-70 wt% silica, 19-21 wt% soda, 6-11 wt% lime, 2-3 wt% potash, 4-5 wt% magnesia, <1 wt% alumina, and <1 wt% iron oxide. Cobalt-blue glasses were found at almost every LBA Egyptian site, except for Lisht, suggesting this colour was very popular in LBA Egypt. All the Egyptian cobalt-blue glasses have a natron-based glass composition, having a typical LBA cobalt-blue signature of low potash and high alumina content.

Glass-making in Egypt during LBA seems to be centralised to some degree having similar minor base oxide contents, especially magnesia and potash contents. However, it is more likely that there were colour specialisations among LBA Egyptian glass workshops as the Uluburun findings and as the majority of the LBA Egyptian sites produced some glasses locally with some other colours sourced from different sites. Large-scale glass workshop sites, such as Amarna and Qantir, seem to produce almost all the colours found from the site locally.

Some peculiar base compositions were seen among green glasses from LBA Egyptian sites. This may be simply due to the technicality during the colouring process rather than suggesting different sources.

Red, purple, and opaque green glasses are difficult to produce, thus the craftsmen need to be very familiar with the technicality of the process. Both redox conditions and temperatures have to be carefully monitored to produce red glass, as mentioned earlier (Chapter 2, section 2.6). Similarly, purple glasses need special control of melting conditions to leave the manganese

ions present in the glass at exactly the correct state of chemical oxidation, the trivalent state, to produce its colour (Sayre & Smith 1974). In the more modern colourless glasses (2nd to 4th centuries AD), even higher manganese contents can be found compared to these strongly coloured LBA purple glasses (Sayre & Smith 1974). Although, colourless glasses were only found from LBA Mesopotamian sites, none of the LBA colourless glass has a higher manganese content.

It is interesting to note that opaque yellow glasses from the Mesopotamian sites, except for Nimrud, have antimony oxide contents of only 0.1 wt% with an average lead oxide content below 5 wt%, while most of the opaque yellow glasses from Egyptian sites have those of about 1.0 wt% and more than 5 wt% (except for Lisht having below 1 wt% PbO), respectively, suggesting different colorant sources were used in Mesopotamian and Egyptian sites. Lead content in the yellow glasses tends to be higher than that of antimony since the colorant was added saturated with lead due to difficulty of producing this colour. Shortland's (2002) experimental work showed that the lead antimonate is very susceptible to temperature, and difficult to produce. It has to be integrated into the glass at relatively low temperatures (when the glass is extremely viscous) otherwise the formed glass will be of a poor quality having yellowish patches within a creamy coloured glass. However, Shortland's (2002) experimental study on lead antimonate colorant is still not complete and may not reflect the full technicality of the colorant.

In addition, Brill and co-workers' (1993) analyses of Mesopotamian glasses showed that they can be easily distinguished, isotopically, from the lead in

Egyptian yellow glasses, as mentioned above, suggesting that opaque yellow glasses were produced both in Mesopotamia and Egypt. Shortland's (2002, Shortland *et al.* 2000) lead isotope analyses of lead antimonate glasses from Amarna and Malkata showed that they were produced using the same lead source, possibly from Gebel Zeit on the Red Sea coast of Egypt. The earliest Tuthmosis III glasses contain lead that is isotopically different, probably from a Mesopotamian source, but since the time of Malkata and Amarna, almost all the glasses contain lead that is from Egyptian sources (Lilyquist *et al.* 1993, Shortland *et al.* 2000). It makes sense that although opaque yellow glass is difficult to produce, the skilled Mesopotamian craftsmen, who were brought back to Egypt when Tuthmosis III conquered Mesopotamia, used locally available raw materials.

7.1.2.2. LBA Mesopotamian sites vs. LBA Egyptian sites (in general)

The chemical compositions (base glass compositions) of glass samples from Mesopotamian sites varies by their colours, even within the same site, while those of LBA Egyptian glasses are much more consistent, as mentioned above. Base glass compositions of glasses from Egyptian sites are more consistent within each individual site compared to Mesopotamian glass samples. This may be due to the fact that glass samples from Mesopotamian sites tend to be in poorer conditions and are less well dated compared to the glasses from Egyptian sites. In addition, both magnesia and potash contents of LBA Mesopotamian glasses tend to be up to 1 wt% higher than those of LBA Egyptian glasses of the same colour (see Table 7.16, above). Nimrud glass compositions are exempt from the comparison here, except for Group 1 & Group 2 glasses (plant-ash based) since the most

Table 7.16: Comparison of the base glass composition between Mesopotamian and Egyptian LBA glasses* [wt%].

	SiO ₂	Na ₂ O	CaO	K ₂ O	MgO	Al ₂ O ₃	Fe ₂ O ₃
Mesopotamian	65 - 72	13 - 20	4 - 11	2 - 4	3 - 6	<1	<0.5
Egyptian	65 - 70	19 - 21	6 - 11	2 - 3	4 - 5	<1	<1

Note*: Regardless of their colours (all the colours combined, excluding cobalt-blue).

recent interpretation on Nimrud glasses suggested that both plant ash glasses and natron glasses were present or produced at Nimrud, as discussed earlier in this chapter.

In general, minor oxide contents that relate to colorant and opacifiers vary accordingly, reflecting the colorants and/or opacifiers added to produce the colour. There are nine different colours (i.e. cobalt-blue, copper-blue, red, purple, white, green, yellow/amber, black, and colourless), either transparent or opaque, and light or dark hue, found among analysed LBA glass samples discussed above. Judging from the chemical compositions, it seems that the colorants and opacifiers used at Mesopotamian LBA sites are the same as those used at LBA Egyptian sites (Table 7.1, above). The amount of colorants and opacifiers in the glass varies according to the depth of the colour. In general, the more the amount of colorants and opacifiers, the deeper the colour will become. However, not only the colorants but also the main raw materials, such as quartz (either in sand or pure pebble form), plant ash, and natron, can contribute to variety of minor oxides in the glass. Moreover, there are always contaminant(s) in these deliberately added materials that have a potential of accidentally contaminating the batch during the glass-making (e.g. clay from the partial melting of glass-making crucibles,

copper and bronze from tools and stirrers, and old glass from the reuse of these tools or vessels) (Shortland 2005). Shortland's (2005) analysis on LBA colourless glass compositions show that there are many minor oxides in the glasses that could be coming from the plant ash or one of the possible sources of accidental contamination. However, Shortland (2005) does not discuss about this matter in depth in his publication. Therefore, the contaminations caused by plant ash will be discussed more in detail in the later section (section 7.2) and the general composition variables that are coming from colorants will be mainly discussed in this section.

Blue is the most popular colour and blue glasses were found from every LBA site. However, it is interesting to note that cobalt-blue, red, and purple glasses were mostly found from Egyptian LBA sites.

As long established (Lilyquist *et al.* 1993; Kaszmarczyk 1986), all the LBA cobalt-blue glasses have a characteristic composition of high alumina contents, and typically a lower potash content as well as a suite of transition metal oxides together with the cobalt oxide. However, there is a difference between Mesopotamian and Egyptian cobalt-blue base compositions. Although all the LBA cobalt-blue glasses have low potash and high alumina contents, Egyptian cobalt-blue glasses tend to have lower potash contents (around 1 wt%) than those of Mesopotamian origin (1-2 wt%). Moreover, base glass compositions of Egyptian cobalt-blue is more consistent between sites than those between Mesopotamian sites, with opaque cobalt-blue glass from Nimrud having very extreme high alumina content of up to 7 wt%, while all the other LBA cobalt-blue glasses have about 2 wt% alumina.

In summary, the trend that purple, red, black and cobalt-blue can be found predominantly from Egyptian LBA sites, while some colours can be found everywhere, and the technical difficulty to produce certain colours suggest that there existed some specialisation among LBA glass workshops which colour(s) to be produced, especially for the cobalt-blue and red glasses. More details on cobalt-blue glasses will be discussed more in detail in the later section (section 8.2.2., in Chapter 8).

It is interesting to note that there is no tin in Mesopotamian copper-blue glasses while almost all the Egyptian copper-blue glasses discussed above have 0.1-0.2 wt% SnO_2 . Similarly, Shortland's (2005) analyses of LBA copper-blue glasses from Malkata, Amarna, and Tell Brak, showed that 75 % of analysed Egyptian copper-blue glasses contained tin while Mesopotamian copper-blue glasses have no tin in all of them. This suggest that copper-containing colorant used in Egypt may be based on bronze or bronze scrap (Shortland 2005).

Moreover, opaque green glass produced by mixing lead antimonate (yellow) and copper oxide (blue) has not been found from LBA Mesopotamian sites, while it can be found often in LBA Egyptian sites. A green glass from Nimrud has a peculiar composition, having very low copper (0.02 wt%), no lead, and low antimony (0.2 wt%) contents. This pattern highly suggests that the technique of producing green glass by mixing yellow and blue to make green was an Egyptian speciality.

The previous section has concentrated on the presence or absence of

particular oxides as a reflection of different raw materials and added colorants; this variability is strongly controlled by geological conditions and therefore regionally specific. However, one of the main aims of this thesis was to identify possible directly human-controlled parameters, such as firing temperatures, in the glass compositions. Therefore, further comparisons using three reduced oxides (ternary diagrams with SiO_2 , Na_2O , CaO , and fixed content of 5 wt% MgO) and by plotting the LBA glass compositions by their colours were conducted below.

7.1.2.3. Reduced compositions (ternary diagram, by colour)

All the collected LBA glass compositions, discussed above, were reduced (see Table 7.17, below) and plotted on the ternary diagrams by their colours (see Figure 7.1-7.6, below). The compositions were reduced to three major oxides, silica**, lime**, and soda**, with fixed value of 5 wt% MgO (see Chapter 2 for data handling). It is very unfortunate that there were not enough samples available to come up with any detailed interpretation of the plots, except for cobalt-blue and copper-blue. Therefore, the combined plots of all the LBA glasses, except for blue glasses (i.e. cobalt-blue and copper-blue) are shown in Figure 7.6, below.

In general, almost all the LBA glasses, regardless of the colour, can be plotted below 1000 °C, with just a few glasses plotting at around 1050 °C. This is supporting the current view that the upper limit of the firing temperature used for glass-making is around 1050 °C. Conversely, only very few glasses plot at temperatures below the 800 °C isotherm; this could either indicate that there is indeed a practical lower limit of glass-forming with the part of the phase

Table 7.17: Reduced compositions of various LBA glass samples [wt%] (data from Oates *et al.* 1997, Rehren 1997, Brill 1999a, 1999b, Shortland 2000b, Shortland 2002, Reade *et al.* 2005, Schoer & Rehren 2007).

SiO ₂	Na ₂ O	CaO	K ₂ O	MgO	Al ₂ O ₃	Fe ₂ O ₃	Total	Reduced & Normalized to 95%			Sample Description
								SiO ₂ **	Na ₂ O**	CaO**	
71.0	9.8	6.5	2.6	6.6	2.03	1.44	100	74.8	11.6	8.6	Tell Brak #1235, opaque dark cobalt-blue
72.7	12.7	4.3	3.1	4.3	2.30	0.50	100	76.9	14.7	3.2	Tell Brak #Br3, cobalt-blue
71.7	16.3	5.2	2.3	4.0	0.30	0.20	100	73.2	18.0	3.8	Tell Brak #Br5, dark cobalt-blue
65.2	16.5	3.2	1.0	6.3	6.52	1.33	100	73.3	16.9	4.8	Nimrud #3231, opaque dark cobalt-blue
65.7	15.3	4.3	0.8	4.9	7.11	1.77	100	75.1	15.8	4.1	Nimrud #3232, opaque dark cobalt -blue
64.6	17.0	4.2	0.8	4.7	7.40	1.32	100	74.2	17.4	3.4	Nimrud #3233, opaque dark cobalt -blue
63.6	17.3	4.2	0.9	4.7	8.00	1.28	100	73.8	17.8	3.4	Nimrud #3234, opaque dark cobalt -blue
71.1	16.4	4.9	0.3	2.1	4.21	0.99	100	77.6	16.8	0.6	Nimrud #3230, transparent dark cobalt-blue
68.3	19.2	3.0	0.4	3.4	5.18	0.52	100	74.9	19.4	0.7	Nimrud #3229, transparent dark cobalt-blue
63.0	22.6	6.5	1.9	3.5	1.53	0.91	100	66.5	24.2	4.3	Malkata #3901, transparent dark cobalt-blue
65.1	19.3	7.9	1.1	4.0	1.76	0.79	100	68.3	20.2	6.4	Malkata #3900, transparent dark cobalt-blue
61.9	19.6	8.4	2.0	5.0	2.19	0.98	100	65.8	21.1	8.1	Malkata #3902, opaque dark cobalt-blue
63.2	21.3	7.8	1.2	3.5	1.98	1.02	100	67.1	22.4	5.5	Malkata #3903, opaque dark cobalt-blue
67.6	18.1	7.7	0.8	3.7	1.61	0.53	100	70.5	18.7	5.8	Amarna #3357, transparent dark cobalt-blue
61.3	20.7	7.9	0.9	5.0	3.28	0.92	100	66.0	21.3	7.7	Amarna #3358, transparent dark cobalt-blue
67.2	19.0	6.5	1.0	3.5	2.21	0.52	100	70.8	19.8	4.3	Amarna #3359, transparent dark cobalt-blue
63.1	19.1	9.2	1.9	4.2	1.75	0.75	100	66.4	20.6	7.9	Amarna #3360, transparent dark cobalt-blue

Table 7.17: continued

SiO ₂	Na ₂ O	CaO	K ₂ O	MgO	Al ₂ O ₃	Fe ₂ O ₃	Total	SiO ₂ ^{wt}	Na ₂ O ^{wt}	CaO ^{wt}	Sample Description
62.8	18.6	9.5	0.9	4.7	2.82	0.73	100	66.8	19.2	9.1	Amarna #3361, transparent dark cobalt-blue
64.9	18.4	9.1	0.9	4.0	2.08	0.62	100	68.2	19.1	7.7	Amarna #1521, transparent dark cobalt-blue
69.2	16.4	7.5	1.3	3.6	1.32	0.68	100	72.0	17.4	5.6	Amarna #3364, transparent light cobalt-blue
64.6	17.9	6.5	0.3	4.3	4.24	2.17	100	71.5	18.1	5.4	Qantir #88/0386b, dark cobalt-blue
70.1	20.5	4.7	0.5	1.7	1.91	0.62	100	73.8	21.1	0.0	Uluburun #5950, transparent dark cobalt-blue
65.1	18.9	7.4	1.3	4.0	2.58	0.76	100	69.2	19.9	5.9	Uluburun #5951, transparent dark cobalt-blue
67.9	17.2	7.4	1.0	4.0	1.98	0.48	100	71.0	18.0	6.0	Uluburun #5954, transparent dark cobalt-blue
64.9	19.7	8.9	1.0	3.3	1.59	0.61	100	67.9	20.5	6.5	Uluburun #5955, transparent dark cobalt-blue
68.0	17.7	7.5	1.5	2.9	1.68	0.61	100	71.4	18.9	4.7	Uluburun #5956, transparent dark cobalt-blue
66.3	19.3	8.3	0.9	3.0	1.49	0.62	100	69.3	20.1	5.6	Uluburun #5957, transparent dark cobalt-blue
68.4	18.0	6.8	1.2	2.8	1.83	0.89	100	72.1	19.1	3.8	Uluburun #5961, transparent dark cobalt-blue
69.0	16.7	7.2	1.3	3.4	1.82	0.57	100	72.2	17.7	5.0	Uluburun #5962, transparent dark cobalt-blue
69.1	20.1	5.2	0.9	2.0	2.01	0.59	100	72.9	21.0	1.1	Uluburun #5975, transparent dark cobalt-blue
68.5	15.1	8.6	3.2	4.0	0.41	0.22	100	70.4	17.5	7.1	Nuzi #1214, transparent dark copper-blue
65.3	18.3	6.7	2.4	4.8	1.41	1.03	100	68.5	20.1	6.5	Nuzi #1217, transparent light copper-blue
71.2	15.8	5.2	2.4	4.7	0.43	0.24	100	72.7	17.6	4.7	Nuzi #1219, transparent light copper-blue
65.5	17.2	8.0	2.9	4.9	0.95	0.50	100	67.8	19.4	7.8	Nuzi #1221, transparent light copper-blue
67.2	15.5	9.7	2.5	3.6	0.51	1.01	100	70.0	17.5	7.6	Nuzi #1209, opaque light copper-blue

Table 7.17: continued

SiO ₂	Na ₂ O	CaO	K ₂ O	MgO	Al ₂ O ₃	Fe ₂ O ₃	Total	SiO ₂ **	Na ₂ O**	CaO**	Sample Description
70.0	13.6	9.7	2.4	3.2	0.43	0.69	100	72.5	15.5	7.0	Nuzi #1210, opaque light copper-blue
65.4	17.5	7.4	3.8	4.9	0.72	0.29	100	67.5	20.3	7.2	Nuzi #1216, opaque light copper-blue
69.4	16.8	8.6	1.7	3.1	0.25	0.10	100	70.9	18.2	5.8	Tell Brak #1230, opaque light copper-blue
65.6	15.6	11.1	2.0	4.3	0.88	0.38	100	67.8	17.2	10.0	Tell Brak #1231, opaque light copper-blue
73.3	14.9	6.9	1.7	2.7	0.40	0.11	100	75.2	16.2	3.5	Tell Brak #1232, opaque light copper-blue
70.8	16.6	5.2	2.3	4.6	0.41	0.21	100	72.3	18.3	4.4	Tell Brak #Br4, light copper-blue (turquoise)
71.2	16.1	4.9	2.3	4.8	0.42	0.31	100	72.8	17.8	4.5	Tell Brak #Br7, light copper-blue (turquoise)
63.4	19.0	6.5	2.6	7.3	0.51	0.51	100	64.5	20.8	9.7	Tell Brak #Br12, light copper-blue (turquoise)
68.3	17.4	5.0	3.3	5.3	0.51	0.20	100	69.8	19.8	5.4	Tell Brak #Br14, light copper-blue (turquoise)
71.5	13.0	9.1	2.1	3.3	0.62	0.41	100	73.8	14.6	6.6	Tell Brak #Br8, opaque light copper-blue
63.6	16.4	6.2	3.8	7.7	1.94	0.31	100	66.2	18.9	9.9	Tell Brak #Br9, opaque light copper-blue
64.3	17.3	8.1	3.4	5.4	1.03	0.62	100	66.8	19.8	8.4	Tell Brak #Br10, opaque light copper-blue
62.0	17.2	12.5	2.4	4.3	0.90	0.65	100	64.7	19.2	11.1	Malkata #3905, opaque light copper-blue
62.6	18.5	10.6	2.4	4.2	0.90	0.76	100	65.2	20.4	9.4	Malkata #3907, opaque light copper-blue
72.3	14.8	7.8	1.0	2.8	0.72	0.56	100	74.7	15.8	4.6	Malkata #3904, transparent light copper-blue
60.8	18.7	11.9	2.4	4.0	0.98	1.13	100	64.4	20.8	9.8	Malkata #3908, opaque dark copper-blue
66.1	17.2	9.2	2.6	3.9	0.58	0.33	100	68.2	19.3	7.6	Amarna #3362, transparent light copper-blue
58.2	23.3	10.7	1.2	4.8	1.11	0.63	100	60.4	24.2	10.3	Amarna #3363, transparent light copper-blue

Table 7.17: continued

SiO ₂	Na ₂ O	CaO	K ₂ O	MgO	Al ₂ O ₃	Fe ₂ O ₃	Total	SiO ₂ ^{**}	Na ₂ O ^{**}	CaO ^{**}	Sample Description
64.5	20.8	8.0	1.7	3.3	1.02	0.62	100	67.1	22.2	5.7	Amarna #1515, transparent light copper-blue
62.3	19.2	10.1	2.6	4.5	0.53	0.76	100	64.6	21.3	9.1	Amarna #3367, transparent dark copper-blue
65.9	18.9	7.5	2.9	3.6	0.65	0.52	100	68.2	21.2	5.6	Amarna #3366, transparent dark copper-blue
65.8	18.3	8.9	1.7	4.1	0.76	0.46	100	67.8	19.7	7.5	Amarna #3365, opaque light copper-blue
66.2	19.6	7.5	1.2	3.2	0.84	1.34	100	69.2	20.7	5.0	Lisht #3940, transparent dark copper-blue
64.0	19.8	8.6	2.4	3.3	0.74	1.03	100	66.9	21.8	6.3	Lisht #3941, transparent dark copper-blue
68.5	19.9	4.4	2.3	3.0	0.82	1.06	100	71.6	21.8	1.6	Lisht #3943, transparent light copper-blue
63.7	22.8	6.0	2.3	3.9	0.49	0.85	100	65.9	24.7	4.4	Lisht #3944, transparent light copper-blue
63.6	20.6	7.9	2.0	4.9	0.73	0.31	100	65.4	22.1	7.5	Qantir #83/0110, transparent copper-blue
71.3	17.9	5.9	1.6	1.9	0.89	0.56	100	74.2	19.3	1.5	Uluburun #5964, transparent light copper-blue
66.9	20.1	7.0	1.5	3.5	0.59	0.42	100	68.7	21.3	4.9	Uluburun #5969, transparent light copper-blue
68.3	17.1	7.2	1.6	3.2	1.22	1.32	100	71.8	18.5	4.7	Amarna #3355, opaque red
66.2	20.9	5.3	2.2	3.9	0.74	0.82	100	68.8	22.7	3.5	Lisht #3957, opaque brownish-red
64.5	18.0	8.8	1.8	4.8	1.58	0.45	100	67.8	19.5	7.7	Qantir #87/0824, opaque red
66.4	18.2	8.8	2.0	3.5	0.84	0.32	100	68.9	19.8	6.3	Qantir #80/0044, opaque red
67.4	20.0	4.2	2.0	3.8	2.15	0.41	100	71.0	21.6	2.4	Tell Brak #Br4, purple
64.3	17.8	9.8	2.0	4.5	0.81	0.71	100	66.5	19.4	9.1	Malakata #3913, purple
66.0	19.4	8.9	2.2	2.9	0.41	0.20	100	67.9	21.3	5.8	Amarna, purple

Table 7.17: continued

SiO ₂	Na ₂ O	CaO	K ₂ O	MgO	Al ₂ O ₃	Fe ₂ O ₃	Total	SiO ₂ **	Na ₂ O**	CaO**	Sample Description
65.5	19.3	6.8	2.4	4.5	0.78	0.74	100	67.8	21.1	6.1	Light #3950, purple
64.4	17.9	9.2	2.2	4.9	0.60	0.72	100	66.3	19.6	9.1	Uluburun #5968, transparent purple
69.5	13.7	8.7	2.3	5.4	0.30	0.08	100	70.5	15.4	9.2	Tell Brak #1234, opaque white
65.2	16.4	7.6	3.9	5.4	1.02	0.54	100	67.7	19.1	8.1	Tell Brak #1236, opaque white
65.6	18.1	9.5	2.2	3.8	0.62	0.31	100	67.5	19.8	7.7	Amarna, opaque white
67.0	18.2	6.6	2.2	4.0	0.93	1.04	100	69.9	20.0	5.1	Amarna #3352, opaque white
67.2	15.1	9.3	2.5	4.2	1.12	0.61	100	69.9	17.0	8.1	Amarna, opaque green
68.2	18.7	6.7	1.1	2.9	1.06	1.48	100	71.9	19.7	3.4	Amarna #3354, opaque light-green
68.0	18.8	7.0	1.1	3.2	0.90	0.99	100	70.7	19.7	4.6	Light #3952, opaque green
70.5	13.1	6.0	3.6	5.4	1.01	0.31	100	72.7	15.6	6.7	Nuzi #1213, Amber or yellow
67.6	16.4	7.4	3.1	5.0	0.40	0.08	100	68.9	18.7	7.4	Tell Brak #1233, opaque dark amber/yellow
77.1	7.9	6.2	1.5	5.2	1.27	0.86	100	79.9	9.0	6.2	Tell Brak #1237, opaque yellow
73.8	13.0	4.0	2.8	5.2	0.83	0.31	100	75.8	15.0	4.2	Tell Brak #Br5, brown
68.7	17.8	4.1	2.6	6.6	0.20	0.00	100	69.1	19.7	6.2	Tell Brak #Br10, brown
68.3	16.9	4.8	2.6	7.1	0.20	0.10	100	68.7	18.7	7.6	Tell Brak #Br11, brown
67.1	18.3	8.0	1.8	4.0	0.43	0.43	100	69.1	19.8	6.1	Amarna, opaque yellow
65.5	17.9	7.8	2.9	4.2	0.65	1.09	100	68.5	20.3	6.3	Amarna #3353, opaque yellow
65.6	19.5	7.2	2.0	4.2	0.61	0.85	100	67.9	21.1	6.0	Light #3956, opaque yellow

Table 7.17: continued

SiO ₂	Na ₂ O	CaO	K ₂ O	MgO	Al ₂ O ₃	Fe ₂ O ₃	Total	SiO ₂ **	Na ₂ O**	CaO**	Sample Description
65.2	19.3	4.7	3.5	6.3	0.71	0.31	100	66.8	21.8	6.5	Tell Brak #Br6, black
69.6	18.1	5.3	2.0	3.3	0.82	0.89	100	72.4	19.7	2.9	Lisht #3960, black
63.1	20.8	6.1	2.2	5.2	0.91	1.70	100	66.1	22.4	6.4	Lisht #3962, black
66.3	19.8	6.1	2.3	3.6	0.86	0.94	100	69.1	21.7	4.3	Lisht #3958, black
65.5	17.2	8.8	2.4	5.0	0.80	0.31	100	67.2	18.9	8.9	Nuzi #1215, colourless
72.3	14.5	9.1	0.1	2.1	1.70	0.16	100	75.2	14.7	5.1	Tell Brak #1238, colourless
65.2	17.1	6.8	3.6	5.6	1.08	0.64	100	68.0	19.8	7.2	Nimrud Group 1, mainly colourless
70.8	14.1	8.8	1.5	3.2	1.02	0.49	100	73.4	15.3	6.2	Nimrud Group 2

: Initially, obtained data is reduced to 7 oxides (above) and then reduced further to 3 oxides, SiO₂^{}, Na₂O^{*}, and CaO^{*}, based on the calculation published in Rehren (2000).

** : The values of SiO₂^{*}, Na₂O^{*}, and CaO^{*} were normalised to 95 wt% and are shown as SiO₂^{**}, Na₂O^{**}, and CaO^{**}, since the ternary diagram have the fixed magnesia content of 5 wt%.

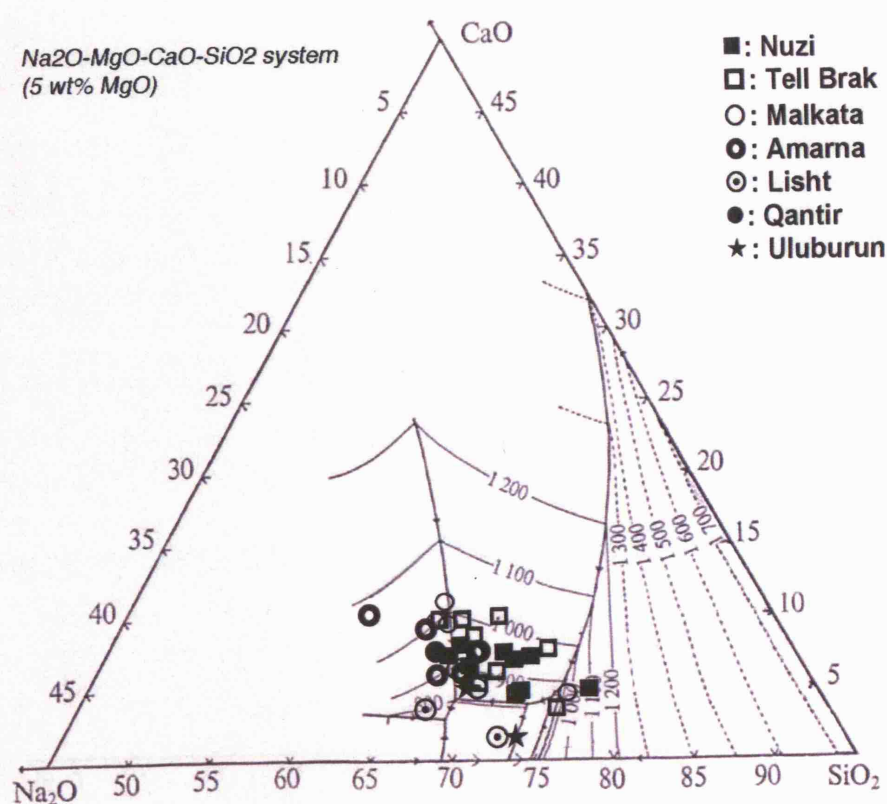
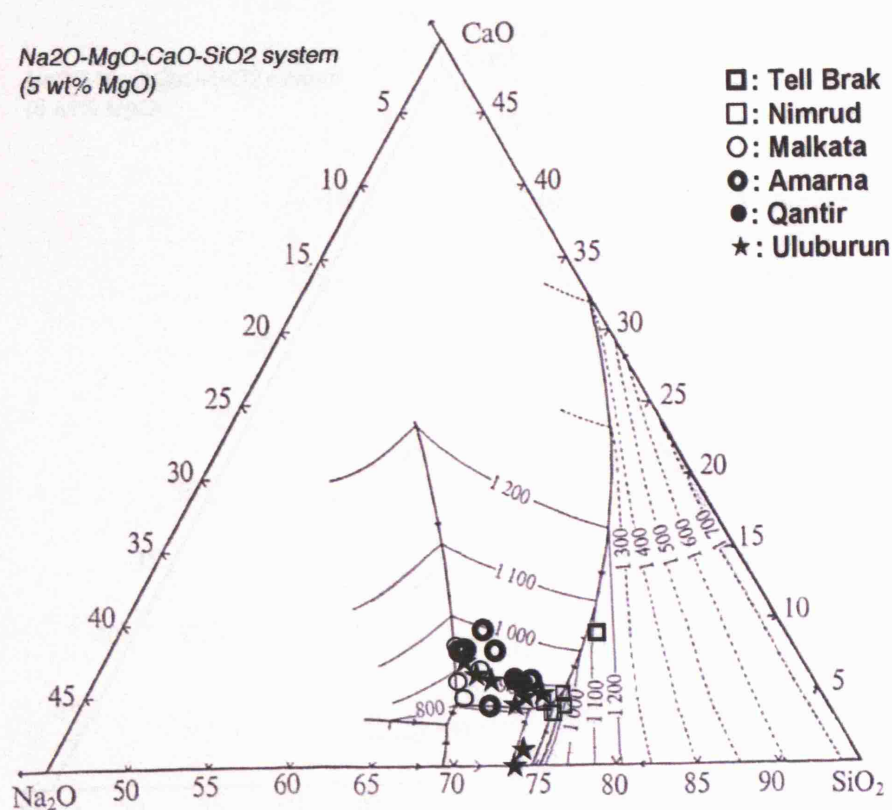


Figure 7.1: Plots of reduced chemical compositions of LBA cobalt-blue (top) and copper-blue (bottom) glasses.

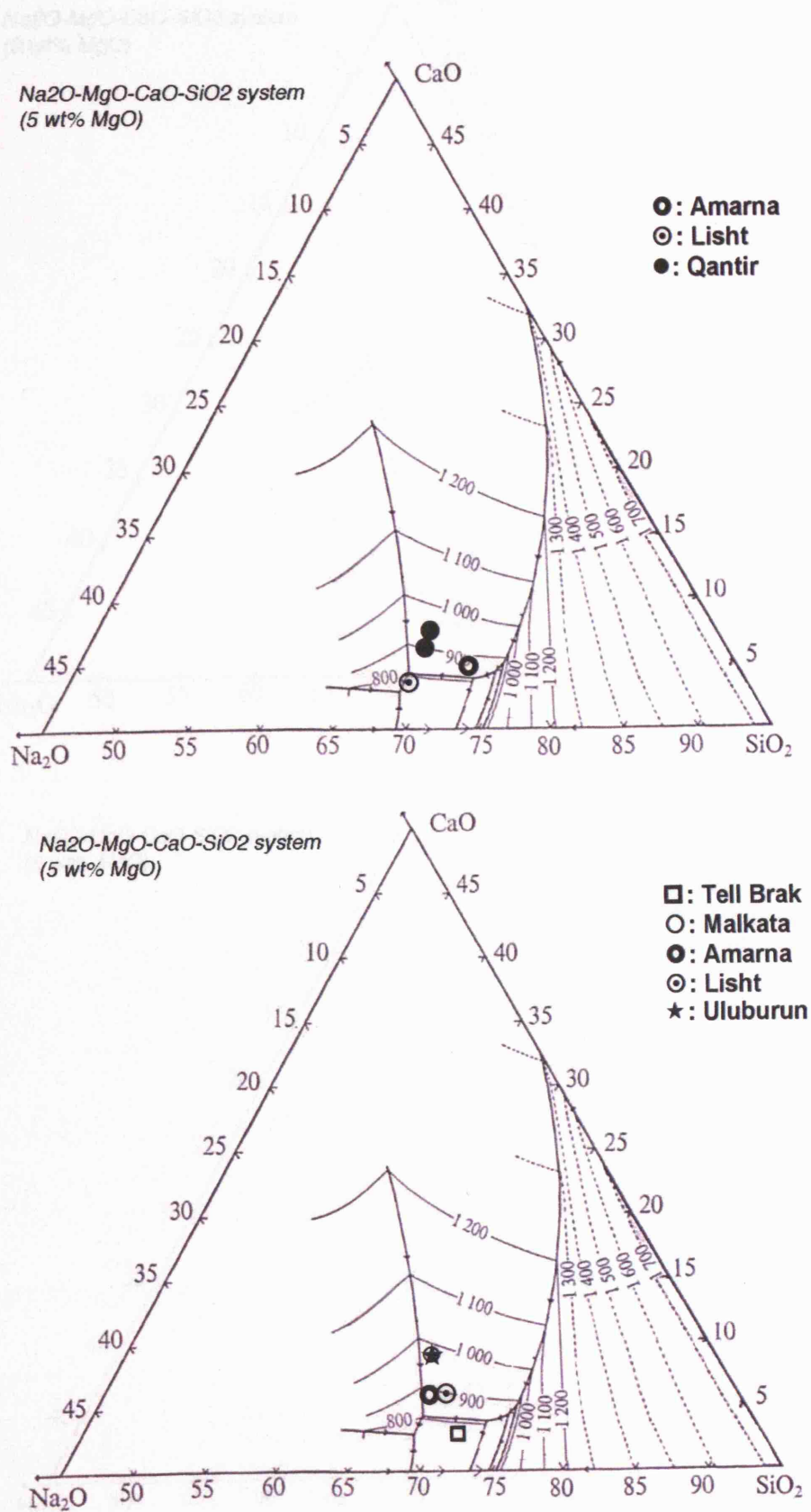


Figure 7.2: Plots of reduced chemical compositions of LBA red (top) and purple (bottom) glasses.

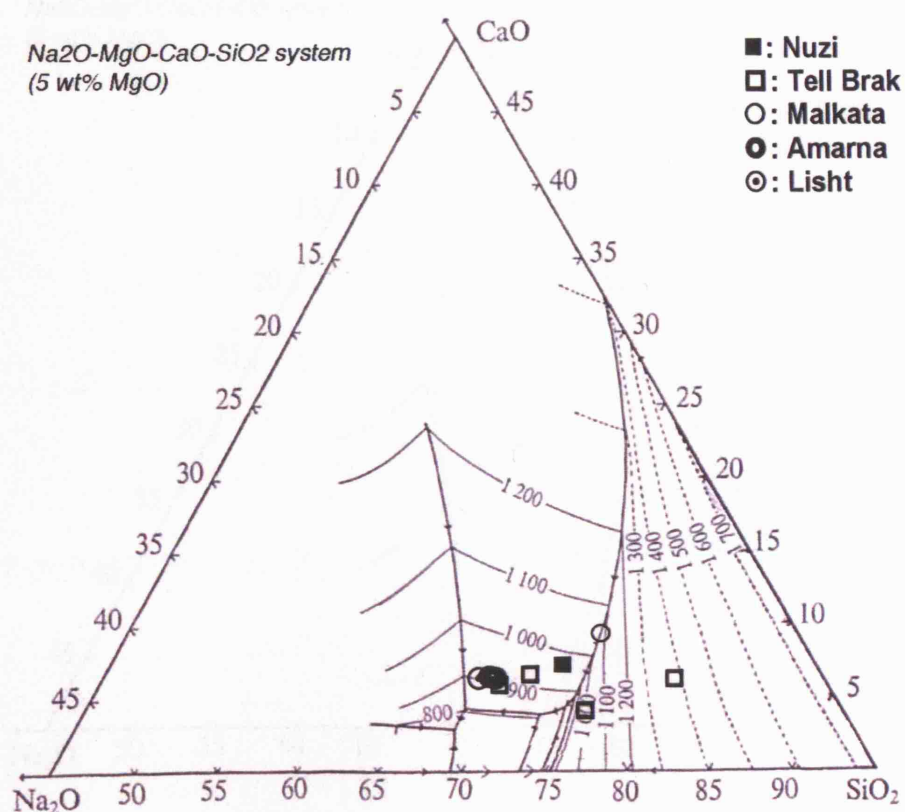
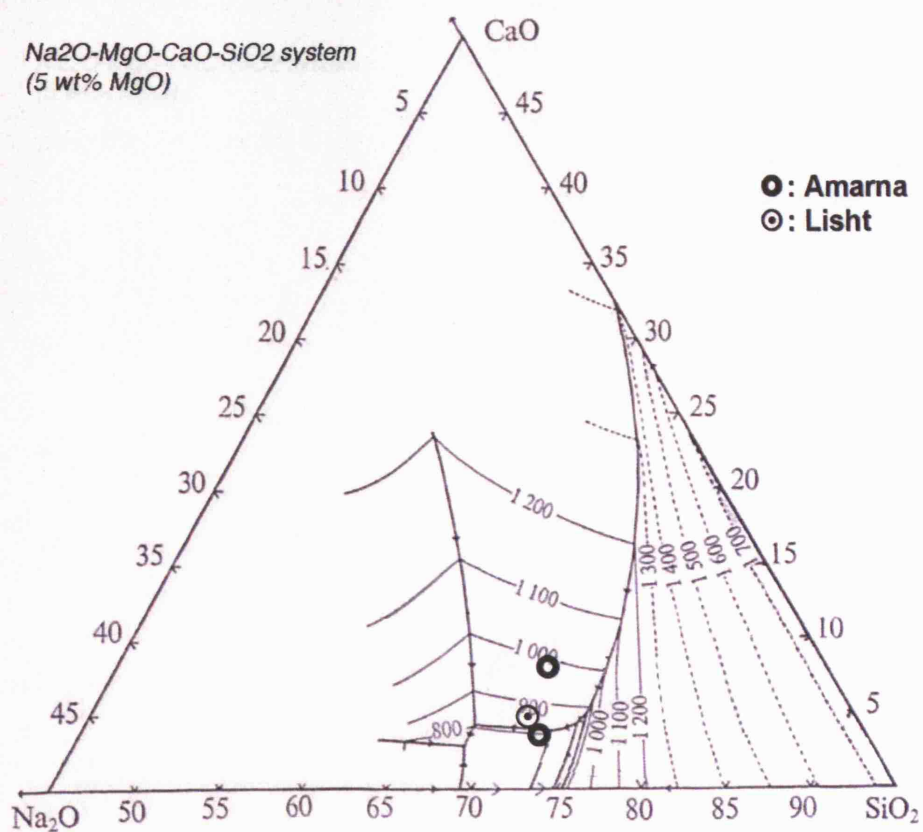


Figure 7.3: Plots of reduced chemical compositions of LBA green (top) and yellow (bottom) glasses.

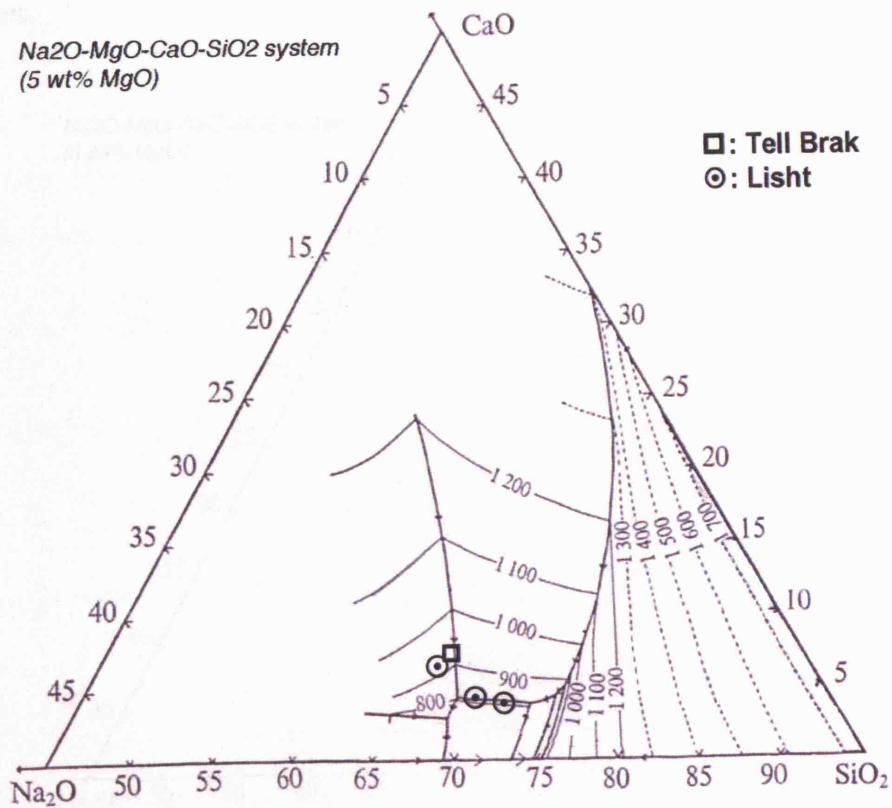
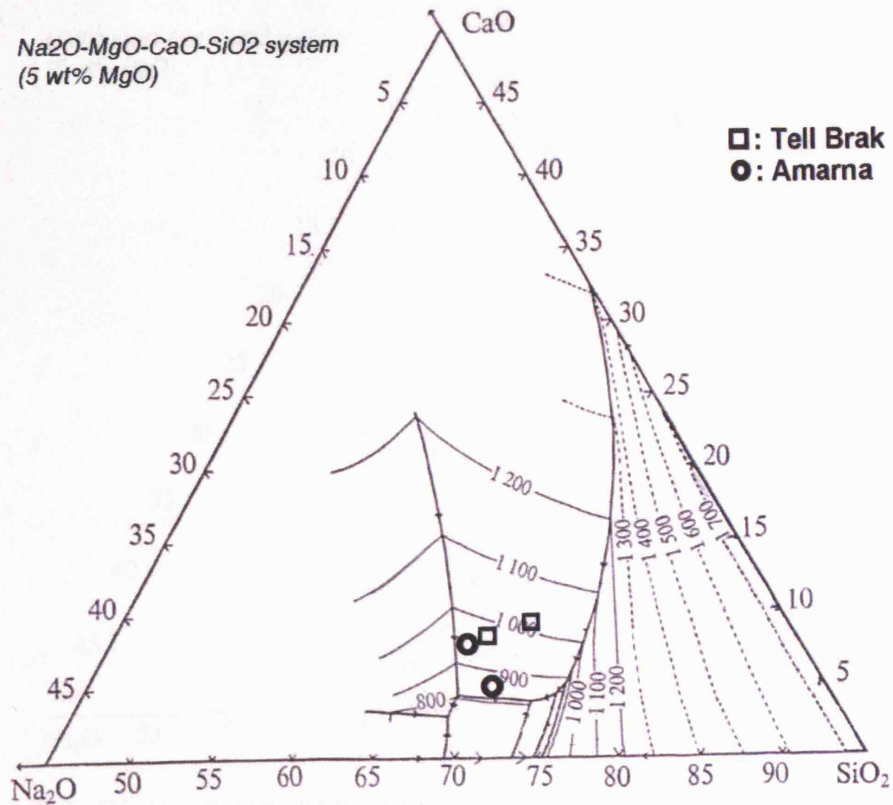


Figure 7.4: Plots of reduced chemical compositions of LBA white (top) and black (bottom) glasses.

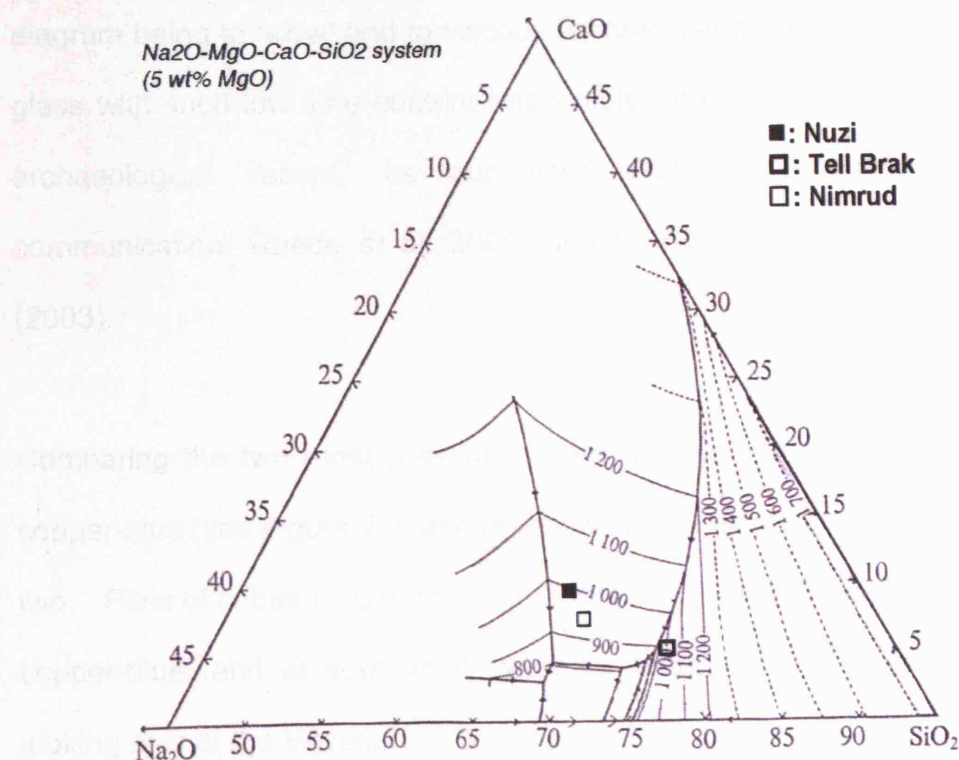


Figure 7.5: Plots of reduced chemical compositions of LBA colourless glasses.

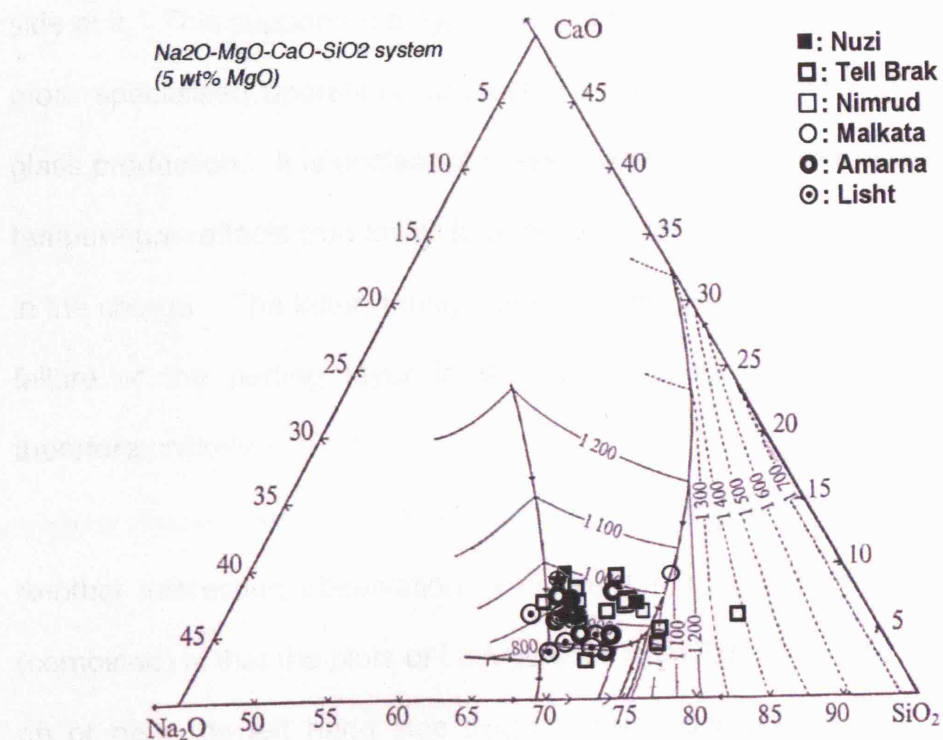


Figure 7.6: Combined plots of reduced chemical compositions of LBA red, purple, green, yellow, white, black, and colourless glasses.

diagram being to 'slow' and to viscous for practical glass-forming, or that any glass with such low lime content has simply weathered and is lost from the archaeological record, as suggested first by Freestone (personal communication/ Raede *et al.* 2005) and by Schlick-Nolte and Werthmann (2003).

Comparing the two most popular colours among LBA glasses, cobalt- and copper-blue (see Figure 7.1, above) shows interesting difference between the two. Plots of cobalt-blue glasses are more closely clustered than the plots of copper-blue, and at somewhat lower temperatures. On the other hand, looking only at the Egyptian glasses, the cobalt-coloured ones appear slightly shifted towards the silica-rich corner of the diagram, while the copper-coloured glasses are firmly centered along the Egyptian trough and scatter on either side of it. This supports the hypothesis that the cobalt-blue production was a more specialised operation, conducted at fewer sites than the copper-blue glass production. It is unclear at present whether the lower apparent melting temperature reflects true lower furnace temperatures, or simply a lack of lime in the charge. The latter, though, would have resulted in an increased risk of failure of the parting layer in the glass-colouring crucibles, and seems therefore unlikely.

Another interesting observation in Figure 7.1 (copper blue) and Figure 7.6 (combined) is that the plots of LBA glasses from Egyptian sites tend to gather on or near the left hand side trough (more soda-rich area) of the ternary diagram, while the plots of glasses from Mesopotamian sites tend to gather on the right hand side, towards or on the Roman trough (more silica-rich area).

Moreover, Nimrud Group 2 glasses (plant ash based) tend to plot along and close to the “Roman” cotectic trough, on the right hand side of the ternary diagram although they are not natron based, while Nimrud Group 1 (colourless, plant ash based) glasses plot near Egyptian trough. This trend contradicts the current hypothesis that the difference between the “Egyptian” cotectic trough (on the left of the ternary diagram) and the “Roman” cotectic trough is thought to relate to the type of alkali used to produce the glass, either plant ash (“Egyptian”, soda-rich) or natron (“Roman”). However, no causal explanation for this different preference has yet been given.

The sample numbers of most other colours are too small to permit sensible interpretation of their position in the ternary diagram; a puzzling observation is that the three Egyptian green opaque glasses all plot almost exactly half way between the two troughs. This green glass is thought to be based on mixing light blue and yellow glass, both of which plot on or near the Egyptian trough. Only one Malkata yellow glass plots on the Roman trough, but more analyses are clearly necessary to understand this phenomenon.

The three black glasses from Lisht, apparently coloured mostly by their somewhat elevated iron oxide content, plot at the lower temperature range, possibly related to the need to keep the furnace conditions more reducing to produce an iron-based black colour (Kaczmarczyk & Hedges 1983).

The observed dispersion of data points in most of the ternary diagrams (Figure 7.1-7.6, above) is as much evident in horizontal direction as in the vertical direction. That is, the lime contents that vary in vertical direction in the ternary

diagram in most colours of LBA glass are similarly variable in absolute terms compared to the contents of silica, which changes horizontally. The main exception from this is the Egyptian copper-blue glass which shows the best adherence to the Egyptian trough with a nominal range in lime** from 4 to 11 wt% with two exceptionally low values of around 1.5 wt%. The silica** values of these glasses, in contrast, scatter mostly from 64 to 68 wt%, with only very few exceptionally low (60 wt%) and high (74 wt%) values. The cobalt-blue glass, in comparison, has a slightly smaller spread in lime** content than in its silica** range, with 5 to 10 wt% CaO** and 66 to 74 wt% SiO₂** respectively, omitting the two Uluburun samples with very low lime** levels.

As mentioned earlier, the inclusion of the Mesopotamian glasses in these diagrams shifts the spread considerably towards the silica-rich Roman trough, suggesting a systematic difference in raw material selection and batch mixing recipes. Useful data sets are only available for light blue and white glasses from Nuzi and Tell Brak; they scatter around or below the 1000 °C isotherm linking the Egyptian and the Roman trough, with no particular preference for either trough.

7.1.3. Interpretation of the variables in chemical composition of LBA glasses by comparing with the finds from the experimental melts

It is clear that most variables in minor oxide contents are direct reflection of raw materials (such as quartz, sand, plant ash, and natron), and the colorant composition added to produce the glass, as mentioned above. However, the interpretations of the variables in the remaining oxide contents among LBA glasses are discussed below in view of experimental data shown above.

As mentioned earlier, all the LBA glasses can be plotted within the range of firing temperature 800–1050 °C. The experimental findings have shown that the lime content is proportional to the firing temperature, provided that a source or buffer rich in lime is available for the glass melt to absorb more lime as the temperature increases. Recent archaeological and ongoing experimental work has shown that for Egyptian glassmaking, this buffer material is most likely the lime-based parting layer (Merkel & Rehren 2007, Rehren 1997, Schoer & Rehren 2007, Turner 1954a). The firing temperatures that can be achieved from the LBA furnace designs are limited by the nature of the ceramic material used in building the furnaces and the glassmelting vessels. Turner (1954a) has shown that this limit is around 1100 °C, which is in very good agreement with the estimated firing temperatures observed here.

It has been noted above that LBA Egyptian glasses tend to disperse on the left hand side of the ternary diagram (more soda-rich and less silica) and those of Mesopotamian origin disperse on the right (more silica and less soda). Moreover, since the experimental studies in this thesis did not identify a scientific force that would govern the soda to silica ratio (other than the initial batch composition), the only factor/force that can make plots of glass compositions to disperse horizontally on ternary diagram is a fundamental human factor, choice of raw materials and how they are mixed. Therefore, the variability of raw materials, particularly plant ash will be discussed below.

7.2. Variability of plant-ash glasses in general, grouping potentials

As mentioned earlier, the compositions of plant ash varies drastically even

among ashes of the same species or of different parts from the same stem. In addition, as seen from Figure 3.1 (in Chapter 3), there is a wider dispersion along the silica** axis among plots of recently published LBA glass compositions than shown in Rehren (2000b). This suggests that the homogeneity of LBA glass compositions is not as tight as initially proposed. That is, both the ratio of soda** to silica** in the reduced data and the absolute concentrations of minor oxides in the base glass compositions need to be taken into consideration when discussing LBA glass compositions.

The detailed interpretation of base glass compositions between Egyptian and Mesopotamian glasses has revealed that there is a systematic difference in their minor oxide content, particularly in potash and magnesia. Both are in general higher in Mesopotamian glasses, although a broad overlap exists between the ranges of composition for both regions. In contrast, both iron oxide and alumina are generally somewhat lower in Mesopotamian glasses. Both pairs of minor oxides are likely to reflect differences in raw materials, with the magnesia and potash representing the plant ash, while alumina and iron oxide are more likely to come at least in part from the silica source. Although the main source of silica, crushed quartz pebbles, is theoretically pure silica, there are several major contaminants to be considered. Firstly, most quartz pebbles contain varying amounts of rutile and zircon inclusions, resulting in elevated titania and zirconia levels in the glass. In fact, the minerals rutile and zircon are both almost insoluble in water and therefore unlikely to be metabolised/absorbed by plants; one would assume that the plant ash is very low in these elements, and that most if not all titania and zirconia in the glass originates from the silica source. Secondly, the crushing

of quartz pebbles requires grinding tools, which are well known archaeologically. These tools consist of hard-wearing rocks, such as granite or metamorphic igneous rocks. These rocks consist of a certain amount of quartz plus a range of other minerals, such as feldspar, amphibole and mica. These individual minerals, however, are all softer than quartz, and the crushing and grinding of quartz pebbles will result in a considerable contamination of the finely ground material. The contaminating minerals directly reflect the composition of the grinding tools, and are likely to add not only silica, alkali and earth alkali oxides to the quartz powder, but also alumina and iron oxides. While the addition of alkali and earth alkali oxides from this source will be not noticeable next to the overwhelming amount of these oxides from the plant ash, both alumina and iron oxide are less likely to be present in these plant ashes (generally both alumina and iron contents in the plant ash is below 1 wt%, Brill 1999a, b).

Therefore, the observed systematic differences in minor oxides between Mesopotamian and Egyptian glasses are reflecting the different geological environments of the two regions, either via the soil composition and different ratios of alkali and earth alkali oxides in the plant ashes, or via the availability of different rock types for grinding tools and accordingly different contamination of the quartz powder used as silica source.

The technical study presented earlier indicates that the magnesia content of these glasses is not entirely determined by the plant ash composition. In the presence of sufficient earth alkali oxides and suitable cooling conditions, magnesia levels will be capped by around 5 wt% through the formation of

diopside instead of wollastonite (see chapter 4). Thus, the observed level of magnesia of around 4 to 5 wt% in most Mesopotamian glasses could be due to the technical limit inherent in the system. However, the typically lower levels of magnesia in Egyptian glass are likely to directly reflect the plant ash composition.

It is important to stress that the ratio of lime to magnesia is not likely to be very meaningful, as the lime content of the Egyptian glass is to a considerable extent increased through the absorption of additional parting layer material, and hence artificially enhanced compared to the original plant ash composition. The absolute level of magnesia, up to about 5 wt%, however should be a reliable indicator of raw material composition. The important exception to this is cobalt-blue glass, whose magnesia content is most likely heavily influenced by the added colorant (Rehren 2001, Shortland *et al.* 2006, Tite & Shortland 2003).

A considerable portion of this thesis has focussed on the potential factors influencing the ratio soda to potash in LBA glasses. Both are very strong fluxes and likely to react in their carbonated form with free silica to form clear glass. The regional variability in this ratio has been mentioned already, and offers some potential provenancing information. However, the key problem in this respect is how to explain the particularly low potash level in most cobalt-blue glasses. Shortland and Tite (2000) had suggested that this is due to the use of mineral natron as the flux for this particular glass only. Rehren (2001) has argued against this assumption and suggested instead that either a particular low-potash plant ash was used, or that there is a

technical factor from the added colorant influencing the potash content of the resulting glass.

The experiments in this thesis have demonstrated that indeed the presence of large quantities of chloride salt in the glassmelting process will reduce the amount of potash in the glass melt, due to the preferential partitioning of potash into the chloride phase. This salt phase is then either washed out of the glass by water later in the process, or simply separates again as a second, lighter layer on top of the glass ingot. On the basis of the experiments, it is estimated that the glass charge has to include about the same amount of chloride salt as that of sodium carbonate in order to bring the potash content down from the usual 2 wt% to the typical 1 wt% in cobalt-blue glasses.

Recent experimental work (Shortland *et al.* 2006) has indicated that the pre-treatment of cobaltiferous alum necessary to produce a useable colorant can be achieved by adding (mineral) natron to the alum solution, and precipitating the transition metals as hydroxides, together with varying amounts of alumina and magnesia. However, it is unlikely that large quantities of chloride salt will form in this or any other relevant process, let alone be co-precipitated with the colorant. Therefore, and although a technical explanation for the particularly low potash content of these glasses is feasible, it is more likely that this low content is due to a particularly potash-poor, or a particularly chloride-rich, plant ash. Further fieldwork is necessary to investigate whether particularly soda-rich environments, such as in the Wadi Natrun, will yield halophytic plants capable of producing such a particularly potash-poor glass.

In this context it is noteworthy that the potash-poor signature is not restricted to cobalt-blue glasses; there are several published analyses of LBA glasses which are similarly low in potash (Brill 1999b, 1999a, Lilyquist *et al.* 1993). This may indicate that this particular plant ash was used predominantly, but not exclusively for the production of cobalt-blue glass, a scenario in good agreement with the recently suggested idea of a predominant, but not exclusive specialisation of individual glass workshops on specific colours while at the same time producing others, in particular copper-blue, too (Rehren 2006 = Archaeometry conference presentation).

This chapter has demonstrated that there is a good potential for grouping LBA glasses based on their minor base glass oxides as well as their characteristic colorants. Recent work by Shortland (2005, and ongoing) is extending this to include a much larger number of trace elements, which is hoped to eventually offer a provenancing tool. This, however, is beyond the scope of my thesis that is more concerned with the identification of technical constraints of glass composition from relatively wide range of raw materials, as presented earlier.

Chapter 8: Summary and Outlook

As mentioned at the beginning of this thesis, this research is based on two fundamental questions. One is why there is very little archaeological evidence related to LBA glass-making, despite the popularity of the material during the Late Bronze Age? Another is why LBA glasses are so homogeneous despite the compositional variability of the raw materials available across the region at the time (during LBA)?

Therefore, in order to address these fundamental questions as pertinently as possible, there are two main aims to this thesis. Firstly, to contribute to the better understanding of the physical and chemical reactions that take place during LBA glass-making given the constraints of materials and technologies available at the time. Secondly, to use this better understanding to identify the possible nature of glass-making remains and how these immanent factors control glass composition and limit glass-making practice. It is hoped to help identify and better interpret possible glass-making remains in the archaeological record and to reveal the cultural or configurational parameters at work in LBA glass-making.

In order to achieve these aims, the following objectives were addressed. At first, the relevant archaeological publications were studied for descriptions of glass-making remains or workshop evidence, both from Mesopotamia and Egypt.

Secondly, two possible glass-making models or scenarios that could influence the glass composition were experimentally studied. The “Partial Melting

Model (PMM)" is thought to influence the earth alkali oxide content of the glass, while the "Two Melt Model (2MM)" is thought to influence the alkali oxide content of glass. These scenarios were initially proposed by Rehren (Rehren 2000a, 2000b, Shugar & Rehren 2002) and explored further in detail in this research. Nowadays, all the raw materials are placed in one crucible and all the raw materials will react completely in modern glass-making technology, without any residual materials, to form a clear glass (namely, "total batch melting model", Rehren 2000b: 1225). However, this need not have been the case in antiquity, such as for example from India (Sode & Kock 2001) where the glass was made to give a glass phase mixed with residual phase. Both models were tested through a series of experimental melts under controlled conditions, using industrial grade raw materials, focussing on the contents of lime and potash, respectively.

Not only are LBA glasses chemically homogeneous, but also there is an interesting trend observed among archaeological glasses. Rehren (2000a, 2000b, Shugar & Rehren 2002) noted that the compositions of the majority of LBA glasses, published by Lilyquist and Brill (Lilyquist *et al.* 1993) are closely related to the cotectic trough originating from the eutectic region of the soda-lime-silica (SLS) system on the soda-rich side and extending towards more lime-rich cotectic compositions. Similarly, almost all the Roman/Hellenistic glasses are found within the more silica-rich cotectic trough region (see Figure 3.2). Rehren (2000a, 2000b) argues that these glass compositions and the liquidus surface morphology of the relevant phase diagrams are too closely linked to be coincidental, and that the variability in chemical composition is too small to be derived from simple initial raw

material control. The variability of raw material compositions, especially plant ash, is absolute (Jackson *et al.* 2005, Jackson & Smedley 2004). Therefore, it is likely that some inherent factors within the glass-making system itself rather than some variable or configurational human factors (e.g. choice of materials) control the composition of glass made with variable raw material compositions. That is, there may be some self-adjusting mechanism (i.e. buffering system) within ancient glass-making being responsible for the final glass composition.

The PMM assumes the formation of a cotectic glass melt in the presence of crystalline material that acts as a buffer material from which the melt draws upon as it forms (Shugar & Rehren 2002). This means that the formation of glass is not a sudden and complete process, but that there are different stages in which different parts of the batch material have already reacted to form a glass, while others are either partly reacted to form an intermediate crystal phase, or are semi-reacted, residual due to lack of time or temperature to form a glass. Therefore, during glass-formation, the glass will evolve and have different compositions at different stages of the process; therefore, it is bound to have also a different composition than the original batch until all components are fully reacted and molten. Incomplete or partial melting means that there are intermediate lime-rich phases such as wollastonite or residual phases such as silica present when the glass-making process finishes.

In contrast, the 2MM is based on the fact that not only does the composition of plant ash and mineral soda vary, but that there are always substantial

amounts of non-reactive salts present as part of the flux used in ancient glass-making (Jackson *et al.* 2005, Tite *et al.* 2006, Turner 1956c) and the partitioning coefficient (PC) of these salts influences the amount of alkalis that will be incorporated into the glass. That is, at melting temperature, the SLS glass and common chloride- or sulphate-based salts form a system of two immiscible melts, like oil and water. However, exchanges of ions are expected to occur between these two separate melts. The boundary between the two melts acts like a permeable membrane and ions can move between the two to react, and to concentrate in one or the other. Silica, for example, partitions completely into the glass melt, while sulphur and chlorine partition preferably, but not completely, into the salt melt. The maximum amount of chlorine, on the other hand, that can go into the silicate melt is limited to less than 2 wt% (for details see below). The behaviour of the alkalis under these conditions is as yet unknown, but clearly very relevant in the context of early glass-making. Therefore, it was tested in this research.

This replication process is important since it enables us to better evaluate to what extent the composition of finished glass is controlled by human behaviour and to what extent it is controlled by chemical reaction.

Lastly, these explorations of possible LBA glass-making technologies will contribute scientific information where little archaeological evidence is available yet. However, the experimental data was also tested by comparing it to new archaeological finds from Dr Pusch's ongoing excavation at the ancient Ramesside capital of Piramesses in the eastern Nile Delta, Qantir, and to published data of LBA glasses and ideas concerning these

compositions. All the published LBA glass compositions to test differences in the base glass compositions were reviewed to better understand the proposed colour specialisation among LBA glass workshops and the geographical distributions.

This research has focussed on aspects of the production of LBA glass, particularly between 1500 BC, when glass industries had become well developed and glass was routinely produced, and 1000 BC. This cut-off point was decided to coincide with the earliest known production of natron-based glass around 1000 BC, as reported by Schlick-Nolte and Werthmann (2003), whereas typical LBA glass is plant-ash-based. The changes in the flux (alkali source) will have major implications for the process of glass-making. Therefore, this thesis has focused on plant-ash-based LBA (1500-1000 BC) glass only.

The geographical framework of this research is limited mainly to Mesopotamia and Egypt, leaving aside the Aegean (except for the Uluburun shipwreck), and other parts of Asia etc. This is mostly a reflection of the virtual absence of published evidence for glass workshops in areas outside Mesopotamia and Egypt during the Late Bronze Age.

8.1. Summary of outcomes from the research on the relevant archaeological publications

Almost all glass evidence published from LBA archaeological sites is for glass-working or for consumption of glass in palace complex, temples and graves, rather than glass-making. That is, most of the published evidence

relates either to the manipulation of glass objects, or to the long-distance trade in coloured glass ingot form, rather than producing raw glass from the raw materials. In addition, the number of possible glass-working sites or artistic workshops is much larger than the number of possible primary glass-making factories, suggesting centralised glass production during the LBA (see Table 2.3 and Table 2.4).

However, a few LBA Egyptian sites, particularly Amarna and Qantir, have yielded more substantial evidence of glass workshops. Therefore, these two sites were studied in more detail in this thesis.

Numerous fragments of cylindrical vessels (crucibles) were found from both Amarna and Qantir, some of them having fused glass attached, suggesting glass-making could have been taken place at the site. Moreover, these sites suggest that there may be a colour specialisation among LBA glass-making sites since they both appear to have evidence for glass of a certain colour, particularly cobalt-blue in Amarna and red glasses in Qantir, which were both rare in LBA Mesopotamia. There are still ongoing studies on the technicality of producing cobalt-blue glass and their unique composition, having low potash and high alumina contents. This matter will be discussed later in section 8.2.2.

The most recent evidence from Qantir seem to prove local glass-making from raw materials and gives more insights into LBA glass-making practice, including possible raw materials and the firing temperatures used (see below).

8.2. New contributions from this research

8.2.1. Replication of two possible glass-making models

8.2.1.1. Earth alkali contents in SLS glass (PMM):

A series of experimental melts has demonstrated that the concept of partial melts is possible and probably has a major influence on the melt composition, within the technical constraints of ancient glass-making practice. The indication for this can be seen as either a crystalline phase above the glass phase, or as pockets of semi-reacted materials within the melt, acting as a buffer for the forming glass to draw upon during the melt. The residual crystalline phase can more or less easily be separated from the formed glass phase, depending on their proportion. Moreover, re-firing the isolated glass fraction at the same or higher temperature at which the initial batch was fired produces a good quality glass of consistent composition ready for further manipulation, such as coloration or working.

In the Late Bronze Age SLS system, lime being characterised as the main buffer material, the content of calcium oxide in the glass melt is primarily being controlled by the melting temperature. The experiments showed that the composition of the glass phase regularly matched the composition expected for the melting/firing temperature rather than the initial batch composition, with only slight shifts depending on the amount and types of crystals present. The forming melt uses the crystalline material newly formed from the reactions within the initial batch material as a buffer to draw on as the temperature allows. Residual and intermediate phases present in the partially molten material included silica, wollastonite, and the mixture of lime-rich soda-lime-silicate phases in various ratios, depending on where the

phase was found and the firing temperature. It represents local heterogeneities of the melt phase near what used to be limestone lumps. It is important to note that there was no soda-rich phase or nucleus formation observed throughout the samples while residual quartz grains and lime-rich phases were found frequently. This may suggest that within the range of temperature used in this experiment soda diffuses quickly and completely, and will be distributed into the glassy phase. Moreover, the distribution of the phases, including residual quartz grains, may indicate how the heat is transferred during the glass-forming process. The presence of a lime-rich nucleus and/or residual quartz grains may tell us whether the glass/melt was produced by primary glass-making process.

The results also suggest that the chlorine content in LBA SLS glasses is primarily controlled by their calcium oxide content but is affected neither by the soda content nor by the firing temperature. Therefore, chlorine cannot be used as a thermometer, as initially proposed by Rehren (2000b). It is beyond the aim of this project to study the exact mechanisms controlling chlorine content in glass melts but published work (Gerth *et al.* 1998) shows that the chlorine loss by vaporization as NaCl, or at least Cl from NaCl, below 1400 °C is far too low to be of major effect. In essence, the investigation of the relationship between the raw materials, the lime content of the glass, and the manufacturing process demonstrate that under PMM conditions, and with a lime-rich buffer phase available during the glass-forming reactions, the lime content of the glass is primarily controlled by the melting temperature during glass-making.

As a result, two possible buffer materials that affect earth alkali contents are suggested. One is the crystalline phase formed within the glass phase as a result of local heterogeneity, such as semi-reacted raw materials. To identify whether crystals in the glass are indeed residual or semi-reacted raw materials, it is important to establish a way to determine whether the crystalline phase is formed from raw materials or by devitrification. Once this is established, by identifying what crystalline phase(s) is present, one may be able to determine whether a certain archaeological glass was originally made at the site or recycled. The other possible buffer is the fabric of the surface material of the furnace or crucible, in which the glass is formed. This was studied by Rehren (1997) and Merkel (Merkel & Rehren 2007) and the interaction between the lime partition layer and the glass was observed, affecting the lime content of the formed glass.

Melting temperatures of around 900 °C, as postulated by Rehren and Pusch (2005) for the initial melting of the raw materials in the reaction vessels, would result in a glass with about 6 wt% CaO, at a nominal level of 5 wt% MgO (see Figure 3.4). An increase in temperature to around 1000 °C increases the possible CaO content to about 10 wt%, provided that a source for the additional CaO is available. In the case of LBA glass-making, this source is most likely to be the parting layer in the crucibles. In fact, mass balance calculation based on the assumption that the lime present in the parting layer is completely absorbed/transferred into the glass melt, shows the degree of the parting layer effect on the formed glass composition and gives a plausible support to this idea. The parting layer accounts for about 5 % of the volume of glass ingot by comparing the volume of a typical LBA glass ingot and the

volume of the parting layer. This mass balance calculation suggests that at least a few extra wt% CaO can be sourced from the parting layer, if the layer is completely absorbed into the glass phase.

8.2.1.2. Alkali proportions in SLS glass (2MM):

The second series of experimental melts concerned the interaction between SLS glass and a salt melt. The compositions of the glass phase, whose volume and recipe was kept consistent throughout the series, were almost identical, except for the sodium and potassium content in this series of experiment. Despite the presence of large excess amounts of alkali chloride(s) in the batch, chlorine levels throughout the series remained below about 1.5 wt% in soda-rich glasses, and even below 1 wt% in glasses with more than about 5 wt% potash. Earlier experimental melts had shown that the maximum chlorine content in soda-lime-silica glass is negatively correlated with the lime content, but not affected by variation in the soda content. These experiments demonstrated that potash has a similar, if not stronger, effect on maximum chlorine concentrations in these glasses. This confirms the earlier observation that there is a chemically controlled solubility limit of chlorine in the glass, and any excess amount of chlorine will form a separate salt phase that floats on top of the glass melt, and can be easily separated from the glass melt. The metal ions necessary to form this salt phase are taken from the batch. It is important to note that during the glass-forming process significant interaction between the glass-forming components and the salt phase occurs. These interactions and ion exchanges are limited to the alkali metals. There is no noticeable change in the earth alkali concentrations in any of the experiments here, nor was any

calcium or magnesium found in the XRF analyses of the salt phase after the reactions had occurred.

This series of experiments has demonstrated that the presence of a salt phase in the batch has a potentially significant influence on the alkali composition of the forming glass. The salt phase within the initial batch acts as a buffer that can provide alkali metal ions as well as receive them from the glass melt. Thus, the 2MM is highly relevant only for alkali oxide content in glass.

There is a strong tendency for low concentrations of potassium to enter the glass phase even when it is provided as potassium chloride, KCl to the batch. It is possible for formed glass melt to contain up to a couple of percent of potassium (K_2O) by simple absorption of potassium chloride, up to the saturation level of chlorine in the glass. The following series of experiments had overall low potassium content in the batch, provided as chloride, and in the presence of increasing amounts of sodium chloride. The results showed a clear preference for potassium to enter into the glass melt when compared to the much higher available amount of sodium chloride. However, when looking at the absolute quantities involved and estimating the potassium content in the salt phase it becomes apparent that the potassium concentration in the salt phase is higher than in the glass phase.

Addition of increased quantities of potassium chloride to the glass batch instead of sodium chloride confirms the picture of free interaction between the two melt systems, with large quantities of potassium going into the glass melt

as potash, and matching amounts of sodium going into the salt phase even if there is no NaCl originally present in the batch. That is, sodium and potassium can coexist in various ratios and be exchanged relatively freely between the two melts, but the total content of alkalis ($\text{Na}_2\text{O} + \text{K}_2\text{O}$) in the glass is kept similar to the total alkali carbonate content in the batch. This may appear surprising since the non-stoichiometric glass structure can absorb a very wide range of alkali oxide to silica ratios, and therefore should be able to increase alkali oxide contents in the glass when more alkali metal ions are available in the batch. However, the molar ratio between alkali metals and chlorine has to be kept constant at 1 (KCl or NaCl), and there is no significant evaporation loss of chlorine at temperatures below c. 1400 °C (Gerth *et al.* 1998). Therefore, the soda content in the glass is reduced when an excess amount of KCl is present, even if all the sodium is introduced as Na_2CO_3 and when this is the only alkali carbonate form present in the batch. The total alkali amount in the glass is determined by the amount of reactive carbonate plus a small amount of absorbed alkali chloride, that is, by the batch recipe and not by any temperature or other technical constraint. The ratio of soda to potash within the glass, however, is not equal to the ratio of alkali oxides present as carbonates, but is modified by the interaction with the co-existing salt melt.

The last series of experiments was undertaken to test whether the distribution factors for sodium and potassium are significantly affected by the original type of alkali compound present in the batch or whether the interaction between the two melt systems is complete so that the distribution of the alkali metals between glass and salt melt is independent of the recipe of the batch. This

series had again 50 g salt and nominally 100 g glass in the batch, although now equal amounts of sodium chloride and potassium chloride were added and various quantities of sodium and potassium carbonate existed in the batch. In effect, this series contained potassium equivalent to between 24 and 42 g potash in the total batch; and the formed glass (100 g) contained between 7.2 and 14.3 g potash, that is about one third of the total potassium initially present. This demonstrates that the mineralogy of the alkali compounds plays a less important role in determining the resulting glass composition than overall alkali ratio and glass to salt ratio.

8.2.1.3 Possible firing temperatures utilized in LBA glass-making (Qantir archaeological samples):

Almost all the LBA glasses, regardless of the colour, can be plotted on the ternary diagram below 1000 °C with just a few glasses plotting at around 1050 °C. This trend supports the current view that the upper limit of the firing temperature used for LBA glass-making is about 1050 °C. In contrast, only very few glasses plot at temperatures below the 800 °C isotherm; this could either indicate that there is a practical lower limit of glass-forming temperature with the part of the phase diagram being too viscous for practical glass-forming, or that any glasses with such a low lime content have merely deteriorated and are lost from the archaeological record, as suggested initially by Freestone (personal communication/ Raede *et al.* 2005) and recently by Schlick-Nolte and Werthmann (2003).

Published works (Rehren & Pusch 2005, Turner 1954a) suggest that the firing temperatures used at Qantir glass workshop(s) are 900-950 °C for initial

melting of the raw materials and 1000-1100 °C for the subsequent firing for coloration and ingot production. These firing temperature ranges for Qantir glasses were judged from the degree of colour change and vitrification of the ceramics of the reaction vessels. Therefore, if the lime content in the glass is proportional to the firing temperature, as discussed earlier, the lime content in the semi-finished glass should be lower than in the finished glass which is supposedly fired at the higher temperature.

In fact, the lime content of Qantir glasses ranges about 2 to 8 wt % CaO** (at nominally 5 wt% MgO), with the two semi-finished glasses (#88/0517,01 and #88/0517,04) and a droplet of glass (#98/0844) having a much lower lime content (2 to 3 wt % CaO**) than the finished glasses from the site. Three aspects are particularly noteworthy when all the chemical compositions of Qantir glasses were reduced and plotted on the SLS ternary diagram. First, it is interesting to note that the plots of finished Qantir glasses disperse largely in a horizontal direction only. That is, the lime contents of Qantir glasses are somewhat consistent whereas their silica and soda contents vary by each sample, suggesting that there was either some good control over the firing temperature or firing temperature was kept relatively consistent due to technical limitations during the LBA.

Secondly, the three archaeological samples of semi-finished glasses plotted near the 1200 °C isotherm towards the silica-rich corner of the system, which is in a very uncommon part of the diagram. This is in sharp contrast to what was expected at the beginning of this analysis and seems to contradict the assumption of a low-temperature firing for semi-finished glass. Indeed, the

calculated temperature is in excess of what is assumed the upper limit of Late Bronze Age glassmaking temperatures (1100 °C). However, this seemingly very high temperature is to a large extent due to the particular way in which the analytical data is reduced from the original seven base glass oxides to only three oxides for the ternary diagram. In this process, both alumina and iron oxide are recalculated into silica** (Rehren 2000b). All three samples have about 3 to 4 wt% of combined alumina and iron oxide, resulting in a much higher converted silica** value. Furthermore, due to their low magnesia content of less than 3 wt% and a typical potash content of around 2 wt%, the total difference between the seven base oxides and the reduced three oxides for the ternary diagram is well above the 5 wt% limit below which this reduction can be considered reasonable (Rehren 2000b). In this case, the iron oxide and alumina levels bring the calculated silica level up from around 75 wt% to near 80 wt%, equivalent to an increase in calculated temperature from around 900 °C to around 1200 °C (see Figure 6.12). However, Morey (1930c: Fig.1) has shown in an experimental study on the effect of alumina on liquidus temperatures of SLS glasses that the liquidus temperature will actually be lowered (by about 40-80 °C) by an addition of alumina up to about 2 wt%. In contrast, the liquidus temperatures will only start to increase when the alumina content is more than 2 wt%. A similar effect is to be assumed for iron oxide, although no experimental study for this has been found in the literature. Therefore, it is very likely that these peculiar Qantir samples were plotted in the higher temperature region (of 1200 °C) due to their high alumina and iron oxide contents but do not represent the actual firing temperature used to produce the glass. This example shows clearly the limitation of the 'tool' ternary diagram for the estimation of

temperatures in more complex systems. The consistently low earth alkali contents of these three samples, however, support the idea of a low-temperature initial firing of semi-finished glass.

Overall, the currently available archaeological data is still insufficient for the intended purpose of these analyses, namely to test the validity of the partial melting model, and to determine the probable melting temperatures for the primary glass making in the reaction vessels. The only surviving samples of likely semi-finished glass are contaminated by a certain amount of clay or ceramic material, making it impossible to estimate the original melting temperatures, or at least a temperature difference between the semi-finished and the finished glass. However, it is remarkable that the measured lime and magnesia content in these two samples is well below the typical levels found in the finished glasses. This indicates that the principle of a relationship between lime content and firing temperature may still be true, even if there is insufficient data to prove it. This low content of stabilizer in the semi-finished glass is also likely to be the reason why so little of it survived in the wet soil of the Nile Delta.

8.2.1.4 Raw materials possibly used in LBA glass-making (Qantir archaeological samples):

Comparison of microscopic analysis of Qantir glass samples and those of experimental melts enable us to discuss the possible raw materials used in Qantir glass-making.

Quartz pebbles, sand (calcareous sand), plant ash, and natron are believed to

be the typical raw materials for ancient soda-lime-silica glass-making. Both quartz pebbles and sand are possible source for silica, and they can be distinguished on the basis of the alumina contents in the finished glass (Tite & Shortland 2003). In addition, both plant ash and natron can be the source for soda (flux) and they can be distinguished according to potash and magnesia contents. However, it is more complex when it comes to the lime content, since both quartz sand and plant ash can contribute. However, if natron (which is mainly sodium carbonate, Na_2CO_3 , and has few other impurities) can be assumed to be the source of the flux (rather than plant ash which has many impurities), then the lime content of the glass can be used to distinguish between crushed quartz pebbles and quartz sand. Otherwise, it is generally assumed that the bulk of the lime content comes from plant ash (Sayre & Smith 1974, Tite & Shortland 2003).

Bearing this in mind, comparison of the preliminary findings from the microscopic examinations of experimental melts and that of Qantir glass samples shows interesting difference between the two. Experimental melts were prepared using quartz sand, sodium carbonate, and calcium carbonate. After firing and incomplete fusion, both lime-rich areas/particles, wollastonite, and quartz grains can be seen microscopically. The wollastonite-rich areas are often surrounding porous cores of very lime-rich material, probably remains of the limestone particles from the batch material. Since only quartz grains are visible in the semi-finished Qantir glass samples and the fact that the glass has a rather low lime content, the possible raw materials used in LBA glass-making in Qantir, and possibly the rest of Egypt, could be crushed quartz pebble and plant ash. In fact, sharp-angular shaped silica crystals

can be seen from the Qantir sample (see Figure 6.13). No full characterisation of mineral phases and grain sizes in plant ash has been found in the literature, but it may be assumed that plant ash contains a very finely intergrown matrix of sodium and calcium carbonate, with few if any areas rich in calcium carbonate. Therefore, during glass melting no such lime-rich areas and therefore no wollastonite clusters are likely to form. However, more experimental work using real plant ash is necessary to be investigated further.

8.2.2. The comparison of the base glass compositions

8.2.2.1 Colour specialisation among LBA glass workshops and geographical distribution of glass:

The comparison of the base glass compositions (all the newly obtained and published composition of LBA glasses were reduced to seven base glass oxides, Brill 1999a, 1999b) showed interesting trends between the two regions, Mesopotamia and Egypt. Moreover, it is suggested that there was a colour specialisation among LBA glass workshops, as discussed below.

The base glass compositions of glasses from Egyptian sites are more consistent not only within each individual site but also as a whole, compared to Mesopotamian glass samples. The base glass compositions of Mesopotamian glasses have wide ranges of major base glass oxide contents with much more narrow ranges of minor base glass oxide contents, except for cobalt-blue glasses. This may be due to the fact that glass samples from Mesopotamian sites tend to be in poorer conditions and are less well dated compared to the glasses from Egyptian sites. In addition, both magnesia

and potash contents of LBA Mesopotamian glasses tend to be up to 1 wt% higher than those of LBA Egyptian glasses of the same colour.

Glass-making during LBA may be centralised to some degree having similar minor base oxide contents, especially magnesia and potash contents, since the similarity in potash and magnesia contents, in particular, generally reflects the source of alkalis used to produce the glass (e.g. plant ash or natron). However, from the current published works, it is not clear if there were one or more centralised glass-making sites in Mesopotamia, the findings only suggest that glass workshops existed at the sites, excavated so far.

Blue is the most popular colour and blue glasses were found from every LBA site. These blue glasses have two types; cobalt- and copper-blue. However, cobalt-blue, red, and purple glasses were mostly found from Egyptian LBA sites and are rare from Mesopotamia.

As long established (Lilyquist *et al.* 1993; Kaszmarczyk 1986), all the LBA cobalt-blue glasses have a characteristic composition of high alumina contents, and typically a lower potash content as well as a suite of transition metal oxides together with the cobalt oxide. However, there is a difference between Mesopotamian and Egyptian cobalt-blue base compositions. Although all the LBA cobalt-blue glasses have low potash and high alumina contents, Egyptian cobalt-blue glasses tend to have lower potash contents (around 1 wt%) than those of Mesopotamian origin (1-2 wt%). Moreover, base glass compositions of Egyptian cobalt-blue glass are more consistent between sites than those between Mesopotamian sites that have opaque

cobalt-blue glass, with Nimrud having very extreme high alumina content of up to 7 wt%, while all the other LBA cobalt-blue glasses have about 2 wt% alumina. The fact that the base glass compositions of Uluburun cobalt-blue ingots are very similar to those of Egyptian cobalt-blue glasses from Amarna, also supports the hypothesis of cobalt-blue specialisation in Egypt.

Plots of cobalt-blue glasses are more closely clustered than the plots of copper-blue, and analysis suggests they were formed at somewhat lower temperatures. On the other hand, looking only at the Egyptian glasses, the cobalt-coloured ones appear slightly shifted towards the silica-rich corner of the diagram, while the copper-coloured glasses are firmly centered along the Egyptian trough and scatter on either side of it. This supports the hypothesis that the cobalt-blue production was a more specialised operation, conducted at fewer sites than the copper-blue glass production. It is unclear at present whether the lower apparent melting temperature reflects true lower furnace temperatures, or simply a lack of lime in the charge. The latter, though, would have resulted in an increased risk of failure of the parting layer in the glass-colouring crucibles, and seems therefore unlikely.

Red, purple, and opaque green glasses are difficult to produce, thus the craftsmen needed to be very familiar with the technicality of the process. Both redox conditions and temperatures have to be carefully monitored to produce red glass. Similarly, purple glasses need special control of melting conditions to leave the manganese ions present in the glass at exactly the correct state of chemical oxidation, the trivalent state, to produce its colour (Sayre & Smith 1974).

In summary, the trend that purple, red, black and cobalt-blue can be found predominantly from Egyptian LBA sites, while some colours can be found everywhere, and the technical difficulty to produce certain colours suggest that there existed some specialisation among LBA glass workshops in relation to which colour(s) they produced, especially for the cobalt-blue and the red glasses. It is interesting to note that there is no tin in Mesopotamian copper-blue glasses while almost all the Egyptian copper-blue glasses discussed in this research have 0.1-0.2 wt% SnO_2 (Shortland 2005).

Moreover, opaque green glass produced by mixing lead antimonate (yellow) and copper oxide (blue) has not been found from LBA Mesopotamian sites, while it can be found often in LBA Egyptian sites. A green glass from Nimrud has a peculiar composition, having very low copper (0.02 wt%), no lead, and low antimony (0.2 wt%) contents. This pattern highly suggests that the technique of producing green glass by mixing yellow and blue to make green was an Egyptian speciality.

Another interesting trend observed during this research is that the plots of LBA glasses from Egyptian sites tend to gather on the left hand side or near the Egyptian trough (more soda-rich area) of the ternary diagram, while the plots of glasses from Mesopotamian sites tend to gather on the right hand side, towards or on the Roman trough (more silica-rich area). Moreover, Nimrud Group 2 glasses (plant ash based) tend to plot along and close to the "Roman" cotectic trough, on the right hand side of the ternary diagram although they are not natron based, while Nimrud Group 1 (colourless, plant ash based) glasses plot near the Egyptian trough. However, the sample numbers of most other

colours are too small to permit sensible interpretation of their position in the ternary diagram; a puzzling observation is that the three Egyptian green opaque glasses all plot almost exactly half way between the two troughs. This green glass is thought to be based on mixing light blue and yellow glass, both of which plot on or near the Egyptian trough. Only one Malkata yellow glass plots on the Roman trough, but more analyses are necessary to understand this phenomenon.

8.2.2.2. Limitations of the ternary diagram:

This research was started based on the observation that LBA glass compositions are very homogeneous despite various raw materials available across time and regions (Rehren 2000b). However, this is not as neat and clear-cut as tentatively proposed by Rehren (2000b), and the situation is more complicated with the plots of individual glass analyses more scattered. One important observation is that the data dispersion is bigger horizontally than vertically in the ternary figure. This supports the view that the lime content is controlled by the firing temperature, resulting in less scatter in compositions vertically (only the lime content changes vertically) since the firing temperature used or possible to achieve with ancient glass-making technology was limited at the upper range by the available refractory materials, and at the lower end by the minimum temperatures necessary to make glass. In fact, most of the LBA glass compositions plot between 800 and 1000 °C, which is about the range of the temperature that is believed to be used in LBA glass-making (initial firing and secondary firing) in the published works. However, it is difficult to explain why LBA glass compositions scatter horizontally. The main compositional differences of horizontally dispersed plots are mainly due to

alkali and silica contents in the glass.

Overall, it should be stressed that some of the Egyptian glasses plot a considerable distance to the right from the Egyptian trough, some even reaching the Roman trough. This is in contradiction to the data presented by Rehren (2000a, b), but in good agreement with the experimental results presented in this thesis. This indicates that there are controlling factors at work, which may be either a direct reflection of raw material choice and batch recipes, or an indirect reflection of furnace temperatures, as argued for the lime content. In any case, they represent configurational, that is human factors and influences, although these are to some extent modulated by the inherent behavior of the glass-forming reactions. There are two main factors controlling the spread of the reduced glass compositions in the diagram, namely the technical limitation in ancient glass-making, such as furnace designs that determine the temperature that can be reached, and variables in the raw materials, especially in plant ash.

Alternatively, the choice of which cotectic trough (i.e. “Egyptian” on the left or “Roman” on the right) to follow as the glass forms, which affects the glass composition to be plotted and scatter horizontally on ternary diagram were studied. However, at present, there does not seem to be any inherent factor that would affect the composition of the melt to go either to the Egyptian or the Roman trough; the main difference appears to be the soda content, and as such, it is probably a configurational effect, depending on the overall amount of flux relative to quartz being added to the batch that controls in which cotectic trough the glass finally follows as it forms. The experimental studies

just suggested that the “Roman” composition needs over-firing (about 50 °C more than its set temperature as shown in the ternary diagram) while the “Egyptian” composition forms more easily and nicely (with lesser foamy crystalline phases) without over-firing. This observed phenomenon provides a clear indication that the preferred choice of earlier LBA glass-makers was for batch compositions closer to the soda-rich cotectic trough. This finding probably relates to the lack of suitable refractory materials in the LBA – and the clay used for the earliest known melting vessels.

Moreover, there is unavoidable limitation of the ternary diagram not representing the whole chemical composition of the glass since it uses reduced oxides, it only shows us the spread in silica** to soda** ratios horizontally. That is, for example, since the potash content is converted and integrated into soda** content, the reduced data does not reflect the alkali difference in the raw materials used to produce a glass. To study such differences, it is necessary to work with the full base glass oxide data, and trace elements.

8.3. Human agency as the remaining aspect: how influential?

Although this study showed that some interaction among alkalis, earth alkalis and firing temperature will control formed glass compositions, the variability within each raw material composition is significant/large enough that human agency is the most influential aspect of LBA glass-making. That is, the composition of LBA glass is not only affected by the variable nature of the raw materials but also by the choices and manipulation of these raw materials by the ancient glassmakers (Jackson *et al.* 2005). Moreover, the fritting stage

during glass-making process, if such a stage was necessary, may have an effect on the final composition of the formed glass.

In addition, as discussed above, dispersion of plots suggests that the homogeneity of LBA glass cannot be simply explained by ternary diagram.

Moreover, there are some coloured glasses with atypical compositions found among LBA glasses, even from the same site. For example, both an atypical high potash cobalt-blue glass rod and a typical copper-blue glass rod with low potash content were found from Amarna (Smiriniou & Rehren 2006). Therefore, although the number of glass workshops during LBA may be limited, a fascination for glass and the high demand for glass might have encouraged the highly skilled glass-makers to experiment with the use of variable raw materials for various reasons, such as using better (pure) quality raw materials and/or using materials that are readily (locally) available.

It is unfortunate that, up till now, there has been so little archaeological evidence available for LBA glass-making workshops. However, this experimental study shows that the human agencies, such as choice of materials, furnace technology, colouring, and workshop organisation, have noticeable effects on the LBA glass composition.

8.4. Future Outlook

This research has made an original contribution to our understanding of LBA glass-making, but further investigation on the following aspects will be necessary so that the relevance of these new contribution to LBA glass-making can be more conclusive.

Detailed research into the chemical and mineralogical composition of plant ash, especially of those derived from Egyptian plant sources, is necessary, in particular to test the replicated model, 2MM, using actual plant ash.

Further 2MM experiments on alkali exchanges needs to be conducted. For example, a series of batches having equal amounts of 4 different alkalis (NaCl, Na₂CO₃, KCl, K₂CO₃) could be used to study how much of each is preferentially absorbed into glass phase.

It would be desirable to gain a better understanding of another possible buffering material that controls the glass composition, namely the lime from the parting layer. It is hoped that the ongoing work on lime parting layer by Merkel and Rehren (2007) will reveal some useful information on the diffusion profiles for lime from the parting layer into the glass melt as a function of time and temperature, and the homogeneity of individual glass ingots.

Finally, recent work on trace elements (Shortland 2005, in press) is likely to make significant contributions to provenancing LBA glasses. It remains to be seen whether the PMM and 2MM are effective even at the sub-percent level, influencing trace elements such as lithium and rubidium (2MM) or strontium and barium (PMM).

It is hoped that this thesis has demonstrated some of the potential for experimental studies to understand the practicalities of ancient glass-making practice, and its significance for the interpretation of archaeological glass data.

References:

- ANGELINI, I., ARTIOLO, G., BELLINTANI, P., DIELLA, V., GEMMI, M., POLLA, A. & ROSSI, A., 2004. Chemical analyses of Bronze Age glasses from Frattesina di Rovigo, Northern Italy. *Journal of Archaeological Science*, **31** (8), 1175-84.
- Assur: Minnesota State University EMuseum Website [On-line]
http://www.mnsu.edu/emuseum/archaeology/sites/middle_east/assur.html
May 2006
- Tour Egypt: The Life of Ancient Egyptians, Glass Making [On-line]
<http://www.touregypt.net/historicalessays/lifeinEgypt12.htm>
23 Oct, 2004
- BACKMAN, R., KARLSSON, K. H., CABLE, M. & PENNINGTON, N. P., 1997. Model for liquidus temperature of multi-component silicate glasses. *Physics and Chemistry of Glasses*, **38** (3), 103-09.
- BAQIR, T., 1946. Iraq Government Excavations at 'Aqar Quf, Third Interim Report, 1944-5. *Iraq*, **8**, 73-93.
- BARAG, D., 1970. Mesopotamian Core-formed Glass Vessels (1500-500 B.C.). IN Oppenheim, Leo A., Brill, R. H., Barag, Dan & Saldern, Axel Von (Eds.) *Glass and Glassmaking in Ancient Mesopotamia*. Corning, New York, The Corning Museum of Glass, 131-97.
- BARAG, D., 1985. *Catalogue of Western Asiatic Glass in the British Museum, Volume I*, London, British Museum Publications Ltd.
- BASS, G. F., 1986. A Bronze Age Shipwreck at Ulu Burun (Kas): 1984 Campaign. *American Journal of Archaeology*, **90**, 269-96.
- BASS, G. F., 1987. Oldest known shipwreck reveals splendors of the Bronze Age. *National Geographic*, **172** (6), 692-733.
- BASS, G. F., PULAK, C., COLLON, D. & WEINSTEIN, J., 1989. The Bronze Age Shipwreck at Ulu Burun: 1986 Campaign. *American Journal of Archaeology*, **93**, 1-29.
- BECK, H. C., 1934. Glass Before 1500 B.C. *Ancient Egypt and The East*, 7-21.

(Hebrew) Bible, 2 Chronicles Chapter 2: 14-16.

http://en.wikisource.org/wiki/Bible%2C_King_James%2C_2_Chronicles#Chapter_2 05 September 2006

BOEHMER, R. M., 1965. Die Entwicklung der Glyptik während der Akkad-Zeit. *UAVA (Untersuchungen zur Assyriologie und Vorderasiatischen Archäologie)*, **4**.

BOYCE, A., 1989. Notes on the manufacture and use of faience rings at Amarna (Chapter 8). IN Kemp, B. J. (Ed.) *Amarna Reports V*. London, The Egypt Exploration Society, 160-68.

BOYCE, A., 1995. Collar and necklace designs at Amarna: a preliminary study of faience pendants (Chapter 11). IN Kemp, Barry J. (Ed.) *Amarna Reports VI*. London, The Egypt Exploration Society, 336-71.

BRAIDWOOD, R. J. & BRAIDWOOD, L. S., 1960. Excavations in the Plain of Antioch (Volume I): The Earlier Assemblages (Phases A-J). *Oriental Institute Publications*, **61**.

BRILL, R. H., 1999a. *Chemical analyses of early glass, The catalogue*, Corning, The Corning Museum of Glass.

BRILL, R. H., 1999b. *Chemical analyses of early glass, Tables of analyses*, Corning, The Corning Museum of Glass.

BRILL, R. H., SHIRAHATA, H., LILYQUIST, C. & VOCKE, J. R. D., 1993. Lead-Isotope Analyses of Some Objects from Egypt and the Near East. IN Lilyquist, C., Brill, R. H. & Wypyski, M. T. (Eds.) *Studies in Early Egyptian Glass*. New York, The Metropolitan Museum of Art, 59-70.

BRUNTON, G. & ENGELBACH, R., 1927. *Gurob*, London, British School of Archaeology in Egypt.

CABLE, M. & YANG, Y. X., 1993. Crystallisation in glasses of the system Na₂O-K₂O-CaO-MgO-Al₂O₃-SiO₂. *Physics and Chemistry of Glasses*, **34** (1), 18-23.

CARROLL, M. R. & HOLLOWAY, J. R., 1994. *Volatiles in Magmas*, Washington D.C., Mineralogical Society of America.

CARTER, T. H., 1965. Excavations at Tell Al-Rimah, 1964. Preliminary Report. *Bulletin of the American Schools of Oriental Research*, **178**, 40-69.

- COONEY, J. D., 1970. A History of Glass in Dynastic Egypt. *Curatorial Files*. The Cleveland Museum of Art, 98-122.
- COONEY, J. D., 1981. Notes on Egyptian glass. IN Simpson, W. K. & Davis, W. M. (Eds.) *Studies in Ancient Egypt, the Aegean, and the Sudan*. Boston, Museum of Fine Arts, Boston, 31-33.
- DELOUGAZ, P., HILL HARLOD, D. & LLOYD, S., 1967. *Private Houses and Graves in the Diyala Region*, Chicago, The University of Chicago Press.
- DITTMANN, R., 1990. Ausgrabungen der Freien Universität Berlin in Assur und Kar-Tuklti-Ninurta in den Jahren 1986-89. *Mitteilungen des Deutschen Orient-Gesellschaft zu Berlin*, **122**, 157-72.
- FOSTER, K. P., 1979. Faience Technology and Terminology. IN Foster, K. P. (Ed.) *Aegean Faience of the Bronze Age*. New Haven and London, Yale University Press, 1-21.
- FRANK, S., 1982. *Glass and Archaeology*, London, Academic Press Inc. London Ltd.
- FRANKFORT, H., 1934. Iraq Excavations of the Oriental Institute, 1932/33: Third Preliminary Report of the Iraq Expedition. *Oriental Institute Communications*, **17**.
- FREED, R. E., 1981. *Egypt's Golden Age: The Art of Living in the New Kingdom 1558-1085B.C*, Boston, Massachusetts, Museum of Fine Arts, Boston.
- FREESTONE, I. C., GORIN-ROSEN, Y. & HUGHES, M. J., 2000. Composition of primary glass from Israel. IN Nenna, M. D. (Ed.) *La route du Verre*. Lyon, Travaux de la Maison de l'Orient Méditerranéen, no. 33, 65-84, 65-84.
- FREESTONE, I. C., GREENWOOD, R. & GORIN-ROSEN, Y., 2002. Byzantine and Early Islamic Glassmaking in the Eastern Mediterranean: Production and Distribution of Primary Glass. IN G., Kordas (Ed.) *1st International Conference, HYALOS VITRUM GLASS*. Athens, 167-74.
- GAMMON, J. B., BORCSIK, M. & HOLLAND, H. D., 1969. Potassium-Sodium Ratios in Aqueous Solutions and Coexisting Silicate Melts. *Science*, **163** (3863), 179-81.
- GARNER, H. S., 1956. An Early Piece of Glass from Eridu. *Iraq*, **18**, 147-49.

- GEOTTI-BIANCHINI, F., DE RIU, L., SGLAVO VINCENZO, M. & MASCHIO, D., 1998. Influence of alumina content and modifiers on phase separation in soda-lime-silica glass. *Glastech.Ber.Glass Sci.Technol*, **71** (2), 42-47.
- GERTH, K., WEDEPOHL, K. H. & HEIDE, K., 1998. Experimental Melts to Explore the Technique of Medieval Woodash Glass Production and the Chlorine Content of Medieval Glass Types. *Chemie der Erde*, **58**, 219-32.
- GIBSON, M., 1990. Nippur, 1990: Gula, Goddess of Healing, and an Akkadian Tomb. *The Oriental Institute News and Notes*, No.125. Chicago, Illinois, Oriental Institute, The University Chicago Press, 1-7.
- GURNEY, O. R., 1953. Further Texts from Dur-Kurigalzu. *Sumer*, **9** (1), 21-34.
- HALL, H. R., 1930. Abu Shahrain. IN Hall, H. R. & Litt, D. (Eds.) *A Season's Work at Ur*. London, Methuen & Co. Ltd, 187-228.
- HAMZA, M., 1930. Excavations of the Department of Antiquities at Qantir (Faqus District) (Season, May 21st-July 7th, 1928). *Annales du Service des Antiquites de L'Egypte*, **30**, 31-68.
- HARDEN, D. B., 1956. Glass and glazes. IN Singer, C., Holmyard, J., Hall, E. J. & Williams, T. I. (Eds.) *A History of Technology*, II.318-19.
- HENDERSON, J., 1991. Industrial specialization in late Iron Age Britain and Europe. *Archaeological Journal*, **148**, 104-48.
- JACKSON, C. M. & SMEDLEY, J. W., 2004. Medieval and post-medieval glass technology: melting characteristics of some glasses melted from vegetable ash and sand mixtures. *Glass Technology*, **45** (1), 36-42.
- JACKSON, C. M., NICHOLSON, P. T. & GNEISINGER, W., 1998. Glassmaking at Tell el-Amarna: an integrated approach. *Journal of Glass Studies*, **40**, 11-23.
- JACKSON, C. M., BOOTH, C. A. & SMEDLEY, J. W., 2005. Glass by design? Raw materials, recipes and compositional data. *Archaeometry*, **47** (4), 781-95.
- KACZMARCZYK, A., 1986. The source of cobalt in ancient Egyptian pigments, (Eds.) *Secondary The source of cobalt in ancient Egyptian pigments*, 369-76. Place Published, Washington D.C., Smithsonian Institution Press.

- KACZMARCZYK, A. & HEDGES, R. E. M., 1983. *Ancient Egyptian Faience: an analytical survey of Egyptian faience from Predynastic to Roman times*, London, Warminster, England: Aris & Phillips.
- KELLER, C. A., 1983. Problems in dating glass industries of the Egyptian New Kingdom: examples from Malkata and Lisht. *Journal of Glass Studies*, **25**, 19-28.
- KOZLOFF, A. P., BRYAN, B. M. & BERMAN, L. M., 1992. Glass Vessels. IN Kozloff, A. P., Bryan, B. M., & Berman, L. (Eds.) *Egypt's Dazzling Sun, Amenhotep III and his world*, Bloomington, The Cleveland Museum of Art in cooperation with Indiana University Press, 373-92.
- KUNIHOLM, P. I., KROMER, B., MANNING, S. W., NEWTON, M., LATINI, C. E. & BRUCE, M. J., 1996. Anatolian tree rings and the absolute chronology of the eastern Mediterranean, 2220-718 BC. *Nature*, **381** (6585), 780-83.
- KÖPSEL, D., 2001. Solubility and vaporization of halides. *Proceedings of International Congress on Glass*. Edinburgh, Scotland, 330.
- LEMONNIER, P., 1986. The Study of Material Culture Today: Toward an Anthropology of Technical Systems. *Journal of Anthropological Archaeology*, **5**, 147-86.
- LILYQUIST, C., BRILL, R. H., WYPYSKI, M. T. & KOESTLER, R., 1993. Part 2. Glass. IN Lilyquist, C. & Brill, R. H. (Eds.) *Studies in early Egyptian glass*. New York, The Metropolitan Museum of Art, 23-58.
- LODING, D., 1981. Lapidaries in the Ur III period. *Expedition*, **23** (4), 6-14.
- MALLOWAN, M. E. L., 1947. Excavations at Brak & Chagar Bazar. *Iraq*, **9** (1-2), 1-266.
- MALLOWAN, M. E. L., 1954. The Excavations at Nimrud (Kalhu). *Iraq*, **16**, 59-163.
- MALLOWAN, M. E. L., 1966. Chapter 13. The Burnt Palace. IN Mallowan, M. E. L. (Ed.) *Nimrud and its remains, Volume 1*. London, Collins, 200-30.
- MASS, J. L., WYPYSKI, M. T. & STONE, R. E., 2002. Malkata and Lisht glassmaking technologies: towards a specific link between second millennium BC metallurgists and glassmakers. *Archaeometry*, **44** (1), 67-82.

- MATTHEWS, R., 2003. Issues and Approaches. IN Matthews, R. (Ed.) *Excavations at Tell Brak, Vol.4: Exploring an Upper Mesopotamian regional centre, 1994-1996*. London, British School of Archaeology in Iraq, 1-6.
- MCDONALD, H., 1997. The Beads. IN Oates, D., Oates, J. & McDonald, H. (Eds.) *Excavations at Tell Brak, Vol.1: The Mitanni and Old Babylonian periods*. London, British School of Archaeology in Iraq, 101-03.
- MCLOUGHLIN, S. D., 2003. The Characterisation of Archaeological Glass Using Advanced Analytical Techniques. *Unpublished PhD Thesis*. London, Imperial College of Science, Technology and Medicine,
- MERKEL, S. & REHREN, Th., 2007. Parting Layers, Ash Trays, and Ramesside Glassmaking: an Experimental Study. IN Pusch, E. B. & Rehren, Th. (Eds.) *Hochtemperaturtechnologie in der Ramses-Stadt*. Hildesheim, Verlag Gebrüder Gerstenberg, 197-216.
- MEYERS, E. M., 1997. *The Oxford Encyclopedia of Archaeology in the Near East*, Oxford University Press.
- MISRA, M. K., RAGLAND, K. W. & BAKER, A. J., 1993. Wood ash as a function of furnace temperature. *Biomass and Bioenergy*, **4** (2), 103-16.
- MOIR, G. K. & GLASSER, F. P., 1976. Phase equilibria in the glass-forming region of the system $\text{Na}_2\text{O}-\text{CaO}-\text{Al}_2\text{O}_3-\text{SiO}_2$. *Physics and Chemistry of Glasses*, **17** (3), 45-53.
- MOOREY, P. R. S., 1994. Glass and Glass-making. *Ancient Mesopotamian Materials and Industries*. New York, Oxford University Press Inc., 189-215.
- MOOREY, P. R. S., 2001. The Mobility of Artisans and Opportunities for Technology Transfer between Western Asia and Egypt in the Late Bronze Age. IN Shortland, A. J. (Ed.) *The Social Context of Technological Change, Egypt and the Near East, 1650-1550 BC*. Oxbow Books, 1-14.
- MORAN, W. L., 1992. *The Amarna Letters*, London, Baltimore MD: The Johns Hopkins University Press.
- MOREY, G. W., 1930a. The devitrification of soda-lime-silica glasses. *Journal of the American Ceramic Society*, **13**, 683-713.

- MOREY, G. W., 1930b. The effect of magnesia on the devitrification of a soda-lime-silica glass. *Journal of the American Ceramic Society*, **13**, 714-17.
- MOREY, G. W., 1930c. The effect of alumina on the devitrification of a soda-lime-silica glass. *Journal of American Ceramic Society*, **13**, 718-24.
- MOREY, G. W. & BOWEN, N. L., 1925. XVII.- The Ternary System Sodium Metasilicate-Calcium Metasilicate-Silica. *Journal of the Society of Glass Technology*, **9**, 226-64.
- NEWBERRY, P. E., 1920. A glass chalice of Tuthmosis III. *The Journal of Egyptian Archaeology*, **6**, 155-60.
- NICHOLSON, P. T., 1993. *Egyptian Faience and Glass*, Buckinghamshire, Shire Publications Ltd.
- NICHOLSON, P. T., 1995a. Glassmaking and glassworking at Amarna: some new work. *Journal of Glass Studies*, **37**, 1-19.
- NICHOLSON, P. T., 1995b. Recent excavations at an ancient Egyptian glassworks: Tell el-Amarna. *Glass Technology*, **36** (4), 125-28.
- NICHOLSON, P. T., 1996. New evidence for glass and glazing at Tell el-Amarna (Egypt). *Annales of the 13th AIHV Congress*. AIHV, 11-19.
- NICHOLSON, P. T. & HENDERSON, J., 2000. Glass. IN Nicholson, P. T. & I., Shaw (Eds.) *Ancient Egyptian Materials and Technology*. Cambridge, Cambridge University Press, 195-224.
- NICHOLSON, P. T., JACKSON, C. M. & TROTT, K. M., 1997. The Ulu Burun glass ingots, cylindrical vessels and Egyptian glass. *The Journal of Egyptian Archaeology*, **83**, 143-53.
- NOLTE, B., 1968. *Die Glasgefäße im alten Ägypten*, Berlin, Verlag Bruno Hessling Berlin.
- OATES, D., 1965. The Excavations at Tell al Rimah, 1964. *Iraq*, **27**, 62-80.
- OATES, D., 1966. The Excavations at Tell al Rimah, 1965. *Iraq*, **28**, 122-39.
- OATES, D., 1967. The Excavations at Tell al Rimah, 1966. *Iraq*, **29**, 70-96.

- OATES, D., 1982. Excavations at Tell Brak, 1978-81. *Iraq*, **44**, 187-204.
- OATES, D. & OATES, J., 1991a. A Human-headed Bull Statue from Tell Brak. *Cambridge Archaeological Journal*, **1** (1), 131-35.
- OATES, D. & OATES, J., 1991b. Excavations at Tell Brak 1990-91. *Iraq*, **53**, 127-45.
- OATES, D. & OATES, J., 1994. Tell Brak: A Stratigraphic Summary, 1976-1993. *Iraq*, (56), 167-76.
- OATES, D., OATES, J. & MCDONALD, H., 1997. Glass, Frit and Faience. IN Oates, D., Oates, J. & McDonald, H. (Eds.) *Excavations at Tell Brak, Vol. 1: The Mitanni and Old Babylonian periods*. London, British School of Archaeology in Iraq, 81-100.
- OPPENHEIM, L. A., BRILL, R. H., BARAG, D. & SALDERN, A. V., 1970. *Glass and Glassmaking in Ancient Mesopotamia*, New York, The Corning Museum of Glass.
- OWENS-ILLINOIS-GLASS-COMPANY-GENERAL-RESEARCH-LABORATORY, 1944. Effect of substituting MgO for CaO on properties of typical soda-lime glasses. *Journal of American Ceramic Society*, **27** (8), 221-25.
- PAYNTER, S. & TITE, M., 2001. The Evolution of Glazing Technologies in the Ancient Near East and Egypt. IN Shortland, A. J. (Ed.) *The Social Context of Technological Change, Egypt and the Near East, 1650-1550 BC*. Oxford, Oxbow Books, 239-54.
- PETRIE, F. W. M., 1891. Medinet Gurob. IN Petrie, F. W. M. (Ed.) *Illahun, Kahun and Gurob. 1889-90*. London, David Nutt, 15-21.
- PETRIE, F. W. M., 1894. *Tell el Amarna*, London, Methuen & Co.
- PETRIE, F. W. M., 1926. XX.- Glass in the Early Ages. *Journal of the Society of Glass Technology*, **10**, 229-34.
- PULAK, C., 1998. The Uluburun shipwreck: an overview. *The International Journal of Nautical Archaeology*, **27**, 188-224.

- PULAK, C., 2003. Paired Mortise-and-Tenon Joints of Bronze Age seagoing Hulls. IN Beltrame, C. (Ed.) *Boats, Ships, and Shipyards. IX International Symposium on Boat and Ship Archaeology*. Oxford, 28-34.
- PULAK, C., 2005. Who were the Mycenaens aboard the Uluburun Ship? IN Laffineur, R. & Greco, E. (Eds.) *Emporia: Aegeans in the Central and Eastern Mediterranean. Proceedings of the 10th International Aegean Conference, Athens, Italian School of Archaeology, 14-18 April 2004, Aegaeum 25, Liège - Austin.*, 295-312.
- PULAK, C., 2006. The Ship of Uluburun: A comprehensive compendium of the exhibition catalogue "The Ship of Uluburun - World Trade 3.000 Years Ago". IN Yalçın, Ünsal (Ed.) *Handouts Uluburun Workshop*. Bochum, Deutsches Bergbau-Museum Bochum, 6-40.
- READE, W., FREESTONE, I. C. & SIMPSON, S. J., 2005. Innovation or continuity? Early first millennium BCE glass in the Near East: the cobalt blue glasses from Assyrian Nimrud. *Annales du 16^e Congrès de l'Association Internationale pour l'Histoire du Verre, London 2003*, 23-27.
- REHREN, Th., 1997. Ramesside glass-colouring crucibles. *Archaeometry*, **39** (2), 355-68.
- REHREN, Th., 2000a. New aspects of ancient Egyptian glassmaking. *Journal of Glass Studies*, **42**, 13-23.
- REHREN, Th., 2000b. Rationales in Old World Base Glass Compositions. *Journal of Archaeological Science*, **27**, 1225-34.
- REHREN, Th., 2001. Aspects of the production of cobalt-blue glass in Egypt. *Archaeometry*, **43** (4), 483-89.
- REHREN, Th. & PUSCH, E. B., 1997. New Kingdom glass-melting crucibles from Qantir-Piramesses. *The Journal of Egyptian Archaeology*, **83**, 127-41.
- REHREN, Th. & PUSCH, E. B., 2000. Glass and glass making at Qantir-Piramesses and beyond. *Egypt and the Levant: International Journal for Egyptian Archaeology and Related Disciplines*, **4**, 171-79.
- REHREN, Th. & PUSCH, E. B., 2005. Late Bronze Age Glass Production at Qantir-Piramesses, Egypt. *Science*, **308**, 1756-58.

- REHREN, Th., PUSCH, E. B. & HEROLD, A., 1998. Glass coloring works within a copper-centered industrial complex in Late Bronze Age Egypt. IN Mccray, P. & Kingary, P. (Eds.) *The Prehistory and History of Glassmaking Technology*. 227-50.
- REHREN, Th., PUSCH, E. B. & HEROLD, A., 2001. Qantir-Piramesses and the organisation of the Egyptian glass industry. IN Shortland, Andrew J. (Ed.) *The Social Context of Technological Change, Egypt and the Near East, 1650-1550 BC, Proceedings of a conference held at St Edmund Hall, Oxford 12-14 September 2000*. Oxford, Oxbow Books, 223-38.
- SALDERN, A. V., 1966. Glass (Appendix III). IN Mallowan, M. E. L. (Ed.) *Nimrud and its remains, Volume 2*. London, Collins, 623-34.
- SAYRE, E. V., 1967. Summary of the Brookhaven Program of Analysis of Ancient Glass. IN Young, W. J. (Ed.) *Application of Science in Examination of Works of Art: Proceedings of the Seminar, September 7-16, 1965, conducted by the Research Laboratory, Museum of Fine Arts, Boston, Massachusetts*. Boston, Museum of Fine Arts, 145-54.
- SAYRE, E. V. & SMITH, R. W., 1974. Analytical studies of ancient Egyptian glass. IN Bishay, A. (Ed.) *Recent advances in science and technology of materials: proceedings, Cairo Solid State Conference 2nd, 1973*. New York, Plenum Press, 47-70.
- SCHAIRER, J. F., 1957. Melting relations of the common rock-forming oxides. *Journal of the American Ceramic Society*, **40** (7), 215-35.
- SCHAIRER, J. F. & YODER, H. S., 1971. *Carnegie Institution of Washington, Year Book 1969-1970*. 157-63.
- SCHLICK-NOLTE, B. & WERTHMANN, R., 2003. Glass Vessels from the Burial of Nesikhons. *Journal of Glass Studies*, **45**, 11-34.
- SCHOER, B. & REHREN, Th., 2007. The Composition of Glass and Associated Ceramics from Qantir. IN Pusch, E. B. & Rehren, Th. (Eds.) *Hochtemperaturtechnologie in der Ramses-Stadt*. Hildesheim, Verlag Gebrüder Gerstenberg, 165-95.
- SHAHID, K. A. & GLASSER, F. P., 1972. Phase equilibria in the glass forming region of the system Na₂O-CaO-MgO-SiO₂. *Physics and Chemistry of Glasses*, **13** (2), 27-42.

- SHAW, I., 2000. *The Oxford History of Ancient Egypt*, New York, Oxford University Press, Inc.
- SHAW, I. & NICHOLSON, P. T., 1995. *British Museum Dictionary of Ancient Egypt*, London, British Museum Press.
- SHERRATT, A. & SHERRATT, S., 1991. From luxuries to commodities: The nature of Mediterranean Bronze Age trading systems. IN Gale, N.H. (Ed.) *Bronze Age Trade in the Mediterranean*. 351-86.
- SHORTLAND, A. J., 2000a. The number, extent and distribution of the vitreous materials workshops at Amarna. *Oxford Journal of Archaeology*, **19** (2), 115-34.
- SHORTLAND, A. J., 2000b. *Vitreous Materials at Amarna, The production of glass and faience in 18th Dynasty Egypt*, Oxford, Archaeopress.
- SHORTLAND, A. J., 2001. Social Influences on the Development and Spread of Glass Technology. IN Shortland, A. J. (Ed.) *The Social Context of Technological Change, Egypt and the Near East, 1650-1550 BC*. Oxbow Books, 211-22.
- SHORTLAND, A. J., 2002. The use and origin of antimonate colorants in early Egyptian glass. *Archaeometry*, **44** (4), 517-30.
- SHORTLAND, A. J., 2004. Evaporites of the Wadi Natrun: seasonal and annual variation and its implication for ancient exploitation. *Archaeometry*, **46** (4), 497-516.
- SHORTLAND, A. J., 2005. The raw materials of early glasses: the implications of new LA-ICPMS analyses. *Annales du 16^e Congrès de l'Association Internationale pour l'Histoire du Verre, London 2003*, 1-5.
- SHORTLAND, A. J., **in press**. Who were the glassmakers? Social and technological interaction in mid-second millennium glass production. *Oxford Journal of Archaeology*.
- SHORTLAND, A. J. & TITE, M. S., 2000. Raw materials of glass from Amarna and implications for the origins of Egyptian glass. *Archaeometry*, **42** (1), 141-51.

- SHORTLAND, A. J., TITE, M. S. & EWART, I., 2006. Ancient exploitation and use of cobalt alums from the Western Oases of Egypt. *Archaeometry*, **48** (1), 153-68.
- SHUGAR, A. & REHREN, Th., 2002. Formation and composition of glass as a function of firing temperature. *Glass Technology*, **43C**, 145-50.
- SILVERMAN, W. B., 1940. Effect of alumina on devitrification of sodium oxide-dolomite lime-silica glasses. *Journal of American Ceramic Society*, **23** (9), 274-81.
- SMIRINIOU, M. & REHREN, Th., 2006. Investigating the production origins of Egyptian blue glass from New Kingdom Amarna. *36th International Symposium on Archaeometry (ISA 2006)*. Quebec City, Canada,
- SODE, T. & KOCK, J., 2001. Traditional Raw Glass Production in Northern India: The Final Stage of an Ancient Technology. *Journal of Glass Studies*, **43**, 155-69.
- STARR, R. F. S., 1939. Nuzi, Text. *Reports on the excavations at Yorgan Tepa near Kirkrk, Iraq, conducted by Harvard University in conjunction with the American Schools of Oriental Research and The University Museum of Philadelphia, 1927-1931*. Cambridge, Massachusetts, Harvard University Press,
- STEIN, D. L., 1989. A Reappraisal of the "Saustartar Letter" from Nuzi. *Zeitschrift für Assyriologie und Vorderasiatische Archäologie*, **79**, 36-58.
- STERN, M. E. & SCHLICK-NOLTE, B., 1995. *Early Glass of the Ancient World: 1600 B.C. - A.D. 50*, Ostfildern, Hatje Cantz Publishers.
- SWIFT, H. R., 1947. Effect of magnesia and alumina on rate of crystal growth in some soda-lime-silica glasses. *Journal of American Ceramic Society*, **30** (6), 170-74.
- TATTON-BROWN, V. & ANDREWS, C., 1991. Before the Invention of Glassblowing. IN Tait, H. (Ed.) *Five Thousand Years of Glass*. London, British Museum Press, 20-61.
- THOMAS, S., 2000. *Aspects of Technology and Trade in Egypt and the Eastern Mediterranean during the Late Bronze Age*, PhD Thesis, unpublished. University of Liverpool.

- TIRADRITTI, F., 1999. *The Cairo Museum: masterpieces of Egyptian art*, London, Thames & Hudson.
- TITE, M. S., 1987. Characterisation of Early Vitreous Materials. *Archaeometry*, **29** (1), 21-34.
- TITE, M. S. & BIMSON, M., 1986. Faience: an investigation of the microstructures associated with the different methods of glazing. *Archaeometry*, **28** (1), 69-78.
- TITE, M. S. & SHORTLAND, A. J., 2003. Production technology for copper- and cobalt-blue vitreous materials from the New Kingdom site of Amarna - a reappraisal. *Archaeometry*, **45** (2), 285-312.
- TITE, M. S., FREESTONE, I. C. & BIMSON, M., 1983. Egyptian faience: an investigation of the methods of production. *Archaeometry*, **25** (1), 17-27.
- TITE, M. S., SHORTLAND, A. J., MANIATIS, Y., KAVOUSSANAKI, D. & HARRIS, S. A., 2006. The composition of the soda-rich and mixed alkali plant ashes used in the production of glass. *Journal of Archaeological Science*, **33**, 1284-92.
- TURNER, W. E. S., 1939. XIX.- A Note on the Solubility of Sodium Chloride in a Soda-Lime-Silica Glass. *Journal of the Society of Glass Technology*, **23**, 265-67.
- TURNER, W. E. S., 1954a. XXIII.- Studies of ancient glass and glass-making processes. Part II. The composition, weathering characteristics and historical significance of some Assyrian glasses of the Eighth to Sixth Centuries B.C. from Nimrud. *Journal of the Society of Glass Technology*, **38**, 445-56.
- TURNER, W. E. S., 1954b. XXII.- Studies of ancient glass and glass-making processes. Part I. Crucibles and melting temperatures employed in ancient Egypt at about 1370 B.C. *Journal of the Society of Glass Technology*, **38**, 436-44.
- TURNER, W. E. S., 1956a. X.- Studies in ancient glasses and glassmaking processes. Part IV. The chemical composition of ancient glasses. *Journal of the Society of Glass Technology*, **40**, 162-86.
- TURNER, W. E. S., 1956b. XIV.- Studies in ancient glasses and glassmaking processes. Part V. Raw materials and melting processes. *Journal of the Society of Glass Technology*, **40**, 277-300.

- TURNER, W. E. S., 1956c. V.- Studies in ancient glasses and glassmaking processes. Part III. The chronology of the glassmaking constituents. *Journal of the Society of Glass Technology*, **40**, 39-52.
- TYTUS, R. D., 1903. *A Preliminary Report on the Re-excavation of the Palace of Amenhetep III*, New York, The Winthrop Press.
- VANDIVER, P., 1982. Mid-Second Millennium B.C. Soda-Lime-Silicate Technology at Nuzi (Iraq). IN Wertime, T. A. & Wertime, S. F. (Eds.) *Early Pyrotechnology*. Washington, D.C., Smithsonian Institution Press, 73-92.
- VANDIVER, P., 1983. Glass technology at the mid-second-millennium B.C. Hurrian site of Nuzi. *Journal of Glass Studies*, **25**, 239-47.

APPENDICES:

Appendix 1: Semi-quantitative analysis of salt melts (2MM*, analysed by XRF)

Note: Elements with their contents higher than 0.05 wt%, respectively, are only shown here.

	salt-1	salt-2	salt-3	salt-4	salt-5	salt-6	salt-7
	batch: Base A* + 20 g NaCl. (This batch composition was prepared twice. Hence, different two salt melts were produced.)	batch: Base A-4* + 20 g NaCl	batch: Base A-5* + 20 g NaCl	batch: Base A-6* + 20 g NaCl	batch: Base A-4* + 20 g KCl	batch: Base A-6* + 20 g KCl	
Na	56.4 ± 1.6	58.4 ± 1.8	56.6 ± 1.5	54.1 ± 1.6	50.5 ± 1.6	33.0 ± 1.7	32.0 ± 1.8
Cl	44.9 ± 0.06	43.5 ± 0.05	43.7 ± 0.05	43.5 ± 0.05	45.1 ± 0.06	45.3 ± 0.06	45.2 ± 0.06
K	1.7 ± 0.042	1.1 ± 0.036	2.6 ± 0.048	5.3 ± 0.064	7.3 ± 0.075	24.6 ± 0.14	25.8 ± 0.14
SUM	103	103	103	103	103	103	103

2MM: two melts model (see Chapter 5).

Base A: 65.0 wt% SiO₂ (65.0 g of sand), 10.5 wt% CaO (18.8 g of calcium carbonate, CaCO₃), 19.5 wt% Na₂O (33.3 g of soda ash, mainly Na₂CO₃), and 5.0 wt% MgO (5.0 g of magnesium oxide, MgO).

Base A-4: 65.0 wt% SiO₂ (65.0 g of sand), 10.5 wt% CaO (18.8 g of CaCO₃), 5.0 wt% MgO (5.0 g of MgO), 18.5 wt% Na₂O (32 g of soda ash), and 0.5 wt% K₂O (0.79 g potassium chloride, KCl).

Base A-5: 65.0 wt% SiO₂ (65.0 g of sand), 10.5 wt% CaO (18.8 g of CaCO₃), 5.0 wt% MgO (5.0 g of MgO), 16.2 wt% Na₂O (28 g of soda ash), and 1.7 wt% K₂O (2.6 g potassium chloride, KCl).

Base A-6: 65.0 wt% SiO₂ (65.0 g of sand), 10.5 wt% CaO (18.8 g of CaCO₃), 5.0 wt% MgO (5.0 g of MgO), 14.5 wt% Na₂O (25.0 g of soda ash), and 2.5 wt% K₂O (3.95 g potassium chloride, KCl).